"KINETIC STUDIES OF POLYENE EXCHANGE AND SUBSTITUTION IN LOW VALENT OCTAHEDRAL METAL COMPLEXES"

by

NEIL F. ASHFORD B.Sc. Hons. (LEICESTER)

A thesis submitted to the University of Keele
in partial fulfilment of the requirements for
the Degree of Doctor of Philosophy

Department of Chemistry
University of Keele

July 1987

TEXT BOUND CLOSE TO THE SPINE IN THE ORIGINAL THESIS

To Lauren and Jamie

This thesis is the author's own account of work carried out by the author under the supervision of Dr. J.A.S. Howell. No part of the work incorporated in this thesis has been incorporated in a thesis presented for a Higher Degree at any other university.

Acknowledgements

The following people and institutions are gratefully acknowledged:

Dr. J.A.S. Howell for his guidance and supervision of the project.

Professor G. Jones and the Department of Chemistry for the generous provision of Laboratory facilities.

The Science and Engineering Research Council for the Award of a Studentship.

Dr. D.T. Dixon for his help in the derivation of rate equations.

Dr. P. Borrell for the use of his computer programmes and all help with computing.

Mr. K.T. Alston for help in adapting special equipment and Mr. J. Clews for technical services.

Mr. T. Bolam and Mr. L.F. Ashford for assistance with reproduction of diagrams.

Mr. C. Cork for glassblowing expertise.

Miss P. Stockton (Elizabeth Charles Agency) for typing of the thesis.

Finally special thanks to my family for their support and encouragement throughout the period of my work.

ABSTRACT

The kinetics of polyene exchange and substitution in (polyene)$Cr(CO)_3$ complexes has been investigated. The exchange reaction involving displacement of complexed polyene for free polyene (Chapter 2) has shown two competing rate determining pathways to be operative; a ligand independent pathway giving rise to the exchange product and under certain conditions small amounts of $Cr(CO)_6$, and a ligand dependent pathway involving exclusive formation of the exchange product. Both reactions are postulated to originate from a common reaction intermediate. Structural interpretations of this intermediate are discussed in the light of theoretical molecular orbital calculations.

Phosphite substitution of (polyene)$Cr(CO)_3$ complexes to form $[P(OMe)_3]_3Cr(CO)_3$ is discussed in Chapter 3. In contrast to the exchange reactions, limiting rates at high ligand concentrations are apparent, indicating the presence of a ligand free intermediate. Such an intermediate is consistent with that postulated in the exchange reaction and enables interpretation of both exchange and substitution reactions in terms of a common mechanism under different limiting conditions.

Formation of isomeric products fac-$L_3Cr(CO)_3$ and mer-$L_3Cr(CO)_3$ from the substitution reactions together with a study of the fac $\rightleftharpoons$ mer isomerisation of these octahedral complexes are the subject of Chapter 4. Kinetic information indicates the isomeric product formation to be a result of a preceeding fluxional five-coordinate intermediate, whilst the isomerisation reaction proceeds via an intramolecular mechanism involving a six-coordinate trigonal **prismatic** intermediate.

CONTENTS

CHAPTER 3 Page Number

POLYENE SUBSTITUTION IN (Polyene)$Cr(CO)_3$ COMPLEXES

CHAPTER 4

ISOMERISATION REACTIONS OF $L_3M(CO)_3$ COMPLEXES

1. EXCHANGE AND SUBSTITUTION REACTIONS OF 18-ELECTRON ALKENE AND POLYENE TRANSITION METAL COMPLEXES

1.1 Introduction

One of the most interesting and rapidly developing areas of inorganic chemistry is that of organometallic chemistry. Historically the subject dates back to 1827 with the discovery of Zeise's Salt[1]. Other notable early landmarks include the syntheses of methyl and ethyl derivatives of zinc[2] by Frankland in 1848 and Victor Grignard's synthesis of organomagnesium halides[3] in 1900, for which he was awarded the Nobel Prize. The chemistry of metal carbonyls dates back to 1890 with the discovery by Mond of $Ni(CO)_4$[4], closely followed by $Fe(CO)_5$[5]; later years have witnessed an extensive development of the chemistry of metal carbonyls and their derivatives. More recently the discovery of ferrocene[6] in the early 1950's has led to an extensive application of organometallic complexes in stoichiometric organic syntheses.

The interest and expansion in organometallic chemistry arises not only from the variety of structures and bonding observed, but equally importantly from the potential of such compounds to act as heterogeneous or homogeneous catalysts for chemical reactions. Major developments in homogeneous catalysis, which is the main industrial application of organotransition metal chemistry, include hydroformylation (1938) catalysed by metal carbonyls, Zeigler-Natta polymerisation of alkenes (1955), the Wacker process (1959), alkene metathesis (1964), and the rhodium catalysed carbonylation of methanol, which has recently been re-investigated and shown to involve $cis\text{-}Rh(CO)_2I_2^-$ as the catalytically active species[7].

The continuing growth in the fine chemicals industry to provide materials for agricultural, pharmaceutical and electronic applications provides probably the main future area of application of organometallic complexes in both stoichiometric and catalytic synthesis. The more rigorous requirement for selectivity in such reactions, particularly enantioselectivity, is a subject of much current research. Other current areas of interest include the anchoring of homogeneous catalysts on polymer supports involving inorganic or organic backbones; such materials have potential in designing systems with selective permeability or specific electronic adsorption properties.

The significance of catalysis has undoubtedly accelerated the development of a systematic study of organometallic chemistry. Though the synthesis of new compounds still provides great stimulus, there has been an increasing effort over the last two decades devoted to a mechanistic understanding of reactivity using kinetic studies and other methods. Such studies provide not only a stimulating intellectual challenge, but also practical applicability in the design and operation of catalysts, including the increasing important area of metal cluster chemistry. Finally, the recent development of theoretical techniques, such as the fragment molecular orbital approach of Hoffmann[8] which may be applied to both ground state structures and reaction pathways, has provided an additional stimulus towards research in the area of reactivity and mechanism in both catalytic and stoichiometric organometallic reactions, since the latter may provide "model" systems for particular steps in a catalytic cycle which are not amenable to direct study.

1.2 Bonding in Organometallic Complexes

The chemical properties of organometallic compounds are determined to a a large exent by the nature of the bonds between metal and ligand. The traditional type of 2-electron, 2-centre bond can only in part explain the bonding characteristics of some metal atoms attached to organic ligands.

Of the numerous amount of organometallic compounds reported, bonding may be classified into five main categories:

1. Ionic bonds - occuring in alkali metals and alkaline earth metals.
2. Electron deficient bonds, such as the formation of M---CH_3---M bridges.
3. Metal-metal bonds, such as in metal cluster compounds.
4. Sigma donor bonds.
5. Pi donor bonds.

The latter two are the most commonly encountered types of bonding in low valent transition metal chemistry and deserve extra consideration.

1.2.1 Sigma (σ) Donor Bonding.

Sigma covalent bonds are formed from the overlap of ligand orbitals of σ symmetry with suitably orientated metal orbitals of σ symmetry. The bonds are to some degree polar in character depending upon the differences in electronegativity. The carbon σ donors may be formally subdivided into two classes: (a) anionic σ-donors and (b) neutral σ-donor/π-acceptor Compounds in the first class include metal alkyls. Type (b) compounds are formed almost exclusively by transition metals in low valence states bonded to ligands such as carbon monoxide, isonitriles, phosphines and phosphites.

Carbon monoxide has a filled σ orbital and two filled π orbitals localised between the carbon and oxygen atoms. As carbon is less electronegative than oxygen, the spatial extent of its lone pair is greater than that of oxygen. Associated with the filled π orbitals are empty π^* orbitals mainly localised on carbon as the filled π orbitals are predominantly localised on oxygen. The interaction of the metal with a CO molecule is linear, such that if the d_{z^2} orbital overlaps with the lone pair orbital on carbon then the d_{xz} and d_{yz} filled metal orbitals can overlap with π_x^* and π_y^* empty orbitals.

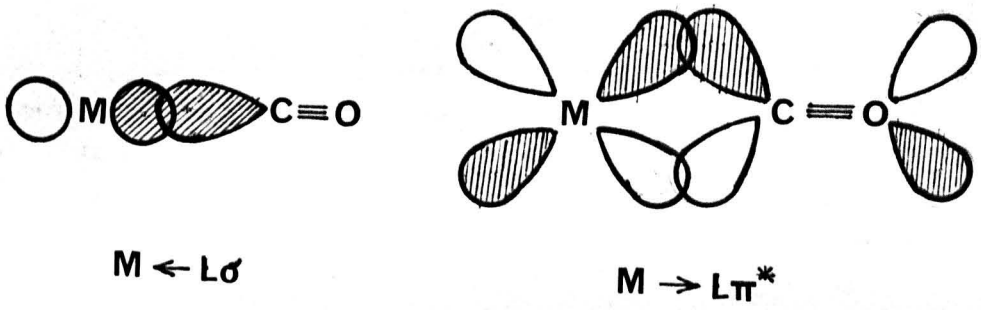

Fig. 1.1

The net effect is that carbon monoxide donates electron density to the metal via overlap of orbitals of σ symmetry and accepts electron density from the metal via overlap of orbitals of two π symmetry adapted orbitals. Carbon monoxide and other ligands which bond to the metal in a similar manner are termed σ-donor, π-acceptor ligands.

1.2.2 Pi(Π) Donor Bonding

The majority of metal compounds with Π-donor ligands involve low valent transition metals. The reason for this becomes clear when examining the Dewar, Chatt, Duncanson (DCD) model[9] whereby interactions consist of donation of Π electron density from a filled pΠ molecular orbital to a metal orbital of σ symmetry directed towards the centre of the ligand system, and back donation from the filled metal d orbitals to the Π^* orbital on the ligand.

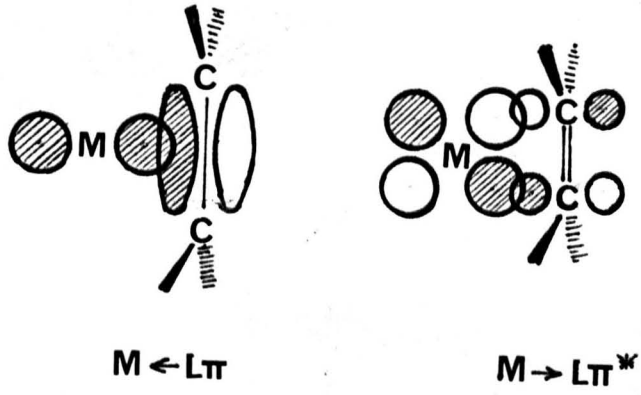

Fig. 1.2

The bonding of compounds containing unsaturated organic ligands such as allyls, conjugated dienes, cyclopentadienyls, trienes or arenes can be explained using essentially an extension of the DCD model, with all being examples of this synergistic model of donor-acceptor bonding.

1.3 Mechanisms of Ligand Substitution Pathways.

The classical categories introduced by Hughes and Ingold[10] to define organic reactions were based on the molecularity of the rate determining step of the reaction. The categorisation of inorganic substitution mechanisms as described by Langford and Gray[11] includes examples seemingly bimolecular in nature but which are related to unimolecular cases. This latter approach, which effectively provides a continuum from one limiting mechanism to the other, has been adopted in transition metal complex chemistry and provides the framework for a classification of reaction mechanism. Three possible simple pathways have been identified:

1.3.1 The Dissociative Pathway.

The dissociative (D) pathway involves loss of the leaving group to form an intermediate of reduced coordination number, which is subsequently attacked by the entering group to form the product. The rate determining step of the reaction is the initial dissociation of the leaving group. The transition state, formed prior to the intermediate has no entering group participation, hence the complete absence of an energetic role for the entering group is a characteristic feature of this mechanism. Scheme 1.1 illustrates a particular example of a reaction proceeding via a D mechanism.

$$ML_x \underset{k_{-1}}{\overset{k_1}{\rightleftharpoons}} ML_{x-1} + L' \xrightarrow{k_2} ML_{x-1}L'$$

Scheme 1.1

A true D mechanism usually gives rise to large positive activation enthalpies and entropies, with negligible effects due to solvation. Application of steady state theory to the intermediate ML_{x-1}, under pseudo first order reaction conditions yields the rate equation

$$R = \frac{k_1 k_2 [ML_x]\,[L']}{k_{-1} + k_2[L']} \qquad (1.1)$$

For the condition $k_2[L'] >> k_{-1}$ this reduces to

$$R = k_1[ML_x] \qquad (1.2)$$

1.3.2 The Associative Pathway.

The associative (A) process involves an initial addition of the entering group to substrate producing an intermediate of increased coordination number. The transition state and associated activation energies are affected by both entering and leaving groups; hence larger variations in rate can occur by altering entering or leaving groups, a characteristic feature of this mechanism. True A mechanisms are not observed in ligand substitution reactions of 18-electron organometallic complexes, though this is the most common pathway for substitution processes in 16-electron square planar complexes[11]. Scheme 1.2 illustrates an example of a reaction proceeding via an A mechanism.

$$ML_x + L' \underset{}{\overset{K_{diff}}{\rightleftharpoons}} ML_x.L' \overset{k_2}{\underset{k_{-2}}{\rightleftharpoons}} ML_xL' \xrightarrow{k_3} ML_{x-1}L' + L$$

Scheme 1.2

As k_2 is the rate determining step, the rate equation is

$$R=K_{diff}k_2[ML_x][L'] \qquad (1.3)$$

K_{diff} is the equilibrium constant for the diffusion together of ML_x and L' to form the "caged" species $ML_x.L'$ (analogous to the ion pair formation constant when considering ionic species). As with the dissociative mechanism, proof is provided by detection of the intermediate, in this case one of increased coordination number.

1.3.3 The Interchange Pathway.

The interchange (I) pathway is illustrated in Scheme 1.3

$$ML_x + L' \underset{}{\overset{K_{diff}}{\rightleftharpoons}} ML_x.L' \xrightarrow{k_2} ML_{x-1}L' + L$$

Scheme 1.3

and involves a diffusion controlled caged combination whereby the leaving group moves from the inner to the outer coordination sphere, and the entering group moves from the outer to the inner. The process could involve a multi-step path since the formation and dissociation of the outer sphere complex may consist of discrete steps of a reaction, but characteristic of the interchange is the absence of an intermediate related to any coordination change of the metal.

The subdivision of the mechanism into I_a and I_d classifications acts as a useful distinction between those reactions whose activation parameters are sensitive to changes in the entering ligand, I_a (interchange-associative) and those more sensitive to changes in leaving ligand, I_d (interchange-dissociative).

The I_a mechanism involves a transition state in which bond formation predominates over bond cleavage, while the I_d mechanism involves a transition state in which considerable bond cleavage has taken place. The implicit assumption is made that k_2 is the rate determining step, the applicable rate law is

$$R = K_{diff}k_2[ML_x][L'] \qquad (1.4)$$

Reactions of 18-electron complexes which depend on [L'] have been shown to be I_d in nature although many reactions exhibit competing D and I_d pathways. Figure 1.3 reflects the differences in the general rate behaviour for A, D and I mechanisms, and Figure 1.4 the accompanying energy profile diagrams.

1.3.4 The Ring-Opening Mechanism

The mechanisms described, do in the main, explain reactions at metal centres involving sustitutions of monodenate ligands. However, substitution reactions of polydentate chelating ligands often exhibit rate behaviour which is more complicated than the simple picture. The ring-opening mechanism (Scheme 1.4) proposed by Dobson and co-workers[12,13] provides an explanation for substitution reactions of polydenate ligands

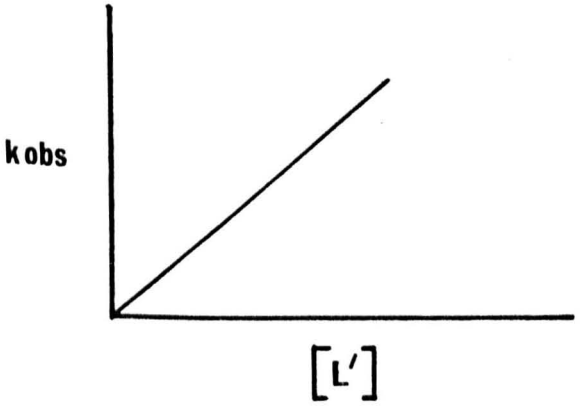

A-pathway

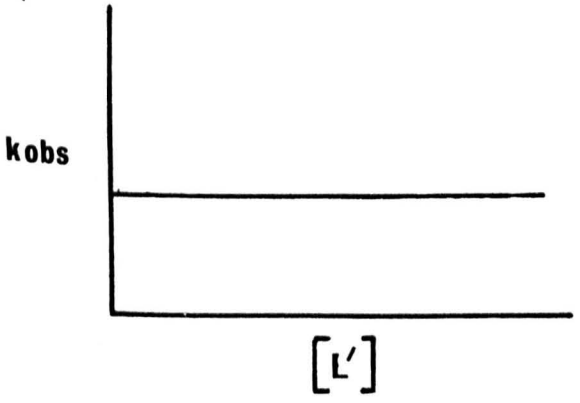

D-pathway

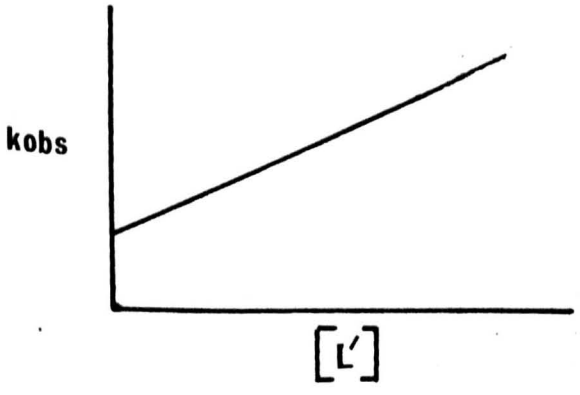

Ia, Id pathways

kobs = pseudo 1st order rate constant

Fig. 1.3

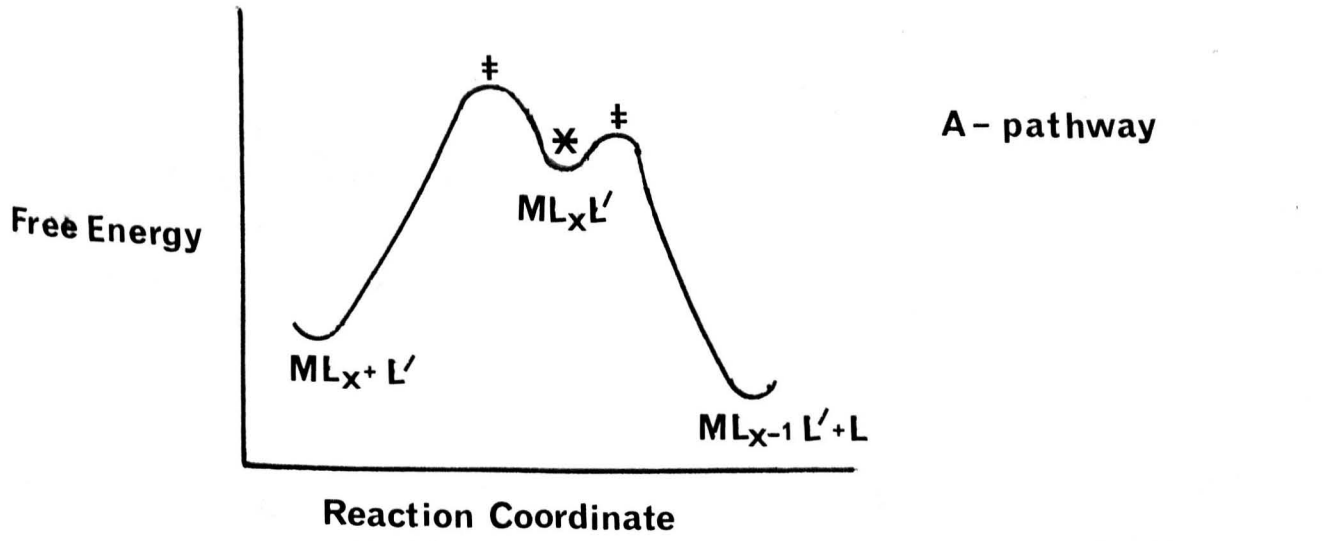

A – pathway

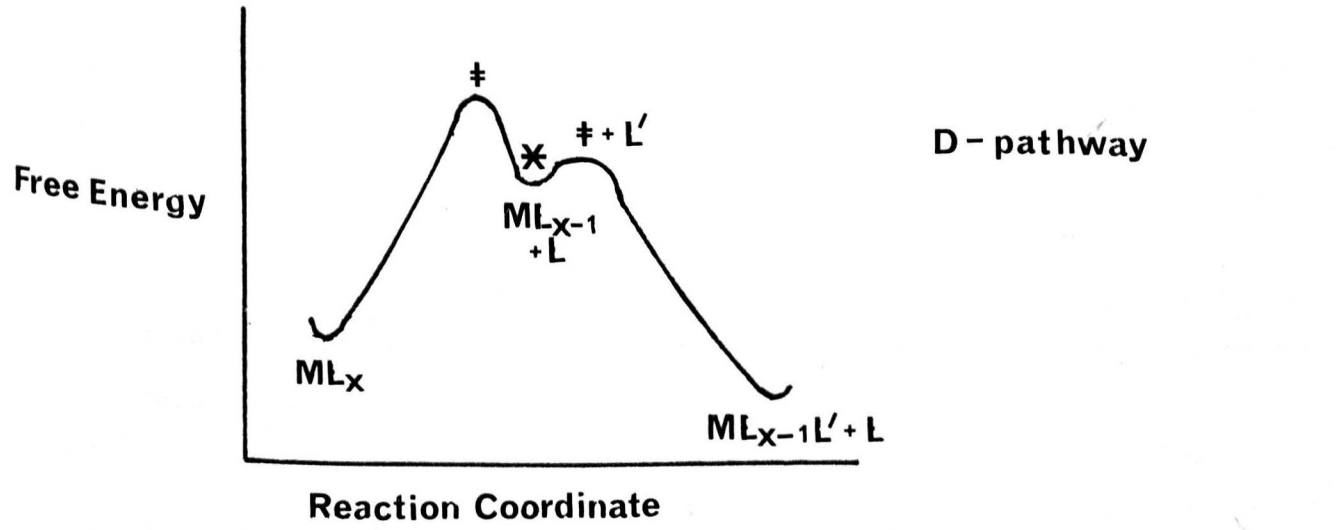

D – pathway

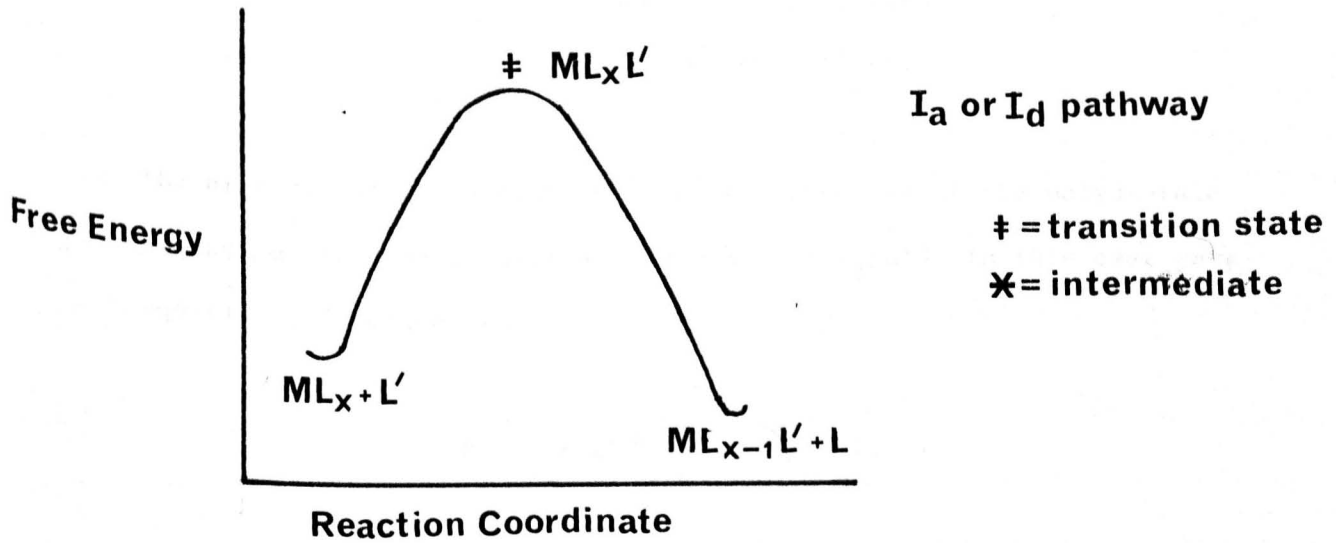

I_a or I_d pathway

‡ = transition state

* = intermediate

Fig. 1.4

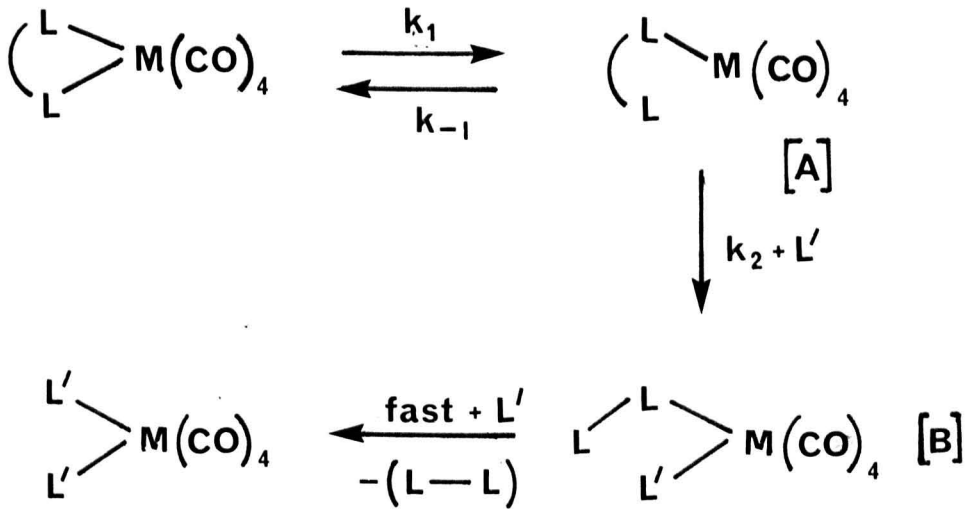

Scheme 1.4

Assuming steady state concentration of the intermediate (A), the derived rate law is

$$R = \frac{k_1 k_2 [S][L']}{k_{-1} + k_2[L']} \qquad (1.5)$$

where [S] and [L'] are substrate and ligand concentrations.

The high "local concentration"[14] of the free end of the polydentate ligand may provide conditions where $k_{-1} >> k_2[L']$. In this case rate equation 1.5 reduces to

$$R = \frac{k_1 k_2 [S][L']}{k_{-1}} \qquad (1.6)$$

Under conditions such that the $k_2[L']$ term greatly exceeds the re-chelation term (k_{-1}), the rate law becomes

$$R = k_1 [S] \qquad (1.7)$$

Intermediate conditions with $k_2[L'] \simeq k_{-1}$ have been observed in a number of cases, such as reactions of:
(2,2,7,7-tetramethyl-3,6-dithiaoctane)$W(CO)_4$ with alkyl and aryl phosphines and phosphites[15]. Plots of k_{obs} against [L'] are curved; the corresponding plots of $1/k_{obs}$ against $1/[L']$ are linear with a common non-zero intercept.

Rearranging equation 1.5 leads to such a linear equation

$$\frac{1}{k_{obs}} = \frac{1}{k_1} + \frac{k_{-1}}{k_1 k_2 [L']} \qquad (1.8) \quad \text{where } k_{obs} = R/[S]$$

Support for the ring-opening mechanism has come from linear plots of this type, with added confirmation from reactions in which the intermediate (A) in scheme 1.4 has been trapped, such as the reaction of bidentate $M(CO)_4(Ph_2P(CH_2)_nNR_2)$ (M=Cr,Mo,W) complexes (R=Me,Et;n=2,3) with CO, in which the five coordinate intermediate can be trapped as $M(CO)_5P\text{-}N^+H$ in the presence of acid[16]. An intermediate (B) has also been isolated from the reaction of bidenate $M(CO)_4(Me_2N(CH_2)_3NMe_2)$ and bicyclic phosphite[17]. Rate plots of the three cases are illustrated in Figure 1.5.

(1)

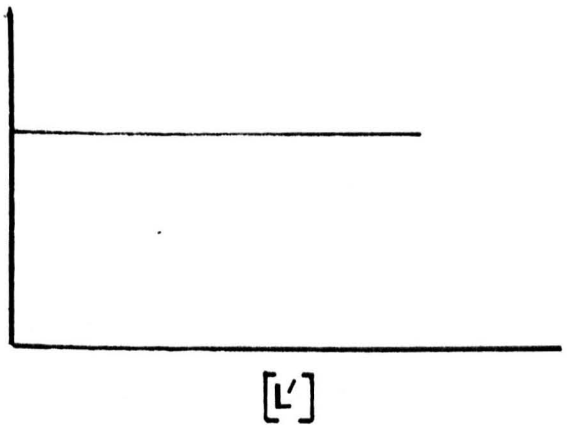

$k_2[L'] >> k_{-1}$

(2)

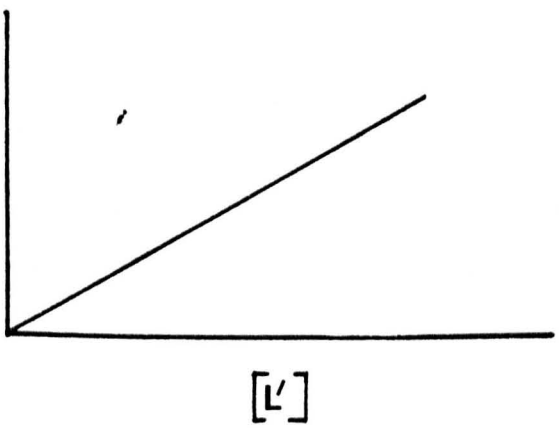

$k_{-1} >> k_2[L']$

$(3)_a$

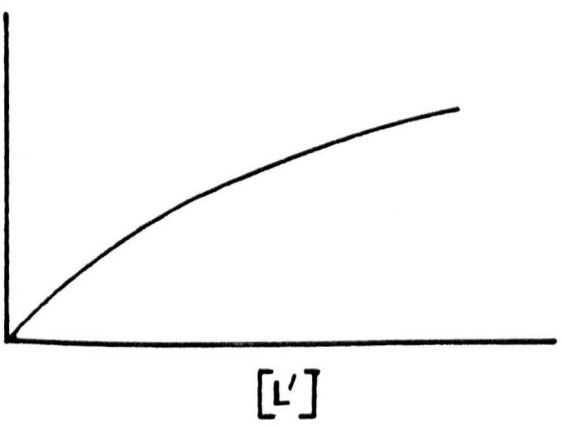

$k_{-1} \simeq k_2[L']$

$(3)_b$

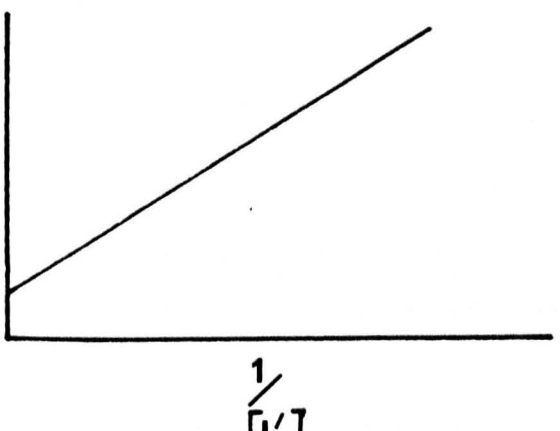

$k_{-1} \simeq k_2[L']$

Fig. 1.5

It is apparent from the plots that, if $k_2[L'] >> k_{-1}$ it is kinetically indistinguishable from a D pathway, and that if $k_{-1} >> k_2[L']$, the rate law is likewise indistinguishable from an I or A pathway. The magnitude of $\Delta S^{\ddagger}$ (entropy of activation) has been used to distinguish these possible mechanisms in the reaction of (2,5-dithiahexane)$M(CO)_4$ (M=Cr,Mo) with triphenyl phosphite; $\Delta S^{\ddagger}$ for the molybdenum complex is -83 J K^{-1} mol^{-1} indicating some form of associative reaction, while $\Delta S^{\ddagger}$ for the chromium complex is 8 J K^{-1} mol^{-1} consistent with an intermediate of unchanged coordination number[18].

The above outlined mechanisms can account for the majority of organometallic ligand substitution processes involving chelate ligands. Examples involving competing mechanisms, particularly applicable to the ring-opening mechanism, are frequently encountered and information from other sources is necessary to establish the overall mechanistic pathway.

1.4 Properties Contributing to Reactivity in Transition Metal Complexes

Reactivities of transition metal complexes, and the mechanisms by which they react, may be influenced by structural and bonding features of the ground state structure, or those developed in a subsequent transition state or intermediate. The following are some of those features believed to be of influence.

1.4.1 Effective Atomic Number

The sixteen and eighteen electron rule or effective atomic number rule (E.A.N.) was proposed by Tolman[19] to provide a basis for the systematisation of much of the structural chemistry of organotransition metals, and also acted as a useful guide to reactivity.

The main points of the rule are:

(1) "Diamagnetic organometallic complexes of transition metals may exist in significant concentration at moderate temperatures only if the valence shell of the metal contains 16 or 18 electrons. A significant concentration is one that may be detected spectroscopically or kinetically and may be in the gaseous, liquid or solid state.

(2) Organometallic reactions, including catalytic ones, proceed by elementary steps involving only intermediates with 16 or 18 electrons."

The rule, although empirical, has some theoretical support[20] which depends on full utilisation of metal valence orbitals. However an increasing number of stable 17-electron and 14-electron complexes are being found and implicated as intermediates in organometallic substitution reactions[21-23].

1.4.2 Transition State and Ground State Configurations.

The relative magnitude of donor-acceptor character in a metal-ligand bond remains difficult to quantify, although theoretical molecular orbital calculations can give some idea of relative orbital populations. Using such calculations on ground state molecules, it is possible to rationalise the greater affinity of metals in low oxidation states for π-acceptor ligands on the basis of greater $p\pi$ -$d\pi$ ligand-metal orbital overlap. However, though both ground state and transition state arguments have been used to explain reactivity, evidence suggests that information gained from reaction rates (and activation parameters associated with them) may be more closely related to electronic and geometric changes in transition states or intermediates of a reaction. These changes can only be evaluated by calculation when the intermediate is not directly observable. One area of conflicting argument between ground state and transition state calculation lies in the CO dissociation from $Mn(CO)_6^+$ and $Mn(CO)_5Br$

While ground state calculations suggest similar reactivities, transition state calculations[24] suggest that energy changes associated with geometrical relaxation of the 5-coordinate complex fragment [$Mn(CO)_5^+$ or $Mn(CO)_4Br$)] are of sufficient magnitude to strongly influence the energetics of the CO dissociation. This transition state approach predicts $Mn(CO)_6^+$ to be relatively inert, as observed experimentally.

The angular overlap method, which is a simple approximation of the full molecular orbital theory involving key orbital interactions has been successfully applied to associative substitution at square planar d^8 metal centres which proceed via a trigonal bipyramidal intermediate. The potential surface derived from this procedure contains two transition states, one associated with bond making, the other with bond breaking, between which is the trigonal bipyramidal intermediate[25]. The calculations predict that, if the height of the entering barrier is rate determining, as it is in the majority of cases, then decreasing the height causes an increase in the rate of the reaction. This increased rate of reaction can be achieved by:

a) Increasing σ-donor strength of entering ligand

b) Increasing the entering ligand polarisibility

c) Increasing σ strength of cis ligand

d) Decreasing σ strength of leaving group

e) Decreasing σ strength of trans ligand

f) The presence of better π-acceptor orbitals on entering ligand

g) Good interaction of metal (n+1)s and p orbitals with entering ligand

If the leaving barrier is rate determining the height of the barrier increases with:

a) Decreasing σ-donor strength of trans ligand

b) Better Π-acceptor characteristics of trans ligand

c) Good interaction of (n+1)s and p orbitals of metal with trans ligand

d) Polarisability of trans ligand

The conclusions agree well with experimental data from reactions involving hydrolysis, ammoniolysis and anation reactions of $Pt(NH_3)_x(H_2O)_yCl_{4-x-y}$ and related systems[25].

1.4.3 Coordination Number and Geometry.

The fragment molecular orbital approach[20,26] has helped to provide an explanation for chemical reactivity of different metals possessing similar coordination number and geometry. A detailed construction of frontier orbitals derived from fragments such as $M(CO)_3$ and M(arene)[27] gives information regarding symmetry properties, energy and spatial extent of these orbitals for determining interaction with other ligands completing the metal coordination sphere. Similar arguments can be applied to frontier orbitals derived from isolobal systems containing other ligands, for example $CpM(CO)_n$[28] (Cp=cyclopentadienyl) and M(polyene)[29].

A number of experimental studies examining the behaviour of a series of complexes with similar coordination number and geometry have provided information relating changes in reactivity to electronic and steric effects. One example of this approach is provided by the reactions of $Ni(CO)_4$, $Co(NO)(CO)_3$ and $Fe(NO)_2(CO)_2$ with various chelating ligands[30].

In this case, increasing the electron density at the metal on passing from Ni to Fe increases the importance of the ligand dependent term in the rate law derived from kinetic measurements.

Finally, reactivity can be assessed in terms of relative stabilities of complexes displaying similar electron configurations but different geometries. The structural preference energy plots[31] derived from a consideration of angular overlap analysis show, for example, that for a d^6 atom, the ML_6 geometry is strongly preferred relative to either ML_5 or ML_4 since $d\sigma^*$ molecular orbitals are vacant. For a d^8 atom the ML_5 trigonal bipyramidal structure is preferred relative to octahedral ML_6 or tetrahedral ML_4, but square planar ML_4 structures show equal preference, hence the large number of 16-electron square planar complexes of d^8 metals. For a d^{10} atom the $d\sigma^*$ molecular orbitals are equally populated for all coordination numbers and geometries and σ-only angular overlap considerations provide no distinction. The tetrahedral geometry, is however, structurally preferred due to minimisation of ligand-ligand repulsions. The existence of tetrahedral ML_4 complexes, in view of the equally filled bonding and antibonding orbitals, is due to the mixing of metal (n+1)p orbitals with metal nd orbitals of similar symmetry leading to d molecular orbital stabilisation. However, such compounds do tend to decompose more readily, or to undergo dissociation in solution. Thus, $Ni(CO)_4$ decomposes readily to metallic nickel and CO gas, and the solid $Pt(PPh_3)_4$ dissolves to give solutions containing largely the 16-electron $Pt(PPh_3)_3$ species[32]. Square planar 16-electron complexes undergo ligand substitution via an associative mechanism involving an 18-electron intermediate. Thus the reaction of trans-$RPtCl(PEt_3)_2$ with pyridine proceeds via the 5-coordinate intermediate $RPtCl(PEt_3)_2py$ which subsequently loses chloride ion[33].

The differing mechanistic pathways between tetrahedral 18-electron complexes and 16-electron square planar complexes provide clear evidence that decreased metal coordination number does not always equate with a greater tendency to undergo associative reaction pathways. Better correlations exist between mechanism and the number of valence electrons in the complex.

1.5 Exchange and Substitution Reactions of Alkene and Polyene Metal Complexes at d^{18} Metal Centres

Published work on exchange and substitution reactions of ene and polyene complexes of transition metals is focused primarily on five- and six-coordinate geometries possessing 18-electron metal centres. The results of some of these studies, and the mechanistic conclusions derived therefrom are presented below.

1.5.1 η^2-Alkene Metal Complexes

Reactions involving the substitution of alkene in 5-coordinate iron complexes have been well studied[34-38]. The rate of the reaction,

$$(CH_2{=}CHX)Fe(CO)_4 + L \rightarrow Fe(CO)_4L + CH_2{=}CHX$$

$X = OEt, Ph, Bu, CHO, CO_2Me, CN$

$L = PPh_3, AsPh_3, Py, CO$

is independent of the concentration of added ligand and the experimental rate law is

$$R = k_A[(CH_2{=}CHX)Fe(CO)_4] \qquad (1.9)$$

The reaction of $(CH_2=CHX)Fe(CO)_4$ with PPh_3 gives, in addition the disubstituted complex $Fe(CO)_3(PPh_3)_2$ under conditions where $Fe(CO)_4PPh_3$ is not known to undergo thermal substitution. Enthalpies of CO loss from iron carbonyl species obtained from electron affinity and appearance potential measurements[39,40] support CO dissociation from $Fe(CO)_4$ giving $Fe(CO)_3$, and subsequently the disubstituted product. A plot of $1/k_{obs}$ against the concentration of added alkene is linear with a non-zero intercept. The mechanism proposed to explain the above observation is shown in Scheme 1.5

$$(CH_2=CHX)Fe(CO)_4 \underset{k_{-1}}{\overset{k_1}{\rightleftharpoons}} CH_2=CHX + Fe(CO)_4$$

$$Fe(CO)_4 \underset{k_{-3}}{\overset{k_3}{\rightleftharpoons}} Fe(CO)_3 + CO$$

$$Fe(CO)_4 \xrightarrow{k_2 + L} Fe(CO)_4L$$

$$Fe(CO)_3 \xrightarrow{fast + 2L} Fe(CO)_3L_2$$

Scheme 1.5

Neglecting the k_3 pathway and assuming steady state conditions for the intermediate $Fe(CO)_4$, the mechanistic rate law is

$$R = \frac{k_1k_2[(CH_2=CHX)Fe(CO)_4][L]}{k_{-1}[alkene] + k_2[L]} \qquad (1.10)$$

If the condition $k_2[L] >> k_{-1}[alkene]$ is satisfied the equation reduces to

$$R = k_1[(CH_2{=}CHX)Fe(CO)_4] \qquad (1.11)$$

which is the same as the experimental rate law (equation 1.9) where $k_1{=}k_A$.

Rearrangement of equation 1.10 gives

$$\frac{1}{k_{obs}} = \frac{k_{-1}[alkene]}{k_1k_2[L]} + \frac{1}{k_1} \qquad (1.12)$$ where $k_{obs} = R/[S]$ and $[S]=[(CH_2{=}CHX)Fe(CO)_4]$

and is in agreement with the linearity of the plot of $1/k_{obs}$ against concentration of alkene.

The alkene exchange reaction has also been investigated[41]

$$(CH_2{=}CHPh)Fe(CO)_4 + alkene \longrightarrow (alkene)Fe(CO)_4 + PhCH{=}CH_2$$

alkene = methyl acrylate, cyclohexane, cyclooctene, cycloheptene.

The rate is independent of the concentration of added alkene, and the experimental rate law (equation 1.9) also applies. The reaction proceeds via rate determining loss of styrene, and the effect of added styrene on the rate of the reaction is consistent with the proposed mechanism shown in Scheme 1.6

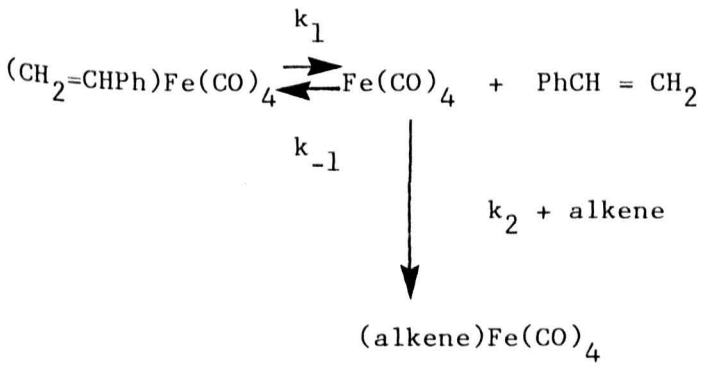

Scheme 1.6

Application of the steady state approximation to $Fe(CO)_4$ gives the same rate equation (1.10) as the ligand substitution reaction. Values of k_2/k_{-1} obtained from the plots of $1/k_{obs}$ against 1/[alkene] may be taken as a measure of the nucleophlicity of the ligands compared to the substrate styrene, and are in the order C_5H_5N > PPh_3 > $AsPh_3$ $SbPh_3$ > CO > methyl acrylate. Alkene rather than CO dissociation is consistent with ground state bond enthalpy contributions, $Fe\text{-}C_2H_4$(96.7 **kJ** mol^{-1}) < Fe-CO(116)[42].

One of the first kinetic studies involving (η^2-alkene)$M(CO)_5$ species was the substitution of acetone by alkenes in (acetone)pentacarbonyltungsten[43]

$$(acetone)W(CO)_5 + alkene \longrightarrow (alkene)W(CO)_5 + acetone$$

alkene = acyclic pentenes, hexene, heptene

Although this study does not directly relate to alkene substitution, it does provide information on the affinity of $W(CO)_5$ for different alkenes. The rate of the reaction is independent of the concentration of added alkene, and the mechanism proposed to support the kinetic results is outlined in Scheme 1.7

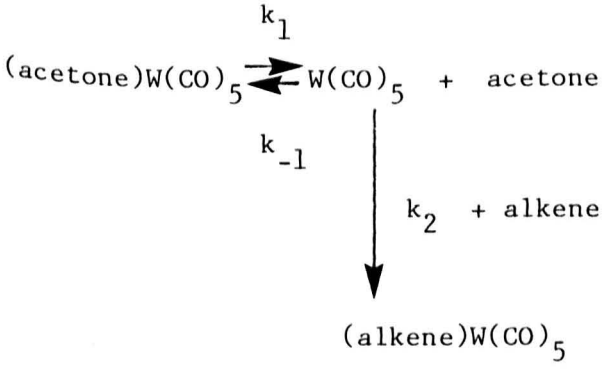

Scheme 1.7

Assuming a steady state concentration of the intermediate $W(CO)_5$, the mechanistic rate law is

$$R = \frac{k_1 k_2[(\text{acetone})W(CO)_5][\text{alkene}]}{k_{-1}[\text{acetone}] + k_2[\text{alkene}]} \qquad (1.13)$$

The ratio of the rates of capture of $W(CO)_5$ by acetone and alkene can be evaluated from the slope to intercept ratio of a plot of $1/k_{obs}$ against $1/[\text{alkene}]$ where

$$\frac{1}{k_{obs}} = \frac{1}{k_1} + \frac{k_{-1}[\text{acetone}]}{k_1 k_2[\text{alkene}]} \qquad (1.14)$$

Comparing these ratios for different alkenes, the ordering of relative kinetic affinity of $W(CO)_5$ follows the order 1-heptene > 1-hexene > cis-2-pentene > 1-pentene > trans-2-pentene > 2-methyl-2-butene. The equilibrium constant for the reaction, K_{eq} is also dependent upon the nature of the alkene, where

$$K_{eq} = \frac{[(\text{alkene})W(CO)_5][\text{acetone}]}{[(\text{acetone})W(CO)_5][\text{alkene}]}$$

[1-hexene(>20)>1-heptene(21.5)>1-pentene(20.7)>cis-2-pentene>(8.2)> trans-2-pentene(2.7)>2-methyl-2-butene(0.9)]

The equilibrium constants within the C-5 series appear to be largely dependent on steric factors. 1-pentene with only one alkyl substituent on the double bond is more stable than the 2-pentenes which have two alkyl substituents. 2-methyl-2-butene having three alkyl substituents is the least stable. The difference between cis- and trans-pentene may also be due to a steric effect. Although both possess alkyl substituents the cis-pentene can adopt a configuration in which the substituents are both directed away from the $W(CO)_5$, whereas the trans-2-pentene does not allow such a configuration. The kinetic effects are not easily rationalised since they do not closely relate to the equilibrium constants. Cis-2-pentene is bound less firmly than 1-pentene, but the former reacts more rapidly with $W(CO)_5$. This indicates that interactions which dominate binding are not fully developed in the transition state.

The reaction involving substitution of alkene

$$cis\text{-}M(CO)_4(PR_3)(alkene) + P(OPr\text{-}i)_3 \rightarrow cis\text{-}M(CO)_4(PR_3)P(OPr\text{-}i)_3 + alkene \quad [44]$$

alkene = dimethyl fumarate, maleic anhydride, dimethyl maleate

$PR_3 = P(Pr\text{-}i)_3, PPh_3, PPh(Pr\text{-}i)_2, PPh_2(Pr\text{-}i). PEt_3$

obeys the rate law

$$R = k_A[M(CO)_4(PR_3)(alkene)] \qquad (1.15)$$

and proceeds via rate determining loss of alkene. in agreement with the positive entropy of activation (Table 1.1). The reactivity of the metal-alkene bond is governed by substituents on the alkene. Electron withdrawing substituents lower the π^* levels, thereby increasing the metal-to-ligand donation, hence the metal-ligand bond becomes stronger.

The phosphine ligands employed vary little in electronic character, however the rate of alkene substitution increases with respect to PR_3 in the order $(P(Pr\text{-}i)_3 > PPh_3 > PPh(Pr\text{-}i)_2 > PPh_2(Pr\text{-}i) > PEt_3$ which parallels the order of ligand cone angle. The order of lability in terms of the metal (Cr>>Mo>>W) differs from the order usually found in substitution reactions involving these metals (Mo>>Cr>W)[45]. Analogous dissociative behaviour has been found for alkene derivatives of manganese[46].

1.5.2 η^3-Allyl Metal Complexes

Few investigations into the mechanisms of η^3-allyl metal complexes have been undertaken despite their considerable importance as intermediates in metal-catalysed reactions.

Kinetic studies of the reaction between $(\eta^3\text{-}C_3H_5)Co(CO)_3$ and trivalent phosphorous ligands have been reported[47].

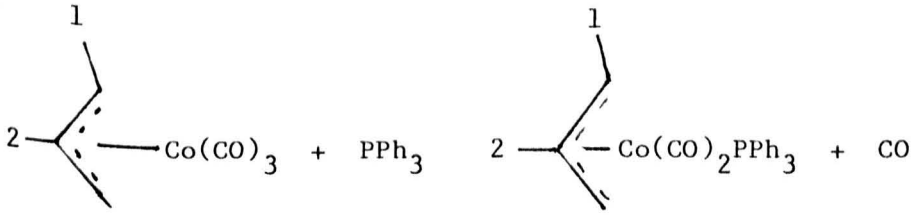

Limiting plots of k_{obs} against concentration of ligand are obtained, and interpreted in terms of Scheme 1.8

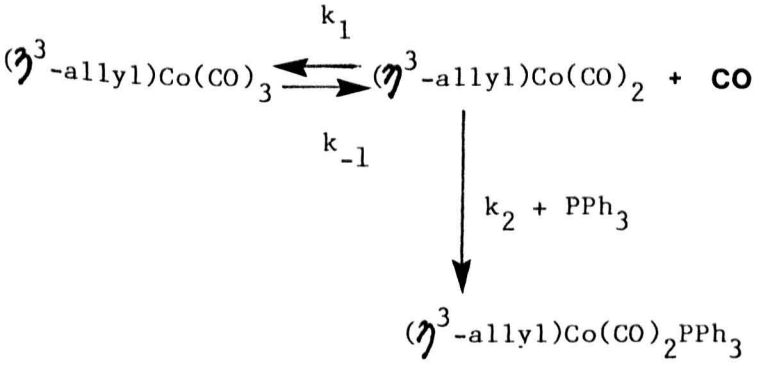

Scheme 1.8

Assuming a steady state concentration of the intermediate, the mechanistic rate law is

$$R = \frac{k_1 k_2[(\eta^3\text{-allyl})Co(CO)_3][PPh_3]}{k_{-1}[CO]+k_2[PPh_3]} \qquad (1.16)$$

Substituents in the 1-position decrease the rate of reaction, whereas an increased rate is observed for substituents in the 2-position, though no clear explanation to these findings is apparent. Similar results are obtained for phosphite substitution of CO, although the reaction proceeds to the disubstituted product[48]. In contrast studies on the CO substitution reactions of $(\eta^3\text{-}C_3H_4X)Fe(CO)_2NO$[49-52] (X=H,1-Me,2-Me,1-Ph,1-CN,1-Cl,2-Cl, or 2-Br) give an experimental rate law

$$R = k_A[\eta^3\text{-}C_3H_4X)Fe(CO)_2NO][PR_3] \qquad (1.17)$$

Entropies of activation are negative (Table 1.1), reflecting the associative nature of the reaction. The mechanism proposed (Scheme 1.9) involves an η^1-coordinated intermediate.

$$(\eta^3\text{-}C_3H_4X)Fe(CO)_2(NO) + PR_3 \xrightarrow{k_2} (\eta^1\text{-}C_3H_4X)Fe(CO)_2(NO)$$

$$\downarrow k_3 - CO$$

$$(\eta^3\text{-}C_3H_4X)Fe(CO)(NO)(PR_3)$$

Scheme 1.9

Electron-donating groups in either the 1- or 2- position decrease the rate of reaction, whereas electron-withdrawing groups increase the rate. For strongly electron-withdrawing groups (X=CN,Cl,Br) the intermediates have been isolated and shown to involve η^1-allyl coordination. An explanation of these effects concluded, that electron-donating groups increase the electron density on the metal thereby hindering nucleophilic attack, whereas electron-withdrawing groups produce opposite effects. The difference in mechanism of the above reactions has been explained by considering the effect of the NO group[53]. Acting as a 3-electron donor, it increases electron density at the metal which subsequently is dissipated via back-donation to the CO groups, hence increasing Fe-C bond strengths. Thus the iron system in its reactions requires more participation from the entering nucleophile, which might account for its second order reactivity.

A recent kinetic investigation of the reaction $(\eta^3\text{-allyl})Mn(CO)_4$ with phosphine ligands[54] has shown the substitution to proceed by rate determining loss of CO, with rate law

$$R = k_A[(\eta^3\text{-allyl})Mn(CO)_4] \qquad (1.18)$$

Activation parameters (Table 1.2) reflect the dissociative nature of the reaction. The mechanism proposed to account for the experimental results is shown in Scheme 1.10

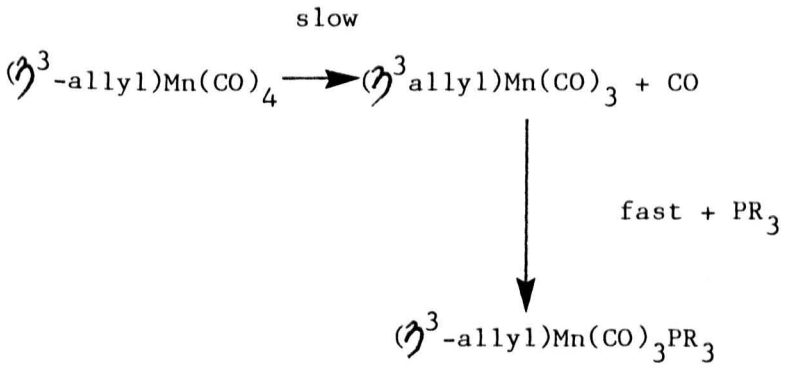

Scheme 1.10

1.5.3 η^4-Diene Metal Complexes

Before proceeding further, it is useful to discuss in more detail the difficulties and ambiguities which can arise in the mechanistic interpretation of experimental rate laws involving substitution or exchange reactions of complexes containing chelate or polydentate unsaturated ligands.

The major difficulty arises in the interpretation of chelate substitution reactions which obey the experimental rate law

$$R = k_B[S][L] \qquad (1.19)$$

and the ambiguities may be illustrated with reference to reactions of $(X\text{-}Y)M(CO)_4$ systems where X-Y may represent a bidentate nitrogen or phosphorus donor, or more particularly in our context a conjugated or non-conjugated diene ligand. This rate law may be interpreted mechanistically in two ways:

(a) An I_d ring-opening of the type

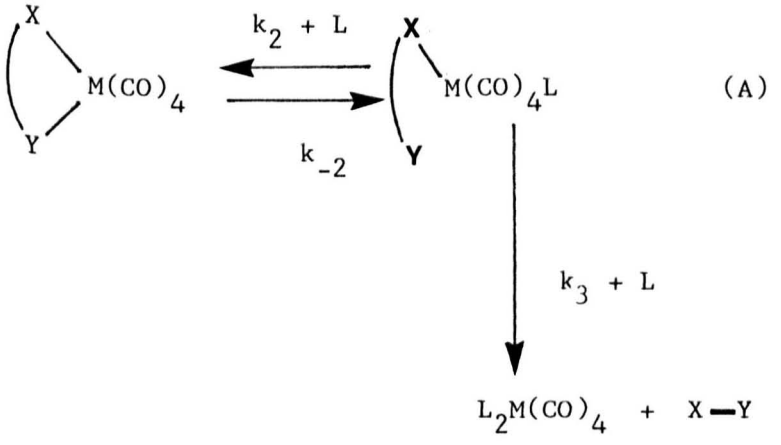

Scheme 1.11

On application of the steady state approximation to intermediate (A), the rate law

$$R = \frac{k_2 k_3 [S][L]^2}{k_{-2}+k_3[L]} \qquad (1.20)$$

is obtained which, when $k_3[L] >> k_{-2}$ reduces to

$$R = k_2[S][L] \qquad (1.21)$$

which is the same as equation 1.19 where $k_2 = k_B$, or

(b) A dissociative ring-opening of the type

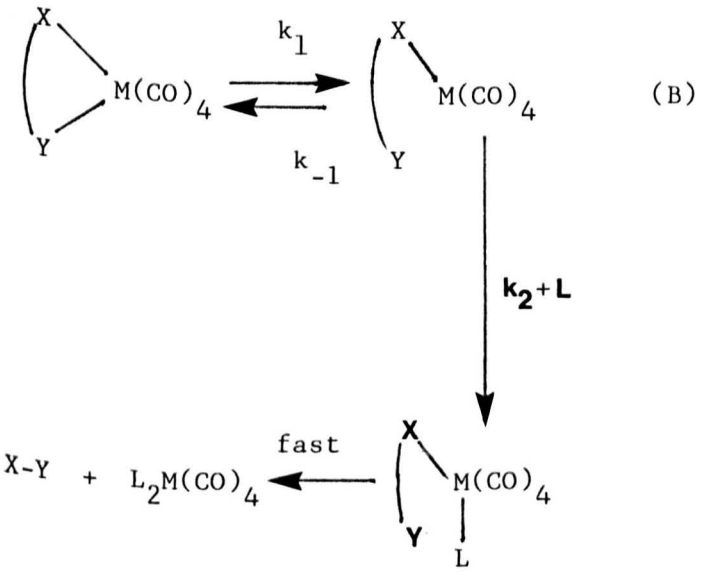

Scheme 1.12

Application of the steady state approximation to the intermediate (B) gives the rate law

$$R = \frac{k_1 k_2[S][L]}{k_{-1} + k_2[L]} \qquad (1.22)$$

which, under the conditions $k_{-1} >> k_2[L]$ reduces to

$$R = \frac{k_1 k_2[S][L]}{k_{-1}} \qquad (1.23)$$

which is again of similar form to equation 1.19 where $k_B = k_1 k_2 / k_{-1}$. The energy profile diagrams associated with these pathways are shown in Figure 1.6.

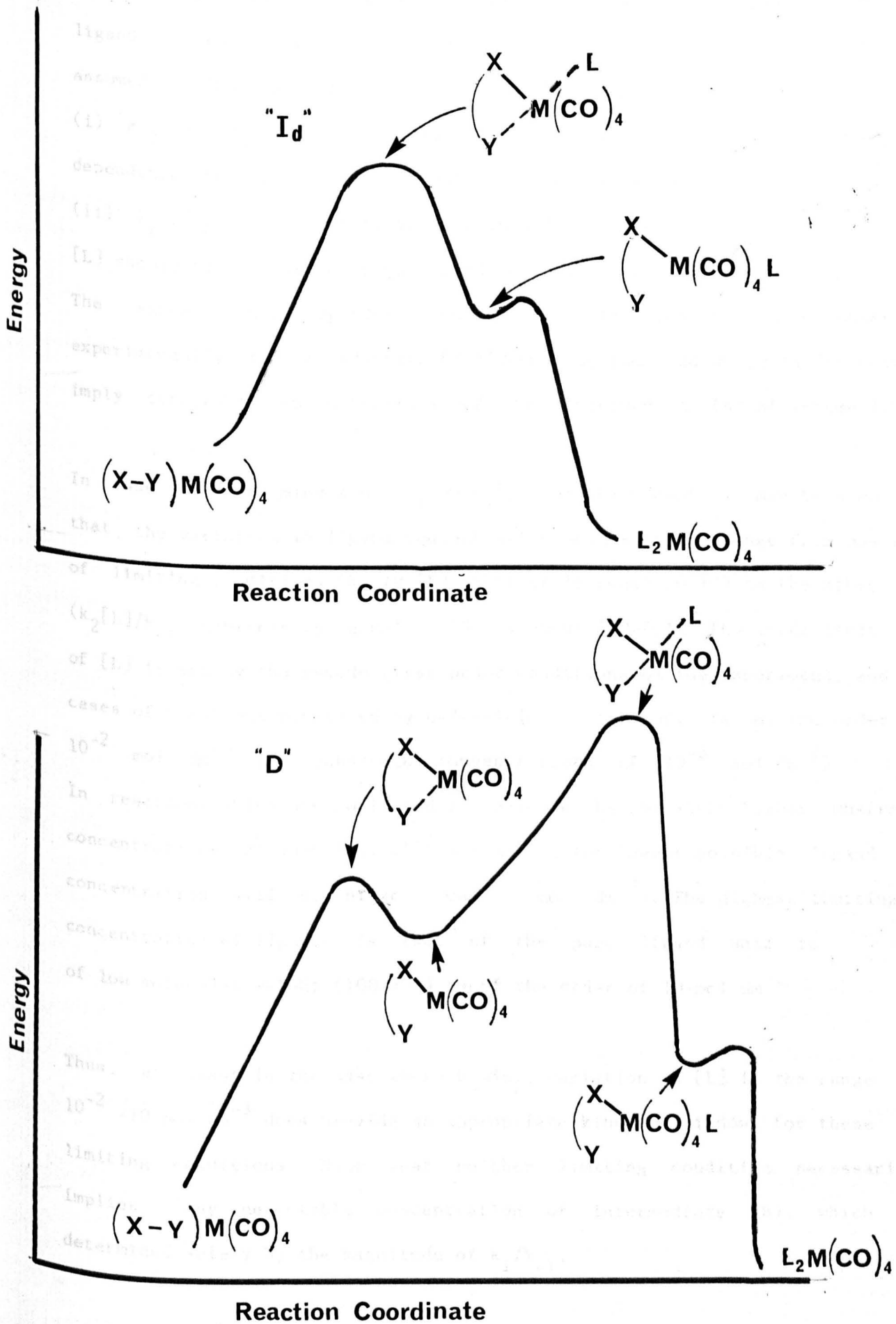
"I_d"
X
L
M(CO)$_4$
Y
X
M(CO)$_4$ L
Y
(X-Y)M(CO)$_4$
L$_2$M(CO)$_4$
Energy
Reaction Coordinate
"D"
X
M(CO)$_4$
Y
X
M(CO)$_4$
Y
X
L
M(CO)$_4$
Y
X
M(CO)$_4$ L
Y
(X-Y)M(CO)$_4$
L$_2$M(CO)$_4$
Energy
Reaction Coordinate

Fig. 1.6

Kinetic differentiation between these two alternatives is possible only if ligand concentrations can be varied such that, the opposite of the two assumed limiting conditions can be attained or approached, ie. (i) $k_{-2} >> k_3[L]$ for equation 1.20 in which case a second order dependence on [L] at low ligand concentration should be observed, or (ii) $k_2[L] >> k_{-1}$ for equation 1.22 in which a zero order dependence on [L] should be observed at high ligand concentration.
The second order dependence outlined in (i) has not been observed experimentally for a bidentate $(X\text{-}Y)M(CO)_4$ system, and would in any case imply detectable concentrations of the intermediate (A) of scheme 1.11.

In case (ii), assuming that $k_{-1} >> k_2[L]$ for the moment, it may be seen that the variation in ligand concentration necessary to change from one set of limiting conditions ($k_{-1}/k_2[L]$ arbitrarily equal to 10) to the other ($k_2[L]/k_{-1}$ arbitrarily equal to 10) is about 100-fold. The lower limit of [L] is set by the pseudo-first order conditions of the experiment, and in cases of reactions monitored by uv/visible spectroscopy, is of the order of 10^{-2} mol dm^{-3} (ie substrate concentrations of 10^{-3} mol dm^{-3})
In reactions which are monitored for example, by nmr where higher substrate concentrations are used (ca. 10^{-1} mol dm^{-3}), the lowest possible ligand concentration will be higher (ca. 1 mol dm^{-3}). The highest limiting concentration of ligands is that of the pure ligand, which for ligands of low molecular weight (100-200) is of the order of 10 mol dm^{-3}.

Thus, at least in the case where $k_{-1} \simeq k_2$, variation in [L] in the range 10^{-2} -10 mol dm^{-3} does provide an appropriate kinetic "window" for these limiting conditions. Note that neither limiting condition necessarily implies any detectable concentration of intermediate (B), which is determined solely by the magnitude of k_1/k_{-1}.

The relative magnitude of k_{-1} and k_2 will be both substrate and ligand dependent. Thus, stabilisation of the intermediate (B) may be slight for example, simply an alteration in solvation energy, which in hydrocarbon solvents will be small, or more substantial involving intramolecular stabilisation. Similarly, k_2 may be dependent on both the size and nucleophilicity of the ligand and intermediate.

Based on the "chelate effect" in aqueous coordination chemistry, it would be chemically reasonable to assume that in most cases, $k_{-1} > k_2$. If the two rate constants differ by more than a factor of 10, then it is unlikely, except at very high concentrations of [L] to see any deviation from rate law (1.19). Such deviations have indeed been observed, though some caution must be shown in cases where the ligand and solvent differ appreciably in character (for example, substitution reactions involving RCN, studied in hydrocarbon or halocarbon solvents).

For a chelate substitution reaction whose experimental rate law is (1.19) and which is interpreted mechanistically as dissociative ring-opening, the experimental activation parameters must be associated with the combination of rate constants k_1k_2/k_{-1} such that

$$\Delta H^{\ddagger}_{exp} = \Delta H^{\ddagger}_1 + \Delta H^{\ddagger}_2 - \Delta H^{\ddagger}_{-1}$$

which if $k_{-1} >> k_1$ and k_2 reduces to

$$\Delta H^{\ddagger}_{exp} = \Delta H^{\ddagger}_1 + \Delta H^{\ddagger}_2$$

and $$\Delta S^{\ddagger}_{exp} = \Delta S^{\ddagger}_1 + \Delta S^{\ddagger}_2 - \Delta S^{\ddagger}_{-1}$$

Thus measurement of $\Delta H^{\ddagger}_{exp}$ provides no absolute value for $\Delta H^{\ddagger}_1$ and $\Delta H^{\ddagger}_2$ in reactions which do not show limiting rate behaviour. In entropy terms, it may perhaps be the case that reactions with the more strongly negative $\Delta S^{\ddagger}$ values, are those in which $\Delta H^{\ddagger}_2 << \Delta H^{\ddagger}_1$

One further point may be made which may be particularly applicable to cases where k_{-1} and k_2 are comparable (ie, $\Delta G^{\ddagger}_{-1}$ and $\Delta G^{\ddagger}_2$ are comparable). It is possible that competing I_d and dissociative ring-opening pathways may be observed. Thus, the difference in energy between attack of L on the ring-opened intermediate compared to attack at some point prior to the transiton state, which leads to the intermediate, may be small with both pathways being kinetically accessible. Based on Scheme 1.13, such reactions might be expected to exhibit three types of rate behaviour.

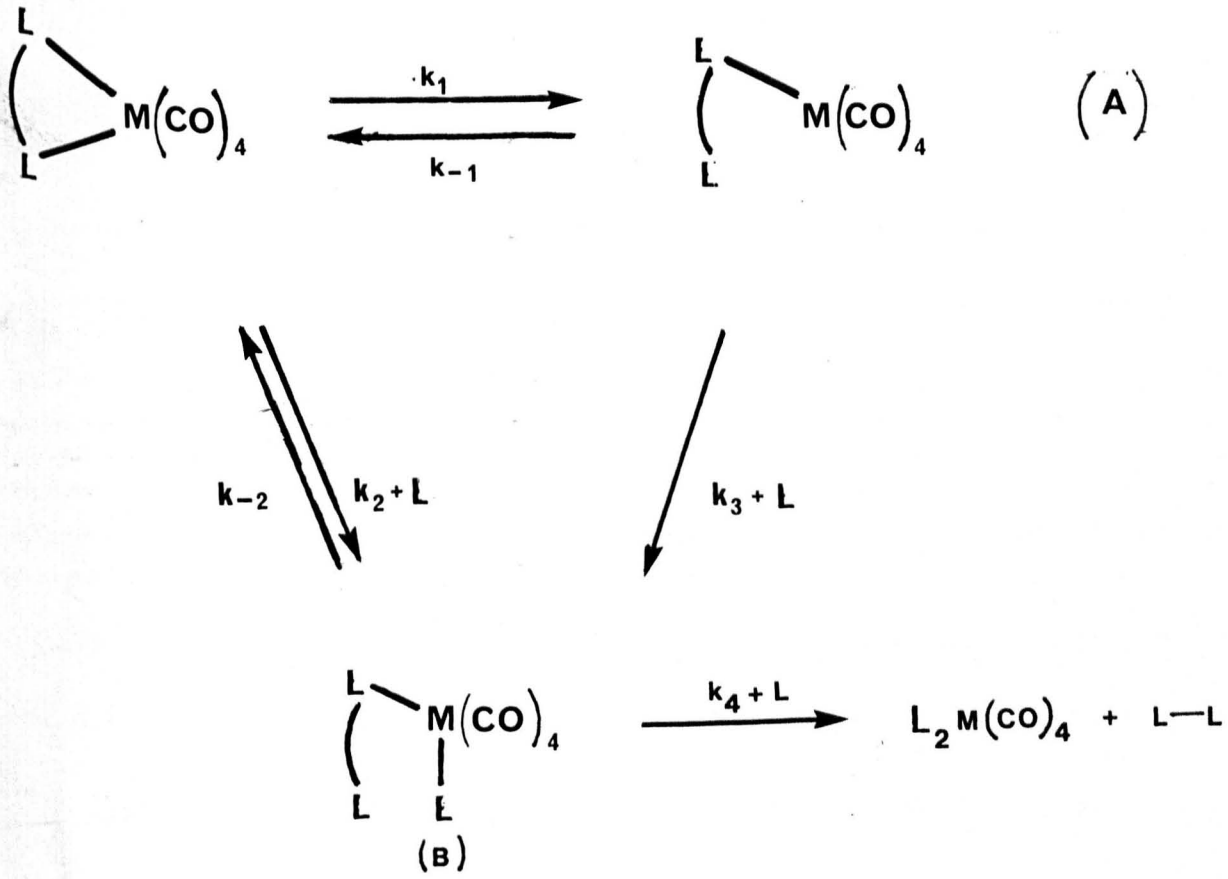

Scheme 1.13

Steady state treatment of (A) and (B) yields the rate law

$$R = \frac{k_1 k_3[S][L]}{k_{-1}+k_3[L]} + \frac{k_2 k_4[S][L]^2}{k_{-2}+k_4[L]} \qquad (1.24)$$

which if $k_4[L] >> k_{-2}$ reduces to

$$R = \frac{k_1 k_3[S][L]}{k_{-1}+k_3[L]} + k_2[S][L] \qquad (1.25)$$

If $k_{-1} >> k_3[L]$ over the whole concentration range, this reduces to

$$R = \left[\frac{k_1 k_3}{k_{-1}} + k_2\right][S][L] = k_B[S][L] \qquad (1.26)$$

ie, first order in [L] with zero intercept.

If the limiting condition $k_3[L] >> k_{-1}$ applies, the above reduces to

$$R = k_1[S] + k_2[S][L] = k_A[S] + k_B[S][L] \qquad (1.27)$$

ie, first order in [L] but with a non-zero intercept.

In cases where the "window" of ligand concentration ($k_{-1} \simeq k_3[L]$) has an effect the rate behaviour may be represented as shown in Figure 1.7.

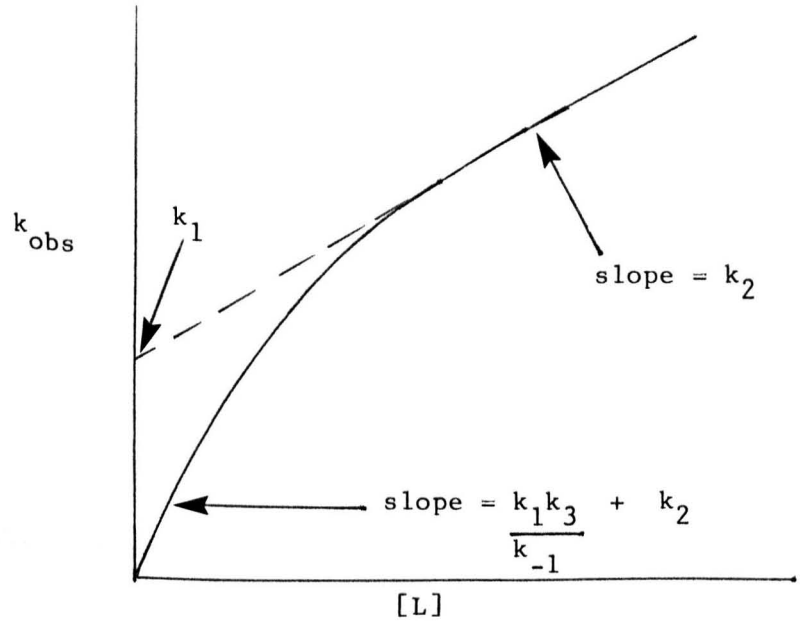

Fig 1.7

The substitution reactions of complexes containing polydentate unsaturated ligands, to be discussed now, provide examples of most, if not all, of these possibilities.

Tricarbonyl complexes of iron bound to 1,3-diene ligands have been studied and found to undergo substitution reactions with group V ligands. Of the two types of diene systems studied, conjugated 1,3-alkadiene and conjugated 1,3-heterodiene, the latter is the more labile. Both systems adopt square pyramidal geometry[55], in contrast to the trigonal bipyramidal structures adopted by $Fe(CO)_4L$ and $Fe(CO)_3L_2$ type complexes. Heterodiene systems studied are

(i)[56]

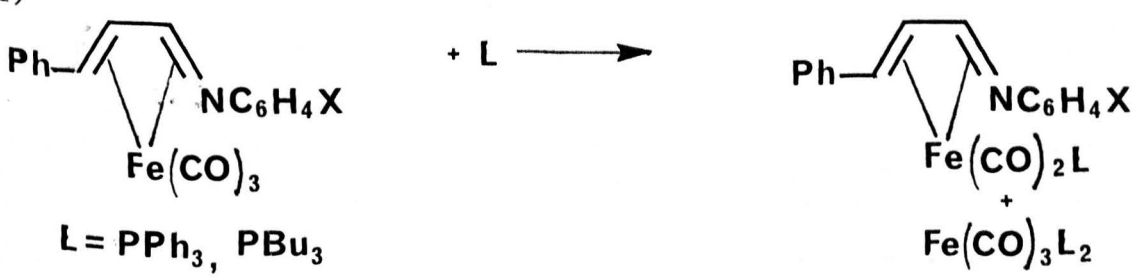

(ii)[57]

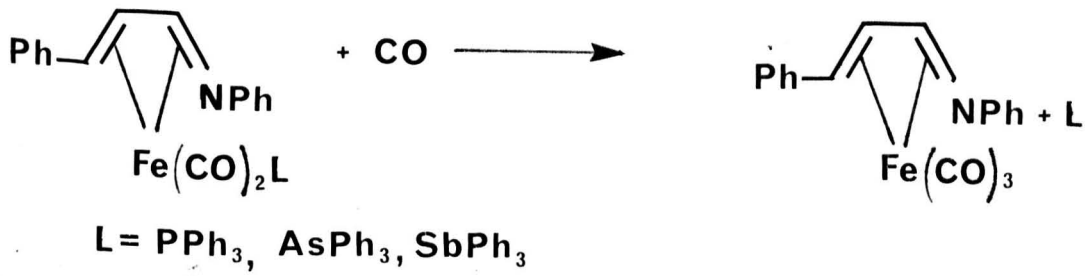

L= PPh_3, $AsPh_3$, $SbPh_3$

(iii)[58]

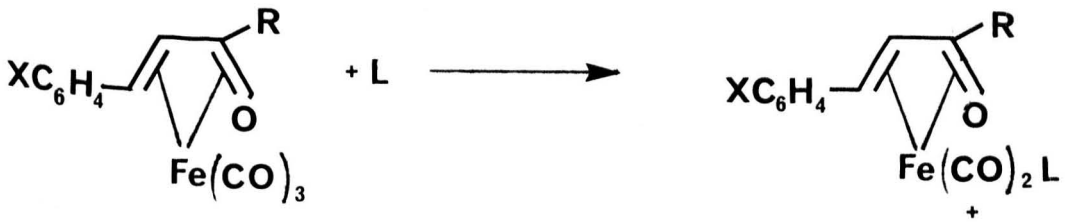

L= PPh_3, $SbPh_3$

The experimental rate law is given by

$$R = \frac{k_A[S][L]}{1 + k_B[L]} + k_C[S][L] \qquad (1.28)$$

with plots of k_{obs} against ligand concentration curved but non-limiting (Figure 1.8), indicating two competing pathways.

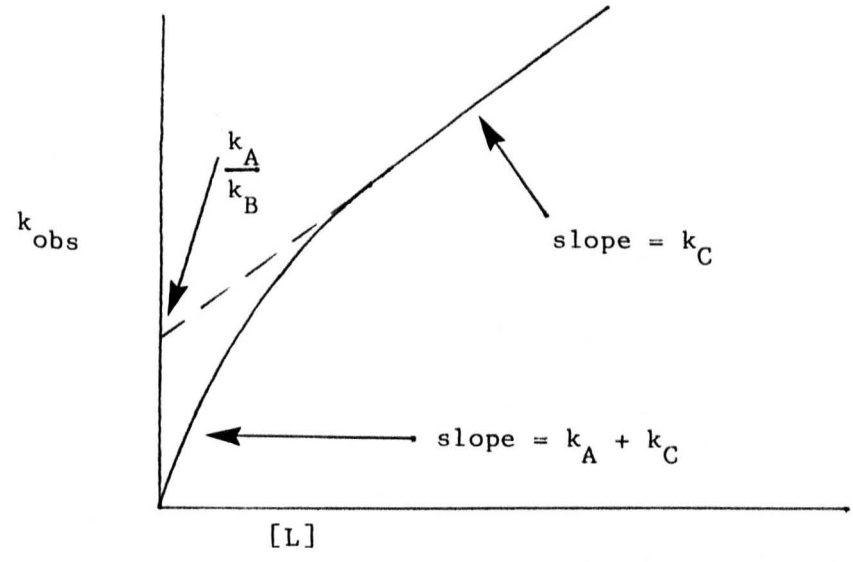

Fig. 1.8

Under the conditions $1 >> k_B[L]$ (at low concentration of L) equation 1.28 reduces to

$$R = (k_A + k_C)[S][L] \qquad (1.29) \quad (\text{slope}, k_A + k_C)$$

If, $k_B[L] >> 1$ (at high concentration of L) equation 1.28 reduces to

$$R = \frac{k_A[S]}{k_B} + k_C[S][L] \qquad (1.30) (\text{intercept}, \frac{k_A}{k_B}; \text{slope}, k_C)$$

The overall mechanisms (Schemes 1.14A and 1.14B) have been rationalised in terms of competing ring-opening, and I_d dechelation of the alkene bond in (i) and (ii), and the ketonic bond in (iii). Steady state treatment of the σ-bonded intermediates (A) and (A') (Scheme 1.14A), and the π^2-coordinated intermediates (B) and (B') (Scheme 1.14B) yields the rate law

$$R = \frac{k_1 k_3[S][L]}{k_{-1} + k_3[L]} + k_2[S][L] \qquad (1.31)$$

which is the same as equation 1.28 where $k_A = k_1 k_3 / k_{-1}$, $k_B = k_3 / k_{-1}$ and $k_C = k_2$. Intermediates (B) and (B') may be observed spectroscopically[59] and in some cases isolated[60].

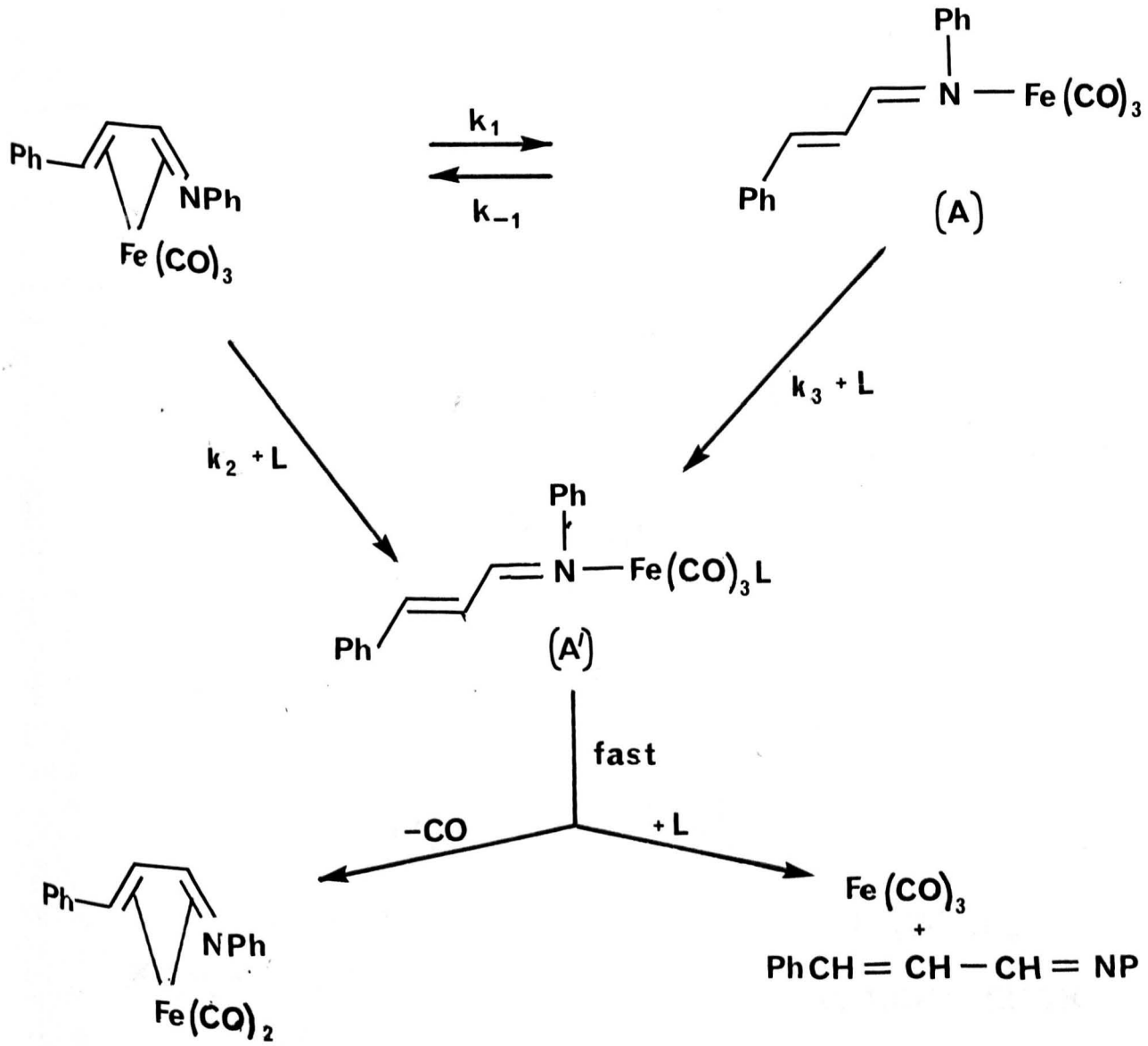
Ph
NPh
Fe(CO)3
k1
k−1
Ph
N — Fe(CO)3
Ph
(A)
k3 + L
k2 + L
Ph
N — Fe(CO)3L
Ph
(A')
fast
−CO
+L
Ph
NPh
Fe(CO)2
Fe(CO)3
+
PhCH = CH — CH = NP

Scheme 1.14 A

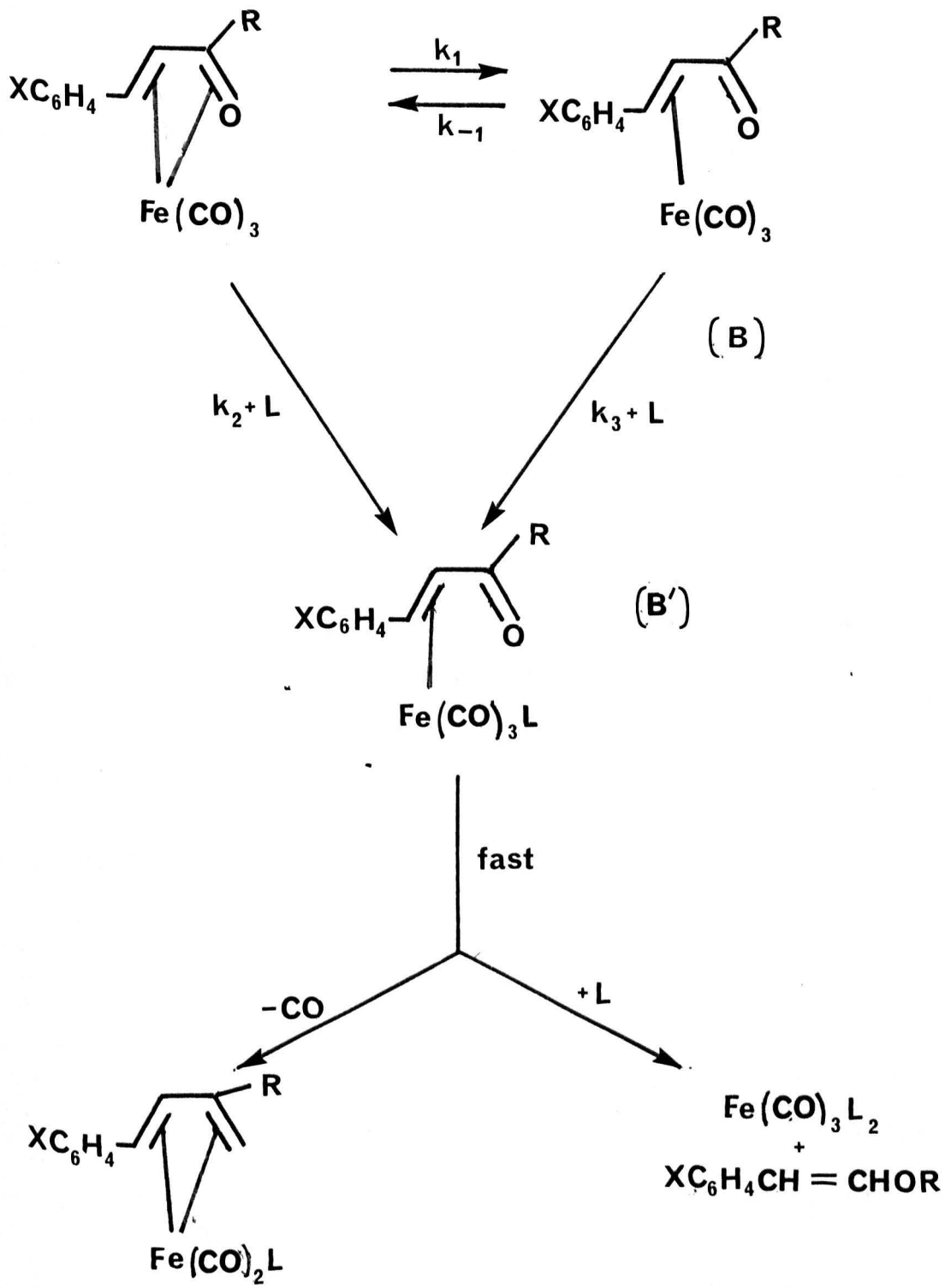
R
XC6H4
O
Fe(CO)3
k1
k−1
(B)
k2 + L
k3 + L
(B′)
Fe(CO)3L
fast
−CO
+L
Fe(CO)2L
Fe(CO)3L2
+
XC6H4CH = CHOR

Scheme 1.14B

Reaction (ii) proceeds to equilibrium, but the approach can be accommodated by rate law 1.28, although in this example the I_d pathway governed by k_2 is very small (0.05%) compared to the ring-opening pathway. In reaction (iii), for $L=SbPh_3$, only the dissociative ring-opening pathway ($k_2=0$) appears to be operating. Substituent (X) effects show that electron-donating groups increase the value of k_1.

Substitution of the less labile (1,3-alkadiene)$Fe(CO)_3$ has been studied kinetically

(iv)[61] $(\eta^4\text{-1-4-cot})Fe(CO)_3 + 2L \rightarrow cot + Fe(CO)_3L_2$

cot = 1,3,5,7-cyclooctatetraene

2L = PPh_3, PPh_2Et, PBu_3 L_2 = diphos

(v)[62] $(\eta^4\text{-1,3-cod})Fe(CO)_3 + 2PPh_3 \rightarrow cod + Fe(CO)_3(PPh_3)_2$

cod = 1,3-cyclooctadiene

(vi)[63] $(\eta^4\text{-1,4-chpd})Fe(CO)(\eta^4\text{-1,3-chd}) + 2L \longrightarrow$

$chpd + (\eta^4\text{-1,3chd})Fe(CO)L_2$

chpd = 1,4-cycloheptadiene L = PPh_3, CO

chd = 1,3-cyclohexadiene

(vii)[62] $(\eta^4\text{-1-4-chpt})Fe(CO)_3 + PPh_3 \rightarrow (\eta^4\text{-1-4-chpt})Fe(CO)_2PPh_3$

$+ Fe(CO)_3(PPh_3)_2$

chpt = 1,3,5-cycloheptatriene

(viii)[63] $(\eta^4\text{-1,3-chd})Fe(CO)_3 + PPh_3 \longrightarrow$

$(\eta^4\text{-1,3-chd})Fe(CO)_2PPh_3 + CO$

Plots of k_{obs} against ligand concentration for reactions (iv) and (v) are linear with zero intercepts, with the rate law being

$$R = k_B[S][L] \qquad (1.32)$$

Activation parameters (Table 1.2) reflecting the associative nature of reaction (iv) have led to a proposed I_d mechanism. However the favoured mechanism for reaction (v) involves dissociative ring-opening to form a η^2-coordinated intermediate (Scheme 1.15), as the activation entropy for this reaction is somewhat less negative than that for reaction (iv).

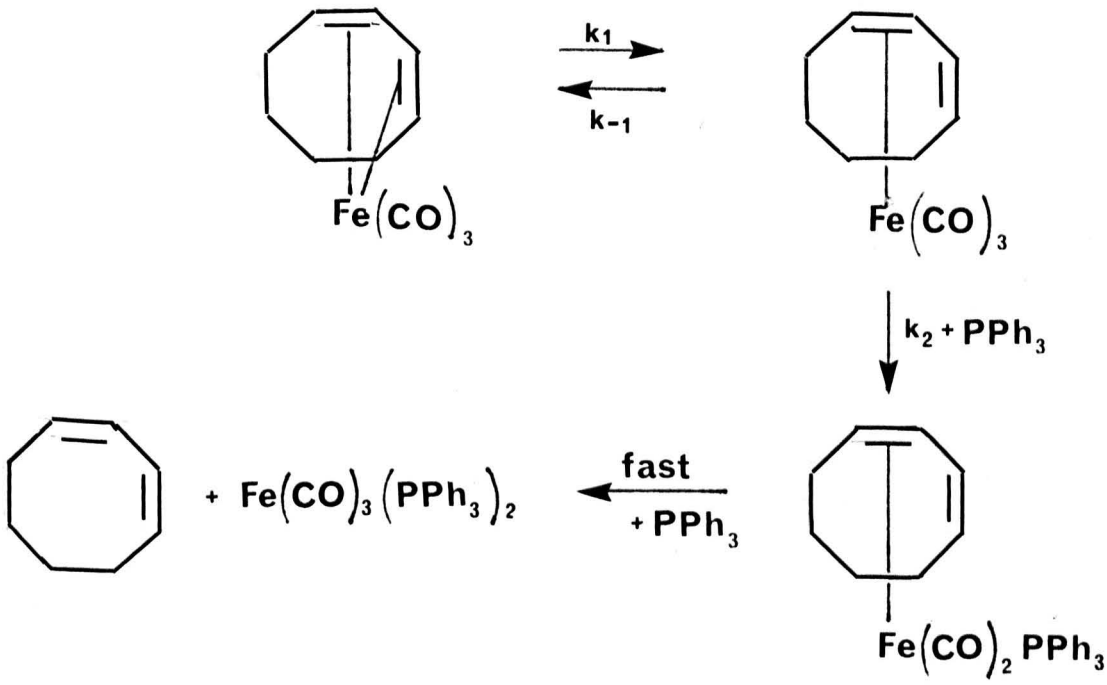

Scheme 1.15

This problem of I_d versus ring-opening mechanism occurs in reaction (vi) with plots of k_{obs} against ligand concentration linear with a non-zero intercept, giving an experimental rate law

$$R = k_1[S] + k_2[S][L] \qquad (1.33)$$

The bimolecular term may again be related to initial ring-opening, and the intercept, in view of the associated positive entropy involves rate determining CO dissociation to give (η^4-chpt)$Fe(CO)_2PPh_3$. The rate of reaction (viii) is independent of ligand concentration, the rate law being

$$R = k_A[\eta^4\text{-1,3-chd})Fe(CO)_3] \qquad (1.34)$$

Positive entropies of activation (Table 1.2) reflect the dissociative nature of the reaction and support a mechanism which involves rate determining loss of CO.

Diene lability in these complexes is in the order chd < chpt < 1,3 cod < cot and is primarily enthalpy controlled. The mechanism of the reaction may depend to some extent on the relative bond enthalpy contributions; the estimated diene-Fe bond enthalpy is 184 kJ mol^{-1} [42] compared to the Fe-CO bond enthalpy of 116 kJ mol^{-1}. Enhanced reactivity towards loss of diene from the tricarbonyl complex may result from steric factors, as the order of lability parallels the order of size of the complexed diene.

Diene exchange reactions of (η^4-diene)$Fe(CO)_3$ complexes have been studied kinetically

(ix)[64] (η^4-$MeCH{=}CH{-}CH{=}CH{-}CO_2Me$)$Fe(CO)_3$ + $MeO_2C{-}CH{=}CH{-}CH{=}CH{-}CO_2Me$ ⟶

(η^4-$MeO_2C{-}CH{=}CH{-}CH{=}CH{-}CO_2Me$)$Fe(CO)_3$ + $MeCH{=}CH{-}CH{=}CH{-}CO_2Me$

(x)[41] 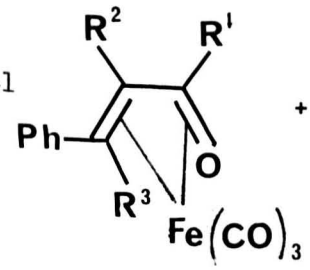

+ 1,3-diene → (η^4-1,3-diene)$Fe(CO)_3$ + enone

R_1 = H,Me,Ph R_2 = H R_3 = H,Me

1,3-diene = cycloheptatriene, cyloheptadiene

cyclohexadiene, cyclooctadiene

Reaction (ix) gives a bimolecular rate law of the type

$$R = k_B[S][L] \quad (1.35)$$

and the authors attribute this to an I_d mechanism. Reaction (x) is more complicated, plots of k_{obs} against ligand concentration conform to the following non-limiting rate law.

$$R = \frac{k_A[S][L]}{1 + k_B[L]} + k_C[S][L] \quad (1.36)$$

The experimental results have been interpreted using competing I_d and dissociative ring-opening pathways shown in Scheme 1.16. Application of the steady state approximation to intermediates (A) and (B) yields the simplified mechanistic rate equation

$$R = k_{A'}[S][L] + \frac{k_{B'}[S][L]}{k_{C'} + k_{D'}[L]} \quad (1.37)$$

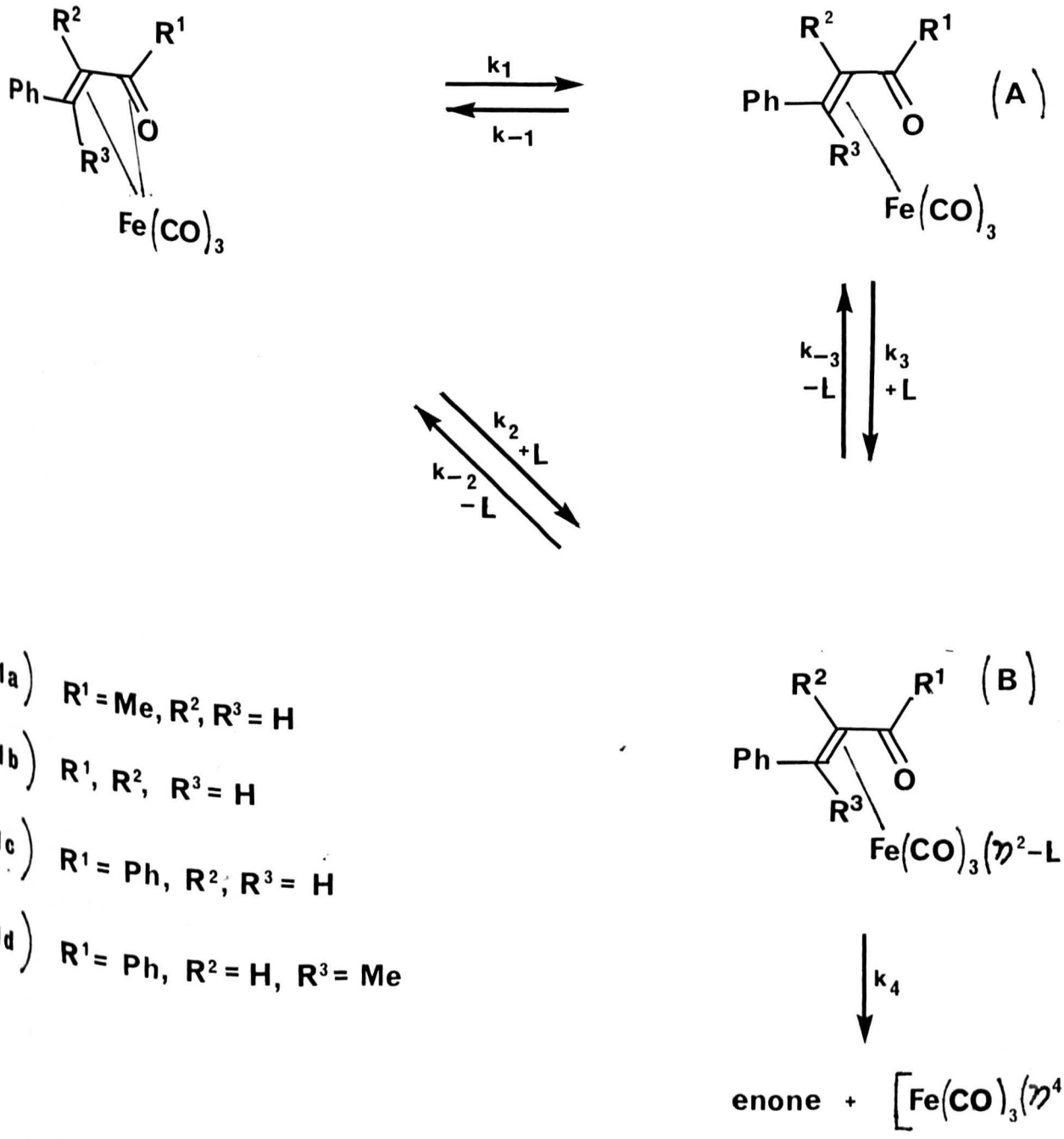
R2
R1
Ph
O
R3
Fe(CO)3
k1
k−1
(A)
k−3
−L
k3
+L
k2
+L
k−2
−L
(1a) R1 = Me, R2, R3 = H
(1b) R1, R2, R3 = H
(1c) R1 = Ph, R2, R3 = H
(1d) R1 = Ph, R2 = H, R3 = Me
(B)
Fe(CO)3(η2−L)
k4
enone + [Fe(CO)3(η4−L)]

Scheme 1.16

where $k_{A'} = k_4k_2/(k_{-2} + k_4)$

$k_{B'} = k_4(k_1k_3k_2 + k_1k_3k_4 - k_2k_{-3}k_{-1}/(k_{-2} + k_4)$

$k_{C'} = k_{-2}k_{-1} + k_{-3}k_{-1} + k_4k_{-1}$

$k_{D'} = k_{-2}k_3 + k_4k_3$

In view of the complexity of the rate law, it is difficult to draw conclusions relating to entering and leaving group effects. However the fit of the theoretical curve of k_{obs} against ligand concentration to that of the experimental results provides some confirmation as to the validity of the mechanism. Similar plots of k_{obs} against ligand concentration are obtained for the reaction,

(η^4-enone)$Fe(CO)_2L$ + chd → (η^4-chd)$Fe(CO)_2L$ + enone

L = PPh_3, PPh_2Me, $P(OPh)_3$

enone = trans-4-phenyl-3-buten-2-one

or trans-3-phenylpropenal

with the mechanism interpreted in the same way[65]. The decreased lability of these complexes compared to the tricarbonyl complexes probably results from the increased electron donor ability of the phosphine or phosphite, which enhances back donation to the enone and carbonyl ligands. Crystal structure determinations and infrared spectroscopy demonstrate the shortening of the M-CO bond lengths, consistent with increased back donation.

Diene substitution and exchange reactions of (η^4-diene)$M(CO)_4$ complexes which have been studied kinetically are listed below

(xi)[66] (η^4-1,4-nbd)$M(CO)_4$ + 2L ⟶ $L_2M(CO)_4$ + nbd

nbd = 1,4-norbornadiene M = Cr,Mo,W

(xii)[67,68] (η^4-1,5-cod)$Mo(CO)_4$ + 2L ⟶ $L_2Mo(CO)_4$ + cod

cod = 1,5-cyclooctadiene L_2 = diphos,bipy,phen

2L = PPh_3,$AsPh_3$,$SbPh_3$,PBu_3

(xiii)[69] (η^4-butadiene)$Cr(CO)_4$ + $2P(OMe)_3$ ⟶ $[P(OMe)_3]_2Cr(CO)_4$ + butadiene

(xiv)[70-72]

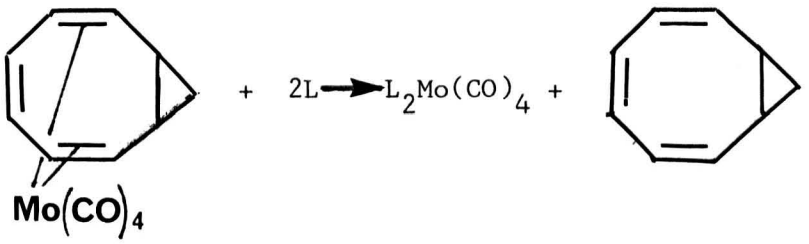

2L = PPh_3,$SbPh_3$,$P(OPh)_3$,$P(OMe)_3$

L_2 = diphos,N,N,N',N'-tetramethylethylenediamine

N,N,N',N'-tetramethyl-1,3-diaminopropane

Reaction (xi) proceeds by the experimental rate law

$$R = k_B[S][L] \qquad (1.38)$$

any may thus be interpreted in terms of either an I_d ring-opening or a dissociative ring-opening in which $k_{-1} >> k_2[L]$. In one case, the substitution of (η^4-nbd)$Cr(CO)_4$ with phosphines, a limiting rate at high concentration of ligand is evident (see ref. 41 of 73), and therefore a dissociative ring-opening seems more likely to be correct.

The order of reactivity of metals in this reaction (Mo>>W>Cr) does not exhibit the same trend as bond enthalpy contributions, Mo-nbd(187 kJ mol^{-1})>Cr-nbd(80)[74], but does parallel behaviour in other substitution reactions involving these metals.

The experimental rate law for reactions (xii) and (xiii) is

$$R = k_A[S] + k_B[S][L] \qquad (1.39)$$

with the butadiene chromium complex showing the greater lability. Hoffmann and Elian[26] have demonstrated the preference of a $Cr(CO)_4$ fragment for a non-conjugated diene system over the conjugated diene system, which accounts for the greater lability of the latter. The two different mechanisms consistent with this rate law are

(a) Competing I_d and dissociative ring-opening, with the limiting condition $k_3[L] >> k_{-1}$ applied to the dissociative pathway (Scheme 1.13)

(b) In the rate law $R = k_A[S] + k_B[S][L]$ (equation 1.39), if the k_B term is interpreted as dissociative ring-opening as in the reaction of (η^4-nbd)$W(CO)_4$ with phosphines, then the intercept corresponds to a pathway other than ring-opening ie. dissociation to $M(CO)_4$, Scheme 1.17.

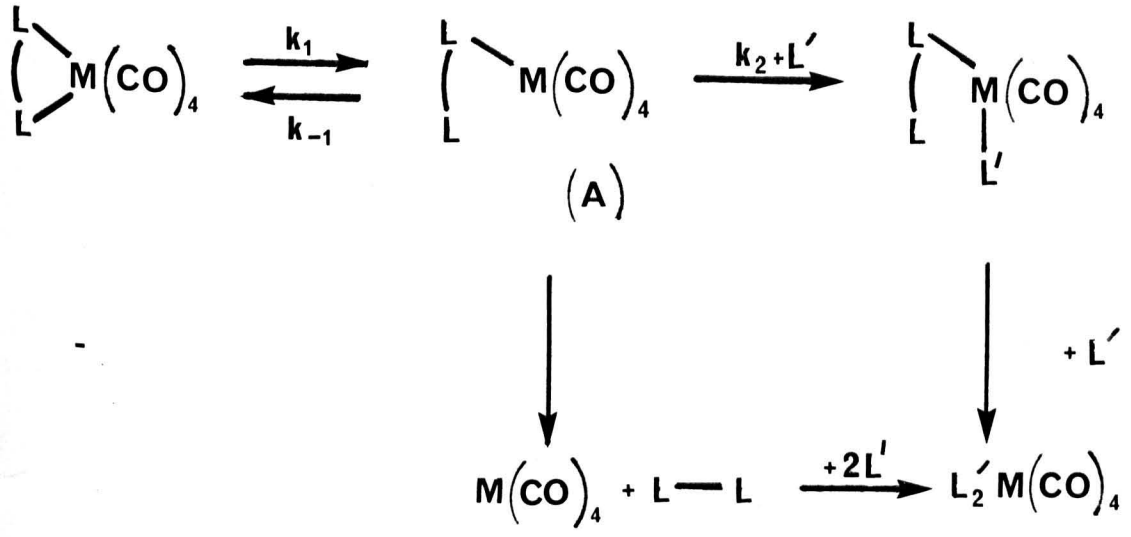

Scheme 1.17

Assuming a steady state concentration of the intermediate (A), the rate law is

$$R = \frac{k_1k_3[S] + k_1k_2[S][L']}{k_{-1} + k_3 + k_2[L']} \qquad (1.40)$$

Under the conditions $k_{-1} >> k_3 + k_2[L']$ the equation reduces to

$$R = \frac{k_1k_3[S]}{k_{-1}} + \frac{k_1k_2[S][L']}{k_{-1}} \qquad (1.41)$$

which is the same as equation 1.39 where $k_A = k_1k_3/k_{-1}$ and $k_B = k_1k_2/k_{-1}$. Large positive activation entropies (Table 1.3) associated with the intercept are consistent with the dissociative pathway.

Reaction (xiv) although not quantitatively studied is thought to proceed by a ring-opening pathway.

(Butadiene)$Cr(CO)_4$ also undergoes diene exchange [69]

(η^4-butadiene)$Cr(CO)_4$ + diene $\rightarrow$ (η^4-diene)$Cr(CO)_4$ + butadiene

diene = 1,4-norbornadiene, 1,5-cyclooctadiene

with a rate law

$$R = k_A[(\text{butadiene})Cr(CO)_4] \qquad (42)$$

The k_{obs} value is the same as the intercept value obtained in reaction (xiii).

On the basis of the dissociative ring-opening pathway, complete ligand loss to form $Cr(CO)_4$ ($k_2 = 0$) is consistent with the lower nucleophilicity of diene compared to $P(OMe)_3$. The existence of the coordinatively unsaturated $Cr(CO)_4$ species has been demonstrated by flash photolytic studies of $Cr(CO)_6$ [75].

1.5.4 η^5-Cyclopentadienyl Metal Complexes

Some systems studied kinetically are shown below. It may be noted that in all cases, the product is a result of loss of ligand other than cyclopentadienyl, though the cyclopentadienyl may not play a passive role in the reaction.

(xv) [76] (η^5-C_5H_5)$V(CO)_4$ + L $\rightarrow$ (η^5-C_5H_5)$V(CO)_3L$ + CO

L = PBu_3, $P(OBu)_3$

(xvi)[77,78] $(\eta^5\text{-}C_5H_5)Mn(CO)_2(\text{alkene}) + L \longrightarrow (\eta^5\text{-}C_5H_5)Mn(CO)_2L + \text{alkene}$

L = phosphines, amines.

alkene = cyclic and acyclic hydrocarbons

(xvii)[79] $(\eta^5\text{-}C_5H_5)Mn(CO)_2SR_2 + L \rightarrow (\eta^5\text{-}C_5H_5)Mn(CO)_2L + SR_2$

L = phosphines, phosphites

R = Me,Et,nPr,nBu,Ph,PhMe

(xviii)[80] $(\eta^5\text{-}C_5H_5)M(CO)_2 + L \rightarrow (\eta^5\text{-}C_5H_5)M(CO)L + CO$

L = phosphines, phosphites M = Co, Rh, Ir

Reactions (xv)-(xvii) show no rate dependence on ligand concentration and proceed by a rate determining loss of the respective leaving groups, as reflected by the positive entropies of activation (Tables 1.3 and 1.4). Reaction (xviii) however, shows a linear dependence on ligand concentration with the rate law

$$R = k_B[(\eta^5\text{-}C_5H_5)M(CO)_2][L] \qquad (1.43)$$

Activation entropies (Table 1.4) are strongly negative for the reaction, and in accordance with this an I_d slippage mechanism is proposed (Scheme 1.18), though a mechanism with a discrete η^3-intermediate cannot be excluded.

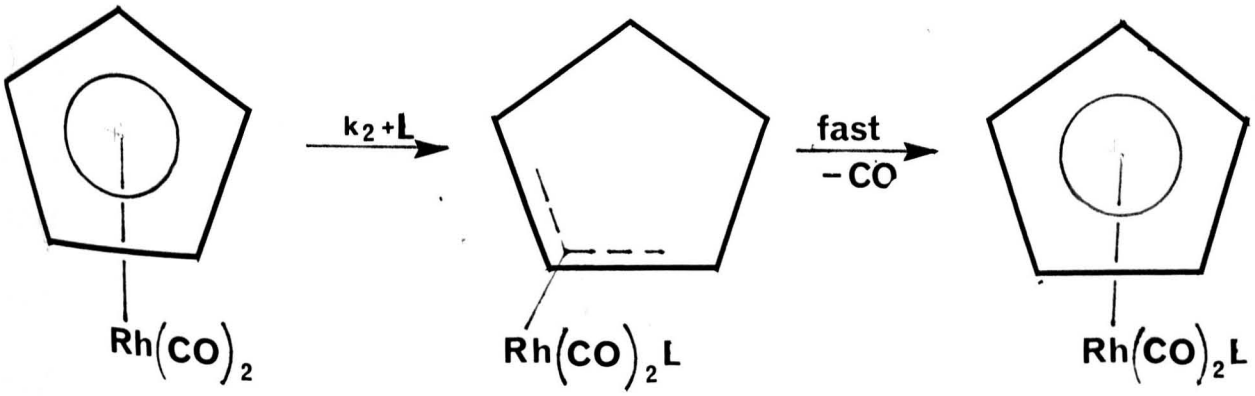

Scheme 1.18

The order of metal reactivity is Co<Rh>Ir.

A recent kinetic study of the ligand displacement reactions of (η^5-N-heterocycle)$Mn(CO)_3$ (N-heterocycle = pyrrolyl, indolyl) with phosphines and phosphites[81] shows the reaction to proceed via rate law (1.43). However, a large rate enhancement is observed relative to the substitutionally inert (η^5-C_5H_5)$Mn(CO)_3$. The reaction is interpreted in terms of an I_d ring-slippage mechanism, with the large rate enhancement arising from the greater localisation of electron density on the more electronegative nitrogen atom compared to carbon in the allylic transition states of the pyrrolyl and cyclopentadienyl ligands.

The substitution reaction

(xix)[82] $(\eta^5\text{-ring})_2M(CO)_2 + L \longrightarrow (\eta^5\text{-ring})_2M(CO)L + CO$

L = phosphines, phosphites M = Ti, Zr, Hf

(η^5-ring) = C_5H_5, $C_5(Me)_5$, indenyl

For M=Ti, plots of k_{obs} against [L] are curved, and limiting at high concentration of [L]. The mechanism used to explain the results is

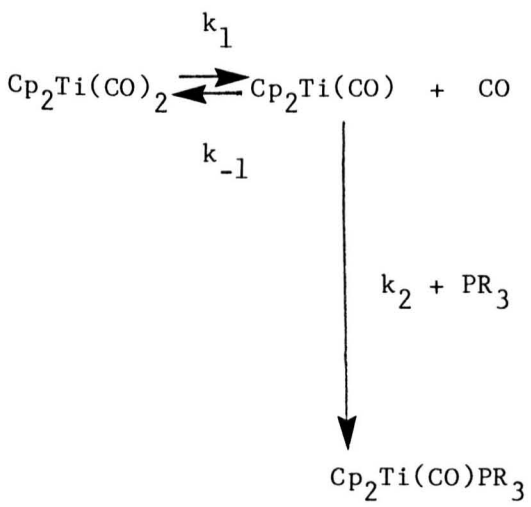

Scheme 1.19

Assuming that the steady state approximation applies to the intermediate $Cp_2Ti(CO)$, then the rate law is

$$R = \frac{k_1 k_2 [Cp_2Ti(CO)_2][PR_3]}{k_{-1}[CO] + k_2[PR_3]} \qquad (1.44)$$

At low concentrations of PR_3, such that $k_{-1}(CO) >> k_2[PR_3]$ the equation reduces to

$$R = \frac{k_1 k_2 [Cp_2Ti(CO)_2][PR_3]}{k_{-1}[CO]} \qquad (1.45)$$

and a linear dependence on $[PR_3]$ is found. However at concentrations above 0.5M, rate constants level off, hence under these conditions $k_2[PR_3] >> k_{-1}[CO]$ and the equation (1.44) reduces to

$$R = k_1[Cp_2Ti(CO)_2] \qquad (1.46)$$

and shows no dependence on concentration of PR_3.

The zirconium and hafnium complexes give a second order experimental rate expression

$$R = k_B[Cp_2M(CO)_2][PR_3] \qquad (1.47)$$

An I_d associative mechanism involving concerted ring slippage of one of the cyclopentadienyl rings from $\eta^5 \rightarrow \eta^3$ coordination is thought to be operative. Loss of CO is then accompanied by re-chelation of the slipped ring.

Reactions receiving much attention at present are those based on the indenyl system

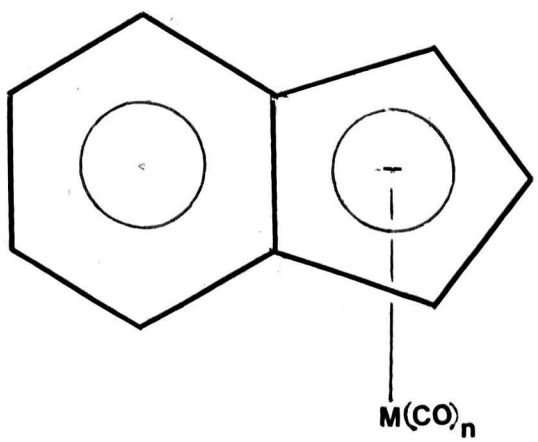

Fig 1.9

Substitution reactions of these η^5 type complexes proceed at up to 10^8 times the rate of the corresponding cyclopentadienyl systems.

In contrast to the inertness of $CpMn(CO)_3$, reaction of $(\eta^5\text{-}C_9H_7)Mn(CO)_3$ with trivalent phosphorus ligands[83] yields a rate law of the type (1.47). An I_d slippage mechanism (Scheme 1.20) has been proposed, in view of the rate law and corresponding negative activation entropies.

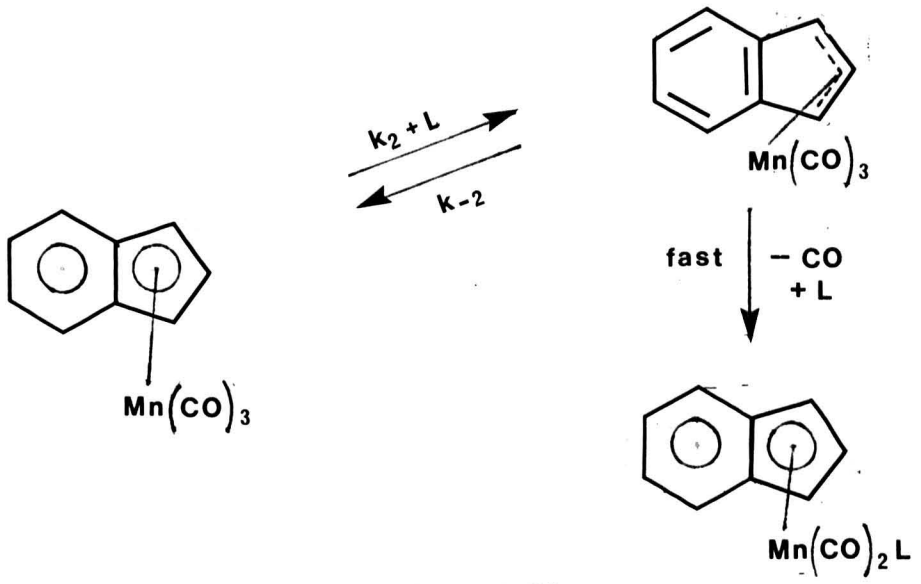

Scheme 1.20

The rate enhancement, known as the "indenyl effect"[83,84], can be attributed to the increased stability of the transition state in the indenyl system relative to the cyclopentadienyl system, resulting from aromatisation of the benzene ring[85,86]. Alternatively the rate enchancement may arise from the resonance stabilisation of the η^3-allyl transition state. An alternative mechanism also consistent with the kinetics, and noted by the authors, involves reversible formation of a discrete coordinatively unsaturated η^3-intermediate. Activation parameters for the reaction are given in Table 1.4. Note that the activation entropies for reaction with PBu_3 and $P(OEt)_3$ are similar. In contrast, the activation entropies for the reaction of these ligands with $(\eta^5$-pyrrolyl$)Mn(CO)_3$ are numerically widely different.

Thus, these values may therefore indicate that reaction of (η^5-pyrrolyl)$Mn(CO)_3$ with the more nucleophilic PBu_3 proceeds via an I_d pathway, whereas reaction with $P(OEt)_3$ proceeds via initial slippage followed by rate determining attack at the η^3-intermediate.

1.5.5 η^6-Polyene and Arene Metal Complexes

Kinetic studies of the displacement of η^6-polyenes and η^6-arenes from η^6-coordinated metal complexes are listed below

(xx)[87] (η^6-chpt)$M(CO)_3$ + 3L → fac-$M(CO)_3L_3$ + chpt

chpt = 1,3,5-cycloheptatriene M = Cr, Mo, W

L = $P(OMe)_3$

(xxi)[88,89] (η^6-polyene)$M(CO)_3$ + 3RCN → fac-$M(CO)_3(RCN)_3$ + polyene

polyene = 1,3,5-cycloheptatriene, C_6H_6, $C_6H_3(Me)_3$

M = Cr,Mo,W R = Me, C_6H_5

(xxii)[90,91] (η^6-polyene)$M(CO)_3$ + 3L → fac-$M(CO)_3L_3$ + polyene

polyene = C_6H_6, C_6H_5Me, o-, m-, p-$C_6H_4(Me)_2$, $C_6H_2(Me)_4$, $C_6H_3(Me)_3$, C_6Me_6, $C_6H_5NMe_2$

L = $P(OMe)_3$, PBu_3, PCl_2Ph, PCl_3 M = Mo

For M=W[92] polyene = C_6H_6, C_6H_5Me, $C_6H_3(Me)_3$, $C_6H_5NMe_2$, p-C_6H_5OMe

(xxiii)[93] $R_3B_3N_3R'_3Cr(CO)_3$ + 3L → fac-$Cr(CO)_3L_3$ + $R_3B_3N_3R'_3$

L = $P(OMe)_3$, $P(OEt)_3$, $P(OPh)_3$ R = alkyl

(xxiv)[94] $[(\eta^5\text{-}C_5H_5)Ru(\eta^6\text{-polyene})]^+ + 3MeCN \longrightarrow [(\eta^5\text{-}C_5H_5)Ru(MeCN)_3]^+ + \text{polyene}$

polyene = naphthalene, pyrene, chrysene, anthracene, azulene

(xxv)[95] $(\eta^6\text{-polyene})Cr(CO)_2CX + 3L \rightarrow fac\text{-}Cr(CO)_2(CX)L_3 + \text{polyene}$

polyene = C_6H_5Me, $C_6H_5NMe_2$, $C_6H_5CO_2Me$, o-, p-$C_6H_4(Me)_2$, p-$C_6H_4(CO_2Me)_2$, p-$C_6H_4(OCH_3)_2$

X = S, Se, Te

Reactions (xx), (xxii) and (xxiii) give linear plots of k_{obs} against [L] and obey the experimental rate law

$$R = k_B[S][L] \qquad (1.48)$$

Activation parameters reflect the associative nature of the reactions, which have been interpreted as proceeding via the I_d slippage mechanism as shown in (Scheme 1.21)[96], though again these reactions could be written as involving discrete $(\eta^4\text{-polyene})M(CO)_3$ or $(\eta^4\text{-polyene})M(CO)_3L$ intermediates, ie a dissociative slippage.

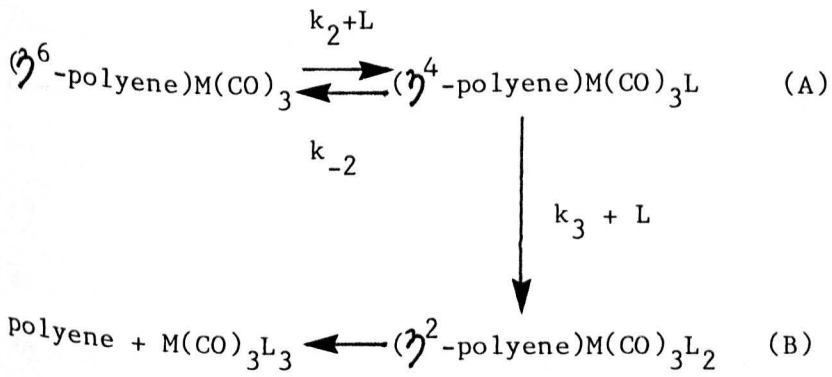

Scheme 1.21

Application of the steady state approximation to the intermediate (A) gives the mechanistic rate law

$$R = \frac{k_2 k_3 [S][L]^2}{k_{-2} + k_3[L]} \qquad (1.49)$$

Applying the limiting assumption $k_3[L] >> k_{-2}$, used in the $(diene)M(CO)_4$ case, equation (1.49) reduces to

$$R = k_2[S][L] \qquad (1.50)$$

Complexes analogous to intermediate (A) have been isolated from reactions of (η^6-cyclooctatetraene)- and (η^6-cyclooctatriene)$Mo(CO)_3$ with CO as (η^4-1,5-diene)$Mo(CO)_4$ [97]. Similar complexes have been obtained from the reactions of (bicyclo[6,1,0]nona-2,4,6-polyene)$Mo(CO)_3$ with CO and $P(OPh)_3$ giving (η^4-1,5-diene)$Mo(CO)_4$ and (η^4-1,5-diene)$Mo(CO)_3P(OPh)_3$ respectively[71,98,99].

For reaction (xxi) (M=Mo, L =C_6H_5CN and M=Cr,Mo,W, L=MeCN) a second order ligand dependence is found, though for M=Cr and L=MeCN, the quoted results appear to be first order in ligand concentration. This reaction may perhaps, therefore, represent a situation so far not observed in $(diene)M(CO)_4$ complexes where $k_{-2} >> k_3[L]$ perhaps as a result of the lower nucleophilicity of MeCN compared to $P(OR)_3$[88,89]. The reaction of (η^6-chpt)$W(CO)_3$ with C_6H_5CN is intermediate in behaviour, apparently with $k_{-2} \simeq k_3$; at low concentration of L a second order dependence on [L] is found, which changes to first order at high concentration of L. Strictly first order ligand dependence is found for the reaction of (η^6-chpt)$Cr(CO)_3$ with C_6H_5CN.

An alternative mechanism proposed by the authors to account for the squared dependence, involves a rapid pre-equilibrium association between the complex and nitrile ligand followed by rate determining addition of a second molecule of nitrile[88].

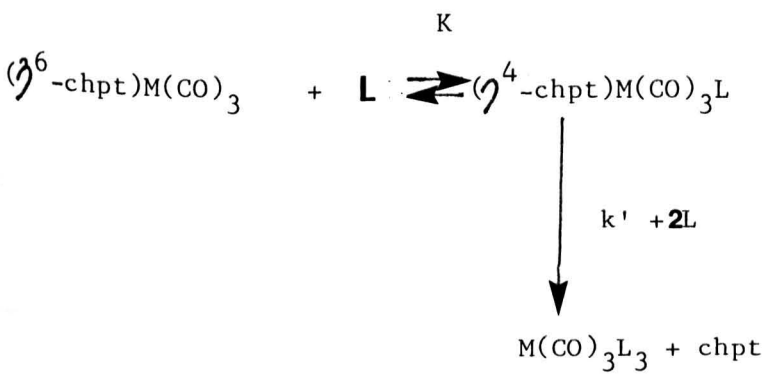

Scheme 1.22

for which the rate equation is

$$R = \frac{k'K[L]^2}{1 + K[L]} \qquad (1.51)$$

However, the results imply a K value of >> 2 mol^{-1} dm^3, meaning that the intermediate $(\eta^4\text{-chpt})M(CO)_3L$ predominates. None is observed spectroscopically.

The reaction of $(\eta^6\text{-naphthalene})Cr(CO)_3$ with MeCN also shows a strict first order dependence on [L] over the concentration range used[100], as does the displacement of $C_7H_7^+$ from $[(\eta^6\text{-}C_7H_7)M(CO)_3]^+$ by MeCN[101].

Some general points regarding ground state bond enthalpies in terms of reactivity may be noted:

(i) The lability of polyenes in these complexes exhibits the same ordering as the calorimetrically determined bond enthalpy contributions;
$Cr\text{-}B_3N_3Et_6$(104 kJ mol^{-1}) < Cr-chpt(150) < $Cr\text{-}C_6H_6$(177) $Cr\text{-}C_6H_5Me$(173) < Cr_6Me_6(202)[74,102]. However, more recent bond enthalpy calculations based on iodination studies have shown the Cr-chpt bond to be stronger than the $Cr\text{-}C_6H_6$ and $Cr\text{-}C_6H_5Me$ bonds[103].

(ii) The lability in terms of metal (Mo>>W>Cr) does not reflect metal-polyene bond enthalpy contributions;
$W\text{-}C_6H_3(Me)_3$(334 kJ mol^{-1}) > $Mo\text{-}C_6H_3(Me)_3$(279) > $Cr\text{-}C_6H_3(Me)_3$(191)[74] and maybe an indication that molybdenum and tungsten complexes can react via a lower energy concerted pathway inaccessible to chromium complex.

The more recently studied reactions (xxiv) and (xxv) show a linear dependence of rate on concentration of ligand, giving a rate law of the type 1.48. Both reactions are interpreted in terms of a dissociative slippage mechanism

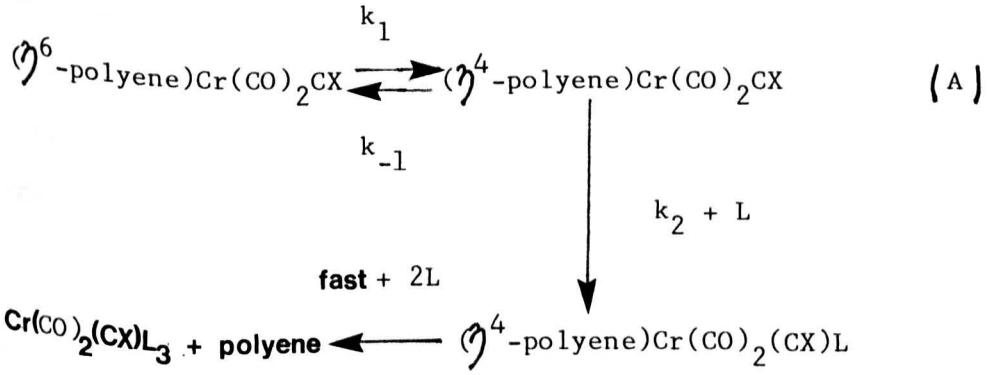

Scheme 1.23

On the assumption that $k_{-1} >> k_2[L]$ the rate equation is

$$R = \frac{k_1 k_2 [S][L]}{k_{-1}} \qquad (1.52)$$

Initial slippage to a discrete η^4-intermediate (as opposed to an associative I_d process) is considered more likely since nucleophilic attack at the metal in the η^6-complex would be energetically unfavourable due to the high electron density located about the metal atom[104]. It is again difficult to differentiate experimentally between this mechanism and the I_d slippage mechanism.

The polyene and chpt exchange reactions (xxvi) and (xxvii) have been kinetically investigated in solvents of differing polarity.

(xxvi)[105-107] $(\eta^6\text{-polyene})M(CO)_3 + \text{polyene}' \rightarrow (\eta^6\text{-polyene}')M(CO)_3 + \text{polyene}$

polyene = polyene' C_6H_6, C_6H_5Me, naphthalene

M = Cr, Mo, W

(xxvii)[105-107] $(\eta^6\text{-chpt})Cr(CO)_3 + \text{chpt}' \rightarrow (\eta^6\text{-chpt}')Cr(CO)_3 + \text{chpt}$

In hydrocarbon solvents both reactions proceed via a two term rate law, with one term common to both and the other dependent on the coordinated polyene. Reaction (xxvi), when the arene is naphthalene and reaction (xxvii) obey the rate equation

$$R = k_A[S] + k_B[S][\text{polyene}'] \qquad (1.53)$$

Exchange reactions involving the less labile monocyclic polyenes proceed via a two term rate law of which one term has a squared dependence on substrate concentration

$$R = k_A[S]^2 + k_B[S][\text{polyene}'] \qquad (1.54)$$

The $k_B[S][polyene']$ term common to both may be interpreted as either a dissociative or I_d slippage pathway. The $k_A[S]^2$ term has more recently been interpreted as a self catalysis of the exchange[108], and will be discussed in more detail in Chapter 2.

Polyene exchange reactions have also been studied in solvents of greater polarity such as cyclohexanone and tetrahydrofuran, and proceed at much faster rates which are independent of the concentration of entering polyene. Solvent assisted mechanisms have been proposed to account for these rate enhancements[109-112]

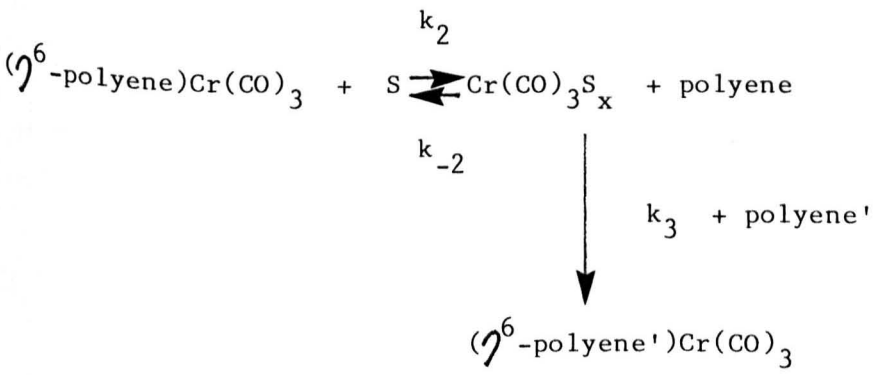

Scheme 1.24

Application of the steady state approximation to $Cr(CO)_3S_x$ leads to the rate equation

$$R = \frac{k_2k_3[(polyene)Cr(CO)_3][polyene'][S]}{k_{-2}[polyene] + k_3[polyene']} \qquad (1.55)$$

which if $k_3[polyene'] >> k_{-2}[polyene]$ reduces to

$$R = k_2[(polyene)Cr(CO)_3][S] \qquad (1.56)$$

The intermediate involving S_x has not been clearly defined in terms of the numerical value of x.

1.5.6 Conclusion

The difficulty in unambiguous assignment of mechanism is apparent, since different reaction pathways may obey the same experimental rate law. Further experiment and theoretical work in this area, directed towards the differentiation of these ambiguous pathways, may provide a more ordered structuring of organometallic reaction mechanisms of particular value in the design and development of transition metal complexes, both in stoichiometric and catalytic organic synthesis.

This is the subject of the work described in Chapters 2 and 3 of this thesis. Chapter 4 describes work arising from these studies and is concerned with the intramolecular rearrangement of six-coordinate octahedral complexes of Cr, Mo and W.

Table 1.1

Reaction	$\Delta H_A^{\ddagger}$	$\Delta S_A^{\ddagger}$	$\Delta H_B^{\ddagger}$	$\Delta S_B^{\ddagger}$
	($\Delta H^{\ddagger}$/ kJ mol^{-1}	$\Delta S^{\ddagger}$/ J K^{-1} mol^{-1})		
$(CO)_4Fe(styrene) + L \longrightarrow$				
$(CO)_4FeL$ + styrene				
L = PPh_3	137	108		
L = $AsPh_3$	127	88		
L = CO	121	54		
cis-$(CO)_4W(dmf)PEt_3 + P(OPr\text{-}i)_3 \longrightarrow$				
cis-$(CO)_4WP(OPr\text{-}i)_3PEt_3$ + dmf	109	39		
$(\eta^3\text{-}C_3H_4X)Fe(CO)_2NO + L \longrightarrow$				
$(\eta^3\text{-}C_3H_4X)Fe(CO)(NO)L + CO$				
X=H, L=PBu_3			28	-221
X=H, L=PPh_3			65	-229
X=H, L=$P(OEt)_3$			59	-117
X=2-Me, L=$P(OEt)_3$			57	-137
X=1-Ph, L=$P(OEt)_3$			48	-133
X=2-Cl, L=PPh_3			57	-134
X=2-Cl, L=PPh_2Et			45	-146
X=2-Br, L=$P(OEt)_3$			55	-113

Table 1.2

Reaction	$\Delta H_A^{\ddagger}$	$\Delta S_A^{\ddagger}$	$\Delta H_B^{\ddagger}$	$\Delta S_B^{\ddagger}$
$(\eta^3\text{-}C_3H_4X)Mn(CO)_4 + PPh_3 \longrightarrow$ $(\eta^3\text{-}C_3H_4)Mn(CO)_3PPh_3 + CO$				
X=H	112	40		
X=2-Me	98	11		
X=1-Ph	111	32		
$(\eta^4\text{-}PhCH{=}CH\text{-}CH{=}NC_6H_4X)Fe(CO)_3 + L \longrightarrow$ $(\eta^4\text{-}PhCH{=}CH\text{-}CH{=}NC_6H_4X)Fe(CO)_2L + CO$				
X=4NMe, L=PPh_3	26	5		
X=H, L=PPh_3	31	20	20	-16
$(\eta^4\text{-cot})Fe(CO)_3 + 2L \longrightarrow$ trans-$Fe(CO)_3L_2$ + cot				
L=PPh_3			48	-159
L_2=diphos			60	-126
$(\eta^4\text{-1,4-chpd})Fe(CO)(\eta^4\text{-1,3-chd}) + 2PPh_3 \longrightarrow$ $(\eta^4\text{-1,3-chd})Fe(CO)(PPh_3)_2$ + 1,4-chpd			**85**	**-12**
$(\eta^4\text{-1,3-cod})Fe(CO)_3 + 2PPh_3 \longrightarrow$ trans-$Fe(CO)_3PPh_2$ + 1,3-cod			87	- 33
$(\eta^4\text{-1,3-chd})Fe(CO)_3 + PPh_3 \longrightarrow$ $(\eta^4\text{-1,3-chd})Fe(CO)_2PPh_3 + CO$	176	70		

Table 1.3

Reaction	$\Delta H_A^{\ddagger}$	$\Delta S_A^{\ddagger}$	$\Delta H_B^{\ddagger}$	$\Delta S_B^{\ddagger}$
$(\eta^4\text{-cod})Mo(CO)_4 + 2L \longrightarrow$				
$L_2M(CO)_4 + cod$				
L_2=bpy	105	21	79	- 46
L_2=diphos	100	8	59	-105
L_2=phen	113	46	84	- 13
L=PPh_3	105	9	88	- 13
L=$AsPh_3$	105	9	71	- 71
L=$SbPh_3$	105	9	80	- 4
L=py	100	13	75	- 50
L=$PPhCl_2$	100	13	83	- 41
$(\eta^4\text{-nbd})Mo(CO)_4 + 2P(OPh)_3 \longrightarrow$				
$[P(OPh)_3]_2Mo(CO)_4$ + nbd			37	-151
$(\eta^5\text{-}C_5H_5)V(CO)_4 + PBu_3 \longrightarrow$				
$(\eta^5\text{-}C_5H_5)V(CO)_3PBu_3 + CO$	230	150		
$(\eta^5\text{-}C_5H_5)Mn(CO)_2SR_2 + PR_3 \longrightarrow$				
$(\eta^5\text{-}C_5H_5)Mn(CO)_2PR_3 + SR_2$				
R_2S = tetrahydrothiophene	154	92		
R=Me	146	75		
R=Et	147	79		
R=Bu	150	92		
R=benzyl	133	54		
R=Ph	133	79		

Table 1.4

Reaction	ΔH_A^*	ΔS_A^*	ΔH_B^*	ΔS_B^*
$(\eta^5\text{-}C_5H_5)Mn(CO)_2ol + PR_3 \longrightarrow$				
$(\eta^5\text{-}C_5H_5)Mn(CO)_2PR_3 + ol$				
ol=C_2H_4	144	79		
ol=cyclooctene	146	120		
ol=propylene	141	115		
ol=cyclopentene	140	115		
ol=1-pentene	139	102		
ol=cycloheptene	135	49		
$CpRh(CO)_2 + L \longrightarrow$				
$CpRh(CO)L + CO$				
L=$PPhEt_2$			63	- 84
L=$P(OBu)_3$			75	- 67
$(\eta^5\text{-}C_4H_4N)Mn(CO)_3 + L \longrightarrow$				
$(\eta^5\text{-}C_4H_4N)Mn(CO)_2L + CO$				
L=PBu_3			63	-156
L=$P(OEt)_3$			95	- 94
$(\eta^5\text{-}C_5H_5)_2M(CO)_2 + PPhMe_2 \longrightarrow$				
$(\eta^5\text{-}C_5H_5)_2M(CO)PPhMe_2 + CO$				
M=Ti	117	63		
M=Hf			64	-130

Table 1.4 continued

	$\Delta H_B^{\ddagger}$	$\Delta S_B^{\ddagger}$
$(\eta^5\text{-}C_9H_7)Mn(CO)_3 + L \longrightarrow$ $(\eta^5\text{-}C_9H_7)Mn(CO)_2L + CO$		
$L=PBu_3$	71	-151
$L=P(OEt)_3$	70	-156

Table 1.5

Reaction	$\Delta H_A^{\ddagger}$	$\Delta S_A^{\ddagger}$	$\Delta H_B^{\ddagger}$	$\Delta S_B^{\ddagger}$
$(\eta^6\text{-arene})Mo(CO)_3 + 3PR_3 \longrightarrow$				
$fac\text{-}(PR_3)_3Mo(CO)_3$ + arene				
arene = toluene, R=Cl			67	- 88
arene = p-xylene, R=Cl			63	-100
arene = mesitylene, R=Cl			71	- 84
arene = mesitylene, R=OMe			72	- 76
$(\eta^6\text{-arene})W(CO)_3 + 3P(OMe)_3 \longrightarrow$				
$[P(OMe)_3]_3W(CO)_3$ + arene				
arene = mesitylene			79	-107
arene = methyl benzoate			74	-102
$(\eta^6\text{-chpt})M(CO)_3 + 3P(OMe)_3 \longrightarrow$				
$[P(OMe)_3]_3M(CO)_3$ + chpt				
M=Cr			69	-105
M=Mo			41	-125
M=W			47	-121
$(R_3B_3N_3R'_3)Cr(CO)_3 + 3P(OMe)_3 \longrightarrow$				
$[P(OMe)_3]_3Cr(CO)_3 + R_3B_3N_3R'_3$				
R=Me, R'=Me			25	-171
R=Et, R'=Me			23	-173
R=Me, R'=Et			33	-158
R=Et, R'=Et			43	-140
R=Pr-n, R'=Me			20	-188
R=Me, R'=Pr-n			48	-113

Table 1.6

Reaction	$\Delta H_A^{\ddagger}$	$\Delta S_A^{\ddagger}$	$\Delta H_B^{\ddagger}$	$\Delta S_B^{\ddagger}$
$(\eta^6\text{-chpt})M(CO)_3 + 3RCN \longrightarrow$				
$fac\text{-}(RCN)_3M(CO)_3 + chpt$				
M=Cr, R=Me			90	- 63
M=Mo, R=Me			47	-129
M=W, R=Me			43	-179
M=Cr, R=Ph			75	-109
M=Mo, R=Ph			53	-109
$(\eta^6\text{-}C_6H_6)Cr(CO)_2CS + 3P(OMe)_3 \longrightarrow$				
$[P(OMe)_3]_3Cr(CO)_2CS + C_6H_6$			74	-117
$[(\eta^5\text{-}C_5Me_5)Ru(\eta^6\text{-anthracene})]^+ + 3MeCN \longrightarrow$				
$[(\eta^5\text{-}C_5Me_5)Ru(MeCN)_3]^+ + anthracene$		62	- 56	
$(\eta^6\text{-}C_6H_6)Cr(CO)_3 + {}^*C_6H_6 \longrightarrow$				
$(\eta^6\text{-}{}^*C_6H_6)Cr(CO)_3 + C_6H_6$			106	- 86

REFERENCES

1. W.C.Zeise, Pogg.Ann., 1827, 9, 632.
2. E.Frankland, J.Chem.Soc., 1848, 2, 263.
3. V.Grignard, Compt.rend., 1900, 130. 1322.
4. L.C.Mond, C.Langer and F.Quinke, J.Chem.Soc., 1890, 57. 749.
   P.Gilmont and A.A.Blanchard, Inorg.Syn., 1946, 2. 242.
5. L.C.Mond and C.Langer, J.Chem.Soc., 1891. 59, 1090.
   M.Berthelot, Compt.rend., 1891, 112. 1343.
6. T.J.Kealy and P.L.Pauson, Nature. 1951. 168. 1039.
   S.A.Miller, J.A.Treboth and J.F.Tremaine, J.Chem.Soc., 1952. 632.
7. S.W.Polichnowski, J.Chem.Educ., 1986, 63, 206.
8. R.Hoffmann, Science, 1981, 211, 995.
9. M.J.S.Dewar, Bull.Soc.Chim., France, 1951, 11. 596.
10. C.K.Ingold, "Structure and Mechanism in Organic Chemistry", Cornell University Press, New York, (1953). Chapt.V.
11. C.H.Langford and H.B.Gray, "Ligand Substitution Processes". W.A.Benjamin, Inc., New York, (1965).
12. G.R.Dobson, Accts.Chem.Res., 1976. 9. 300.
13. G.R.Dobson and L.D.Schultz, J.Organomet. Chem., 1977. 131. 285.
14. R.J.Angelici, Organometallic Chem.Rev., 1968. 3. 173.
15. See G.R.Dobson and G.C.Faber. Inorg.Chim.Acta. 1970. 4. 87 and references cited therein.
16. W.J.Knebel and R.J.Angelici, Inorg.Chem., 1974. 13, 627.
17. G.R.Dobson and A.Moradi-Araghi. Inorg.Chim.Acta. 1978. 31. 263.
18. G.C.Faber and G.R.Dobson, Inorg.Chem., 1968. 7, 584.
19. C.A.Tolman, Chem.Soc.Rev., 1972. 1, 337.
20. D.M.P.Mingos, Adv.Organometallic Chem., 1977. 15. 1.

21. E.L.Muetterties, J.R.Bleeke, Z.Y.Yang and V.W.Day, J.Amer.Chem.Soc., 1982, 104, 2940.

22. C.M.Arewgoda, B.H.Robinson and J.Simpson, J.Chem.Soc., 1982, 284.

23. G.J.Bezems, P.H.Reiger and S.Usco, J.Chem.Soc., Chem.Comm., 1981, 265.

24. D.L.Lichtenberger and T.L.Brown, J.Amer.Chem.Soc., 1978, 100, 366.

25. J.K.Burdett, Inorg.Chem., 1977, 16, 3013.

26. M.Elian and R.Hoffmann, Inorg.Chem., 1975, 14, 1058.

27. M.Elian, M.M.L.Chen, D.M.P.Mingos and R.Hoffmann, Inorg.Chem., 1976, 15, 1148.

28. B.E.R.Schilling, R.Hoffmann, D.L.Lichtenberger, J.Amer.Chem.Soc., 1979, 101, 585.

29. T.A.Albright, P.Hoffmann and R.Hoffmann, J.Amer.Chem.Soc., 1977, 99, 7546.

30. B.J.Plankey and J.V.Rund, Inorg.Chem., 1979, 18, 957.

31. K.F.Purcell and J.C.Kotz, "Inorganic Chemistry", W.B.Saunders, Philadelphia, 1977.

32. J.B.Birk, J.Halpern and A.L.Pickard, J.Amer.Chem.Soc., 1968, 90, 4491.

33. F.Basolo, J.Chatt, H.B.Gray, R.G.Pearson and B.L.Shaw, J.Chem.Soc., 1961, 2207.

34. G.Cardaci, Int.J.Chem.Kinetics, 1973, 5, 805.

35. G.Cardaci and V.Narciso, J.C.S.Dalton, 1972, 2289.

36. G.Cardaci, J.Organomet.Chem., 1974 76, 385.

37. G.Cardaci, Inorg.Chem., 1974, 13, 368.

38. G.Cardaci, Inorg.Chem., 1974, 13, 2974.

39. G.Distephano, J.Res.Nat.Bur.Stand. Section A., 1970, 74, 233.

40. P.C.Engelking and W.C.Lineberger, J.Amer.Chem.Soc., 1979, 101, 5569.

41. P.M.Burkinshaw, D.T.Dixon and J.A.S.Howell, J.C.S.Dalton, 1980, 999.

42. D.L.S.Brown, J.A.Connor, M.L.Leung, M.I.Paz Andrade and H.A.Skinner, J.Organometallic Chem., 1976, 110, 79.

43. M.S.Wrighton, G.S.Hammond and H.B.Gray, J.Amer.Chem.Soc., 1971, 93, 6048.

44. W.A.Schenk and H.Muller, Inorg.Chem., 1981, 20, 6.

45. G.R.Dobson, W.I.Stolz and R.K.Sheline, Adv.Inorg.Chem. Radiochem., 1966, 8, 1.

46. R.J.Angelici and W.Loewen, Inorg.Chem., 1967, 6, 682.

47. R.F.Heck, J.Amer.Chem.Soc., 1963, 85, 655.

48. R.F.Heck, J.Amer.Chem.Soc., 1965, 87, 2572.

49. G.Cardaci and S.M.Murgia, J.Organomet.Chem., 1970, 25, 483.

50. G.Cardaci and A.Foffani, J.C.S.Dalton, 1974, 1808.

51. G.Cardaci, J.C.S. Dalton, 1974, 2452.

52. R.F.Heck and C.R.Boss, J.Amer.Chem.Soc., 1964, 86, 2580.

53. E.M.Thorsteinson and F.Basolo, J.Amer.Chem.Soc., 1966, 88, 3929.

54. G.T.Palmer and F.Basolo, J.Amer.Chem.Soc., 1985, 107, 3122.

55. S.Sorriso and G.Cardaci, J.C.S.Dalton, 1975, 1041.

56. G.Bellachioma and G.Cardaci, J.C.S.Dalton, 1977, 2181.

57. G.Bellachioma, G.Reichenbach and G.Cardaci, J.C.S.Dalton, 1980, 635.

58. G.Bellachioma and G.Cardaci, Inorg.Chem., 1977, 16, 3099.

59. G.Cardaci and S.Sorriso, Inorg.Chem., 1976, 15, 1243.

60. G.Cardaci and G.Concetti, J.Organomet.Chem., 1975, 49, 90.

61. F.Farone, F.Zingales, P.Uguagliati and U.Belluco, Inorg.Chem., 1968, 7, 2362.

62. B.F.G.Johnson, J.Lewis and M.V.Twigg, J.C.S.Dalton, 1974, 2546.

63. B.F.G.Johnson, J.Lewis, I.E.Ryder and M.V.Twigg, J.C.S.Dalton, 1976, 421.

64. M.Cais and N.Moaz. J.Chem.Soc. A, 1971, 1811.

65. J Kola, D.T.Dixon, J.A.S.Howell, M.J.Thomas and P.M.Burkinshaw, J.Organomet.Chem., 1984, 266, 83.

66. J.Kola, D.T.Dixon and J.A.S.Howell, J.C.S.Dalton. 1984 1307.

67. F.Zingales, M.Graziani and U.Belluco, J.Amer.Chem.Soc., 1967. 39, 256.

68. F.Zingales, F.Canziani and F.Basolo, J.Organomet.Chem., 1967. 7, 461.

69. P.M. Burkinshaw, D.T.Dixon, J.A.S.Howell and D.T.Dixon, J.C.S.Dalton, 1980. 2236.

70. D.J.Darensbourg and A.Salzer, J.Amer.Chem.Soc., 1978, 100, 4119.

71. D.J.Darensbourg and A.Salzer, J.Organomet.Chem., 1976, 117, C90.

72. D.J.Darensbourg, L.J.Todd and J.P.Hickey, J.Organomet.Chem., 1977, 131, C1.

73. D.J.Darensbourg, H.H.Nelson III and M.A.Murphy, J.Amer.Chem.Soc., 1976, 99, 896.

74. D.L.S.Brown, J.A.Connor, C.P.Demain, M.L.Leung, J.A.Martinho-Simoes, H.A.Skinner and M.T.Zafarani-Moattar, J.Organomet.Chem., 1977. 142, 321.

75. T.A.Seder, S.P.Church and E.Weitz, J.Amer.Chem.Soc., 1986, 108, 4721.

76. G.C.Faber and R.J.Angelici, Inorg.Chem., 1970, 9, 1586.

77. R.J.Angelici and W.Loewen, Inorg.Chem., 1967, 6, 682.

78. A.E.Fenster and I.S.Butler, Inorg.Chem., 1974, 13, 915.

79. I.S.Butler and T.Sawai, Inorg.Chem., 1975. 14, 2703.

80. H.G.Schuster-Woldan and F.Basolo. J.Amer.Chem.Soc., 1966. 88, 1657.

81. L.-N.Ji, D.L.Kershner, M.E.Rerek and F.Basolo, J.Organomet.Chem., 1985. 83. 296.

82. G.T. Palmer. F.Basolo, L.B.Kool and M.D.Rausch. J.Amer.Chem.Soc., 1986, 108. 4417.

83. M.E.Rerek, L.-N.Ji, and F.Basolo. Organometallics, 1984. 3, 740.

84. M.E.Rerek, L.-N.Ji. and F.Basolo. J.Chem.Soc.. Chem.Comm.. 1983. 1208.

85. A.J.Hart-Davis and R.J.Mawby. J.Chem.Soc.A. 1969. 2403.

86. P.Caddy, M.Green, E.O'Brien, L.E.Smart and P.Woodward J.C.S.Dalton. 1980. 1962.

87. A.Pidcock and B.W.Taylor. J.Chem.Soc. A. 1967. 877.

88. K.M.Al-Kathumi and L.A.P.Kane Maguire. J.C.S.Dalton. 1974. 428.

89. M.Gower and L.A.P.Kane Maguire, Inorg.Chim.Acta. 1979. 37. 79.

90. F.Zingales, A.Chiesa and F.Basolo. J.Amer.Chem.Soc., 1966. 88. 2707.

91. A.Pidcock. J.D.Smith and B.W.Taylor. J.Chem.Soc.A. 1967. 872

92. A.Pidcock. J.D.Smith and B.W.Taylor. J.Chem.Soc.A. 1969 1604.

93. M.Scotti, H.Werner, D.L.S.Brown. S.Cavell. J.A.Connor and H.A.Skinner. Inorg.Chim.Acta. 1977. 25. 261.

94. A.M.McNair and K.R.Mann. Inorg.Chem.. 1986. 25. 2519.

95. I.S.Butler and A.A.Ismail. Inorg.Chem.. 1986 25. 3910

96. P.M.Burkinshaw and J.A.S.Howell. Chem.Rev.. 1983. 83. 557.

97. H.D.Kaesz. S.Winstein and C.G.Kreiter , J.Amer.Chem.Soc., 1966. 88. 1319.

98. A.Salzer. J.Organomet.Chem.. 1976. 107. 79.

99. A.Salzer. J.Organomet.Chem.. 1976. 117. 245.

100. G.Yagupsky and M.Cais. Inorg.Chim.Acta. 1975. 12. L27.

101. K.M.Al-Kathumi and L.A.P.Kane Maguire. J.C.S.Dalton. 1973. 1683.

102. F.A.Adedeji, D.L.S. Brown. J.A.Connor, M.L.Leung. I.M.Paz Andrade and H.A.Skinner. J.Organomet.Chem.. 1975. 97. 221.

103. C.D.Hoff. J.Organomet.Chem.. 1983. 246. C53.

104. E.L.Muetterties. J.R.Blecke, E.J.Wucherer and T.A.Albright. Chem.Rev.. 1982. 82. 499.

105. W.Strohmeier and R.Muller, Z.Phys.Chem. (Wiesbaden). 1964. 40. 85.

106. W.Strohmeier and H.Muller, Chem.Ber. 1960, 93, 2085.

107. W.Strohmeier and H.Mittnacht, Z.Phys.Chem. (Wiesbaden). 1961 29. 339.

108. T.E.Traylor. K.J.Stewart and M.J.Goldberg. J.Amer.Chem.Soc.. 1984. 106. 4445.

109. W.Strohmeier and E.H.Starrico, Z.Phys.Chem. (Wiesbaden). 1963. 38. 315.

110. C.L.Zimmermann, S.L.Shaner, S.A.Roth and B.R.Willeford, J.Chem.Res.(S). 1980. 108.

111. C.A.L.Mahaffy and P.L.Pauson, J.Chem.Res.(S). 1979. 126.

112. M.Cais. D.Fraenkel and K.Wiedenbaum. Coord.Chem.Rev., 1975. 16. 27.

2. POLYENE EXCHANGE IN (POLYENE)$Cr(CO)_3$ COMPLEXES

2.1 Introduction

η^6-polyene complexes of transition metals have been shown to be both useful catalysts and stoichiometric reagents or intermediates for organic synthesis. Catalytic applications of these complexes include homogeneous regioselective hydrogenation of 1,3-dienes to cis-2-monoenes[1,2], and more recently the addition of haloalkanes to alkenes[3]. (Naphthalene)$Cr(CO)_3$ allows both these reactions to be performed at ambient termperatures and pressures. The mechanism of this catalytic behaviour probably involves a reduction of, or loss of coordination of the naphthalene from the $Cr(CO)_3$ moiety, thus allowing empty coordination sites to be filled by reacting species. On this basis, the hydrogenation reaction might proceed as shown.

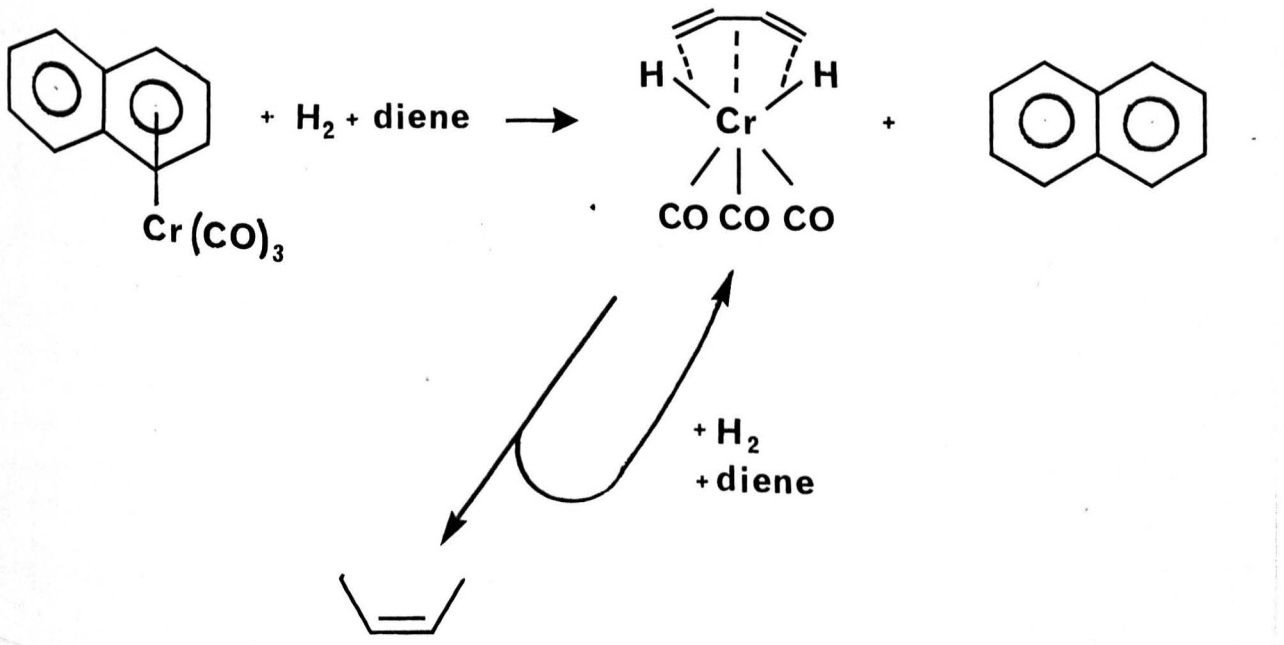

Scheme 2.1

Stoichiometric reactions involving polyene complexes had, until the mid 1960's received little attention. One of the first examples reported by Birch et al involved the aromatisation of 1-methoxycyclohexa-1,4-dienes using $Cr(CO)_6$[4]. The reaction, which proceeds via an (η^6-polyene)$Cr(CO)_3$ complex, has been applied to steroids possessing a 3-methoxy-2,5-diene (ring A) structure converting them into aromatic steroids in 70% yields (Scheme 2.2)[5]. The intermediate complex (A) formed, may be decomplexed by the combined action of light and air, which is generally the method of choice.

Modifications to the chemistry of polyenes when coordinated to the $Cr(CO)_3$ unit are of particular interest to the organic chemist, and are both electronic and stereochemical in nature.

Electronic modifications arise form the strong withdrawal of electron density from the aromatic ring by the $Cr(CO)_3$ moiety. Reactivity changes resulting from this effect are:-

(i) Enhanced nucleophilic substitution of aromatic ring[6]

(ii) Enhanced acidity of the polyene ring hydrogens[6]

(iii) Activation of alkyl side chains[5,7]

Examples of nucleophilic substitution include reactions of (benzene)$Cr(CO)_3$ with lithium alkyls, of which two general reactions are now well defined

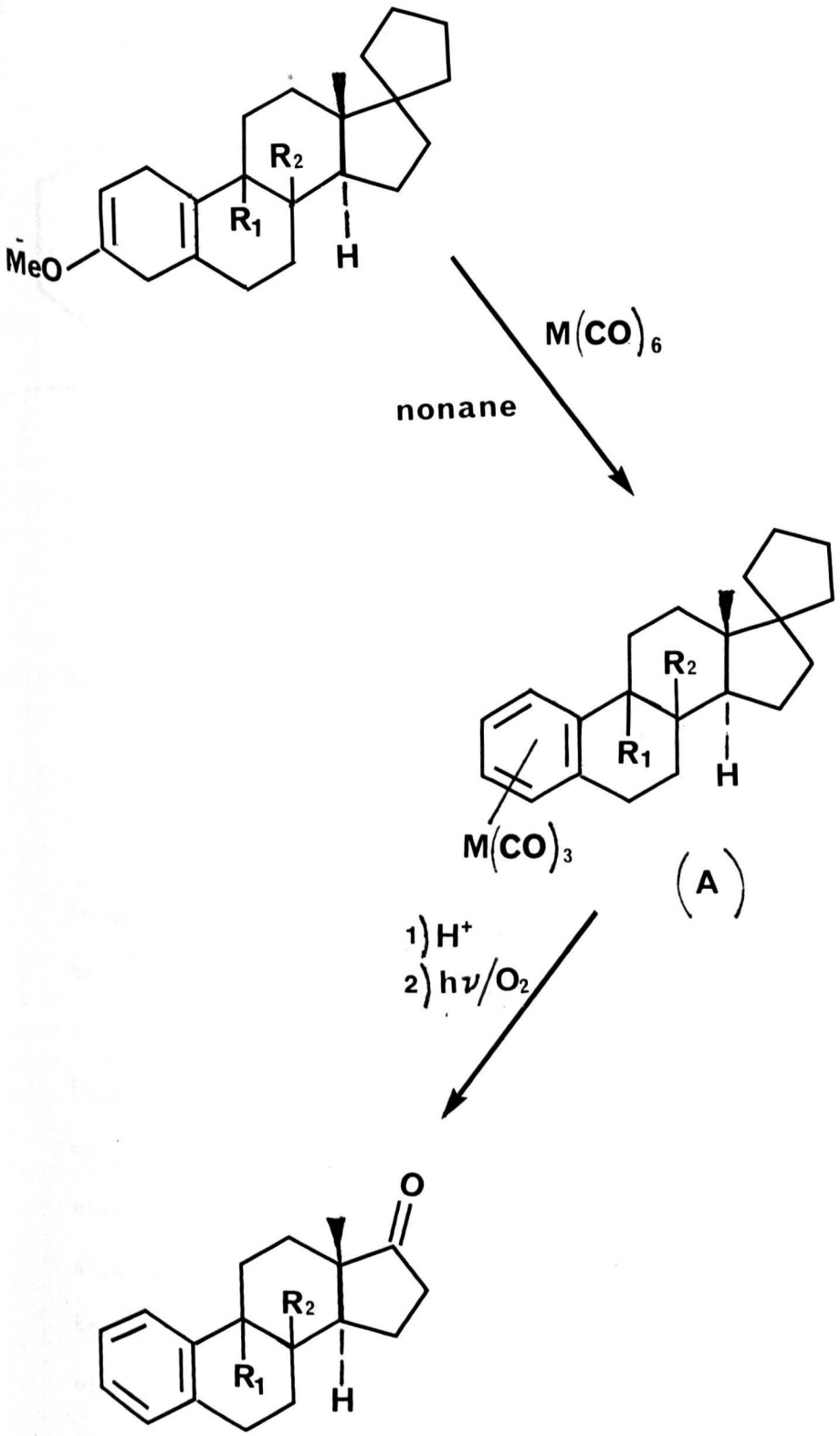

Scheme 2.2

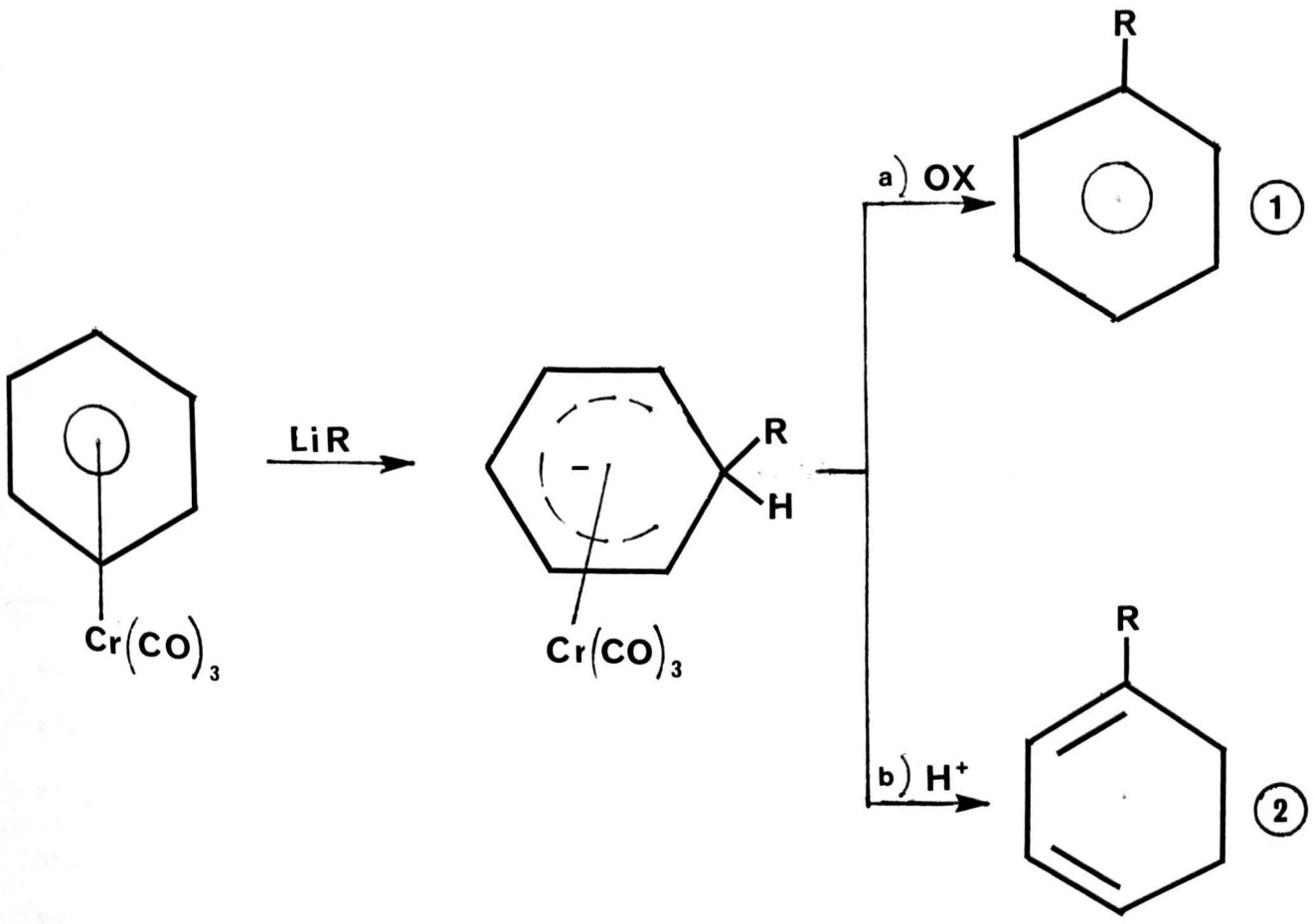

Scheme 2.3

(Chlorobenzene)$Cr(CO)_3$ also undergoes nucleophilic substitution with methoxide ion to give (anisole)$Cr(CO)_3$.

Proton abstraction from an aromatic ring by strong base (metalation) is a method of direct activation of a ring carbon atom as a nucleophile, though alkylarenes undergo preferential side chain metalation. Complexed alkylarenes however, due to their increased acidity allow ring metalation. Reaction of (toluene)$Cr(CO)_3$ with n-butyllithium gives initially mixtures of the meta- and para- metalated complexes, though synthetic uses of these intermediates have yet to be developed.

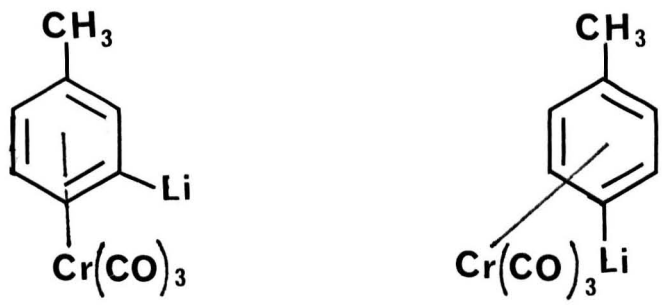

Fig. 2.1

Activation of alkyl side chains involves stabilisation α or β to the ring. Alkylation of anionic sites both in the α and β positions to the complexed ring is possible[5]. Thus whereas free $PhCH_2CO_2Me$ and $PhCH_2CH_2CO_2Me$ are inert to MeI, the $Cr(CO)_3$ complexes of both readily undergo methylation to give $PhMe_2CO_2Me$ and $PhCH_2CMe_2CO_2Me$ respectively. The reasons for β-activation are still unclear. Synthetic applications of the extraordinary stabilisation of α-carbonium ions include preparation of amines (yields 70-80%) from primary, secondary and tertiary alcohol derivatives of (benzene)$Cr(CO)_3$[6].

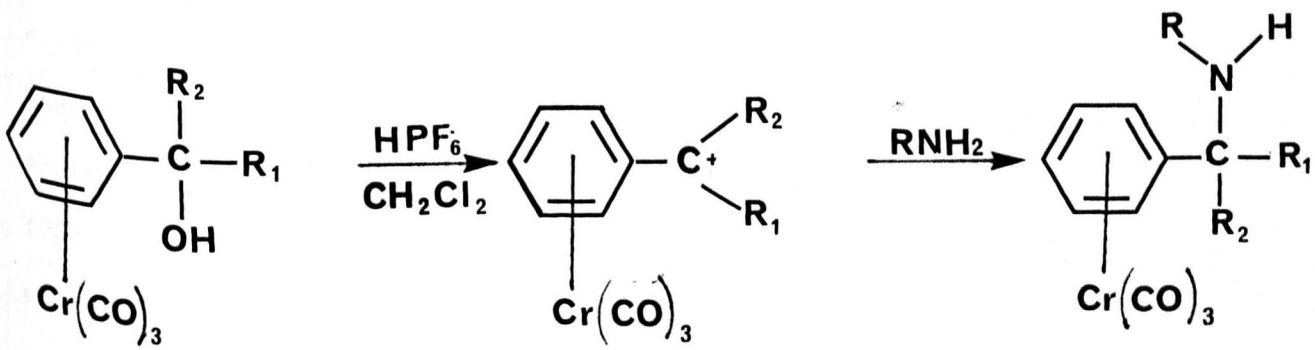

Scheme 2.4

The stereochemical consequence of complexation is shown in Figure 2.2. Arene derivatives containing different ortho or meta substituents exhibit planar chirality, and undergo nucleophilic or electrophilic (α-anionic sites) attack from the opposite side of the ring to that of the $Cr(CO)_3$ moiety (exo attack). An important application of complexes of this nature is therefore in asymmetric synthesis involving enantiomerically pure products.

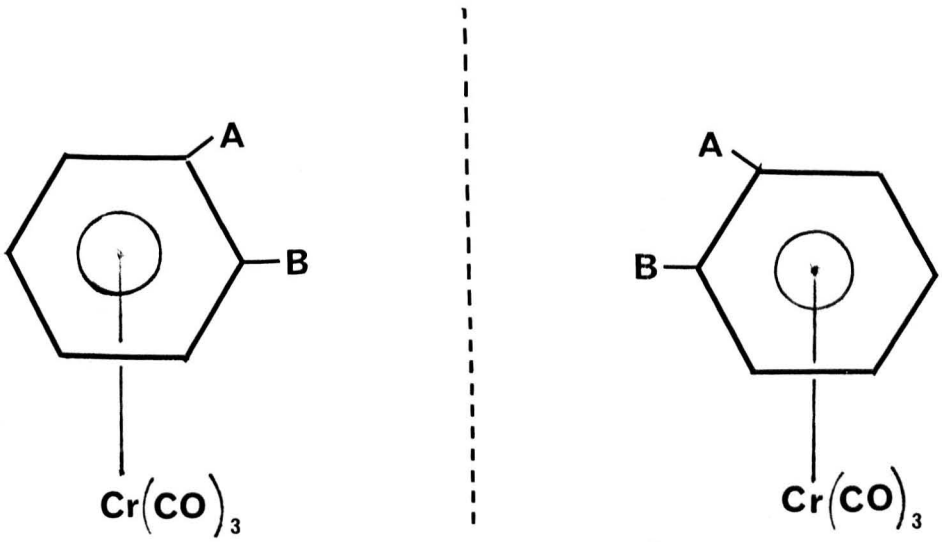

Fig 2.2

A good example of the effect is provided by the route to optically pure ephedrines[8]. Reaction of optically pure complex (Scheme 2.5), with the sodium derivative of nitroethane yields a 70/30 mixture of diastereoisomers (70% erythro) resulting from the orientation of attack by the pro-chiral nitroethane. Asymmetric induction at C_2, nearly 100%, arises from exclusive attack of the nitroethane from the exo side of the molecule to the $Cr(CO)_3$ moiety. These diastereoisomers can be separated by chromatography such that decomplexation affords enantiomerically pure ephedrine.

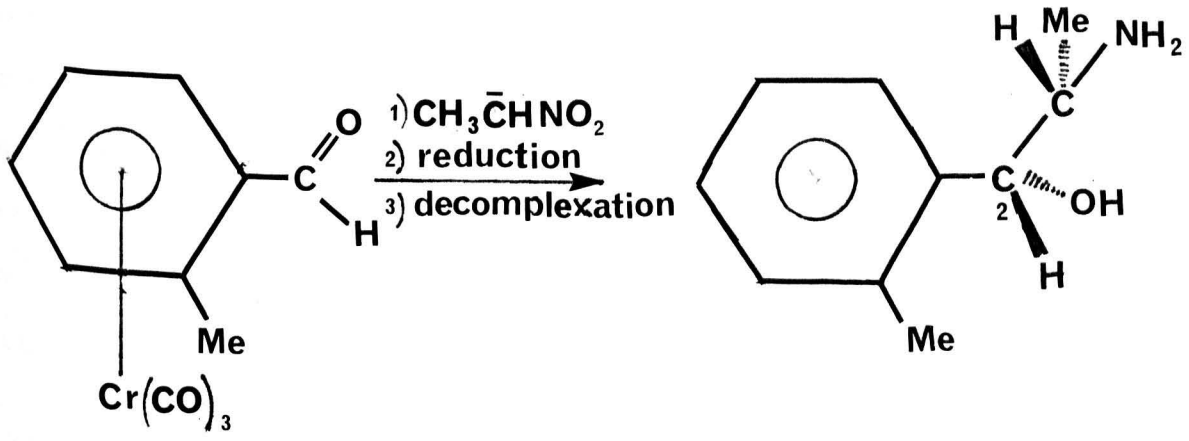

Scheme 2.5

From a synthetic point of view, these reactions suffer in that the activating group, $Cr(CO)_3$ is generally removed oxidatively and cannot be recycled. The advantage of achieving a cyclical process is therefore economically apparent as stoichiometric amounts of the costly chromium(0) compound can be substituted by essentially catalytic amounts. One reaction which would therefore be of great synthetic importance is that of polyene exchange. This approach has been adopted in the preparation of some substituted benzenes[9].

$(ArF)Cr(CO)_3 + X^- \longrightarrow (ArX)Cr(CO)_3 + F^-$

$(ArX)Cr(CO)_3 + ArF \longrightarrow (ArF)Cr(CO)_3 + ArX$

X= OBu^t, cholesteryloxy, menthyloxy, SBu^t, morpholine.

Scheme 2.6

Exchange of the complexed functionalised arene, $(ArX)Cr(CO)_3$ can be accomplished, even though it may be more stable than $(ArF)Cr(CO)_3$[10], by the use of a large excess of fluorobenzene. An example of this approach can be applied to Scheme 2.2 by considering exchange of the complexed arene (A) with reactant polyene. Thus, an understanding of the thermodynamic, kinetic and mechanistic features of the polyene exchange reaction is of some importance.

Surprisingly little work on the kinetics of polyene exchange has been reported. Exchange reactions carried out in coordinating solvents have been studied kinetically[11-14], although information gained from these studies is not directly relevant to the exchange in hydrocarbon solvents. Solvent participation by coordinating solvents significantly increases the rate of reaction, and gives rise to a solvent dependent term in the rate law (See Chapter 1 Section 1.5.5.). Oxidative catalysis by iodine has also been studied[14], with exchange occurring at room temperature. This potentially attractive process is thought to proceed via a 17-electron cationic intermediate

$$(polyene)Cr(CO)_3 \longrightarrow [(polyene)Cr(CO)_3]^+$$

$$[(polyene)Cr(CO)_3]^+ + polyene' \rightarrow [(polyene')Cr(CO)_3]^+ + polyene$$

$$[(polyene')Cr(CO)_3]^+ + (polyene)Cr(CO)_3 \longrightarrow$$

$$(polyene')Cr(CO)_3 + [(polyene)Cr(CO)_3]^+$$

Scheme 2.7

The nature of the reaction however, may prove restrictive for ligands that are sensitive to redox conditions.

The earliest results from kinetic studies of polyene exchange in non-coordinating solvents stem from the work of Strohmeier[12,15-17]. The reactions involve the exchange of ^{14}C labelled polyene

$$(\text{polyene})Cr(CO)_3 + \text{polyene}' \rightarrow (\text{polyene}')Cr(CO)_3 + \text{polyene}$$

polyene = polyene' = naphthalene, benzene, toluene, cycloheptatriene.

The general rate law may be represented as

$$R = \underset{\text{(i)}}{k_A[S]} + \underset{\text{(ii)}}{k_B[S][L]} + \underset{\text{(iii)}}{k_C[S]^2} \qquad (2.1)$$

Terms (i) and (ii) apply to the polycyclic and cycloheptatriene complexes, while only terms (ii) and (iii) are observed in monocyclic complexes. Strohmeier's interpretation of the terms in this rate law are shown below.

The experimental techniques used in this study only allow for the detection of the exchange product $(\text{polyene}')Cr(CO)_3$, which assumes quantitative yield in the calculation of the rate constants. Additionally rate constants are calculated only from initial rate measurements, and may therefore not represent a true value of the rate constant. Furthermore, the entropy value derived from kinetic data for the ligand independent pathway (i) in naphthalene exchange is large and negative, and inconsistent with a dissociative pathway as represented.

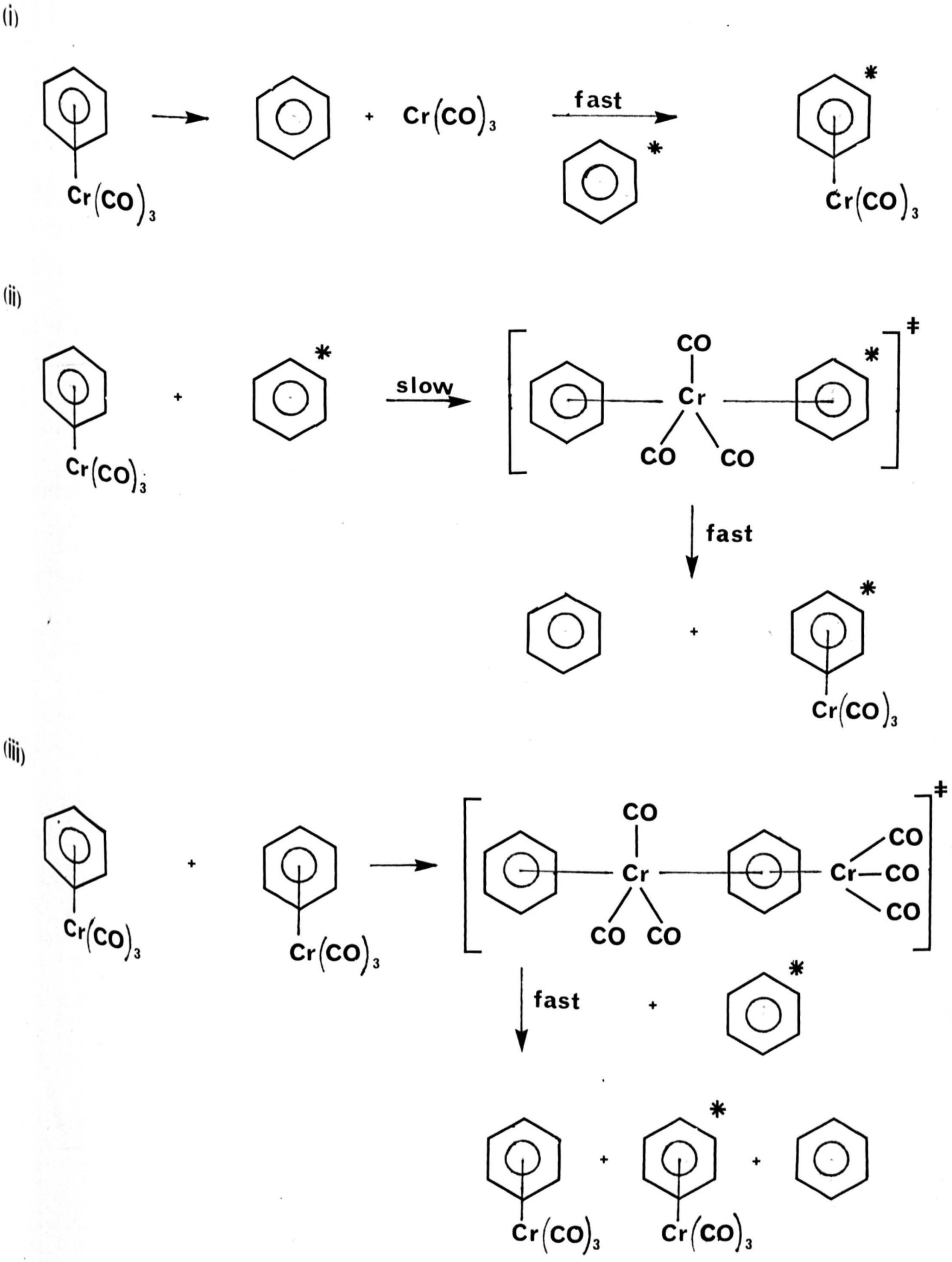
(i)
Cr(CO)3
Cr(CO)3
fast
Cr(CO)3
(ii)
Cr(CO)3
slow
CO
Cr
CO
CO
fast
Cr(CO)3
(iii)
Cr(CO)3
Cr(CO)3
CO
Cr
CO
CO
Cr
CO
CO
CO
fast
Cr(CO)3
Cr(CO)3

Scheme 2.8

Since this work, pathway (i) involving the high energy 12-electron $Cr(CO)_3$ intermediate has also been criticized on energetic grounds[18] and pathway (iii) has been criticized from a stereochemical point of view, since in the absence of added polyene' it would imply an inversion of configuration of the bound polyene. Individual isomers of (alkylindane)$Cr(CO)_3$ (Figure 2.3) were recovered unchanged after being heated under conditions where exchange normally occurs[19].

Fig. 2.3

It therefore appears that this process (iii) cannot be interpreted as represented. More recent work by Traylor[20,21] has however, appeared to confirm this second order substrate dependence term, the postulated pathway involving a carbonyl bridge.

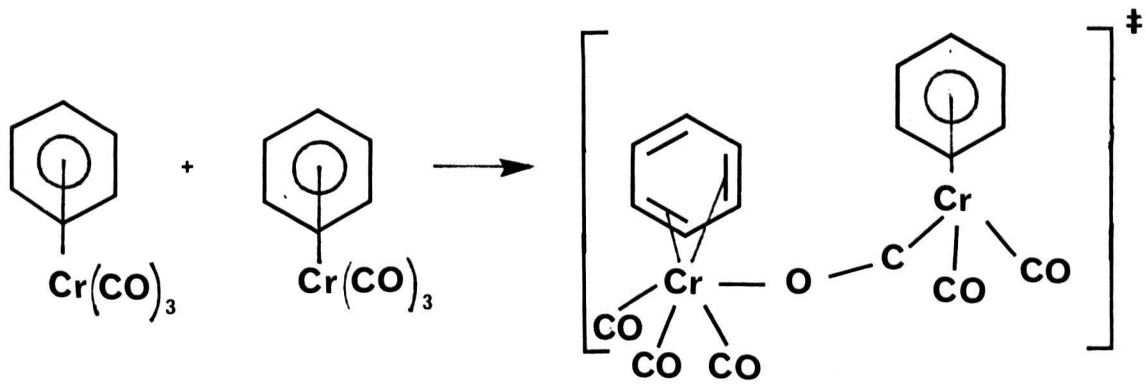

Scheme 2.9

Most recently an investigation of the reaction

$$(\text{naphthalene})Cr(CO)_3 + \text{toluene} \rightarrow (\text{toluene})Cr(CO)_3 + \text{naphthalene}$$

yielded a rate law which is independent of toluene concentration, though the concentration range used was rather limited[22].

In view of the paucity and apparently contradictory nature of the data, a further study into the exchange reactions of these types of complexes has been undertaken. With the aid of theoretical calculations, this work aims to provide a fuller interpretation of the reaction pathways contributing to the overall mechanism of polyene exchange.

2.2 Experimental

2.2.1 Reagents and Materials

All (polyene)$Cr(CO)_3$ complexes were prepared by standard literature methods from $Cr(CO)_6$[23,24], except (styrene)$Cr(CO)_3$ and (2,6-dimethylpyridine)$Cr(CO)_3$ which were prepared from $(NH_3)_3Cr(CO)_3$[25,26]. Polyenes were supplied by Aldrich Chemical Co. Ltd. except for octamethylnaphthalene which was prepared by a literature method[27]. 2,6-dimethylpyridine was purified prior to use to remove non-alkylated impurities. $Cr(CO)_6$ was supplied by Strem Chemicals Inc. Peroxide free tetrahydrofuran, di-n-butyl ether and dioxan were all refluxed and distilled from sodium under a nitrogen atmosphere.

(i) Example of preparation from $Cr(CO)_6$.

$Cr(CO)_6$ (2g 9.1mmol) and pyrene (3g 16mmol) were added to a mixture of 2ml of tetrahydrofuran in 100ml of di-n-butyl ether in a 250ml round bottomed flask, equipped with stirrer, condenser and nitrogen bubbler. After degassing with nitrogen for 15 minutes, the mixture was refluxed at 160 ^{o}C under a nitrogen atmosphere. Any sublimed $Cr(CO)_6$ appearing in the condenser was scraped back into the flask. After reacting for 24 hours, the red mixture was cooled, filtered through a a glass frit containing celite, and solvent removed under reduced pressure. Separation of the complex from free pyrene was effected by passing the mixture down an alumina column (grade III) and first eluting with hexane/diethyl ether (4:1) to remove free pyrene, followed by elution with diethyl ether to remove the complex. After removal of the solvent, recrystallisation from dichloromethane/hexane afforded red crystals of (pyrene)$Cr(CO)_3$ (0.3g 10%).

In all other preparations from $Cr(CO)_6$, except for (naphthalene)$Cr(CO)_3$, 10ml of tetrahydrofuran were used. Purification of both alkyl naphthalene complexes involved the chromatographic procedure outlined with subsequent recrystallisation from hexane. (Naphthalene)$Cr(CO)_3$ was purified by sublimation and the remaining complexes purified by recrystallisation from hexane.

(ii) Example of preparation from $(NH_3)_3Cr(CO)_3$

$(NH_3)_3Cr(CO)_3$[28] (0.9g 5mmol) and 2,6-dimethylpyridine (2.7g 26mmol) were added to 50ml of dioxan in a 100ml round bottomed flask equipped with stirrer, condenser and nitrogen bubbler. After degassing for 15 minutes with nitrogen, the mixture was refluxed for 4 hours after which the resulting brown solution was cooled and filtered through a glass frit containing celite. The yellow filtrate was evaporated to dryness. Recrystallisation of the solid from hexane afforded yellow crystals of the complex (2,6-dimethylpyridine)$Cr(CO)_3$ (0.2g 17%).

All complexes were characterised by ^1H nmr (Jeol Fx-100), infrared (Perkin Elmer 257) and microanalysis. Analytical data are given in Table 2.1

Table 2.1

$Cr(CO)_3$ complex	^1H nmr (ppm, $CDCl_3$)	ν_{CO}/cm^{-1} (decalin)	microanalysis/% found	calc
naphth-	5.52(dd,2)	1974	C = 58.97	59.10
alene	6.12(dd,2)	1910	H = 3.12	3.03
	7.34-7.61(m,4)	1898		
pyrene	5.56(dd,1)	1964	C = 67.36	67.45
	6.00(d,2)	1904	H = 3.22	2.96
	7.45-7.91(m,7)	1898		
2,6-dmn.	2Me 2.41, 2.29	1969	C = 61.79	61.60
	5.38(dd,1)	1905	H = 4.08	4.10
	6.07(m,2)	1891		
	7.15-7.47(m,3)			
2,5-dmt.	2Me 2.18	1984	C = 43.43	43.55
	5.23(s,2)	1824	H = 3.12	3.22
		1914		
2,6-dmp.	2Me 2.38	1984	C = 49.19	49.36
	5.08(d,2)	1924	H = 3.56	3.70
	5.64(t,1)	1914	N = 5.56	5.76

Table 2.1 continued

cyclohep-	1.63(m,1)	1982	C = 52.60 52.63
tatriene	2.88(m,1)	1920	H = 3.47 3.51
	3.32(m,2)	1896	
	4.79(m,2)		
	5.99(m,2)		
styrene	6.25(dd,1)	1978	C = 54.91 55.00
	5.24-5.71(m,7)	1912	H = 3.22 3.30
octamethyl-	4Me 2.28, 2.34	1952	C = 67.13 67.02
naphthalene	2.54, 2.57	1886	H = 6.52 6.38
		1871	
thiophene	5.34	1978	C = 38.29 38.20
	5.57	1905	H = 1.72 1.82
		1897	
toluene	Me 2.15	1977	C = 52.44 52.63
	5.20(m,5)	1902	H = 3.37 3.51
^{t}-butyl-	Bu^{t} 1.27	1972	C = 57.84 57.78
benzene	5.21-5.54(m,5)	1898	H = 5.19 5.19
m-xylene	2Me 2.17	1970	C = 55.19 54.54
	5.0(m,3)	1898	H = 4.25 4.13

Table 2.1 continued

o-xylene		1971	
		1899	
p-xylene		1969	
		1897	
hexamethyl-	6Me 2.26	1952	C = 60.13 60.40
benzene		1876	H = 6.10 6.04
α,α,α-tft.	5.16-5.58(m,5)	1994	C = 42.82 42.55
		1930	H = 1.81 1.77
methylphenylacetate		1980	
		1905	

2,6-dmn. = 2,6-dimethylnaphthalene
2,5-dmt. = 2,5-dimethylthiophene
2,6-dmp. = 2,6-dimethylpyridine
α,α,α-tft = α,α,α-trifluorotoluene

Literature methods[29] for the purification of polyene reactants are outlined below. Toluene, xylenes and t-butylbenzene were purified by first washing with conc.H_2SO_4, followed by aq.Na_2CO_3 and finally water. After drying over anhydrous $CaSO_4$, each solvent was fractionally distilled. α,α,α-trifluorotoluene was treated with boiling aq.Na_2CO_3, dried and fractionally distilled. Methyl phenylacetate was washed with Na_2CO_3 in water, then dried over $CaSO_4$ and distilled from P_2O_5 to remove any alcohol.

Hexamethylbenzene was recrystallised from absolute ethanol and dried under high vacuum. Cycloheptatriene was treated with 2N NaOH and fractionally distilled.

All reactants were stored under an atmosphere of nitrogen.

Decalin (Aldrich Chemical Co. Ltd. and Lancaster Synthesis) and cyclooctane (Fluka) were purified by stirring with conc.H_2SO_4 followed by washing with water, aq.Na_2CO_3 and water respectively. After drying with $CaSO_4$ (decalin) or $MgSO_4$ (cyclooctane), the solvents were passed down an alumina column. Decalin was distilled from sodium under reduced pressure and cyclooctane fractionally distilled from $LiAlH_4$. Both solvents were shown to be pure by glc. The decalin, which shows two peaks on glc, consists of a cis/trans isomeric mixture (76/24). This ratio was consistent between different batches of decalin.

The copoly(divinylbenzene-styrene) used in exchange experiments was obtained from Polymer Laboratories Limited (8% crosslinked. 10μ bead size) and was purified by washing with water. 1;1 water/ethanol. ethanol and acetone followed by Soxhlet extraction with CH_2Cl_2 and drying under vacuum.

2.2.2 Kinetic Measurements

An appropriate amount of complex. to give a 10^{-3} mol dm^{-3} was dissolved in a polyene solvent mixture of the required composition.

The resulting solution was transferred into a 10mm uv/visible glass cell (Figure 2.4) previously internally silylated with a 5% ethereal solution of N-(trimethylsilyl)acetamide to remove any catalytically active surface sites. The solution was degassed for a minimum of 15 minutes with oxygen free and moisture free argon, obtained from passage of the gas through an activated copper catalyst and molecular sieve (4A) trap. The cell was then sealed with a teflon stopcock under a positive pressure of argon (5psi).

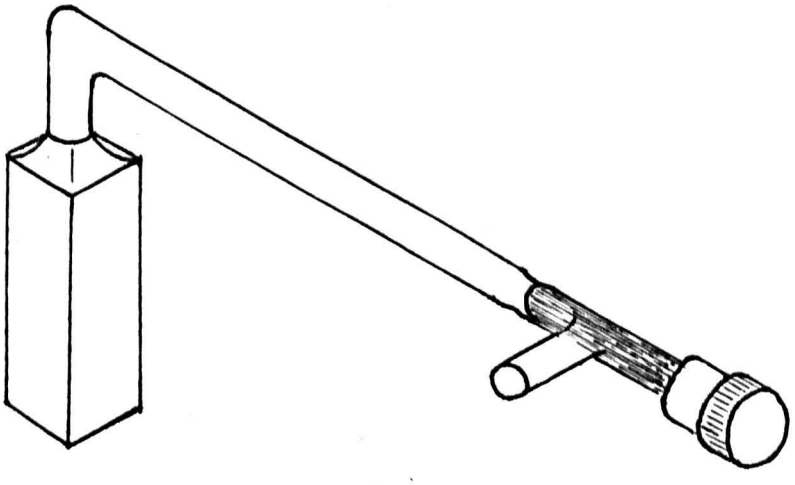

Fig. 2.4

After an initial absorbance reading, the cell was immersed in a constant temperature oil bath ($\pm$0.2 ^{o}C). At appropriate time intervals of not less than 30 minutes, the cell was removed from the bath, quenched in cold petroleum ether and the visible spectrum recorded. A minimum 30 minute time interval was used to ensure that the time taken for the cell to reach bath temperature (approximately 3 minutes) was small in comparison. An average of 10 absorption/time data points at specific wavelengths (See Figure 2.5) were measured on a Varian DMS-100 spectrophotometer and used to calculate the rate constant. All kinetic studies were carried out under pseudo-first order conditions with at least a ten-fold excess of polyene reactant (ie $>10^{-2}$ mol dm^{-3}) and were monitored over not less than three half-lives. The data obtained gave linear plots of $\ln(A_t - A_\infty)$ versus time (where A_t and A_∞ are absorbances at times t and t_∞ respectively) when analysed by a linear least squares program, with correlation coefficients greater than 0.999. All reactions were performed in duplicate with a reproducibility of about $\pm$7%. Yields for the reactions were established by comparing the visible and infrared absorbances of the solutions at t_∞ with absorbances of solutions of known concentrations prepared from authentic samples of the reaction product. Good agreement was found between uv and infrared determinations of the yield. Infrared was also used to detect amounts of any other carbonyl containing products, principally $Cr(CO)_6$. After each kinetic run, acidified potassium bromate was introduced into the cell and boiled to remove any traces of oxidised material which may have been formed during the reaction.

In the solvents used, it was established that the change of absorption with concentration of complex conformed to the Beer-Lambert Law.

UV/visible spectra of (polyene)$Cr(CO)_3$ complexes

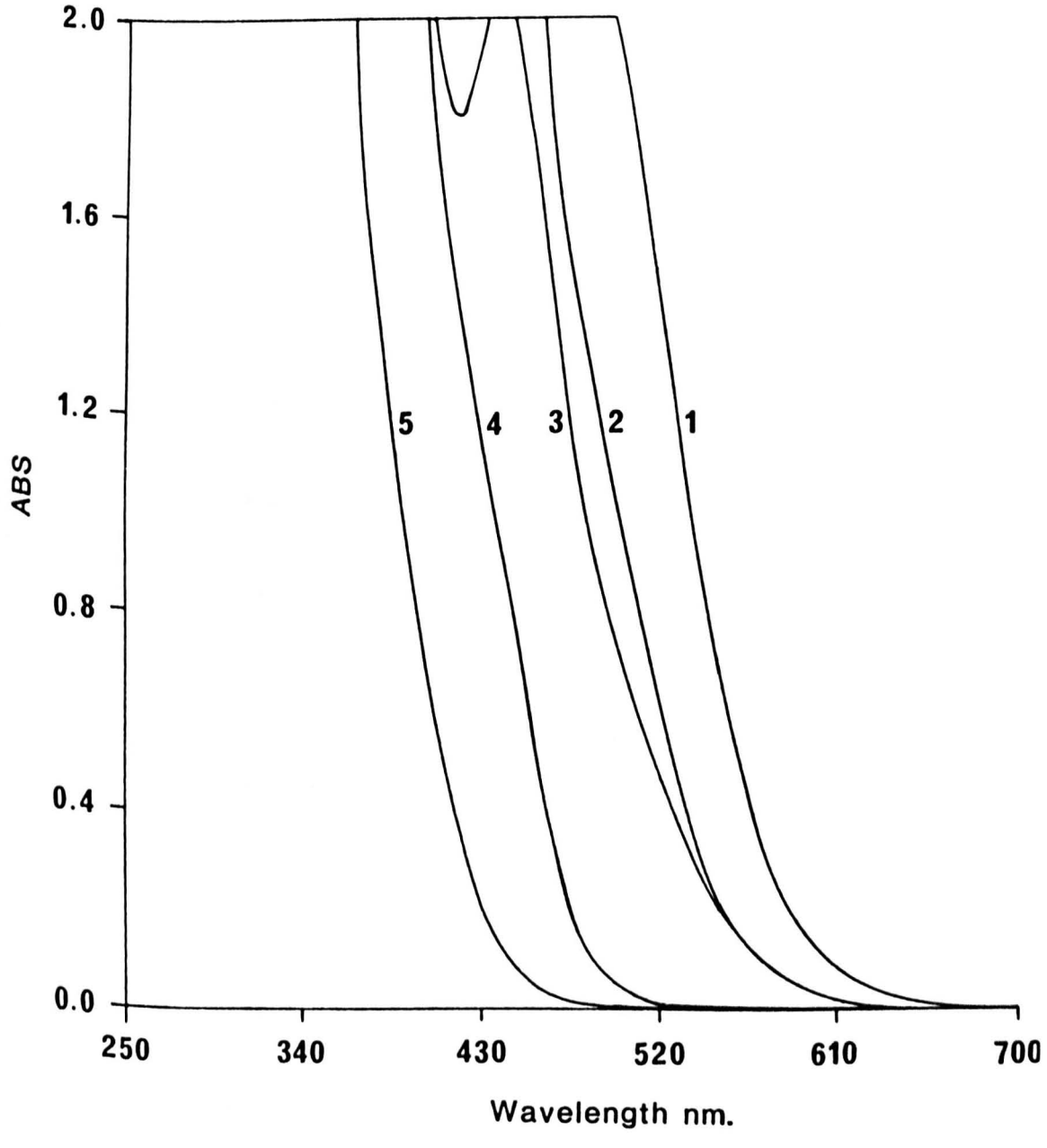

Complex	Wavelength monitored
1. (pyrene)$Cr(CO)_3$	530 nm
2. (2,5-dimethylthiophene)$Cr(CO)_3$	470 nm
3. (naphthalene)$Cr(CO)_3$	470 nm
4. (2,6-dimethylpyridine)$Cr(CO)_3$	440 nm
5. (toluene)$Cr(CO)_3$	

Fig: 2.5

2.2.3 Polymer Studies

(a) Preparation of copoly(divinylbenzene-2-vinylnaphthalene)[30]

1000ml of water was added to a polymerisation vessel equipped with stirrer, thermometer and nitrogen inlet tube. After degassing with nitrogen, 0.125g of copoly(styrene-maleic anhydride) surfactant was added followed by a solution of 5g of 2-vinylnaphthalene (Aldrich Chemical Company Ltd.) and 0.25g benzoyl peroxide dissolved in the minimum amount of toluene. 0.63g of a 63% solution of divinylbenzene in ethylstyrene was added and the mixture stirred for 6 hours at 70 ^{o}C. The resulting yellow polymer was filtered and washed successively with 50ml water, 50ml 1:1 water/ethanol, 50ml ethanol and finally 50ml acetone. The resulting solid was extracted with CH_2Cl_2 and dried under vacuum to give 2g of an off white powder.

Analysis (%) :- C=90.64, H=6.34

Calculated values for each component are:

divinylbenzene:- C=92.3, H=7.7

2-vinylnaphthalene:- C=93.5, H=6.5

(b) Complexation of copoly(divinylbenzene-2-vinylnaphthalene)

0.5g of the copolymer and 0.5g $Cr(CO)_6$ were added to a solution of 2ml tetrahydrofuran in 50ml of di-n-butyl ether. The mixture was refluxed for 10 hours at 160 ^{o}C under argon, and the resulting red powder was filtered and washed with degassed tetrahydrofuran and dried under vacuum (yield 0.7g)

Analysis (%):- C=79.1, H=6.0, Cr=8.6

Infrared (KBr disc)(cm^{-1}):- 1966, 1876

(c) Complexation of copoly(divinylbenzene-styrene)

0.07g of the copolymer beads were suspended in 5ml of decalin containing 0.09g (naphthalene)$Cr(CO)_3$ and the mixture heated at 130°C for 48 hours under argon. The resulting yellow powder was filtered, washed with degassed tetrahydrofuran and dried under vacuum (yield 0.08g).

Analysis (%):- C-77.8, H=6.5, Cr=7.2

Infrared (KBr disc)(cm^{-1}):- 1966, 1882

(d) Exchange studies

All solutions were degassed with argon for a minimum of 15 minutes and sealed under 5psi pressure of argon.

(i) Copoly (divinylbenzene-2-vinylnaphthalene)$Cr(CO)_3$ (0.1g) was heated in decalin (5ml) at 140 °C for 50 hours (a) alone, (b) in the presence of copoly(divinylbenzene-styrene)(0.36g) and (c) in the presence of copoly(divinylbenzene-styrene)(0.36g) and 2,6-dimethylnaphthalene (0.3g). The resulting yellow sediment was filtered and the colourless filtrate analysed by infrared for $Cr(CO)_6$.

(ii) Copoly(divinylbenzene-2-vinylnaphthalene)$Cr(CO)_3$ (0.1g) suspended in hexane (8ml) was reacted with $P(OMe)_3$ (1.0ml) overnight. The resulting yellow sediment was filtered and the colourless solution analysed by infrared for fac-$[P(OMe)_3]_3Cr(CO)_3$. A pure sample of this complex for calibration purposes was prepared using the method outlined in Chapter 3.

(iii) Copoly(divinylbenzene-2-vinylnaphthalene)$Cr(CO)_3$ (0.1g) was heated in toluene (5ml) at 140 ^{o}C for 4 hours. The resulting yellow solution was filtered and analysed by infrared for (toluene)$Cr(CO)_3$.

2.3 Results and Discussion

2.3.1 Experimental

Our initial kinetic studies of the reaction

$$(\text{naphthalene})Cr(CO)_3 + \text{toluene} \rightarrow (\text{toluene})Cr(CO)_3 + \text{naphthalene}$$

were performed in septum sealed vessels, such that samples of the solution could be withdrawn by a syringe. Though similar rate constants were found to those reported in a previous study using the same experimental procedure[22], the relatively poor reproducibility and formation of observable green deposits leading to reduced yields indicated the presence of large amounts of oxygen. In addition, even the trace amounts of oxygen usually present in commercial argon might be expected to effect a catalysis similar in nature to Scheme 2.7 in which O_2 rather than I_2 acts as the initiator. Argon used in the kinetic work was passed through an activated copper catalyst to remove traces of oxygen. If this is not done, although not affecting the yield of $(\text{toluene})Cr(CO)_3$, this catalysis masks the increase in rate with increase in toluene concentration at concentrations less than about 0.1 mol dm^{-3} [31].

The glass cell in which the kinetic work was carried out was designed to minimise the head space above the solution as well as maximising the efficiency of the degassing procedure.

Previous work by Pauson[10] and Traylor[20,21] has demonstrated the catalytic affinity of unsaturated and oxygenated compounds on the reaction; hence solvent impurity is another area of possible catalysis. In this work, the use of unpurified solvents, as received from the supplier, resulted in rate enhancements of up to a factor of 10. The possibility of a catalytic effect of this nature occurring in the work of Strohmeier, where solvent purification was not rigorous, is apparent in view of his higher rate constant values (vide infra).

Finally, internal silylation of the cells to eliminate the possibility of any surface catalysis was carried out. Poorer reproducibility of kinetic results for polyene exchange in unsilylated nmr tubes has been reported by Kundig[32]. Although in this work, rate constants obtained from experiments performed in silylated and unsilylated cells were similar, all reactions were carried out in silylated cells.

As far as possible we are confident that the rate constants reported in this work represent those of a genuine uncatalysed polyene exchange since;

(i) Reproducibility ($\pm$7%) is comparable to other recent studies on monocyclic arene exchange[20], although plots of k_{obs} against [polyene] have better correlation coefficients in this work (>0.999). The slightly poorer reproducibility compared to substitution reactions ($\pm$5%), which take place at much lower temperatures (Chapter 3), may result from the presence of light which is known to catalyse the exchange reaction, and which is difficult to exclude in view of the monitoring technique.

(ii) Although the intercept values of plots of k_{obs} against [polyene] differ for the same reaction performed in the two solvents used (cyclooctane and decalin), the difference is only a factor of 2. In the event of any catalysis due to the impurity in a solvent, a much greater difference would be expected. Additionally, values obtained for the slopes are the same in the two solvents.

(iii) Rate constants obtained using different batches of the same purified solvents are the same. A catalytically active species would give rise to difference values of rate constant, unless coincidentally occuring at similar concentrations in the different batches.

Exchange reactions

$$(\text{polyene})Cr(CO)_3 + \text{toluene} \rightarrow (\text{toluene})Cr(CO)_3 + \text{polyene}$$

polyene = naphthalene, pyrene, 2,5-dimethylthiophene,
2,6-dimethylpyridine

were monitored in hydrocarbon solvent (cyclooctane or decalin) by the decrease in absorbance at the wavelengths indicated in Figure 2.5. At completion, reactions were analysed spectroscopically (uv/visible and infrared) to determine yields of $(\text{toluene})Cr(CO)_3$ and $Cr(CO)_6$.

Kinetic data are presented in Tables 2.3 - 2.5 and plots of k_{obs} against concentration of toluene are shown in Figure 2.6. Activation parameters derived from variable temperature kinetic data for naphthalene and pyrene complexes shown in Table 2.6 were determined from plots of ln(k/T) against 1/T.

Plots of k_{obs} vs. [toluene] for the reaction

(polyene)$Cr(CO)_3$ + toluene ⟶ (toluene)$Cr(CO)_3$ + polyene

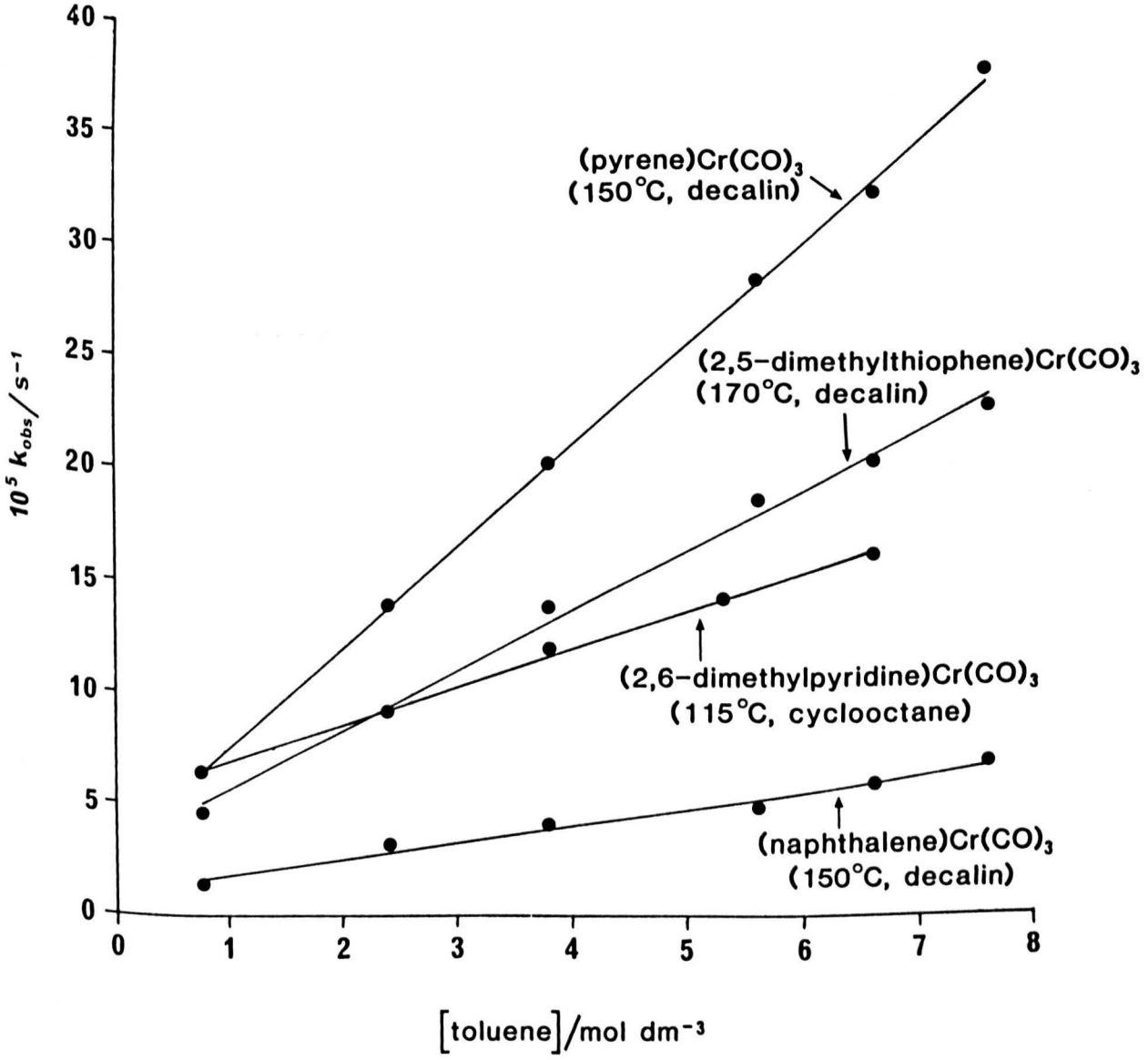

Fig. 2.6

2.3.2 Observed Rate Law and Postulated Mechanism

Polyene lability follows the order 2,6-dimethylpyridine > pyrene > naphthalene > 2,5-dimethylthiophene. At 150 °C exchange between toluene and the $Cr(CO)_3$ complexes of styrene, octamethylnaphthalene and cycloheptatriene were too slow to be kinetically useful. Recent calorimetric results[33-35] show that (cycloheptatriene)$Cr(CO)_3$ is thermodynamically more stable than (toluene)$Cr(CO)_3$ by approximately 20.5 kJ mol^{-1}, equivalent to an equilibrium constant for the reaction

$$(chpt)Cr(CO)_3 + \text{toluene} \rightleftharpoons (\text{toluene})Cr(CO)_3 + chpt$$

at 150 °C of approximately 2.9×10^{-3}. However, at the concentrations used in our experiments [(chpt)$Cr(CO)_3$, 10^{-3} mol dm^{-3}; toluene, 6 mol dm^{-3}], 95% of the bound chromium should be present as (toluene)$Cr(CO)_3$ at thermodynamic equilibrium. The lack of reactivity of (chpt)$Cr(CO)_3$ towards exchange is therefore kinetic rather than thermodynamic in origin, though the opposite may be true to account for the low reactivity of (styrene)$Cr(CO)_3$ and (octamethylnaphthalene)$Cr(CO)_3$, for which there is no thermodynamic data.

All reactions monitored exhibit first order rate behaviour with respect to loss of substrate. Furthermore, the first order rate constant k_{obs} is independent of any variation in initial substrate concentration at both high and low concentrations of toluene, confirming the experimental rate law as

$$\frac{-d[S]}{dt} = k_A[(\text{polyene})Cr(CO)_3] + k_B[(\text{polyene})Cr(CO)_3][\text{toluene}] \quad (2.2)$$

with $k_{obs} = k_A + k_B[\text{toluene}]$ (2.3)

The observed rate law is thus consistent with Strohmeier's exchange study of (naphthalene)$Cr(CO)_3$ using ^{14}C-naphthalene[15] though our k_A value for exchange of (naphthalene)$Cr(CO)_3$ with toluene at 145 °C in cyclooctane (0.98×10^{-5} s^{-1}) is smaller by about a factor of 50 than the value reported by Strohmeier in cyclohexane at 140 °C (45.4×10^{-5} s^{-1}). Comparison of the rate constant k_B is not meaningful because of the difference in entering ligand.

Reactions of all substrates using concentrations of toluene greater than 0.75 mol dm^{-3} provide quantitative yields of (toluene)$Cr(CO)_3$. Though the rate law is maintained (for example, in the pyrene and naphthalene cases) down to almost pseudo-first order limiting conditions ([toluene] = 3×10^{-2} mol dm^{-3}, [substrate] = 1×10^{-3} mol dm^{-3}), reactions below toluene concentrations of about 0.75 mol dm^{-3} result in some formation of $Cr(CO)_6$, with a corresponding reduction in yield of (toluene)$Cr(CO)_3$. Table 2.2 demonstrates the variation of product formation with concentration of toluene for the $Cr(CO)_3$ complexes of pyrene and napthalene.

Table 2.2

	[toluene]/ mol dm^{-3}	% (toluene) $Cr(CO)_3$	% $Cr(CO)_6$
(naphthalene)$Cr(CO)_3$	0.76	>90	<5
	0.19	85-90	5-10
	0.10	80-85	5-10
	0.03	75	15
	0.00	-	30
(pyrene)$Cr(CO)_3$	0.76	>95	0
	0.38	>90	<5
	0.19	>90	5-10
	0.10	85-90	5-10
	0.05	85	10
	0.00	-	20

Thermal decomposition of both (naphthalene) - and (pyrene)$Cr(CO)_3$ in the absence of toluene proceeds at rates which are approximately one-half the value of the extrapolated intercepts of the plots in Figure 2.6. These intercepts, however, represent a genuine kinetic pathway to product, and not simply a competitive decomposition. At concentrations of toluene greater than 0.75 mol dm^{-3} where yields of (toluene)$Cr(CO)_3$ are quantitative, the relative values of k_A and k_B show that the reaction is still carried mainly by the k_A term. Reaction of $Cr(CO)_3$ with toluene under the conditions used in the exchange does not occur, eliminating the possibility of an indirect formation of (toluene)$Cr(CO)_3$.

An experimental rate law of the type, equation 2.2, is not uncommon in organometallic reactions (see Chapter 1), and at least for the exchange or substitution of monodenate ligands, is generally interpreted as reflecting competing dissociative and I_d pathways. A mechanism which is different in character, but which we believe is most consistent with the rate law is shown in Scheme 2.10.

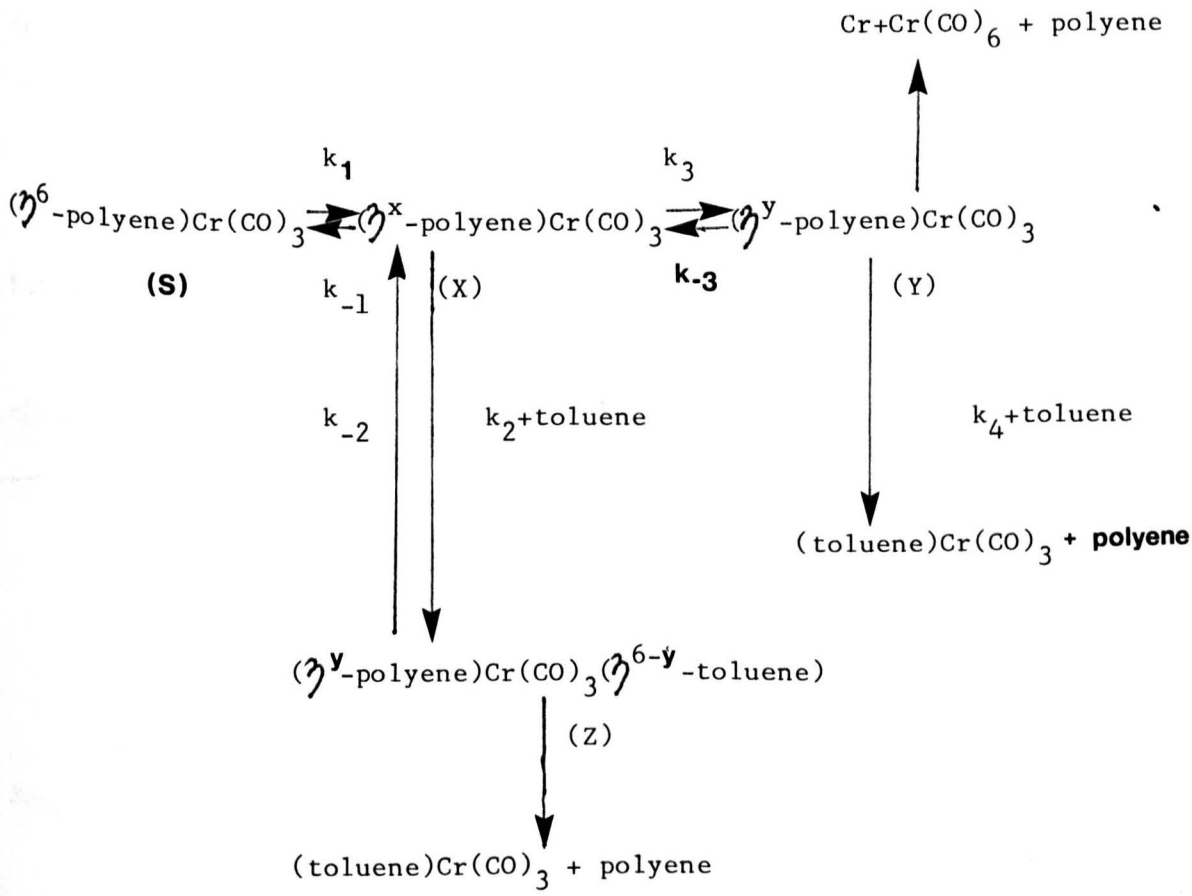

Polyene = naphthalene, pyrene etc.

Scheme 2.10

Derivation of the mechanistic rate law assuming steady state concentrations of the intermediates (X) and (Y) is as follows

$$\frac{-d[S]}{dt} = k_1[S] - k_{-1}[X] \qquad (2.4)$$

Assuming k_{-2} is negligible

$$\frac{d[X]}{dt} = k_1[S] + k_{-3}[Y] - [X](k_{-1} + k_3 + k_2[tol]) = 0 \qquad (2.5)$$

$$\frac{d[Y]}{dt} = k_3[X] - [Y](k_{-3} + k_4[tol]) = 0 \qquad (2.6)$$

$$[Y] = \frac{k_3[X]}{k_{-3} + k_4[tol]}$$

Substituting for [Y] in equation (2.5)

$$\frac{d[X]}{dt} = k_1[S] + \frac{k_3k_{-3}[X]}{k_{-3} + k_4[tol]} - [X](k_{-1} + k_3 + k_2[tol]) = 0$$

$$[X] = \frac{k_1[S](k_{-3} + k_4[tol])}{(k_{-1} + k_3 + k_2[tol])(k_{-3} + k_4[tol]) - k_3k_{-3}}$$

Substituting for [X] in equation (2.4)

$$\frac{-d[S]}{dt} = k_1[S] - \frac{k_1k_{-1}[S](k_{-3} + k_4[tol])}{(k_{-1} + k_3 + k_2[tol])(k_{-3} + k_4[tol]) - k_3k_{-3}}$$

$$= \frac{(k_1k_3k_{-3} + k_1k_3k_4[tol] + k_1k_2k_4[tol]^2)[S]}{(k_{-1} + k_3 + k_2[tol])(k_{-3} + k_4[tol]) - k_3k_{-3}}$$

Assuming $k_{-1} >> k_3 + k_2[tol]$ then

$$\frac{-d[S]}{dt} = \frac{(k_1k_3k_{-3} + k_1k_3k_4[tol] + k_1k_2k_4[tol]^2)[S]}{k_{-1}k_{-3} + k_{-1}k_4[tol]} \qquad (2.7)$$

Assuming k_{-3} is small compared to the rate constants involving the formation of $Cr(CO)_6$ and (toluene)$Cr(CO)_3$ this equation reduces to

$$\frac{-d[S]}{dt} = \frac{(k_1k_3k_4[tol] + k_1k_2k_4[tol]^2)[S]}{k_{-1}k_4[tol]}$$

$$= \frac{k_1k_3[S]}{k_{-1}} + \frac{k_1k_2[tol][S]}{k_{-1}} \qquad (2.8)$$

which is the same as equation 2.1

$$\frac{-d[S]}{dt} = k_A[S] + k_B[S][tol] \qquad (2.1)$$

where $k_A = k_1k_3/k_{-1}$ and $k_B = k_1k_2/k_{-1}$

The mechanism may thus be viewed chemically as a progressive reversible slippage to (X), followed by reversible slippage to (Y), with both intermediates energetically accessible and contributing significantly to the overall reaction rate. Values of x and y cannot be calculated from experimental data but may to some extent be defined from molecular orbital calculations.

2.3.2 Effect of variation of entering arene

The exchange of pyrene in (pyrene)$Cr(CO)_3$ for monocyclic arenes and cycloheptatriene is consistent with the mechanism shown in Scheme 2.10. A series of rate plots is obtained, with slopes which are ligand dependent, but with a common intercept (Figure 2.7).

Omitting hexamethylbenzene, where precision is limited due to the limited solubility of the ligand, no intercept value is further than 4σ from the average, which is consistent with a pathway independent of the nature of the ligand.

The slopes may be taken as a measure of the relative affinity of the different polyenes for intermediate (X) as the rate constant associated with this value is ligand dependent. These values span a range of about 100 and increase in the order $C_6H_5CF_3$ < C_6H_5Me < $m\text{-}C_6H_4Me_2$ < $C_6H_5Bu^t$ < C_6Me_6 < 1,3,5-cycloheptatriene. Measurements of relative rates at a single arene concentration in the xylene series show a reactivity order ortho(1.0) = meta(1.0) < para(1.2). Thermodynamic stability of the (xylene)$Mo(CO)_3$ complexes shows a similar ordering, ortho < meta $\simeq$ para[36]. Exchange between (pyrene)$Cr(CO)_3$ and arenes such as $C_6H_5CH_2CO_2Me$ which contain a Lewis base donor site is complete within minutes at 150 ^oC.

Plots of k_{obs} vs. [polyene] for the reaction

$(\eta^6\text{-pyrene})Cr(CO)_3$ + polyene ⟶ $(\eta^6\text{-polyene})Cr(CO)_3$ + pyrene

in decalin at 150°C

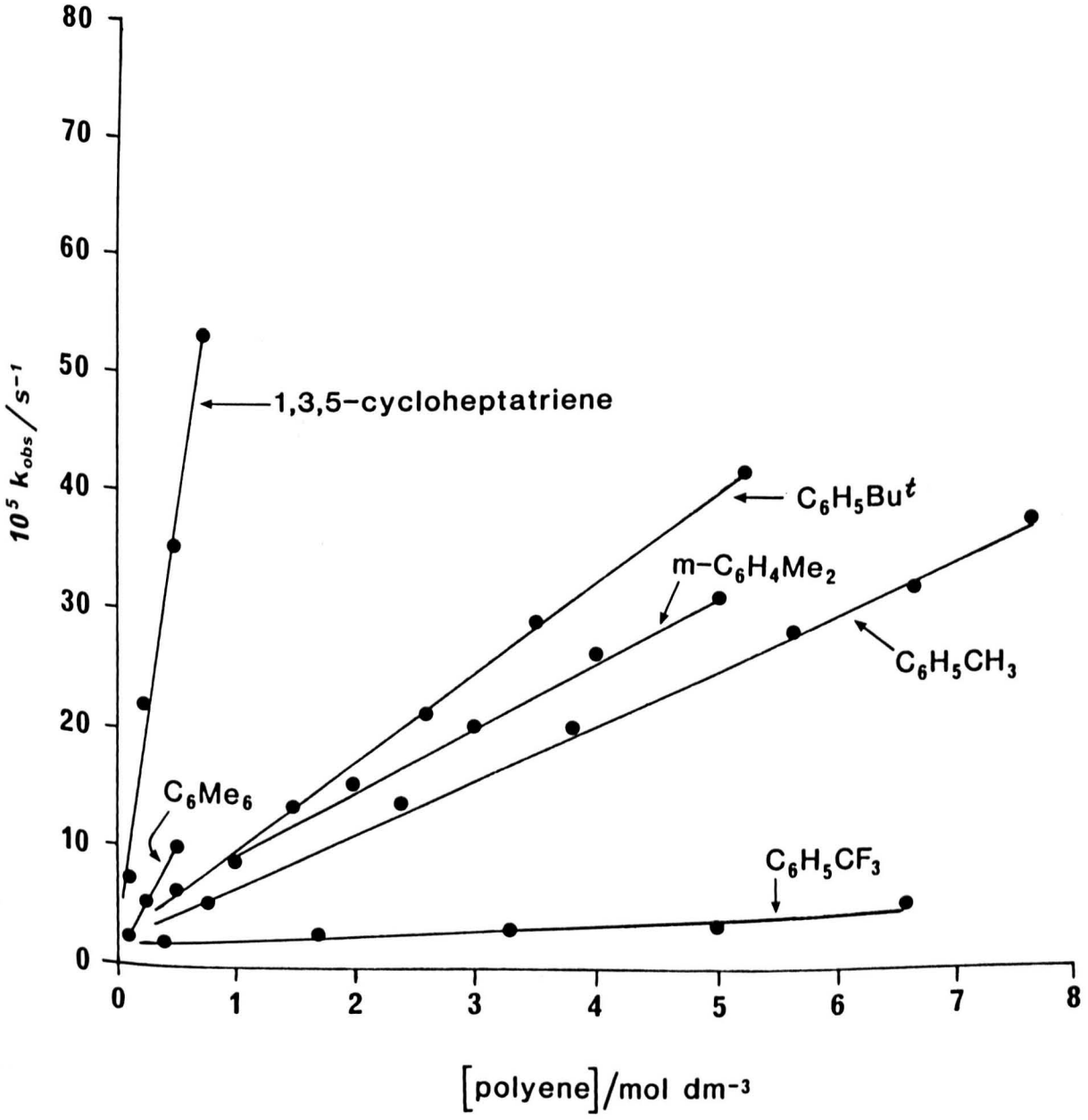

Fig 2.7

The above ordering is the same as that qualitatively observed for the reaction of $Mo(CO)_6$ with these arenes and cycloheptatriene[37-40]. At least for the arenes there is a direct correlation between increasing reaction rate and the increase in thermodynamic stability of the product complex resulting from increased methyl substitution[33-35]. Cycloheptatriene is different; although it exhibits the highest k_B value, recent results show its ground state bond enthalpy contribution to be between Cr-toluene and Cr-mesitylene[33]. It has been suggsted[34] that in the ground state, metal coordination of an arene results in some loss of resonance energy, whereas cycloheptatriene is stabilised by metal coordination, and such arguments, applied to the transiton state interaction of the coordinatively unsaturated (η^x-pyrene)$Cr(CO)_3$ intermediate with incoming ligand, may explain the greater kinetic reactivity of cycloheptatriene. Such a reversal of ordering is not unknown, although cis-2-pentene reacts more rapidly than 1-pentene with $W(CO)_5$(acetone), the terminal alkene forms the more thermodynamically stable $W(CO)_5$(alkene) complex[41].

The k_B[S][toluene] term in equation 2.2 is a typical example of substitution reactions of arene and cycloheptatriene complexes of both Mo and Cr with group V ligands[42-48]. In common with these reactions, this term may be interpreted as either a dissociative slippage shown in Scheme 2.10 (ie a discrete (η^x-polyene)$Cr(CO)_3$ intermediate) or an associative pathway (probably I_d) in which slippage and attack of entering ligand are concerted.

2.3.4 Interpretation of the k_A term

The $k_A[S]$ term requires some comment since at least three different interpretations from that presented in Scheme 2.10 have been discussed in the literature.

(i) As with Strohmeier's original postulate it may represent a dissociation to $Cr(CO)_3$ followed by rapid coordination of incoming polyene[15]. Following Traylor[20], we have sought to examine the potential viability of a $Cr(CO)_3$ intermediate by application of the three phase test[49] in the following reaction

$$(\text{dvb-2-vn})Cr(CO)_3 + \text{dvb-st} \rightarrow (\text{dvb-st})Cr(CO)_3 + \text{dvb-2-vn}$$

dvb-2-vn = copoly(divinylbenzene-2-vinylnaphthalene)

dvb-st = copoly(divinylbenzene-styrene)

The test is a method for the detection of reaction intermediates and involves the generation of an intermediate from an insoluble polymer bound precursor and its trapping by a second solid phase suspended in the same reaction mixture. The insoluble properties required of the two polymers are achieved by incorporation of small amounts (5-10%) of a cross-linking reagent, in this case divinylbenzene. Although the copolymer of divinylbenzene-styrene is commercially available only homopolymeric solvent soluble vinylnaphthalene is available. Hence preparation of its copolymer with divinylbenzene was necessary.

Red $(\text{dvb-2-vn})Cr(CO)_3$ prepared by the complexation method used for $(\text{naphthalene})Cr(CO)_3$ contains about 8% chromium by weight bound to both naphthalene and monocyclic rings (divinylbenzene and ethylstyrene) together with some decomposition product.

Preparation of (naphthalene)$Cr(CO)_3$ also involves formation of this decomposition product. However, preparation of yellow monocyclic aromatic $Cr(CO)_3$ complexes is a relatively clean process with virtually no decompostion product formed. The naphthalene-bound chromium may be determined and differentiated from monocyclic-bound and oxidative chromium deposits by selective reaction of the copolymer with toluene to give (toluene)$Cr(CO)_3$, or with $P(OMe)_3$ to give fac-$[P(OMe)_3]_3Cr(CO)_3$, both under conditions where (dvb-st)$Cr(CO)_3$ is unreactive. The naphthalene-bound chromium may thus be estimated at about 13% of the total amount of chromium present. Polymeric complexes recovered after extraction by toluene or $P(OMe)_3$ are yellow in colour and exhibit infrared spectra which are indistinguishable in the CO stretching region from (dvb-st)$Cr(CO)_3$. In common with (naphthalene)$Cr(CO)_3$ the (dvb-2-vn)$Cr(CO)_3$ complex undergoes thermal decomposition in the absence of toluene to produce about a 30% yield of $Cr(CO)_6$ (based on naphthalene-bound chromium) under conditions where (dvb-st)$Cr(CO)_3$ is unreactive.

Catalysed bead-to-bead exchange may be accomplished; the most efficient catalyst being 2,6-dimethylnaphthalene. Thus reaction of (dvb-2-vn)$Cr(CO)_3$ with copoly(divinylbenzene-styrene) in the presence of 2,6-dimethylnaphthalene initially develops a red solution colour due to formation of (2,6-dimethylnaphthalene)$Cr(CO)_3$ which fades with time to yield yellow beads and an essentially colourless solution containing no $Cr(CO)_6$. In contrast, attempts at uncatalysed bead-to-bead exchange result only in the formation of $Cr(CO)_6$ in an amount equivalent to that formed from the thermolysis of (dvb-2-vn)$Cr(CO)_3$ in the absence of copoly(divinylbenzene-styrene).

The results suggest that any "$Cr(CO)_3$" intermediate produced by Cr-naphthalene bond dissociation has too short a lifetime to allow diffusion to another polyene site before decompositon to "Cr" and CO.

Finally, the substantial negative $\Delta S^{\ddagger}$ values associated with k_A (Table 2.6) are not consistent with such a dissociative process. The values imply a substantially more ordered nature for intermediate (Y), and it is instructive to compare these $\Delta S^{\ddagger}$ values with that of -96 J K^{-1} mol^{-1} obtained for haptotropic ring exchange in (naphthalene)$Cr(CO)_3$[50] for which molecular orbital calculations indicate an η^3-intermediate/transition state[51].

(ii) The k_A term may represent a bimolecular catalysis of the exchange by substrate polyene complex, product polyene complex, or both. Recently[20] the exchange reaction

$$(\text{benzene})Cr(CO)_3 + \text{mesitylene} \rightarrow (\text{mesitylene})Cr(CO)_3 + \text{benzene}$$

has been shown to obey the rate law

$$\frac{-d[S]}{dt} = k_A[(\text{benzene})Cr(CO)_3]([(\text{benzene})Cr(CO)_3] + [(\text{mesitylene})Cr(CO)_3]) + k_B[(\text{benzene})Cr(CO)_3][\text{mesitylene}] \qquad (2.9)$$

While the values of k_A and k_B (3.8×10^{-7} and 2.1×10^{-7} mol^{-1} dm^3 s^{-1} respectively at 170 °C in cyclohexane) are about 100 times less than our results for pyrene/toluene exchange at 150 °C, the k_A/k_B ratio is comparable.

Combined with the demonstration that $(C_6Me_6)Cr(CO)_3$ functions as a catalyst for arene exchange without undergoing exchange itself, the implication of this recent work is that the $k_C[S]^2$ term of Strohmeier may better be represented as

$$\frac{-d[S]}{dt} = k_c[S]([S] + [(\text{polyene})Cr(CO)_3]) \quad (2.10)$$

where $[S] + [(\text{polyene})Cr(CO)_3]$ represents the total $(\text{polyene})Cr(CO)_3$ concentration, and is constant. Catalysis may occur through the formation of an intermediate such as

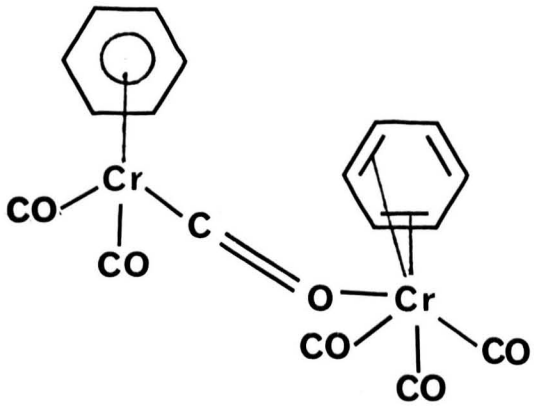

Fig. 2.8

which undergoes rapid exchange of the η^4-ring, with both substrate and product being catalytically active. As written, equation 2.9 implies an equal catalytic activity of both substrate and product, and while this is almost certainly true for the isotopic exchange results of Strohmeier, it would be coincidental in the benzene/mesitylene reaction above. A catalytically more active substrate would render the initial rate of the reaction sensitive to the initial concentration of the substrate. A catalytically more active product would initially show a rate increase, followed by a decrease as substrate is consumed. Added product at the start of a reaction should increase the rate depending on the amount added.

In this work neither substrate nor product catalysis is apparent as the complexes of naphthalene, pyrene and 2,6-dimethylpyridine show no variation of first order rate constant with changes in substrate concentration or added product (Table 2.3). Additionally all kinetic runs give rise to linear plots of ln[substrate] against time. The exchange of $(pyrene)Cr(CO)_3$ with $C_6H_5Bu^t$, is however weakly catalysed by $(C_6Me_6)Cr(CO)_3$ and at 150 ^oC is strongly catalysed by tetrahydrofuran (10:1 molar excess, reaction complete within minutes in 8 mol dm^{-3} toluene)[32].

(iii) As originally postulated by Pauson[10] the k_A term may represent rate determining CO dissociation followed by rapid polyene exchange and recoordination of CO. We have not been able to examine the influence of external CO on the rate of polyene exchange because of rapid formation of $Cr(CO)_6$. However the results of Traylor[52] on monocyclic arene complexes are not consistent with this mechanism. He has recently reported studies on the non-dissociative CO exchange reaction

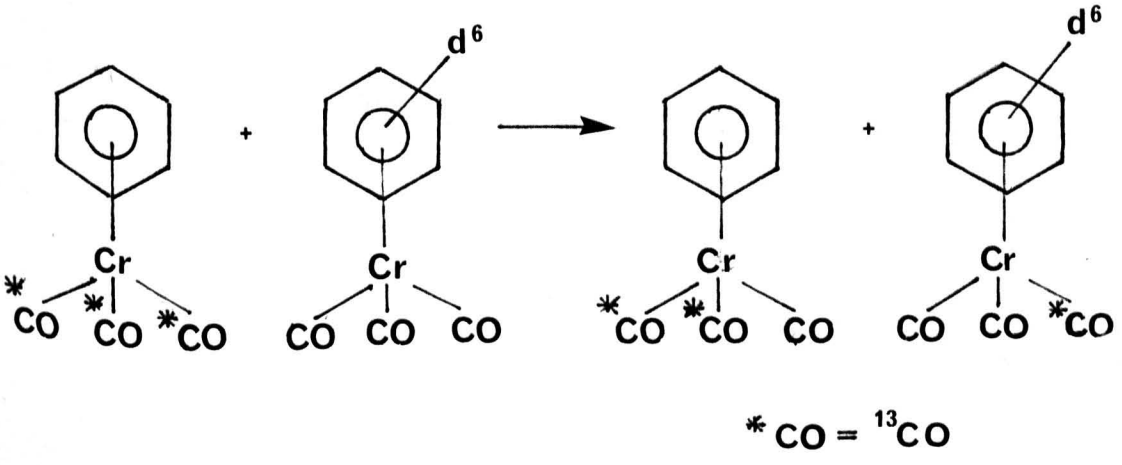

Scheme 2.11

in the absence of free arene and in the presence of free mesitylene which also yields the product of arene exchange. Internal CO exchange and arene exchange are postulated to proceed via the CO-bridged dimer (A) in Scheme 2.12.

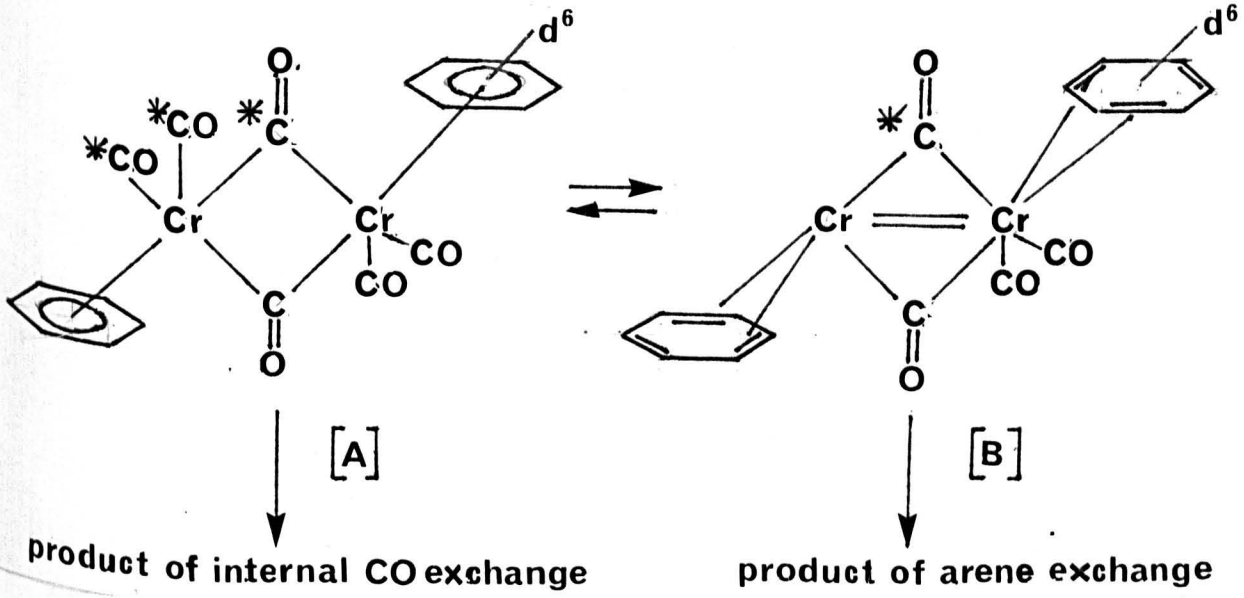

Scheme 2.12

However. the bimolecular rate constant for the formation of the bridge species (A) (8×10^{-5} mol^{-1} dm^3 s^{-1} at 170 °C) is ten times larger than the rate of arene exchange. implying as postulated that a further intermediate assigned structure (B) is responsible for arene exchange and lies at considerably higher energy. From the reported rate constants, the rate of formation of the bridged species (A) at a substrate concentration of 10^{-3} mol dm^{-3} may be calculated as 8×10^{-11} mol dm^{-3} s^{-1} at 170 °C. It seems likely (vide infra) that the rate for such a process in (naphthalene)- or (pyrene)Cr(CO)$_3$ should be similar. The rate of exchange (naphthalene)Cr(CO)$_3$ with toluene at 175 °C at substrate concentration 10^{-3} mol dm^{-3} and toluene concentration of 1 mol dm^{-3} is 3×10^{-8} mol dm^{-3} s^{-1}. Thus it seems unlikely on kinetic grounds that formation of a bridged intermediate of type (A) represents a reasonable mechanistic pathway for exchange in the reaction reported here.

It is reasonable to assume that since formation of the bridged species (A) involves alteration of the M-CO bonding arrangement only, the rate of such a process should not depend significantly on the metal-polyene bonding interaction Indeed, there is no ground state, spectroscopic or crystallographic evidence that in the more ring-labile complexes such as (naphthalene)$Cr(CO)_3$ the M-CO bonds are more labile. A decreasing value for the infrared ν_{CO} stretching frequency has been taken as a measure of increasing M-CO back bonding and therefore M-CO bond strength. Comparison of the highest frequency values for (benzene)$Cr(CO)_3$ (1978 cm^{-1}) and (naphthalene)$Cr(CO)_3$ (1974 cm^{-1}) indicate little difference in the nature of the M-CO bond. Indeed, changes of substituents in monocyclic arene complexes show more substantial variations in these values (for example $C_6H_5CF_3$, 1994 cm^{-1}; C_6Me_6, 1952cm^{-1}). Crystallographic data also show little ground state difference; the M-CO bond length in (benzene)$Cr(CO)_3$ is 1.842 Å, while that for (naphthalene)$Cr(CO)_3$ is 1.821 Å.

Thus these data not only show the unlikelihood of internal CO exchange at the temperatures used in the naphthalene exchange but also provide further circumstantial evidence that neither substrate nor product polyene complex catalyses polyene exchange in the reaction studied in this work.

A reaction profile that most likely represents a realistic picture of the arene exchange pathway is shown in Figure 2.9. $\Delta G^{\ddagger}$ values associated with the rate constants of Scheme 2.10 may be calculated at 150 °C from the activation parameters associated with k_A and k_B (Table 2.6)

Reaction Profile for Polyene Exchange

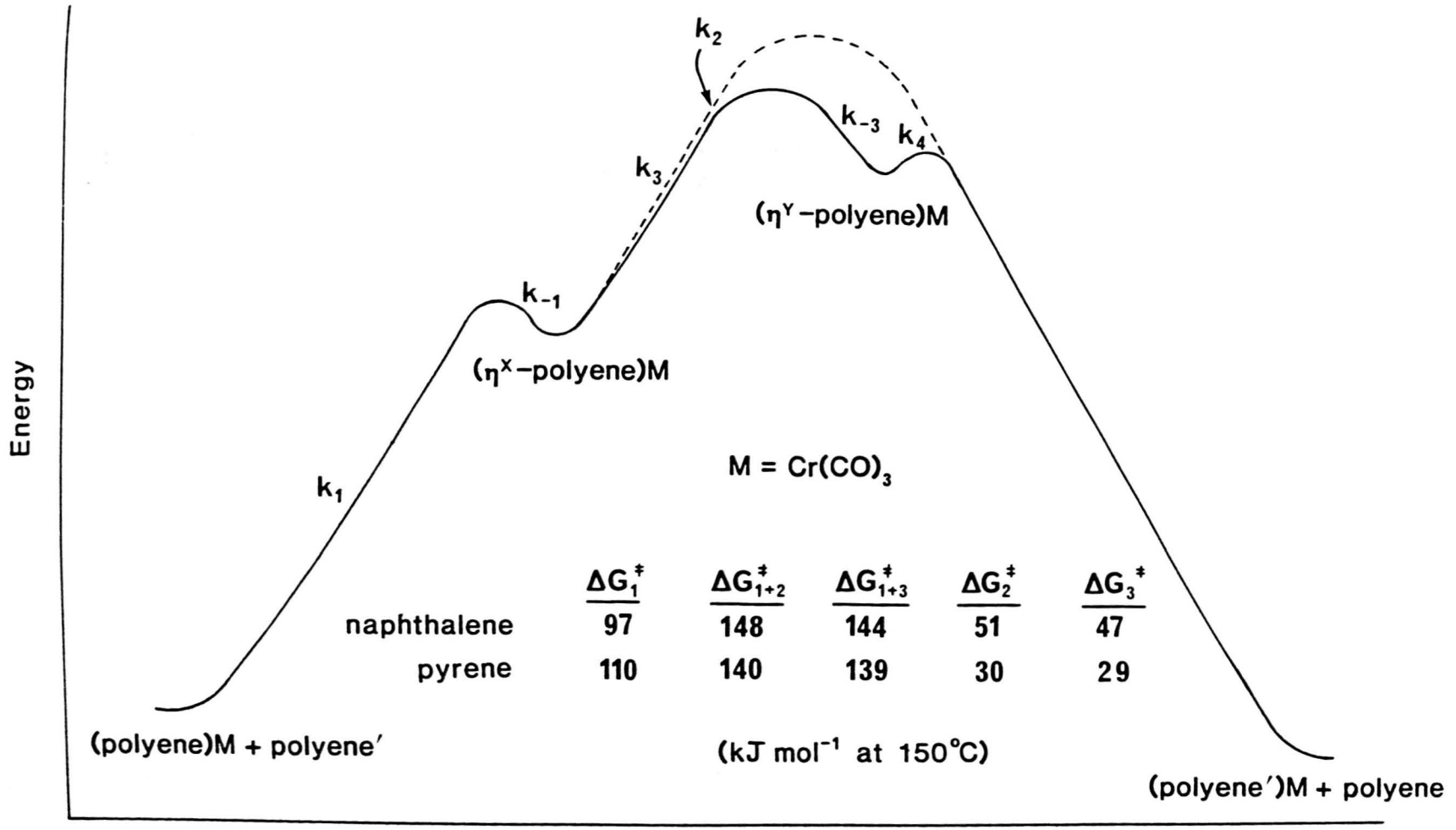

	$\Delta G_1^{\ddagger}$	$\Delta G_{1+2}^{\ddagger}$	$\Delta G_{1+3}^{\ddagger}$	$\Delta G_2^{\ddagger}$	$\Delta G_3^{\ddagger}$
naphthalene	97	148	144	51	47
pyrene	110	140	139	30	29

(kJ mol^{-1} at 150°C)

Fig. 2.9

Thus on the assumption that $\Delta G^{\ddagger}_{-1}$ is relatively small compared to $\Delta G^{\ddagger}_{2}$ and $\Delta G^{\ddagger}_{3}$ (as $k_{-1} >> k_2[\text{toluene}] + k_3$) then.

$$\Delta G^{\ddagger}_{A} = \Delta G^{\ddagger}_{1} + \Delta G^{\ddagger}_{3} \quad (\Delta G^{\ddagger}_{1+3} \text{ Figure 2.9})$$

and $$\Delta G^{\ddagger}_{B} = \Delta G^{\ddagger}_{1} + \Delta G^{\ddagger}_{2} \quad (\Delta G^{\ddagger}_{1+2} \text{ Figure 2.9})$$

Values of $\Delta G^{\ddagger}_{A}$ and $\Delta G^{\ddagger}_{B}$ are very similar, consistent with significant contributions of both k_A and k_B terms to the overall rate. Since limiting rates cannot be seen at high concentration of incoming polyene, individual values of $\Delta G^{\ddagger}_{1}$, $\Delta G^{\ddagger}_{2}$ and $\Delta G^{\ddagger}_{3}$ cannot be evaluated. However, limiting rate behaviour is observed in the phosphite substitution reactions (See Chapter 3)

$$(\eta^6\text{-polyene})Cr(CO)_3 + 3P(OMe)_3 \longrightarrow [P(OMe)_3]_3Cr(CO)_3 + \text{polyene}$$

polyene = pyrene, naphthalene, 2,5-dimethylthiophene, cycloheptatriene

for which the following mechanism may be postulated

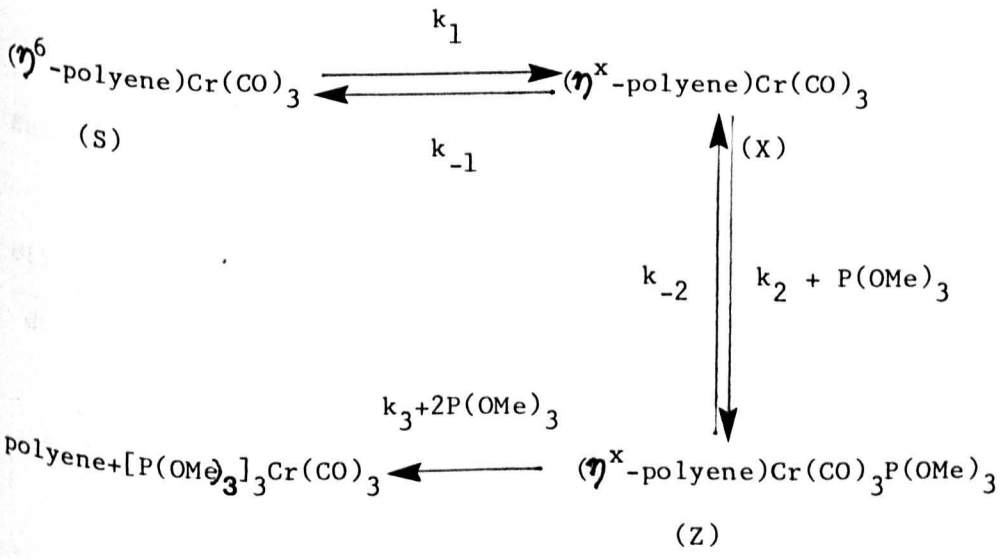

Scheme 2.13

Assuming a steady state concentration of the intermediates (X) and (Z). derivation of the rate equation is as follows

$$\frac{-d[S]}{dt} = k_1[S] - k_{-1}[S][X] \qquad (2.10)$$

$$\frac{d[X]}{dt} = k_1[S] + k_{-2}[Z] - k_{-1}[X] - k_2[X][P(OMe)_3] = 0 \qquad (2.11)$$

$$\frac{d[Z]}{dt} = k_2[X][P(OMe)_3] - k_{-2}[Z] - k_3[Z][P(OMe)_3] = 0$$

$$[Z] = \frac{k_2[X][P(OMe)_3]}{k_{-2}+k_3[P(OMe)_3]}$$

Assuming $k_3[P(OMe)_3] >> k_{-2}$ this reduces to

$$[Z] = \frac{k_2[X]}{k_3}$$

Substituting for [Z] in equation 2.11

$$\frac{d[X]}{dt} = k_1[S] + \frac{k_{-2}k_2[X]}{k_3} - k_{-1}[X] - k_2[X][P(OMe)_3] = 0$$

$$[X] = \frac{k_1[S]}{k_{-1} + k_2[P(OMe)_3] - k_{-2}k_2/k_3}$$

$$= \frac{k_1k_3[S]}{k_{-1}k_3 + k_2k_3[P(OMe)_3] - k_{-2}k_2}$$

Substituting for [X] in equation 2.10

$$\frac{-d[S]}{dt} = k_1[S] - \frac{k_1k_3k_{-1}[S]}{k_{-1}k_3 + k_2k_3[P(OMe)_3] - k_{-2}k_2}$$

$$\frac{-d[S]}{dt} = \frac{k_1k_2k_3[S][P(OMe)_3] - k_1k_2k_{-2}[S]}{k_{-1}k_3 + k_{2\ 3}[P(OMe)_3] - k_2k_{-2}}$$

Again, assuming that $k_3[P(OMe)_3] >> k_{-2}$ this equation reduces to

$$\frac{-d[S]}{dt} = \frac{k_1k_2[S][P(OMe)_3]}{k_{-1} + k_2[P(OMe)_3]} \qquad (2.12)$$

At low $[P(OMe)_3]$ such that $k_{-1} >> k_2[P(OMe)_3]$ this equation becomes

$$\frac{-d[S]}{dt} = \frac{k_1k_2[S][P(OMe)_3]}{k_{-1}} \qquad (2.13)$$

At high $[P(OMe)_3]$ such that $k_2[P(OMe)_3] >> k_{-1}$ equation 2.12 becomes

$$\frac{-d[S]}{dt} = k_1[S] \qquad (2.14)$$

Rearranging equation 2.12 leads to the equation

$$\frac{1}{k_{obs}} = \frac{1}{k_1} + \frac{k_{-1}}{k_1k_2[P(OMe)_3]} \qquad (2.15) \qquad \text{where } k_{obs} = \frac{-d[S]}{dt} \Big/ [S]$$

hence k_1 and k_2k_1/k_{-1} may be evaluated from plots of $1/k_{obs}$ against $1/[P(OMe)_3]$ (See Chapter 3). On the assumption that the value of x is the same in Schemes 2.10 and 2.13, the activation parameters associated with k_1 provide a guide to the value of $\Delta G_1^{\ddagger}$ at 150 °C in Figure 2.9. Hence evaluation of $\Delta G_2^{\ddagger}$ and $\Delta G_3^{\ddagger}$ is possible. For both pyrene and naphthalene complexes, the results imply a significant barrier for interaction of (η^x-polyene)$Cr(CO)_3$ (X) with incoming polyene which is approximately equal to the energy required for further slippage to (η^y-polyene)$Cr(CO)_3$ (Y).

Information relating to the hapticity or structure of intermediates (X) and (Y) cannot be obtained from kinetic data. However, theoretical calculations can provide some indication. By deriving potential energy surfaces, the slippage of an ML_n group across the aromatic ring can be considered in terms of the topology of interacting orbitals. The method, although requiring approximations has been applied to a number of systems, and in some cases can be shown to be consistent with experimental data.

The following discussion is based on such theoretical studies carried out at the University of Houston, USA by Professor T.A.Albright and co-workers[53,54].

Mechanisms for the exchange reaction may involve slippage of the $Cr(CO)_3$ towards a carbon-carbon double bond ($\eta^6 - \eta^4 - \eta^2$ path A Figure 2.10) or towards a carbon atom ($\eta^6 - \eta^3 - \eta^1$ path B figure 2.10)

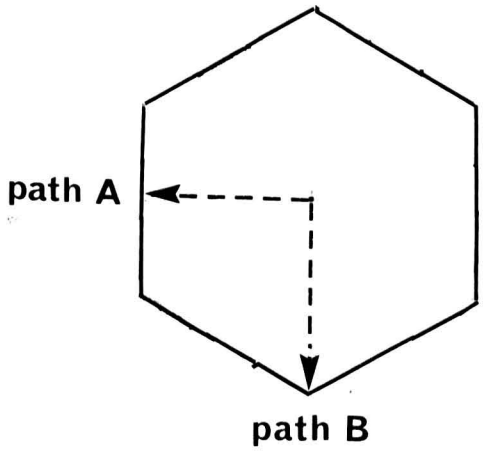

Fig. 2.10

Consider for example slippage of the $Cr(CO)_3$ moiety in (naphthalene)$Cr(CO)_3$. An overall interaction diagram for the ground state complex is shown in Figure 2.11. The orbitals la_1 and le on $Cr(CO)_3$ are filled as it is a d^6 complex. The orbitals are labelled with s or a subscripts according to whether the orbital is symmetric or antiysmmetric to the yz mirror plane. Both the $1\pi_a$ and $2\pi_a$ orbitals on naphthalene are stabilised by the $2e_a$ on the $Cr(CO)_3$ giving a typical 3 orbital pattern; (1) $1\pi_a$ + $2e_a$ containing some $2\pi_a$ bonding with respect to $2e_a$, (2) $2\pi_a$ + $2e_a$ containing some $1\pi_a$ antibonding with respect to $2e_a$, and (3) the highest molecular orbital (not shown) is mainly $2e_a$ antibonding with respect to $1\pi_a$ and $2\pi_a$. The $3\pi_s$ level of naphthalene is stabilised by $2e_s$ giving the molecular orbital $3\pi_s$ + $2e_s$, and the $2\pi_s$ and $1\pi_s$ levels on naphthalene are stabilised by $2a_1$ on $Cr(CO)_3$.

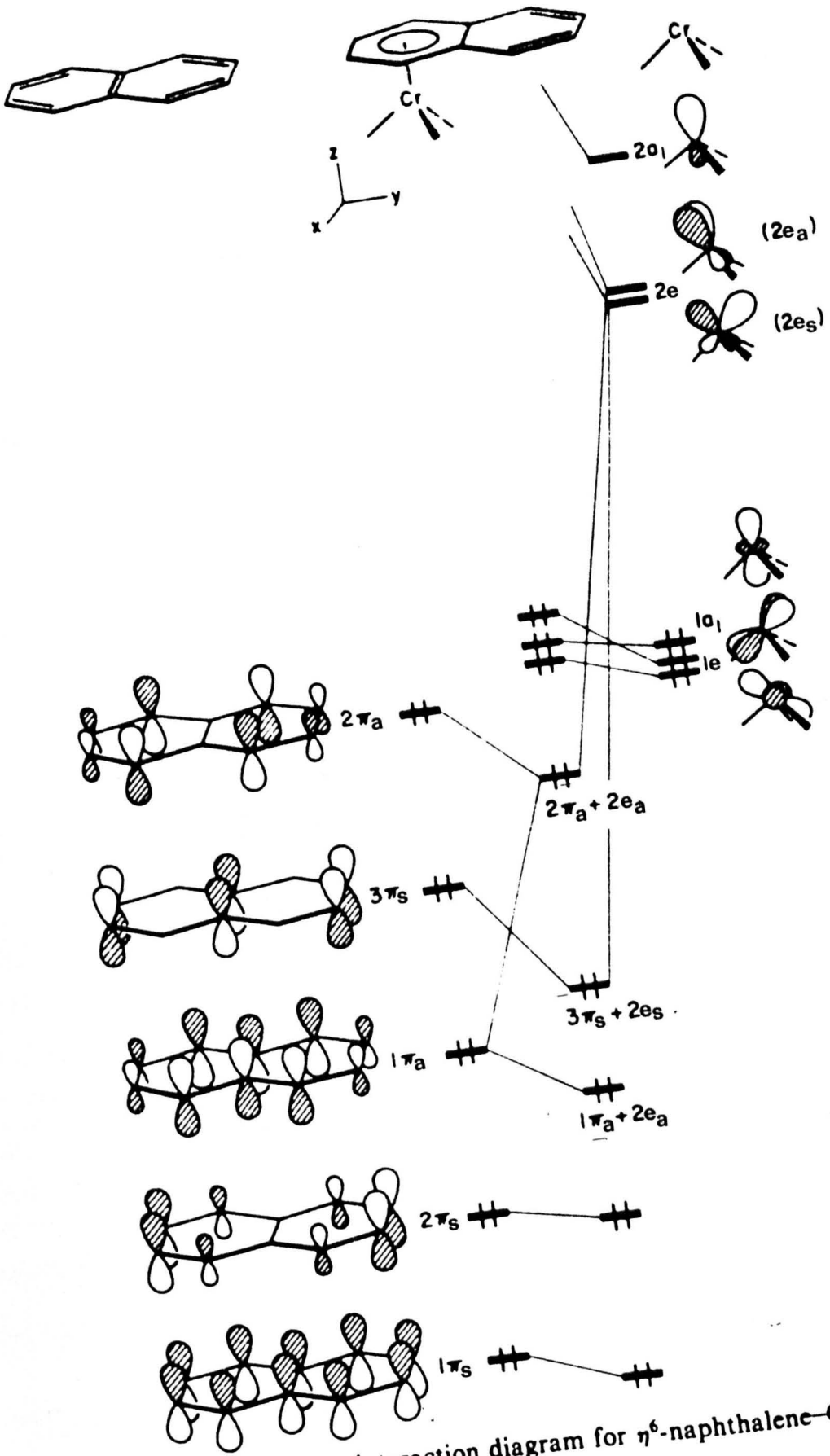

Orbital interaction diagram for η^6-naphthalene–$Cr(CO)_3$.

Fig. 2.11

Slipping the $Cr(CO)_3$ moiety from η^6 coordination to η^4 coordination causes a filled orbital mainly localised on naphthalene shown in Figure 2.12 to rise to an energy higher than it is at η^6 ($3\pi_s + 2e_s$. Figure 2.11)

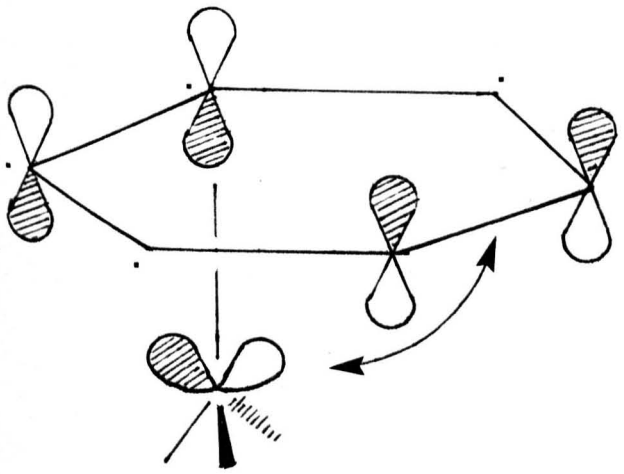

• denotes carbon atom in complexation

only the complexed ring is shown for clarity

Fig. 2.12

These calculations do not indicate that the slipped η^4 structure shown has a discrete energy minimum, and is therefore in disagreement with the substitution reaction kinetics, which in view of the limiting rate at high $[P(OMe)_3]$ indicates a shallow minimum on the energy profile diagram. However, stabilisation of this η^4 species may be achieved by bending the uncomplexed portion of the ring towards the $Cr(CO)_3$ moiety, thus enhancing the interaction between in phase lobes on the chromium and the ring. (Fulvene)$Cr(CO)_3$ complexes (Figure 2.13) provide examples of a distortion of this type in the ground state molecule.

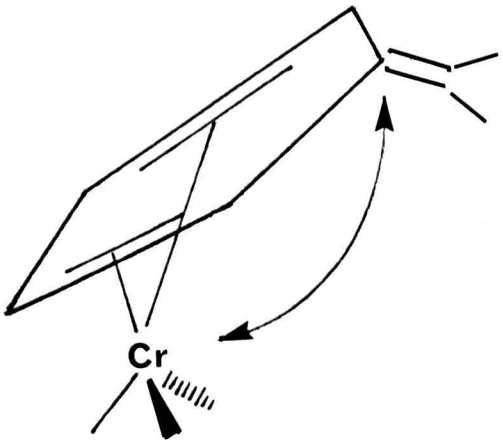

Fig. 2.13

Alternatively increased solvent-complex interactions may produce such a shallow intermediate. Hydrocarbon solvents are known to weakly interact with coordinatively unsaturated complexes such as $Cr(CO)_5$ in both low temperature solid matrices and in hydrocarbon solutions.

Approach of incoming polyene towards the simple slipped 16-electron η^x-structure involves the transfer of electron density from the highest occupied molecular orbital (HOMO) on the polyene to the lowest unoccupied molecular orbital (LUMO) of the complex (Figure 2.14). Population of this orbital generates an antibonding interaction between the metal and the uncomplexed portion of the naphthalene ring, which may be relieved by bending the uncomplexed portion away from the metal. Such a structure may therefore represent the energy minimum for the 18-electron (η^4-polyene)$Cr(CO)_3L$ intermediate, where L represents a 2-electron donor ligand.

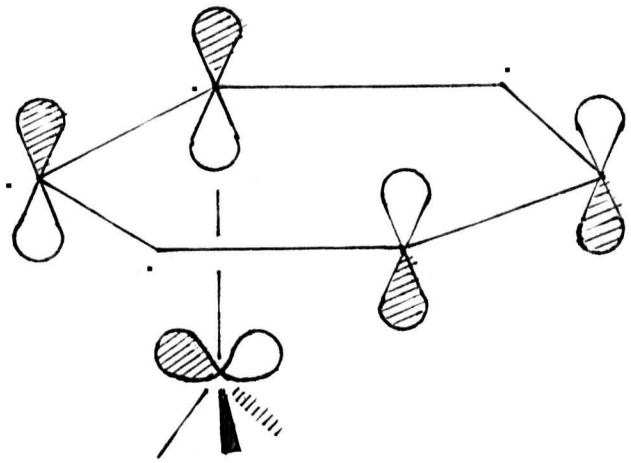

Fig. 2.14

It may also be noted that the orientation of the LUMO in a simple 16-electron η^4-structure is not suitable in steric terms for interaction with incoming ligand. The spatial properties may be improved by either bending of the uncomplexed portion of the polyene away from the metal, or by distortion of the $Cr(CO)_3$ group.

Calculations on (benzene)$Cr(CO)_3$ indicate an energy of 42 kJ mol^{-1} for the simple $\eta^6 - \eta^4$ slippage whereas an additional 63 kJ mol^{-1} is required to bend the uncomplexed C-C unit. Distortion of the $Cr(CO)_3$ group to a more spatially suited structure such as in Figure 2.15 requires a further 70 kJ mol^{-1} making a total of 133 kJ mol^{-1} additional to the 42 kJ mol^{-1} required for the simple $\eta^6 - \eta^4$ slippage[54].

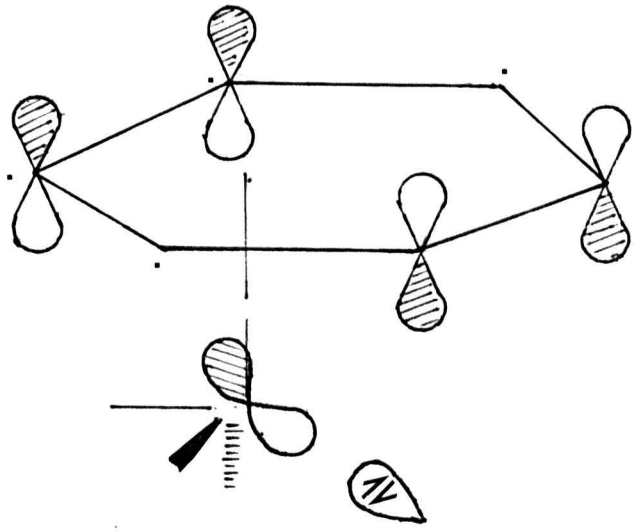

Figure. 2.15

The substitutional energy barrier experimentally found for $\Delta G_2^{\ddagger}$ corresponding to the transformation (η^x-polyene)Cr(CO)$_3$ ⟶ (η^y-polyene)Cr(CO)$_3$(η^{6-y}-polyene') of Scheme 2.10 is therefore consistent with the significant calculated energy barrier for this process in (benzene)Cr(CO)$_3$.

The competing pathway to that of polyene attack at the intermediate (η^x-polyene)Cr(CO)$_3$ is further slippage to (η^y-polyene)Cr(CO)$_3$. Orbitals involving η^2 coordination are shown in Figure 2.16

Fig. 2.16

Both are filled orbitals and mainly localised on naphthalene. Overlap in (A) is essentially zero with some overlap in (B). Establishing an overlap in (A) or strengthening the overlap in (B) is achieved by either tilting the naphthalene ligand such that the uncomplexed portion moves away from the metal and the complexed C-C unit moves towards the metal, or equivalently rotating the $Cr(CO)_3$ group. Both processes allow interaction of in phase lobes on the chromium atom with those on the naphthalene as shown in Figure 2.17. Such a structure may therefore represent the energy minimum for the η^2 coordination.

Fig. 2.17

For (pyrene)$Cr(CO)_3$, $\eta^6 - \eta^3 - \eta^1$ slippage (for which a similar approach to that above may be presented) is predicted in view of the low potential for $\eta^3 - \eta^1$ excursion, whilst $\eta^6 - \eta^4 - \eta^2$ slippage is more likely for the $Cr(CO)_3$ complexes for naphthalene and benzene. Thus, whilst the experimentally determined value of ΔG_1^* for (pyrene)$Cr(CO)_3$ (110 kJ mol^{-1} at 150 °C) is larger than the corresponding value for (naphthalene)$Cr(CO)_3$ (97 kJ mol^{-1} at 150 °C), the values for the slippage ΔG_3^* are 29 kJ mol^{-1} and 47 kJ mol^{-1} respectively, consistent with the above prediction.

Indeed. calculations involving the slippage of the MnCp group (η^6-η^y) in the complexes of pyrene, naphthalene and benzene show the order of reactivity to be pyrene > naphthalene >> benzene, in agreement with the lability order towards exchange in this work.

The order of lability of the complexes studied towards exchange (2.6-dimethylpyridine > pyrene > naphthalene > 2.5-dimethylthiophene > cycloheptatriene) contrasts to that of the lability towards that of substitution (naphthalene > cycloheptatriene > 2.5-dimethylthiophene > pyrene > 2.6-dimethylpyridine). The greatly differing relative labilities of cycloheptatriene and 2.6-dimethylpyridine are of particular interest and will be discussed in Chapter 3.

Table 2.3

Rate data for the Exchange Reaction

$$(\text{polyene})Cr(CO)_3 + \text{polyene}' \longrightarrow (\text{polyene}')Cr(CO)_3 + \text{polyene}$$

(in decalin)

Substrate / M	Entering ligand /M toluene	Added complex /M	$10^5 k_{obs}$ $/s^{-1}$
$(pyrene)Cr(CO)_3$ (150 °C)			
1.0×10^{-2}	7.6		38.8
1.0×10^{-3}	7.6		37.5
1.0×10^{-3}	2.4		13.9
5.0×10^{-4}	2.4		37.7
1.0×10^{-3}	0.76		6.45
5.0×10^{-4}	0.76		5.81
2.0×10^{-4}	0.76		6.1
$(2,6\text{-dmp})Cr(CO)_3$ (115 °C)			
1.0×10^{-3}	0.76		6.62
5.0×10^{-4}	0.76		6.07
$(naph)Cr(CO)_3$ (150 °C)			
2.0×10^{-3}	0.76		1.35
1.0×10^{-7}	0.76		1.48
5.0×10^{-4}	0.76		1.60

M = mol dm^{-3}

Table 2.3 continued

Substrate / M $(pyrene)Cr(CO)_3$ (150 °C)	Entering Ligand / M t-butylbenzene	Added Complex / M $(C_6H_6)Cr(CO)_3$	$10^5 k_{obs}$ / s^{-1}
1.0×10^{-3}	0.52		6.36
1.0×10^{-3}	0.52	1.0×10^{-3}	6.94
1.0×10^{-3}	0.52	2.0×10^{-3}	6.78
1.0×10^{-3}	0.52	5.0×10^{-3}	8.63
1.0×10^{-3}	0.52	1.0×10^{-2}	9.61
		(t-butylbenzene)$Cr(CO)_3$	
1.0×10^{-3}	0.52	5.0×10^{-3}	6.64

M = mol dm^{-3}

Table 2.4

Rate Data for the Exchange Reaction

$(polyene)Cr(CO)_3 + toluene \rightarrow (toluene)Cr(CO)_3 + polyene$

(in cyclooctane)

T °C	polyene[a]	[toluene]/mol dm^{-3}	$10^5 k_{obs}/s^{-1}$ [b]
130	naphthalene	6.6	1.05
		5.3	0.87
		3.8	0.72
		2.4	0.55
		0.76	0.38
	$k_A = 2.88 \times 10^{-6}\ s^{-1}$	(3.43×10^{-7})[c]	
	$k_B = 1.13 \times 10^{-6}\ mol^{-1}\ dm^3\ s^{-1}$	(8.00×10^{-8})[c]	
145	naphthalene	6.6	3.11
		5.3	2.65
		3.8	2.15
		2.4	1.67
		0.76	1.29
	$k_A = 9.8 \times 10^{-6}\ s^{-1}$	(6.73×10^{-7})[c]	
	$k_B = 3.16 \times 10^{-6}\ mol^{-1}\ dm^3\ s^{-1}$	(1.57×10^{-7})[c]	
160	naphthalene	6.6	11.33
		5.3	9.6
		3.8	7.85
		2.4	6.35
		0.76	4.26

Table 2.4 continued

$k_A = 3.38 \times 10^{-5}\ s^{-1}\ (2.57 \times 10^{-6})$

$k_B = 1.19 \times 10^{-5}\ mol^{-1}\ dm^3\ s^{-1}\ (5.98 \times 10^{-7})$

T °C	polyene[a]	[toluene] mol dm^{-3}	$10^5 k_{obs}/s^{-1}$[b]
175	naphthalene	6.6	30.7
		5.3	25.2
		3.8	22.3
		2.4	17.5
		0.76	13.5

$k_A = 1.10 \times 10^{-4}\ s^{-1}\ (7.81 \times 10^{-6})$[c]

$k_B = 2.88 \times 10^{-5}\ mol^{-1}\ dm^3\ s^{-1}\ (1.81 \times 10^{-6})$[c]

115	pyrene	6.6	2.52
		5.3	1.91
		3.8	1.6
		2.4	1.11
		0.76	0.58

$k_A = 3.36 \times 10^{-6}\ s^{-1}\ (5.43 \times 10^{-7})$[c]

$k_B = 3.20 \times 10^{-6}\ mol^{-1}\ dm^3\ s^{-1}\ (1.26 \times 10^{-7})$[c]

Table 2.4 continued

T °C	polyene[a]	[toluene]/mol dm^{-3}	$10^5 k_{obs}$/s^{-1}[b]
130	pyrene	6.6	7.17
		5.3	6.16
		3.8	4.90
		2.4	3.30
		0.76	1.65

$k_A = 1.03 \times 10^{-5}$ s^{-1} (1.20×10^{-6})[c]

$k_B = 9.55 \times 10^{-6}$ mol^{-1} dm^3 s^{-1} (2.80×10^{-7})[c]

140	pyrene	6.6	17.4
		5.3	15.0
		3.8	11.4
		2.4	7.91
		0.76	4.20

$k_A = 2.52 \times 10^{-5}$ s^{-1} (2.02×10^{-6})[c]

$k_B = 2.29 \times 10^{-5}$ mol^{-1} dm^3 s^{-1} (4.70×10^{-7})[c]

150	pyrene	6.6	35.6
		5.3	29.3
		3.8	21.9
		2.4	16.7
		0.76	9.04

$k_A = 5.51 \times 10^{-5}$ (4.23×10^{-6})[c]

$k_B = 4.50 \times 10^{-5}$ mol^{-1} dm^3 s^{-1} (9.83×10^{-7})[c]

Table 2.4 continued

T °C	polyene[a]	[toluene]/mol dm^{-3}	$10^5 k_{obs}$/s^{-1}[b]
115	2,6-dimethylpyridine	6.6	16.1
		5.3	14.1
		3.8	11.8
		2.4	9.16
		0.76	6.62

$k_A = 5.18 \times 10^{-5}$ s^{-1} (2.11×10^{-6})[c]

$k_B = 1.68 \times 10^{-5}$ mol^{-1} dm^3 s^{-1} (4.91×10^{-7})[c]

Notes: a) 1.0×10^{-3} mol dm^{-3}

b) Average of duplicate runs

c) Error (2 standard deviations)

Table 2.5

Rate Data for the Exchange Reaction

$$(\text{polyene})Cr(CO)_3 + \text{toluene} \longrightarrow (\text{toluene})Cr(CO)_3 + \text{polyene}$$

(in decalin at 150 °C)

polyene[a]	[toluene]/mol dm^{-3}	$10^5 k_{obs}/s^{-1}$ [b]
naphthalene	7.6	6.88
	6.6	5.87
	5.6	4.85
	3.8	3.97
	2.4	3.15
	0.76	1.48
	0.19	0.88
	0.10	0.78
	0.03	0.66
	0.00	0.52

$k_A = 1.11 \times 10^{-5}\ s^{-1}\ (1.74 \times 10^{-6})$[c]

$k_B = 7.24 \times 10^{-6}\ mol^{-1}\ dm^3\ s^{-1}\ (3.29 \times 10^{-7})$[c]

2,5-dimethylthiophene	7.6	22.6
	6.6	20.2
	5.6	18.4
	3.8	13.7
	2.4	9.10
	0.76	4.63
	0.00	0.912

$k_A = 2.00 \times 10^{-5}\ s^{-1}\ (5.47 \times 10^{-6})$[c]

$k_B = 2.63 \times 10^{-5}\ mol^{-1}\ dm^3\ s^{-1}\ (1.08 \times 10^{-6})$[c]

Table 2.5 continued

Polyene [a]	[toluene]/mol dm^{-3}	$10^5 k_{obs}/s^{-1}$ [b]
Pyrene	7.6	37.5
	6.6	32.0
	5.6	28.1
	3.8	20.0
	2.4	13.9
	0.76	6.45
	0.38	3.85
	0.19	3.00
	0.10	2.85
	0.05	2.36
	0.00	1.14

$$k_A = 2.84 \times 10^{-5} \times 10^{-5}\ s^{-1}\ (4.7 \times 10^{-6})^{c}$$

$$k_B = 4.50 \times 10^{-5} \times mol^{-1}\ dm^3\ s^{-1}\ (9.36 \times 10^{-7})^{c}$$

Notes:

a) 1.0×10^{-3} mol dm^{-3}
b) Average of duplicate runs
c) Error (2 standard deviations)
k_A and k_B evaluated over concentration range 0.76-7.6 mol dm^{-3}.

Table 2.6

Activation Parameters for the Exchange Reaction

$$(\text{polyene})Cr(CO)_3 + \text{toluene} \longrightarrow (\text{toluene})Cr(CO)_3 + \text{polyene}$$

Polyene	$\Delta H_A^{\ddagger}$ [a,b]	$\Delta S_A^{\ddagger}$ [a,b]	$\Delta H_B^{\ddagger}$ [a,b]	$\Delta S_B^{\ddagger}$ [a,b]
naphthalene	119.7(7.0)	-56.7(16.6)	107(11.0)	-96.2(26.0)
pyrene	100.8(8.0)	-92.8(20.0)	106.2(8.8)	-78.6(22.0)

Notes:

a) Units: $\Delta H^{\ddagger}$/kJ mol^{-1}, $\Delta S^{\ddagger}$/J K^{-1} mol^{-1}
b) Error (2 standard deviations)

1. E.N. Frankel and R.O Butterfield, J.Org. Chem., 1969, 34, 3930.

2. M. Cais and A. Rejoan, Inorg. Chim. Acta., 1970, 4, 509.

3. W.J. Bland, R. Davis and J.L.A Durrant, J. Organomet. Chem., 1985, 280, 95.

4. A.J. Birch, P.E. Cross and H. Fitton, J.C.S. Chem. Comm., 1965, 366.

5. G. Jaouen, Annals New York Academy of Science, 1977, 295, 59.

6. M.F. Semmelhack, G.R. Clarke, J.L. Garcia, J.J. Harrison, Y. Thebtaranonth, W. Wulff and A. Yamashita, Tetrahedron, 1981, 37, 3957.

7. G. Jaouen, A. Meyer and G. Simmoneaux, J.C.S. Chem. Comm., 1975, 813.

8. A. Solladie-Cavallo, G. Lapitajs, P. Buchert, A.C.Deyfuss, F. Sanch and D. Farkhani, Euchem. Comference "Applications of Organo-transition Metal Complexes in Organic Synthesis", 1986.

9. C.A.L. Mahaffy and P.L. Pauson, J. Chem. Res.(S). 1979, 128.

10. C.A.L. Mahaffy and P.L. Pauson, J. Chem. Res.(S). 1979, 126.

11. C.L. Zimmerman, S.L. Shaner, S.A. Roth and B.R. Willeford, J. Chem. Res. (S). 1980, 108.

12. W. Strohmeier and E.H. Starrico, Z. Phys. Chem.(Wiesbaden). 1963, 38. 315.

13. M. Cais, D.Fraenkel and K. Wiedenbaum, Coord. Chem. Rev., 1975, 16, 27.

14. J.J. Harrison, J. Amer. Chem. Soc., 1984, 106, 1487.

15. W. Strohmeier and R. Muller, Z. Phys. Chem, (Weisbaden), 1964, 40, 85.

16. W. Strohmeier and H. Mittnacht, Z. Phys. Chem.(Weisbaden), 1961, 29. 339.

17. W. Strohmeier and R. Muller. Chem. Ber.. 1960. 93. 2085.

18. E.L. Muetterties. J.R. Bleeke and A.C. Sievert. J. Organomet. Chem.. 1979, 178, 197,

19. D.E.F. Gracey, W.R. Jackson, C.H. McMullen and N. Thompson, J. Chem. Soc B, 1969, 1197.

20. T.G. Traylor, K.J. Stewart and M.J. Goldberg, J. Amer. Chem. Soc., 1984, 106, 4445.

21. T.G. Traylor and K. Stewart, Organometallics. 1984. 3. 325.

22. D.T. Dixon. J.A.S. Howell, J. Kola, N.F. Ashford, J. Organomet. Chem., 1985. 294. C1.

23. P.L. Pauson and C.A.L. Mahaffy, Inorg. Synth., 1979. 19, 154.

24. V. Desobry and E.P. Kundig. Helv. Chim. Acta, 1981, 64. 1280.

25. M.D. Rausch, G.A. Moser. E.J. Zaiko and A.L. Lipman, J. Organomet. Chem., 1970, 23, 185.

26. G.A. Moser and M.D. Rausch, Syn. React. Inorg. Metal-org. Chem., 1974, 4, 37.

27. H. Hart and A. Teuerstein, Synthesis, 1979, 683.

28. T.J. McNeese, M.B. Cohen and B.M. Foxman, Organometallics, 1984. 3. 552.

29. D.L. Perrin. W.L.F. Armarego and D.R. Perrin, Purification of Laboratory Chemicals, Pergamon, Oxford, 1966.

30. Reports regarding the preparation of such copolymers exist in the patent literature: (a) C.A. Uraneck and W.M. St. John, Chem. Abstracts. 1959. 53. 17570h; (b) H. Kuyama and Y. Utsunomiya. Chem. Abstracts. 1968. 69. 11111n.

31. Such a catalysis accounts for the independence of rate on [arene] at low arene concentrations reported earlier[22].

32. E.P. Kundig. C. Perret, S. Spichiger and G. Bernardinelli. J. Organomet. Chem., 1985. 286. 183.

33. C.D. Hoff. J. Organomet. Chem., 1983. 246. C53.

34. C.D. Hoff, J. Organomet. Chem., 1985. 282. 20.

35. S.P. Nolan and C.D. Hoff, J. Organomet. Chem., 1985. 290. 365. 2529.

36. S.P. Nolan. R. Lopez de Vega and C.D. Hoff. Organometallics. 1986. 5. 2529.

37. W. Strohmeier, Chem. Ber., 1961. 94. 3337.

38. W. Strohmeier, A.E. Mahagoub and D. von Hobe, Z. Phys. Chem.(Weisbaden). 1962, 35, 253.

39. D.A. Brown, N.J. Gogan and H. Sloan, J. Chem. Soc., 1965, 6873.

40. H. Werner and R. Prinz, J. Organomet. Chem., 1966, 5, 79.

41. M.S. Wrighton, E.S. Hammond and H.B. Gray, J. Amer. Chem. Soc., 1971, 93, 6048.

42. A. Pidcock, J.D. Smith and B.W. Taylor, J. Chem. Soc. A, 1967, 872.

43. A. Pidcock and B.W. Taylor, J. Chem. Soc. A. 1967. 877.

44. A. Pidcock, J.D. Smith and B.W. Taylor, J. Chem. Soc. A. 1969. 1604.

45. F. Zingales, A. Chiesa and F. Basolo, J. Amer. Chem. Soc., 1966, 88, 2707.

46. M. Gower and L.A.P. Kane-Maguire, Inorg. Chim. Acta. 1979, 37, 79.

47. G. Yagupsky and M. Cais, Inorg. Chim. Acta, 1975, 12, L27.

48. I.S. Butler and A.A. Ismail, Inorg. Chem., 1986, 25, 3910.

49. J. Rebek and F. Gavina, J. Amer. Chem. Soc., 1975, 97, 3453.

50. E.P. Kundig personal communication.

51. T.A. Albright, P. Hoffmann, R. Hoffmann, C. Lillya and P. Dobosh. J.Amer. Chem. Soc., 1983, 105, 3396.

52. T.E. Traylor, K.J. Stewart and M.J. Goldberg, Organometallics. 1986, 5, 2062.

53. T.A Albright personal communication.

54. E.L. Muetterties, J.R. Bleeke, J. Wucherer and T.A. Albright, Chem. Rev., 1982, 82, 499.

3. POLYENE SUBSTITUTION IN (POLYENE)$Cr(CO)_3$ COMPLEXES

3.1 Introduction

Mechanistically, polyene exchange of the various $Cr(CO)_3$ complexes studied in Chapter 2 may be interpreted in terms of slippage of the complexed polyene (η^6- η^4- η^2 or η^6 - η^3- η^1). Data from these exchange reactions provide information on the relative energies of the η^2 and η^1 intermediates via the intercepts of the plots of k_{obs} against [polyene]. However, the kinetic data does not provide information regarding the initial slippage to intermediate (X) of Scheme 2.10 in these complexes, and determination of activation parameters for this process is only possible from reactions in which the formation of (X) is rate determining. This chapter describes studies of the substitution reactions of these complexes by Group V ligands, which do provide information relative to the initial slippage. This information has already been discussed (for the pyrene and naphthalene complexes) in the evaluation of the reaction profile for polyene exchange in Chapter 2.

Reactions of (polyene)$M(CO)_3$ complexes (M=Cr, Mo, W) with σ-donor ligands such as phosphines, phosphites and nitriles have been studied kinetically[1-7] and show increased rates of reaction relative to the exchange reaction. Although most have been interpreted as proceeding via an I_d slippage mechanism without a discrete intermediate of type (X) (in view of the linear plots of k_{obs} against [ligand] obtained from limited ligand concentration ranges), one reaction

$$(\text{cycloheptatriene})Cr(CO)_3 + 3P(OMe)_3 \longrightarrow [P(OMe)_3]_3Cr(CO)_3 + \text{cycloheptatriene}$$

provides some evidence that the I_d slippage mechanism proposed in this and other reactions may be incorrect[3]. The reaction gives rise to curved plots of k_{obs} against [phosphite] on extending the ligand concentration range beyond the initial linear region, a feature the authors attribute to a solvent effect resulting from an increase in dielectric constant of the medium on increasing the phosphite concentration. However, one case of a limiting rate involving diene displacement in the reaction of (norbornadiene)$W(CO)_4$ with PBu_3 has been reported[8]. Curvature of plots of k_{obs} against [L] is a common feature of reactions of (chelate)$M(CO)_4$ systems with phosphines and phosphites (chelate = bidentate Group V and Group VI donor ligands, M = Cr,W). The mechanisms which take account of this curvature involve initial dissociative ring-opening (see Chapter 1, Section 1.3.4). Kinetic information relating to this ring opening may be obtained from limiting rate data.

For these reasons, a study of the substitution reactions of the complexes used in the exchange reaction was undertaken.

3.2 Experimental Details

3.2.1 Reagents and Materials

(Polyene)$Cr(CO)_3$ complexes were prepared as outlined in Chapter 2

Preparation of $[P(OMe)_3]_3Cr(CO)_3$

(Cycloheptatriene)$Cr(CO)_3$ (0.3g, 1.3mmol) was added to a mixture of $P(OMe)_3$ (2.0g, 6.0mmol) in 8.0ml of hexane. The red solution was degassed with nitrogen, sealed and left standing at room temperature overnight.

The solvent was removed under vacuum, and the residual white solid recrystallised from hexane. Yield 0.4g (65%)

Analysis

Infrared(decalin) ν_{CO} cm^{-1} 1962 1888 1874

^{31}P nmr ($CDCl_3$) 184.4 ppm relative to 85% H_3PO_4

microanalysis found C = 28.36 H = 5.35

calc C = 28.35 H = 5.31

The substitution product from reaction with PBu_3 was not prepared on a synthetic scale, but infrared data on kinetically monitored solutions at t_∞ showed bands in the area consistent with those obtained from corresponding solutions of $[P(OMe)_3]_3Cr(CO)_3$; $(PBu_3)_3Cr(CO)_3$ - **1930**, 1842 cm^{-1}).

PBu_3 was refluxed over CaH_2 and subsequently distilled. $P(OMe)_3$ was refluxed and distilled from sodium under nitrogen. Butyronitrile was heated with conc. HCl, dried over K_2CO_3 and fractionally distilled. Decalin was purified as outlined in Chapter 2. All solvents and ligands were stored under nitrogen.

3.2.2 Kinetic Measurements

An appropriate amount of complex, to give a 2×10^{-3} mol dm^{-3} solution was dissolved in a decalin/ligand mixture of the required composition. The resulting solution was transferred into a 10mm uv/glass cell of the type described in Chapter 2. The solution was degassed for 15 minutes with nitrogen (commercial grade, oxygen free).

The cell was subsequently sealed with a teflon stopcock under a positive pressure of nitrogen (5 psi), and placed in a constant temperature jacket (± 0.2 °C) suitably positioned in the uv machine (Perkin Elmer 402). The temperature of the circulating water was monitored by means of a thermometer placed in a transparent tube connecting the jacket with the water bath. The temperature in this tube was previously calibrated against the temperature measured inside an open-topped cell placed in the jacket.

Visible spectra were recorded periodically with the reactions monitored by disappearance of substrate. All kinetic studies were carried out under pseudo first order conditions with at least a ten-fold excess of ligand reactant (>2 x 10^{-2} mol dm^{-3}) and monitored over not less than three half-lives. Values of k_{obs} were obtained from linear plots of $\ln(A_t - A_\infty)$ against time, using (in almost all cases) a minimum of 10 absorbance/time data points. All plots gave correlation coefficients greater than 0.9995. Kinetic runs were performed in duplicate and generally showed a reproducibility of better than $\pm 5\%$.

3.3 Results and Discussion

The substitution reactions:

(i) $(\text{polyene})Cr(CO)_3 + 3P(OMe)_3 \longrightarrow fac/mer\text{-}[P(OMe)_3]_3Cr(CO)_3 +$ polyene

polyene = pyrene, naphthalene, 2,5-dimethylthiophene, thiophene, 2,6-dimethylnaphthalene.

(ii) $(\text{chpt})Cr(CO)_3 + 3L \longrightarrow fac/mer\text{-}L_3Cr(CO)_3 + \text{chpt}$

chpt = 1,3,5-cycloheptatriene L = PBu_3, $P(OMe)_3$

were all monitored in decalin at 510 nm except for (pyrene)$Cr(CO)_3$ which was monitored at 560nm. Kinetic data are presented in Tables 3.2 and 3.3 with activation parameters derived from variable temperature studies (evaluated from plots of ln(k/T) against 1/T) given in Table 3.6. A plot of k_{obs} against concentration of $P(OMe)_3$ and a corresponding plot of $1/k_{obs}$ against $1/[P(OMe)_3]$ are shown in Figures 3.1 and 3.2 with a plot of k_{obs} against $[PBu_3]$ shown in Figure 3.3.

It has proved difficult to establish precise yields in these reactions by calibration with pure fac isomers since amounts of the mer isomers are also formed in all reactions, the amount depending upon the particular substrate used and the temperature required for the substitution. For substrates studied at less than 50 ^{o}C, (cycloheptatriene, naphthalene, 2,6-dimethylnaphthalene, thiophene and 2,5-dimethylthiophene), the rate of fac $\rightleftharpoons$ mer isomerisation is slow, and the small amounts of mer observed are derived in the main directly from the substitution reaction; calibration with pure fac isomer shows a yield of >90% fac isomer in all cases. It is assumed that the substitution is quantitative and that the remaining 10% can be ascribed to mer isomer (See Chapter 4).

For substrates requiring temperatures greater than 50 ^{o}C (dimethylthiophene and pyrene) fac $\rightleftharpoons$ mer isomerisation proceeds at a rate which is not insignificant relative to the rate of substitution. Thus, at t_{∞}, fac/mer mixtures which are at or close to thermodynamic equilibrium are obtained, and calibration of yield using pure fac isomer is not possible. These reactions are, however, assumed to proceed quantitatively. No products other than fac/mer isomers can be detected in either the infrared or ^{31}P nmr spectra at t_{∞}.

Plot of k_{obs} vs. $[P(OMe)_3]$ for the reaction

(naphthalene) $Cr(CO)_3 + 3P(OMe)_3 \longrightarrow [P(OMe)_3]_3Cr(CO)_3 +$ naphthalene

in decalin at 31°C

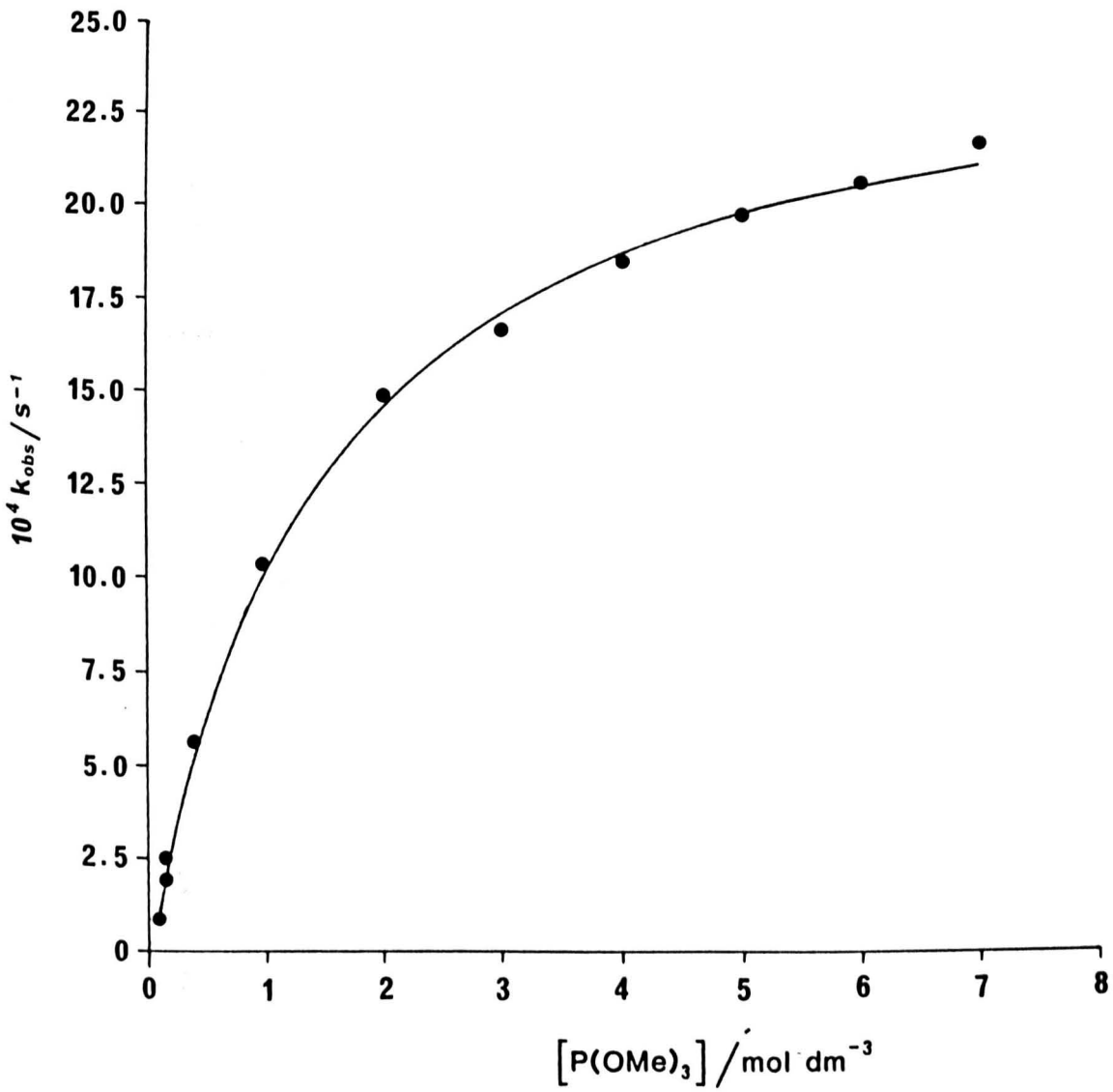

Fig. 3.1

Plot of $\frac{1}{k_{obs}}$ vs. $\frac{1}{[P(OMe)_3]}$ for the reaction

(naphthalene) $Cr(CO)_3$ + $3P(OMe)_3$ $\longrightarrow$ $[P(OMe)_3]_3Cr(CO)_3$ + naphthalene

in decalin at 31°C

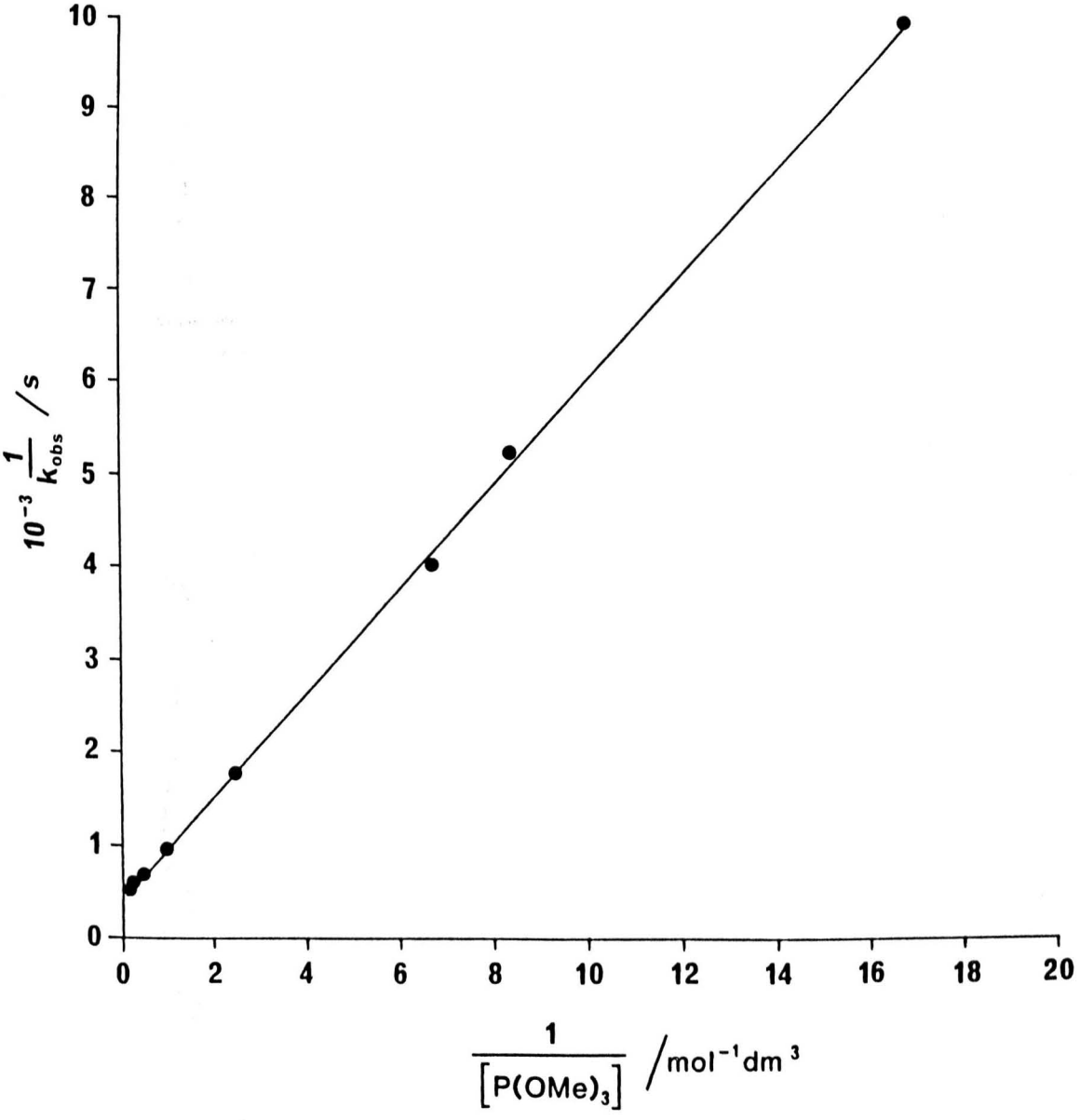

Fig. 3.2

Plot of k_{obs} vs. $[PBu_3]$ for the reaction

$(cycloheptatriene)Cr(CO)_3 + 3PBu_3 \longrightarrow [PBu_3]_3Cr(CO)_3 + cycloheptatriene$

in decalin at 31°C

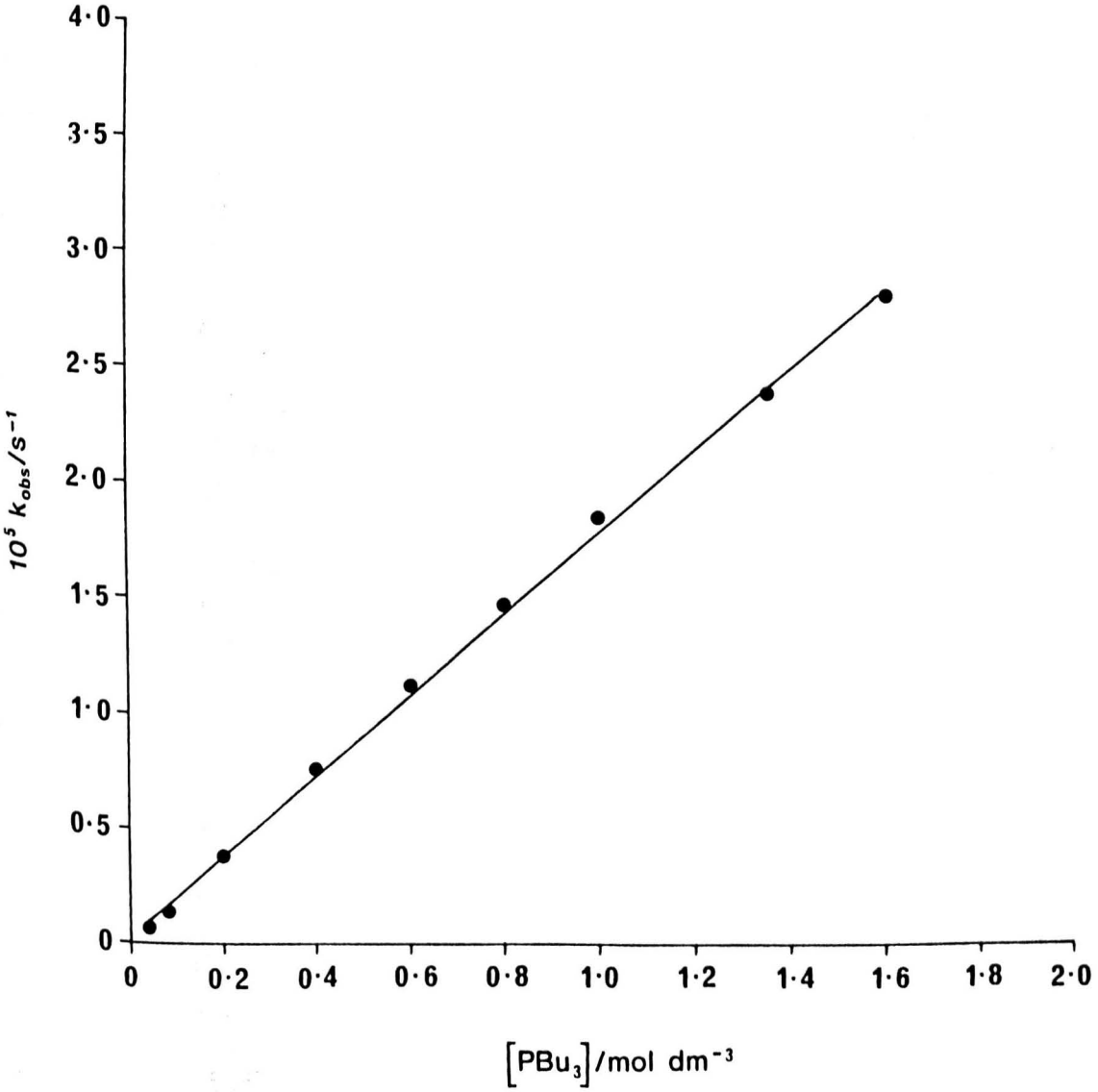

Fig.3.3

The fac - mer isomerisation can be monitored independently by uv/visible spectroscopy (See Chapter 4), and does not interfere with monitoring of the substitution reaction using the disappearance of substrate.

The $Cr(CO)_3$ complexes of styrene, octamethylnaphthalene and 2,6-dimethylpyridine were, under the conditions used (up to 90 ^{o}C), too inert towards phosphite substitution to be kinetically studied. Reaction of (2,6-dimethylpyridine)$Cr(CO)_3$ with PBu_3 does proceed at 70 ^{o}C at measurable rates (about 50 times slower than the rate of reaction of (chpt)$Cr(CO)_3$ with PBu_3), but kinetic monitoring at this temperature proved difficult due to a fac — mer isomerisation of the product $(PBu_3)_3Cr(CO)_3$. The isomerisation which proceeded at similar rates to the substitution, involves uv/visible absorbance changes which overlap with and mask the uv/visible absorbance changes associated with the disappearance of the yellow (2,6-dimethylpyridine)$Cr(CO)_3$ substrate.

The substitution reaction of (chpt)$Cr(CO)_3$ with PBu_3 yields a solution whose infrared and ^{31}P nmr spectra are consistent with fac-$(PBu_3)_3Cr(CO)_3$ as the only product of the reaction. Attempts to synthesize fac-$(PBu_3)_3Cr(CO)_3$ for calibration purposes have, however, not been successful due to its ease of oxidation and its apparent instability in the absence of free phosphine. In the absence of calibration, yields were assumed to be quantitative.

The reaction of (chpt)$Cr(CO)_3$ with butyronitrile (See Section 3.3.3) was carried out in decalin, toluene and dichloromethane. Kinetic data and derived activation parameters for the reaction in toluene are presented in Tables 3.5 and 3.6 with a corresponding plot of k_{obs} against concentration of butyronitrile given in Figure 3.4.

Plot of k_{obs} vs. [butyronitrile] for the reaction

$$\text{(cycloheptatriene)Cr(CO)}_3 + \text{toluene} \xrightarrow[(88.5^\circ C)]{\text{butyronitrile}} \text{(toluene)Cr(CO)}_3 + \text{cycloheptatriene}$$

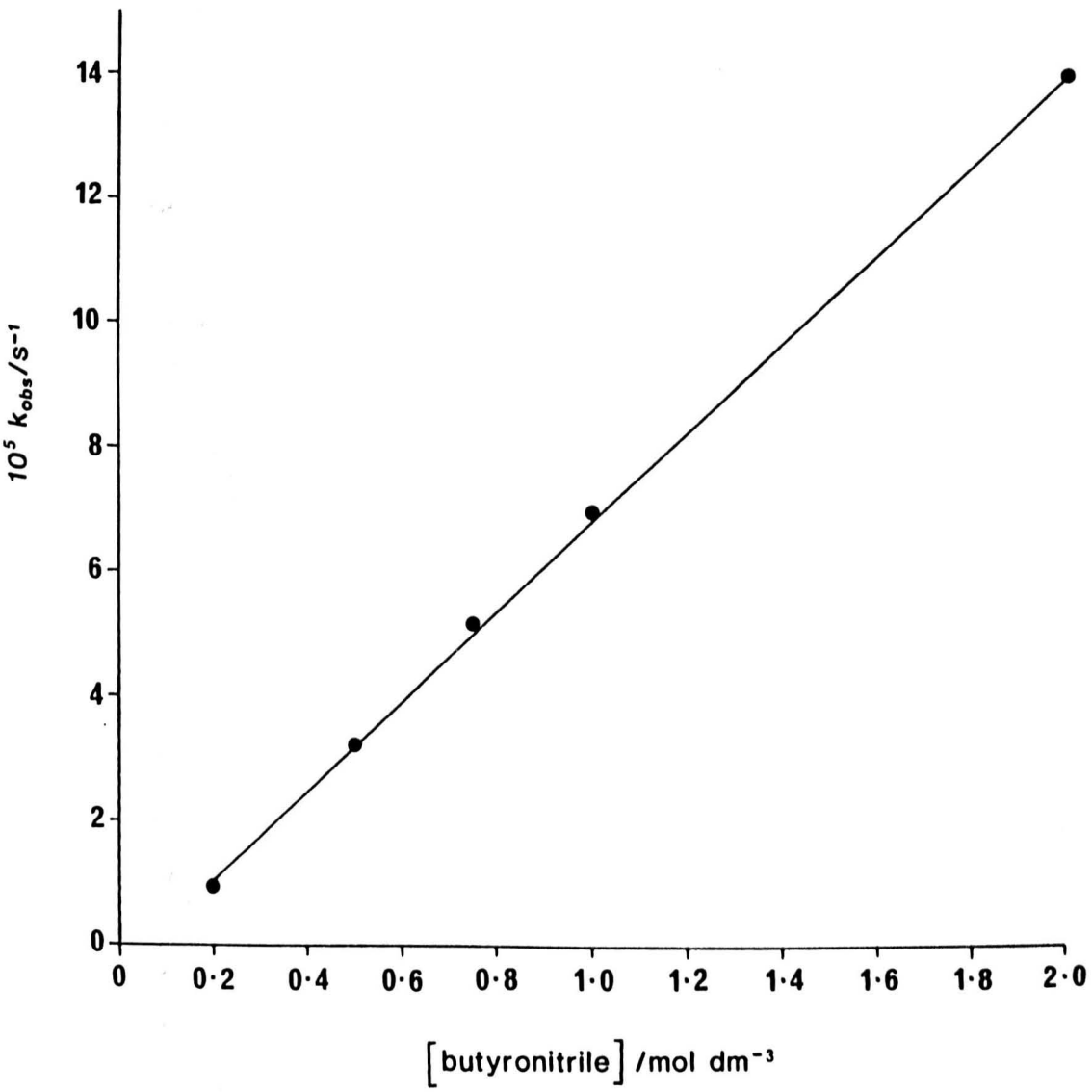

Fig. 3.4

3.3.1 Phosphite Substitution Reactions

The proposed mechanism and derived rate law to account for the phosphite substitution reactions are outlined below

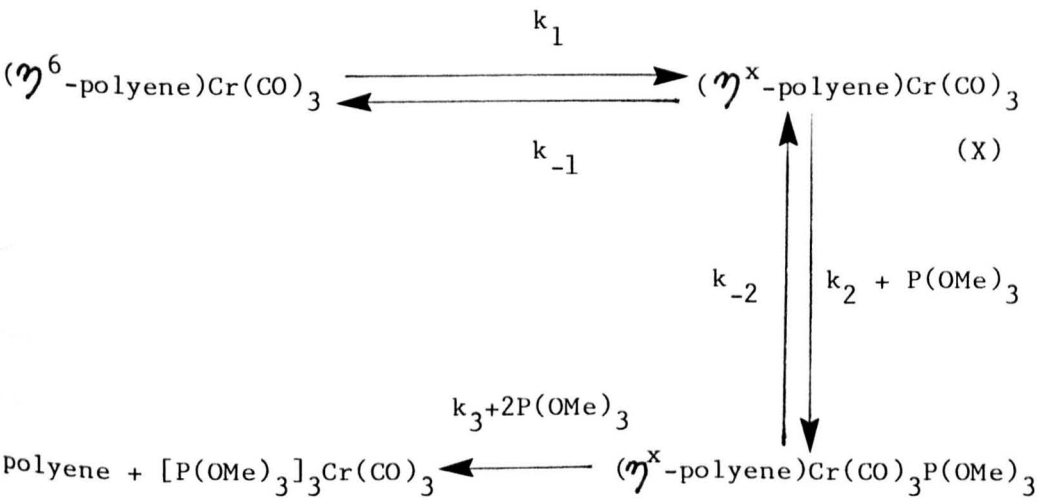

Scheme 3.1

Two main differences may be seen in the plots of k_{obs} against [L] for the phosphite substitution reaction, as compared to the polyene exchange reaction:

(a) the plots which are linear at low concentration of phosphite, pass through the origin implying mechanistically only one available forward pathway for reaction of the intermediate $(\eta^x\text{-polyene})Cr(CO)_3$

(b) deviation from linearity is observed at higher phosphite concentration. The experimental rate law

$$\frac{-d[S]}{dt} = \frac{k_1 k_2 [S][P(OMe)_3]}{k_{-1} + k_2[P(OMe)_3]} \qquad (3.1)$$

thus seems consistent with that derived from the mechanism above in which both conditions ($k_{-1} >> k_2[L]$ and $k_2[L] >> k_{-1}$) can be attained over the ligand concentration range studied. Hence the rate constant k_1 and the expression k_2/k_{-1} can be evaluated by fitting of the experimental data to the equation

$$k_{obs} = \frac{k_B[L]}{1 + K_A[L]} \quad (3.2)$$

where $k_B = k_1k_2/k_{-1}$

and $k_A = k_2/k_{-1}$

$L = P(OMe)_3$

by means of a non-linear least squares program. Initial estimates of k_A and k_B were obtained graphically and then refined by a Taylor differential correction routine. Two additional values have also been calculated: (a) an overall standard deviation which reflects the fit of the experimental k_{obs} values to the equation [(k_{obs} calc - k_{obs} exp)] and (b) the standard deviation of the difference between duplicate runs [(k_{obs}1 - k_{obs}2)], shown in Table 3.4. If the proposed mechanism provides an accurate description of the reaction pathway, it should be expected that the precison of overall fit and the precision of the reproducibility should be similar. If the precision of the reproducibility is much better than the overall fit, the implication is that an incorrect mechanism is being considered for the reaction. In this work it may be seen that the precision of the two quantities is comparable. For example in the reaction of (naphthalene)$Cr(CO)_3$ with $P(OMe)_3$ at 23.5 ^oC, the standard deviation of experimental reproducibility is 1.38×10^{-5} s^{-1} and the standard deviation of the fit 1.37×10^{-5} s^{-1}.

Alternatively values of k_1, and k_2/k_{-1} may be obtained from the intercept and slope respectively of plots of $1/k_{obs}$ against $1/[P(OMe)_3]$. Such linear plots all have correlation coefficients greater than 0.998.

Before proceeding further it is of interest to discuss another mechanism which is consistent with this experimental rate law under certain conditions. This involves a rapid associative pre-equilibrium followed by rate determining dissociative slippage.

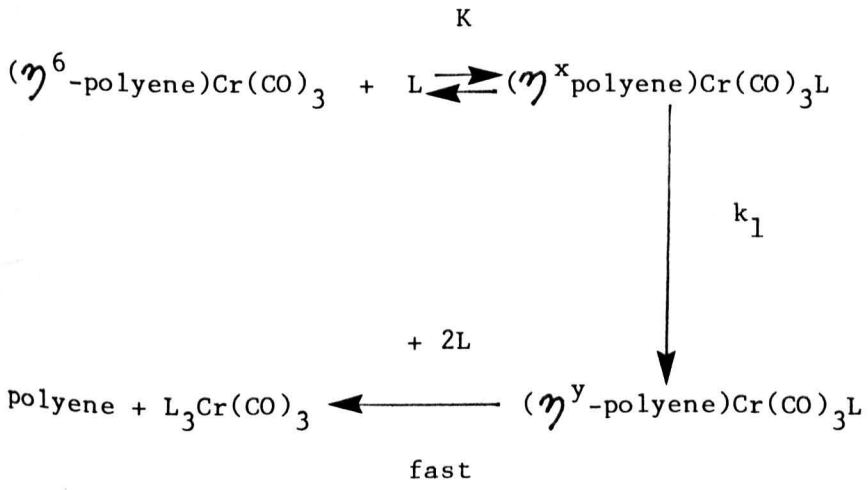

Scheme 3.2

The derived rate law is given by

$$k_{obs} = \frac{k_1 K[L]}{1 + K[L]} \qquad (3.3)$$

which is algebraically equivalent to equation 3.1. Thus under conditions where $K[L] >> 1$, the reaction is independent of [L] and where $K[L] << 1$, the reaction is first order in [L]. At the highest phosphite concentrations used (ca. 10 mol dm^{-3}) the limiting condition $K[L] >> 1$ is approximated thus implying that $K >> 0.1$. There is no evidence, even at high concentrations of phosphite, for detectable concentrations of the $(\eta^x$-polyene)Cr(CO)$_3$P(OMe)$_3$ intermediate from in situ uv/visible, infrared or ^{31}P nmr studies.

The ranges of ligand concentrations used in these substitution reactions (up to 7.0 mol dm^{-3}) deserve some comment as they are higher than those normally reported in other organometallic substitution processes, and much higher than normally used in kinetic studies of aqueous coordination chemistry. Limitations on ligand concentration arise in aqueous systems due to the sensitivity of reaction rates to changes in solvation of the substrate. On increasing the concentration of an ionic ligand, the dielectric effects of the medium (solvent + ligand) change and hence so too does the solvation of the substrate. In addition ion pairing becomes an important feature on increasing either ionic substrate or ligand concentration. Thus, unless studies are done at low concentration, it becomes difficult to separate the reactivity of the simple solvated cation or anion from that of its ion pair. Hence for these reasons ligand concentrations are usually kept well below 0.1 mol dm^{-3}. Substitution reactions in hydrocarbon solvents have, however, been studied at much higher ligand and substrate concentrations. For example, studies of the phosphite substitution reactions of $(\eta^6\text{-}C_6H_3Me_3)Mo(CO)_3$[2], $(\eta^5\text{-}C_9H_7)Mn(CO)_3$[9] and $(\eta^5\text{-pyrrolyl})Mn(CO)_3$[10] have used phosphite concentrations of up to between 0.8 and 1.3 mol dm^{-3}, with plots of k_{obs} against [phosphite] being linear over the whole concentration range. Thus, we believe the curvature of similar plots in the phosphite substitution reactions studied in this work (which occurs at phosphite concentrations about 0.3 mol dm^{-3}) to be a genuine feature of the mechanism, and not, as postulated previously[3], a result of a change in the dielectric constant of the medium. Indeed, added confirmation can be seen in the substitution reactions of $(chpt)Cr(CO)_3$ with PBu_3 and butyronitrile which show strictly linear plots of k_{obs} against [L] over the whole of the concentration range (up to 2 mol dm^{-3}). Though dielectric constant values are not available for $P(OMe)_3$ and PBu_3, the relative dipole moments (PBu_3, 1.94; $P(OMe)_3$, 1.81; butyronitrile, 3.34) may be taken as some measure of comparative dielectric constants.

Thus, if this were indeed responsible for the observed curvature it should be even more apparent in the phosphine and butyronitrile reactions.

The energy profile diagrams relating to substitution and exchange reactions are shown below, **Fig. 3.5**

As noted in Chapter 2 for the exchange reaction

$$\Delta G^{\ddagger}_{A} = \Delta G^{\ddagger}_{1} + \Delta G^{\ddagger}_{3} - \Delta G^{\ddagger}_{-1}$$

and $$\Delta G^{\ddagger}_{B} = \Delta G^{\ddagger}_{1} + \Delta G^{\ddagger}_{2} - \Delta G^{\ddagger}_{-1}$$

On the assumption that $k_{-1} >> k_2[\text{toluene}]$ and k_3, then

$$\Delta G^{\ddagger}_{A} = \Delta G^{\ddagger}_{1} + \Delta G^{\ddagger}_{3}$$

and $$\Delta G^{\ddagger}_{B} = \Delta G^{\ddagger}_{1} + \Delta G^{\ddagger}_{2}$$

For the substitution reaction with $P(OMe)_3$ however, $\Delta G^{\ddagger}_{-1}$ and $\Delta G^{\ddagger}_{2}$ are comparable as the difference $\Delta G^{\ddagger}_{2} - \Delta G^{\ddagger}_{-1}$ can be evaluated from the expression

$$\Delta G^{\ddagger}_{B} = \Delta G^{\ddagger}_{1} + \Delta G^{\ddagger}_{2} - \Delta G^{\ddagger}_{-1}$$

where $\Delta G^{\ddagger}_{1}$ (associated with k_1) and $\Delta G^{\ddagger}_{B}$ (associated with k_B) are known. Values of this difference together with $\Delta G^{\ddagger}_{1}$ and $\Delta G^{\ddagger}_{B}$ are shown below, **Table 3.1**

Substitution Reaction

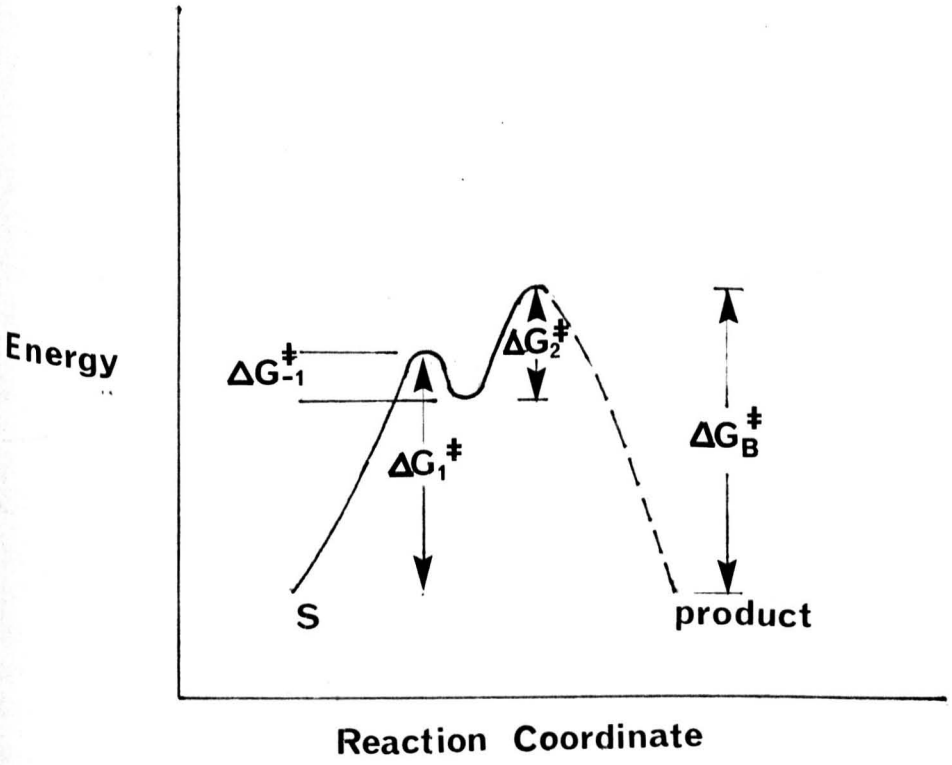

Exchange Reaction

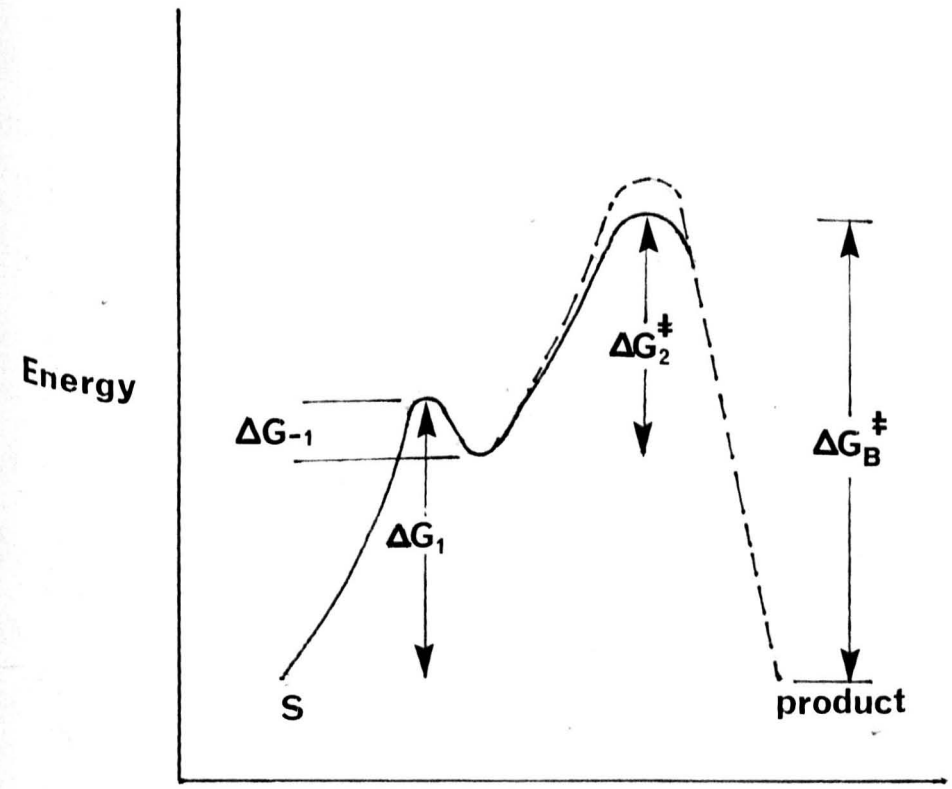

Fig. 3.5

$Cr(CO)_3$ complex	$\Delta G_1^{\ddagger}$	$\Delta G_B^{\ddagger}$	$\Delta G_B^{\ddagger} - \Delta G_1^{\ddagger}$
naphthalene	90.0	91.5	1.5
cycloheptatriene	93.5	96.0	2.5
2,5-dimethylthiophene	96.5	97.0	0.5
pyrene	95.5	98.0	2.5

$\Delta G^{\ddagger}$ / kJ mol^{-1} (evaluated at 40 °C)

Table 3.1

As implied by the shallow minimum on the energy profile diagram, $\Delta G_2^{\ddagger}$ and $\Delta G_{-1}^{\ddagger}$ are assumed to be small compared to $\Delta G_1^{\ddagger}$; justified by theoretical calculations which indicate geometrical distortions could give rise to such a shallow minimum[11]. Experimentally, no spectroscopic evidence is apparent for the intermediate which might be expected for a deep energy minimum.

The lability ordering for phosphite substitution which predominantly reflects the ordering of $\Delta G_1^{\ddagger}$ in view of the above, is naphthalene > 2,6-dimethylnaphthalene ≃ thiophene > cycloheptatriene > 2,5-dimethylthiophene > pyrene > 2,6-dimethylpyridine. Several points may be noted:

a) consistent with kinetic studies of substituted (η^6-arene)$Mo(CO)_3$ complexes is the reduced lability of the methyl substituted derivatives of naphthalene and thiophene compared to the unsubstituted complexes, and is seen to be enthalpy controlled. Although no thermodynamic data is available for these polyene complexes of $Cr(CO)_3$, methyl substituted arene complexes of $Mo(CO)_3$ show arene lability increases [(toluene)$Me(CO)_3$ > (p-xylene)$Mo(CO)_3$ > (mesitylene)$Mo(CO)_3$] on decreasing ground state bond enthalpy contributions[12] [mesitylene - Mo(279 kJ mol^{-1}) > toluene - Mo (273)].

Recent work[13] however, has shown the isomer distribution in the $Cr(CO)_3$ complexes of 1-methylnaphthalene and 2-methylnaphthalene to be markedly different, the $Cr(CO)_3$ bonded predominantly (75%) to the methylated ring in 2-methylnaphthalene. but to the non-methylated ring (75%) in 1-methylnaphthalene. This latter situation would appear to be inconsistent with ground state bond enthalpy contributions in the light of existing thermodynamic data of related complexes.

(b) Although within the substitution lability series, (2,6-dimethylpyridine)$Cr(CO)_3$ is relatively inert, it is more labile than (benzene)$Cr(CO)_3$. Slippage of the $Cr(CO)_3$ moiety towards nitrogen may involve greater stabilisation of the electron deficient metal centre resulting from the greater electron density in the ring π-system around the electronegative nitrogen atom. Hence although no theoretical evidence is available, an $\eta^6 - \eta^3$ slippage towards nitrogen in (2,6-dimethylpyridine)$Cr(CO)_3$ seems likely. Indeed an $\eta^5 - \eta^3$ slippage towards nitrogen in (η^5-pyrrollyl)$Mn(CO)_3$ has been implicated in carbonyl substitution reactions[10,14]. A similar slippage towards sulphur is likely in the thiophene complexes, though in addition the sulphur atom donates two electrons to the ring π-system, further stabilising the electron deficient metal centre, a factor which possibly accounts for the increased reactivity of these complexes compared to the pyridine complex.

(c) Ground state structures have been used to interpret the increased lability of (naphthalene)$Cr(CO)_3$ compared to (benzene)$Cr(CO)_3$ towards substitution[15]. In the naphthalene complex, the metal atom is displaced by ca. 0.03 Å from the centroid of the complexed ring. Increased reactivity is attributed to the maximisation of aromaticity of the uncomplexed ring resulting from a shift of the $Cr(CO)_3$ moiety away from this ring[16].

The metal atom in (benzene)$Cr(CO)_3$ however, is centrally positioned with respect to the ring. The much increased lability of (naphthalene)$Cr(CO)_3$ compared to (benzene)$Cr(CO)_3$ towards substitution is analogous to the tremendous rate enhancement of indenyl complexes relative to cyclopentadienyl complexes towards substitution[9].

The ground state structures of the methyl substituted (pyrrolyl)$Mn(CO)_3$ complex (A) in Figure 3.6 shows a "slip-distortion" of the $Mn(CO)_3$ moiety away from the ring centroid, towards nitrogen, this being attributed to a steric effect[14]. The ground state structure of (2,6-dimethylpyridine)$Cr(CO)_3$ shows the $Cr(CO)_3$ moiety to be centrally positioned with respect to the ring, as is the $Mn(CO)_3$ moiety in complex B

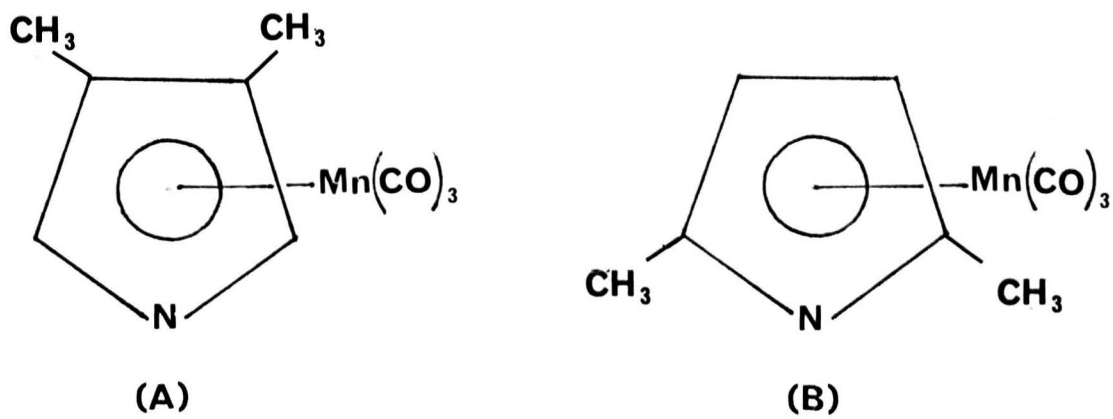

Fig 3.6

In these cases, the methyl groups may exert an opposite effect to that of the nitrogen and "push back" the $M(CO)_3$ moiety into a position which otherwise would also show some "slip-distortion" towards the heteroatom.

Finally, the complex (chpt)$Cr(CO)_3$, of which thermodynamic data has been reported (bond enthalpies have been evaluated at 150 kJ mol^{-1} [17] and 180 kJ mol^{-1} [18]), shows surprising lability towards substitution. An $\eta^6-\eta^4$ slippage in this complex may involve an η^4-coordinated non-conjugated diene intermediate, an arrangement preferred by $Cr(CO)_3L$ relative to an η^4-coordinated conjugated diene system. Hence as only a conjugated arrangement is possible for aromatic polyene complexes, the lability of the cycloheptatriene complex may be due to a lower energy η^4-intermediate.

(d) Activation parameters suggest the relative low lability of (pyrene)$Cr(CO)_3$ is entropy controlled ($\Delta S_1^{\ddagger} = -142.2$ J K^{-1} mol^{-1}) and possibly reflects the greater amount of steric strain associated with distortions of the type discussed in Chapter 2 in the much larger pyrene molecule.

Whilst the reactivity of (polyene)$Cr(CO)_3$ complexes towards phosphite substitution can be predominantly based on the order of $\Delta G_1^{\ddagger}$ values, the exchange reaction requires further consideration as indicated by the lability series towards substitution (naphthalene > cycloheptatriene > 2,5-dimethylthiophene > pyrene > 2,6-dimethylpyridine) and exchange (2,6-dimethylpyridiene > pyrene > naphthalene > 2,5-dimethylthiophene > cycloheptatriene). Notable changes are the positions occupied by 2,6-dimethylpyridine and cycloheptatriene.

The energy barriers $\Delta G_2^{\ddagger}$ for both substitution and exchange reflect the affinity of the intermediate (η^x-polyene)$Cr(CO)_3$ for $P(OMe)_3$ and incoming polyene. Hence whilst $\Delta G_2^{\ddagger}$ is insignificant compared to $\Delta G_1^{\ddagger}$ in the substitution reaction with the relatively basic $P(OMe)_3$, $\Delta G_2^{\ddagger}$ for the exchange (and $\Delta G_3^{\ddagger}$) is significant and makes a substantial contribution to the overall energy barriers $\Delta G_A^{\ddagger}$ and $\Delta G_B^{\ddagger}$.

In view of the above, the much greater reactivity of (2,6-dimethylpyridine)$Cr(CO)_3$ compared to (chpt)$Cr(CO)_3$ towards exchange is due to lower values of $\Delta G_2^{\ddagger}$ and $\Delta G_3^{\ddagger}$. A consideration of the intermediate (η^y-polyene)$Cr(CO)_3$ can provide some indication for these lower values. (2,6-dimethylpyridine)$Cr(CO)_3$ in contrast to the other complexes studied may involve a σ-bonded type intermediate formed between the lone pair on nitrogen and an empty acceptor orbital on the metal, an arrangement sterically and electronically more favourable than an η^1-coordinated intermediate. The same σ-bonded arrangement possibly exists to a lesser extent for (2,5-dimethylthiophene)$Cr(CO)_3$, which is substitutionally 10 times less reactive than (naphthalene)$Cr(CO)_3$, but which shows similar reactivity towards exchange. (Chpt)$Cr(CO)_3$ however is less reactive towards exchange than would be anticipated from its substitutional reactivity. The high values associated with $\Delta G_2^{\ddagger}$ and $\Delta G_3^{\ddagger}$ are difficult to assess, as are the corresponding values associated with the other complexes apart from (pyrene)$Cr(CO)_3$ and (naphthalene)$Cr(CO)_3$ for which theoretical information is available relating to possible slippage pathways.

3.3.2 Substitution of (Cycloheptatriene)$Cr(CO)_3$ by PBu_3

In contrast to the curved plots of k_{obs} against [$P(OMe)_3$] found in the reaction of (chpt)$Cr(CO)_3$ with $P(OMe)_3$, a plot of k_{obs} against [PBu_3] for the reaction of (chpt)$Cr(CO)_3$ with PBu_3 is linear over the whole concentration range studied (up to 1.6 mol dm^{-3}). A mechanism such as that postulated for the phosphite reaction (Scheme 3.1) involving a discrete (η^x-chpt)$Cr(CO)_3$ intermediate and consistent with the linear rate plot, would necessarily require $k_{-1} >> k_2$ [PBu_3] at all concentrations of PBu_3.

As this condition is not always satisfied in the phosphite reaction ie at high concentrations of $P(OMe)_3$, the reverse condition applies $k_2[P(OMe)_3] >> k_{-1}$, it is reasonable to assume the more basic and reactive PBu_3 would reach the same limiting condition ($k_2[PBu_3] >> k_{-1}$) at lower concentrations of PBu_3. Curved plots of k_{obs} against $[PBu_3]$ would therefore be expected with the onset of curvature below 0.3 mol dm^{-3}, the concentration at which curvature is apparent in the phosphite reaction. Hence in view of the above an I_d ring slippage mechanism Scheme 3.3 is likely.

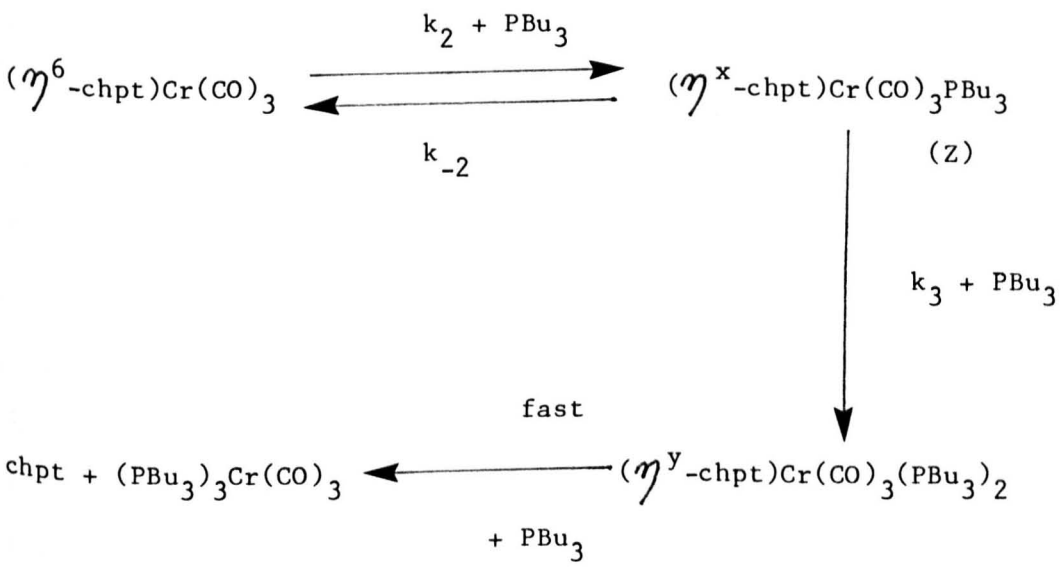

Scheme 3.3

Application of the steady state approximation to intermediate (Z), for which there is no spectroscopic evidence yields the rate equation

$$\frac{-d[S]}{dt} = \frac{k_2k_3[(\eta^6\text{-chpt})Cr(CO)_3][PBu_3]^2}{k_{-2} + k_3[PBu_3]}$$

which if $k_3[PBu_3] >> k_{-2}$ reduces to

$$\frac{-d[S]}{dt} = k_2[(\eta^6\text{-chpt})Cr(CO)_3][PBu_3]$$

Hence the reaction is first order with respect to PBu_3 over the whole of the concentration range of PBu_3. Such different mechanisms have been previously observed for the reaction of 2,2,7,7-tetramethyl-3,6-dithiaoctanetetracarbonyltungsten(0) with PBu_3 and $P(OPr\text{-}i)_3$[20]. Although the rates only differ by a factor of 2 (compared to about a factor of 7 in this work), the phosphine reaction is postulated to proceed via a concerted I_d ring-opening pathway, and the phosphite reaction via an initial dissociative ring-opening pathway.

The entropy value associated with k_2 (-97.9 J K^{-1} mol^{-1}) for the reaction of $(chpt)Cr(CO)_3$ with PBu_3 is significantly more negative than the entropy associated with the rate constant for dissociative ring-slippage k_1 (-32.6 J K^{-1} mol^{-1}) obtained from the reaction of $(chpt)Cr(CO)_3$ with $P(OMe)_3$, and adds support to the associative nature of the PBu_3 transition state. The negative entropy obtained for dissociative ring-slippage may result from loss of electron delocalisation in the ring and/or from geometric distortions. Comparison of these entropy values show the cycloheptatriene complex to be least negative, which may reflect its lack of aromatic resonance stabilisation.

3.3.3 Substitution of (Cycloheptatriene)$Cr(CO)_3$ by Butyrontitrile

Reaction of $(chpt)Cr(CO)_3$ with butyronitrile (PrCN) was kinetically studied in three different solvents; decalin, dichloromethane and toluene. Acetonitrile, which was the initial choice of ligand in view of a previous study, was not suitable due to its immiscibility in decalin.

The reaction in decalin proceeds to equilibrium as indicated by the high uv/visible absorption of the solution (at t_∞) at the monitoring wavelength. Confirmation of this equilibrium

$$(chpt)Cr(CO)_3 + 3PrCN \underset{}{\overset{K}{\rightleftharpoons}} (PrCN)_3Cr(CO)_3 + chpt$$

$K = 7.7 \times 10^{-3}$ mol^{-2} dm^{6} at 110 ^{o}C

(calculated from uv/visible spectroscopy)

was by infrared spectroscopy which revealed absorption bands consistent with that of $(chpt)Cr(CO)_3$. The position of the equilibrium lies appreciably to the left hand side. Infrared spectra (Figures 3.7 and 3.8) at equilibrium show a displacement to the right hand side on increasing the concentration of PrCN from 0.2 to 0.5 mol dm^{-3}. The corresponding reaction of $(naphthalene)Cr(CO)_3$ with PrCN proceeds to near completion as demonstrated by the equilibrium spectrum Figure 3.9. Composition of the equilibrium mixtures from the reactions of $(naphthalene)Cr(CO)_3$ and $(chpt)Cr(CO)_3$ with PrCN reflect the differing thermodynamic stabilities of the two complexes. It has been shown that $(chpt)Cr(CO)_3$ is more stable than $(toluene)Cr(CO)_3$ by approximately 20.5 kJ mol^{-1}, such that an equilibrium exists in the reaction

$$(chpt)Cr(CO)_3 + toluene \underset{}{\overset{K}{\rightleftharpoons}} (toluene)Cr(CO)_3 + chpt$$

$K = 2.9 \times 10^{-3}$ at 150 ^{o}C

Infrared Spectrum at $t=\infty$ of the reaction

$$(chpt)Cr(CO)_3 + 3PrCN \rightleftharpoons (PrCN)_3Cr(CO)_3 + chpt$$

in decalin at 110 °C, $[PrCN] = 0.2$ mol dm^{-3}

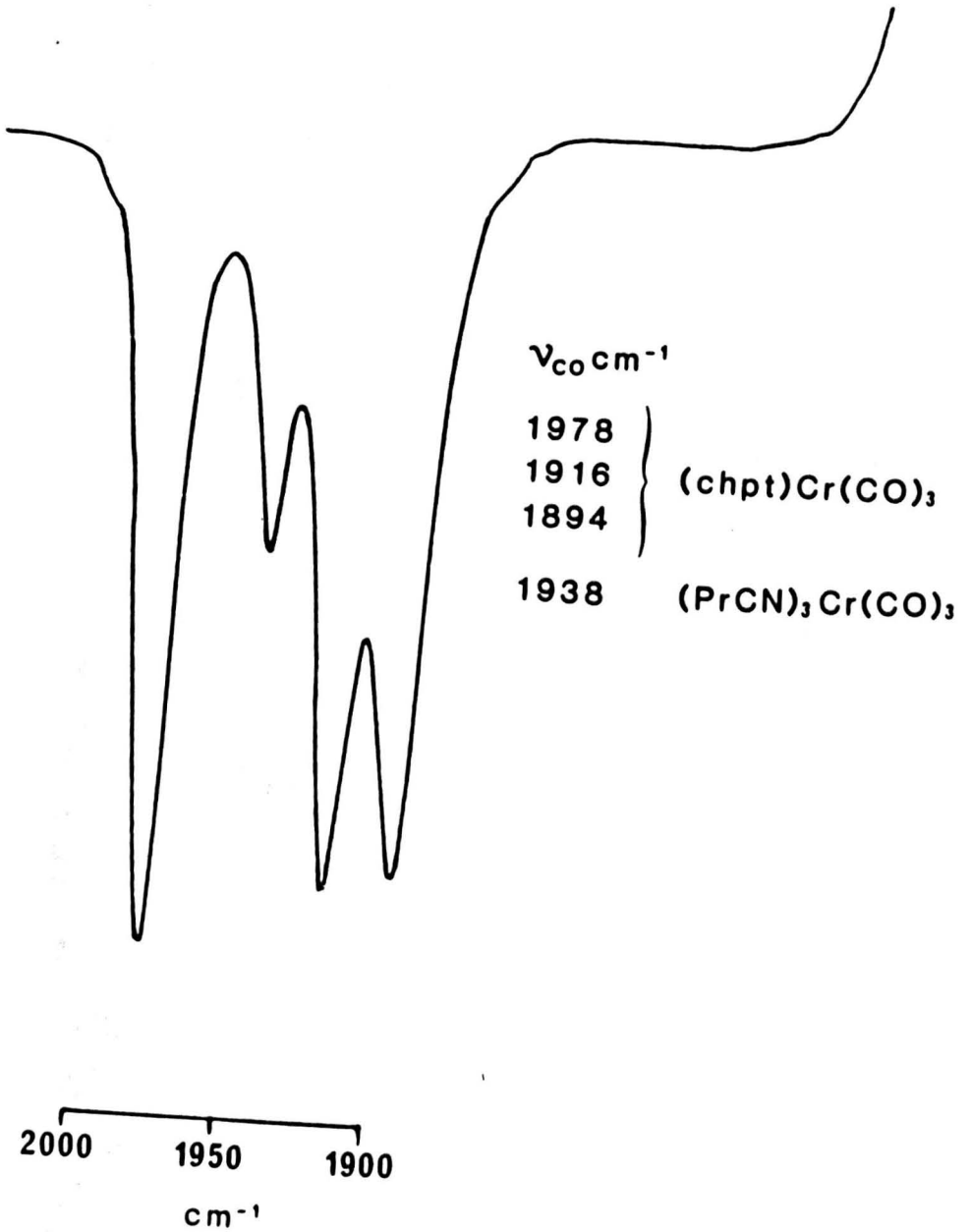

Fig. 3.7

Infrared Spectrum at $t=\infty$ of the reaction

$$(chpt)Cr(CO)_3 + 3PrCN \rightleftharpoons (PrCN)_3Cr(CO)_3 + chpt$$

in decalin at 110 °C, $[PrCN] = 0.5$ mol dm^{-3}

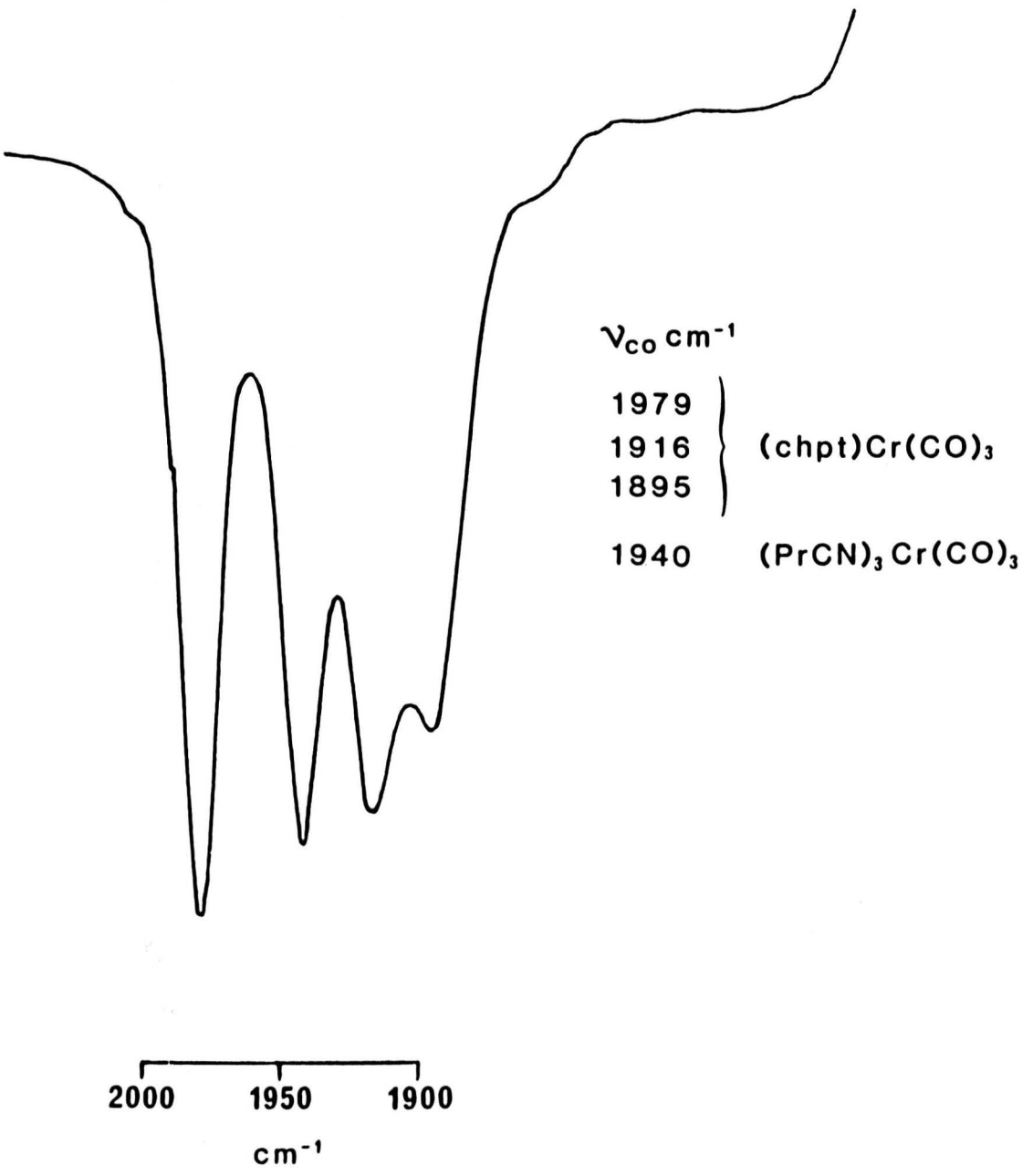

Fig. 3.8

Infrared Spectrum at $t \simeq \infty$ of the reaction

$$(\text{naphthalene})Cr(CO)_3 + 3PrCN \longrightarrow (PrCN)_3Cr(CO)_3 + \text{naphthalene}$$

in decalin at 110°C

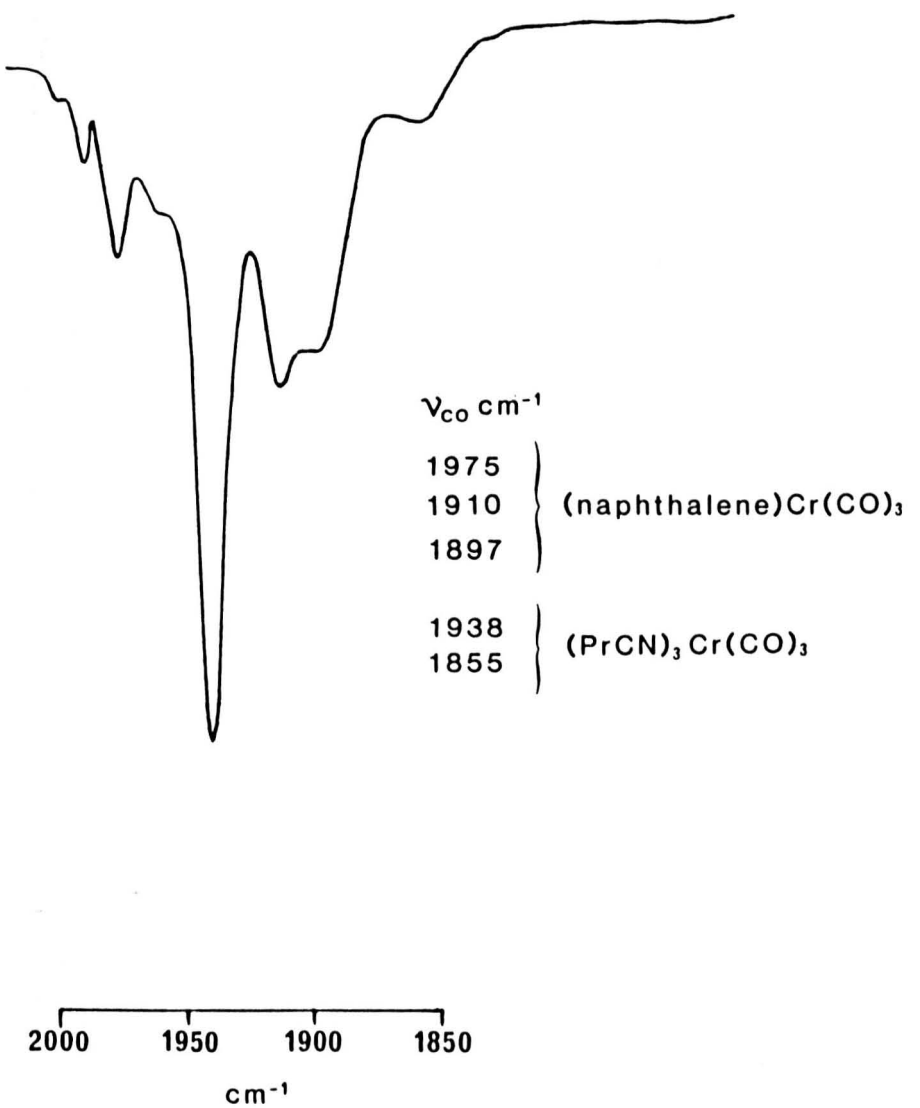

Fig. 3.9

Under the same conditions however, reaction of (naphthalene)$Cr(CO)_3$ with toluene proceeds to completion.

To enable significant variations in ligand, different solvents were used to eliminate an equilibrium and therefore allow greater absorbance changes between initial and final solutions. In the light of the above equilibrium in decalin, the previously reported reaction of (chpt)$Cr(CO)_3$ with acetonitrile in dichloroethane, which proceeds to completion, appeared surprising. However, reaction of (chpt)$Cr(CO)_3$ with PrCN in dichloromethane also proceeds to completion at rates similar to those in decalin. Examination of the colourless product solution at reaction completion (as indicated by zero absorption at the monitoring wavelength), showed only $Cr(CO)_6$ implying an initial substitution to give $(PrCN)_3Cr(CO)_3$ followed by chlorination/decomposition releasing CO, which in the closed cell results in the formation of $Cr(CO)_6$. A similar reaction involving substitution of toluene in (toluene)$Mo(CO)_3$ by $P(OMe)_3$ and carried out in dichloroethane resulted in some formation of $Mo(CO)_6^{2}$.

On changing the solvent from dichloromethane to toluene, quantitative yields of (toluene)$Cr(CO)_3$ were obtained at similar rates to those in decalin (about 3 times higher). Given that slight increases in rates are usually observed in reactions of this type on increasing polarity, the reactions occurring in the three solvents appear to reflect a mechanism involving rate determining substitution by PrCN followed by a) rapid decomposition in dichloromethane and b) rapid displacement by toluene in toluene. Hence the toluene displacement reaction is a measure of the rate of substitution by PrCN and may therefore be mechanistically compared, as far as the rate determining step is involved, to the phosphite and phosphine substitution reactions.

Linear plots of k_{obs} against [PrCN] for the reaction of $(chpt)Cr(CO)_3$ with PrCN are found and are consistent with the results from the previous reactions. Application of the same rate determining mechanism to this reaction as proposed for the phosphite reaction leading to formation of $(\eta^x\text{-polyene})Cr(CO)_3L$ (Scheme 3.1) requires $k_{-1} >> k_2[PrCN]$ over the whole ligand concentration range. This is reasonable due to the much lower basicity of PrCN compared to $P(OMe)_3$. The rate equation applicable is

$$\frac{-d[S]}{dt} = \frac{k_1 k_2[(\eta^6\text{-chpt})Cr(CO)_3][PrCN]}{k_{-1} + k_2[PrCN]}$$

which on the assumption $k_{-1} >> k_2[PrCN]$ reduces to

$$\frac{-d[S]}{dt} = \frac{k_1 k_2[(\eta^6\text{-chpt})Cr(CO)_3][PrCN]}{k_{-1}}$$

and $k_{obs} = k_B[PrCN]$ where $k_B = \frac{k_1 k_2}{k_{-1}}$

Reactivity differences between PrCN and $P(OMe)_3$ are enthalpy controlled as seen from comparison of the corresponding activation parameters associated with k_B for both reactions.

The order of reactivity of $(chpt)Cr(CO)_3$ with the ligands used above and toluene is PBu_3 > $P(OMe)_3$ >> PrCN >> toluene. Whilst a change in mechanism is observed on passing from PBu_3 to $P(OMe)_3$, the reactions of the latter three ligands in the series all proceed via an initial dissociative ring-opening mechanism.

Table 3.2

Rate Data for the Substitution Reaction

$$(\text{polyene})Cr(CO)_3 + 3P(OMe)_3 \longrightarrow [P(OMe)_3]_3Cr(CO)_3 + \text{polyene}$$

Polyene	T/ °C	[L]/mol dm^{-3}	$10^5 k_{obs}/s^{-1}$ [a]
naphthalene	23.5	0.06	5.56
		0.12	11.00
		0.18	14.50
		0.50	35.80
		1.00	51.10
		2.00	65.60
		3.00	75.00
		4.00	80.90
		5.00	88.80
		6.00	91.90
		7.00	101.00
	31.2	0.06	10.15
		0.12	19.30
		0.15	25.20
		0.40	56.30
		1.00	104.00
		2.00	148.00
		3.00	165.00
		4.00	185.00
		5.00	195.00
		6.00	204.00
		7.00	216.00

Table 3.2 continued

polyene	T/ ^{o}C	[L]/mol dm^{-3}	$10^{5}k_{obs}$/s^{-1} [a]
naphthalene	37.1	0.03	7.47
		0.06	14.10
		0.09	21.70
		0.12	28.50
		0.15	35.80
		0.66	132.00
		1.00	169.00
		2.00	231.00
		3.00	263.00
		4.00	289.00
		5.00	320.00
		6.00	346.00
		7.00	370.00
chpt	31.2	0.10	2.56
		0.20	5.03
		0.30	7.50
		0.40	9.50
		1.00	18.80
		2.00	28.10
		3.00	33.90
		4.00	37.30
		5.00	39.40
		6.00	41.90
		7.00	45.00

Table 3.2 continued

polyene	T/ ^{o}C	[L]/mol dm^{-3}	$10^{5}k_{obs}$ s^{-1} [a]
chpt	37.1	0.15	7.12
		0.30	12.50
		0.60	26.50
		0.90	32.60
		2.00	53.30
		3.00	60.90
		4.00	70.00
		5.00	76.20
		6.00	81.40
		7.00	83.30
chpt	48.4	0.06	7.34
		0.12	14.70
		0.18	21.50
		0.24	28.80
		0.30	35.20
		0.60	63.80
		0.90	89.20
		1.80	136.00
		3.00	169.00
		4.00	186.00
		5.00	208.00
		6.00	226.00
		7.00	248.00
2,5-dimethyl -	37.1	0.06	1.80
thiophene		0.09	2.71

Table 3.2 continued

polyene	T/ °C	[L]/mol dm^{-3}	$10^5 k_{obs}/s^{-1}$ [a]
2,5-dimethyl-thiophene	37.1	0.12	3.39
		0.15	4.23
		0.60	14.30
		1.00	19.50
		2.00	26.10
		3.00	29.60
		4.00	31.30
		5.00	32.20
		6.00	33.50
		7.00	34.70
	47.0	0.06	4.45
		0.08	5.73
		0.09	6.80
		0.12	8.87
		0.15	10.50
		0.60	31.20
		1.00	41.90
		2.00	59.60
		3.00	66.60
		4.00	70.50
		5.00	72.70
		6.00	75.20
		7.00	78.50

Table 3.2 continued

Polyene	T/ °C	[L]/mol dm^{-3}	$10^5 k_{obs}/s^{-1}$ [a]
2,5-dimethyl-	56.6	0.03	5.01
thiophene		0.06	10.00
		0.09	14.30
		0.12	18.90
		0.15	23.30
		0.60	70.20
		1.00	93.70
		2.00	129.00
		3.00	144.00
		4.00	162.00
		5.00	164.00
		6.00	173.00
		7.00	178.00
Pyrene	56.6	0.10	3.03
		0.30	7.97
		0.50	12.60
		1.00	20.50
		2.00	31.10
		3.00	44.80
		4.00	49.00
		5.00	55.10
		6.00	64.40
		7.00	72.50

Table 3.2 continued

Pyrene	T/ °C	[L]/mol dm^{-3}	$10^5 k_{obs}/s^{-1}$ [a]
Pyrene	68.7	0.06	5.24
		0.09	7.50
		0.12	10.00
		0.15	13.10
		0.50	37.80
		1.00	54.00
		2.00	91.30
		3.00	117.00
		4.00	137.00
		5.00	155.00
		6.00	167.00
		7.00	192.00
	78.0	0.03	5.38
		0.06	11.08
		0.09	15.70
		0.12	22.00
		0.15	26.40
		0.50	62.00
		1.00	109.00
		2.00	181.00
		3.00	223.00
		4.00	245.00
		5.00	289.00
		6.00	300.00
		7.00	340.00

Table 3.2 continued

polyene	T/ ^{o}C	[L]/mol dm^{-3}	$10^{5}k_{obs}/s^{-1}$ [a]
thiophene	37.1	0.05	5.33
		0.07	7.88
		0.09	9.77
		0.12	12.30
		0.15	15.30
	47.0	0.03	8.46
		0.06	16.20
		0.09	23.20
		0.12	29.80
		0.15	36.80
	56.6	0.03	18.00
		0.06	35.70
		0.09	51.30
		0.12	61.80
		0.15	79.00
2,6-dimethyl-	37.1	0.03	3.12
naphthalene		0.06	6.73
		0.09	9.50
		0.12	11.70
		0.15	15.80

Table 3.2 continued

polyene	T/ ^{o}C	[L]/mol dm^{-3}	$10^{5}k_{obs}/s^{-1}$ [a]
2,6-dimethyl	47.0	0.03	6.86
naphthalene		0.06	14.50
		0.09	20.50
		0.12	27.00
		0.15	33.40
	56.6	0.03	13.00
		0.06	27.20
		0.09	39.20
		0.12	50.50
		0.15	65.80

Notes a) Average of duplicate runs

Table 3.3

Derived Rate Constants for the Substitution Reaction

$$(\text{polyene})Cr(CO)_3 + 3P(OMe)_3 \longrightarrow [P(OMe)_3]_3 Cr(CO)_3 + \text{polyene}$$

polyene	T/ ^{o}C	$10^3 k_1/s^{-1}$ [a]	$10^3 k_B/$ mol^{-1}dm^{3}s^{-1} [a]
naphthalene	23.5	1.17(0.14)	0.94(0.008)
	31.2	2.63(0.17)	1.78(0.14)
	37.1	4.61(0.54)	2.53(0.13)
chpt	31.2	0.62(0.04)	0.27(0.005)
	37.1	1.10(0.10)	0.50(0.008)
	48.4	3.77(0.34)	1.25(0.006)
2,5-dmt	37.1	0.43(0.03)	0.31(0.002)
	47.0	0.95(0.08)	0.78(0.007)
	56.6	2.16(0.10)	1.71(0.005)
pyrene	56.6	2.22(0.42)	0.89(0.009)
	68.7	4.07(0.72)	1.84(0.014)
	78.0	7.41(0.78)	3.13(0.45)
thiophene	37.1	-	0.97(0.03)
	47.0	-	2.35(0.04)
	56.6	-	5.00(0.14)

Table 3.3 continued

Polyene	T/ ^{o}C	$10^{3}k_{1}/s^{-1}$ [a]	$10^{3}k_{B}/$ $mol^{-1}dm^{3}s^{-1}$ [a]
2,6-dmn	37.1	-	1.02(0.03)
	47.0	-	2.18(0.04)
	56.6	-	4.32(0.08)

Notes a) Error (2 standard deviations)

Table 3.4

Errors Associated with Reproducibility and Theoretical Fit for the Reaction as Represented in Table 3.1

Polyene	T/ ^{o}C	$[\lvert k_{obs}\text{calc.} - k_{obs}\text{exp}\rvert]$ $\times 10^{-5}/s^{-1}$	$[\lvert k_{obs}1 - k_{obs}2\rvert]$ $\times 10^{-5}/s^{-1}$
naphthalene	23.5	1.37	1.38
	31.2	1.30	1.40
	37.1	0.63	1.59
chpt	31.2	2.65	3.75
	37.1	0.58	0.86
	38.4	2.05	0.98
2,5-dmt	37.1	2.27	2.10
	47.0	2.13	3.45
	56.6	5.10	4.10
pyrene	56.6	3.89	1.46
	68.7	2.03	0.83
	78.0	9.25	2.08

Table 3.5

Rate Data for the Substitution Reaction

$$(chpt)Cr(CO)_3 + 3L \longrightarrow L_3Cr(CO)_3 + chpt$$

L	T/ °C	[L]/mol dm^{-3}	$10^5 k_{obs}/s^{-1}$ [a]
PBu_3	31.0	0.04	6.20
		0.08	13.40
		0.10	17.50
		0.20	37.00
		0.40	76.20
		0.60	144.00
		0.80	148.00
		1.05	183.00
		1.35	235.00
		1.60	283.00
	40.6	0.04	12.00
		0.08	28.70
		0.10	37.00
		0.20	78.70
		0.30	121.00
		0.40	160.00
	50.4	0.04	19.60
		0.08	50.80
		0.10	66.00
		0.20	158.00
		0.30	243.00

Table 3.5 continued

L	T/ °C	[L]/mol dm^{-3}	$10^5 k_{obs}/s^{-1}$ [a]
PrCN	88.5	0.20	0.92
		0.50	3.17
		0.75	5.10
		1.00	6.85
		2.00	13.80
	100	0.20	2.70
		0.50	7.15
		0.75	11.90
		1.00	16.30
	110	0.20	4.90
		0.50	16.00
		0.75	24.20
		1.00	32.50

Derived Rate Constants for the above Reactions

L	T/ °C	$10^3 k_2/mol^{-1} dm^3 s^{-1}$ [b]	$10^5 k_B/mol^{-1} dm^3 s^{-1}$ [b]
PBu_3	31.0	1.95(.02)	-
	40.6	4.12(.03)	-
	50.4	8.72(.07)	-
PrCN	88.5	-	7.17(0.08)
	100.0	-	17.16(0.50)
	110.0	-	34.70(0.66)

Notes: a) Average of duplicate runs b) Error (2 standard deviations)

Table 3.6

Activation Parameters for the Subsititution Reaction

$$(\text{polyene})Cr(CO)_3 + 3P(OMe)_3 \longrightarrow [P(OMe)_3]_3Cr(CO)_3 + \text{polyene}$$

polyene	$\Delta H_1^{\ddagger}$ a,b	$\Delta S_1^{\ddagger}$ a,b	$\Delta H_B^{\ddagger}$ a,b	$\Delta S_B^{\ddagger}$ a,b
naphthalene	74.9(5.4)	-48.6(19.0)	53.5(7.4)	-122(24.0)
chpt	83.4(7.8)	-32.6(25.0)	69.1(8.4)	- 86.2(26.6)
2,5-dmt	67.5(5.6)	-92.4(17.6)	71.4(2.0)	- 82.0(8.8)
pyrene	51.0(9.4)	-142(27.4)	53.6(2.6)	-141.5(7.6)
thiophene	-	-	69.0(1.8)	- 80.5(5.2)
2,6-dmn	-	-	60.3(3.6)	-108.1(11.0)

Activation Parameters for the Substitution Reaction

$$(\text{chpt})Cr(CO)_3 + 3L \longrightarrow L_3Cr(CO)_3 + \text{chpt}$$

L	$\Delta H_B^{\ddagger}$ a,b	$\Delta S_B^{\ddagger}$ a,b	$\Delta H_2^{\ddagger}$ a,b	$\Delta S_2^{\ddagger}$ a,b
PrCN	81.5(7.6)	-100.4(20.8)	-	-
PBu_3	-	-	60.6(2.4)	- 97.9(7.6)

Notes: a) 2 standard deviations b) Units: $\Delta H^{\ddagger}$ / J mol^{-1}, $\Delta S^{\ddagger}$ / J K^{-1} mol^{-1}

REFERENCES

1. F. Zingales, A. Chiesa and F. Basolo, J. Amer. Chem. Soc., 1966,88, 2707.
2. A. Pidcock, J.D. Smith and B.W. Taylor, J. Chem. Soc. A, 1967, 872.
3. A. Pidcock and B.W. Taylor, J. Chem. Soc. A, 1967, 877.
4. A. Pidcock, J.D. Smith and B.W. Taylor, J. Chem. Soc. A, 1969, 1604.
5. K.M. Al. Kathumi and L.A.P. Kane Maquire J. C. S. Dalton. 1974, 428.
6. M. Gower and L.A.P. Kane Maquire, Inorg. Chim. Acta. 1979, 37, 79.
7. K.M. Al. Kathumi and L.A.P. Kane Maquire, J. C. S., Dalton, 1973, 1683.
8. See ref. 4, J. Amer. Chem. Soc., 1976, 99, 896.
9. L.N. Ji, M.E. Rerek and F. Basolo Organometallics, 1984, 3, 740.
10. L.N. Ji, D.L. Kershner. M.E. Rerek and F. Basolo. J. Organomet. Chem., 1985. 83. 740.
11. T.A. Albright private communication.
12. S.P. Nolan and C.D. Hoff, J. Organomet. Chem., 1985, 290, 365.
13. S. Wyatt and J.A.S. Howell unpublished results.
14. D.L. Kershner and F. Basolo unpublished results.
15. V. Kunz and W. Nowacki. Helv. Chim. Acta. 1967, 50. 1053.
16. E.L. Muetterties. J.R. Bleeke. E.J. Wucherer and T.A. Albright. Chem. Rev., 1982, 82. 499.
17. D.L.S. Brown. J.A. Connor, C.P. Demain. M.L. Leung, J.A. Martinho-Simoes, H.A. Skinner and M.T. Zaffaroni - Moattar, J. Organomet. Chem., 1977, 142, 321.
18. C.D. Hoff, J. Organomet. Chem., 1983, 246, 653.
19. D.T. Dixon, J.C. Kola and J.A.S. Howell, J. C. S. Dalton 1984, 1307.
20. G.R. Dobson, L.D. Schultz, B.E. Jones and M. Schwartz, Inorg. Nuc. Chem., 1979, 41, 119.

4. ISOMERISATION REACTIONS OF $L_3M(CO)_3$ COMPLEXES

4.1 Introduction

A large number of organometallic systems have been studied in which stereochemical non-rigidity is observed under conditions where intermolecular ligand exchange does not occur. It is reasonable to claim that the study of rearrangements of this type has become one of the most exciting areas in reaction mechanisms, particularly since the advent of nmr, which has provided an ideal tool for study.

Early indications of stereochemical non-rigidity were provided by the ^{19}F nmr spectrum of PF_5 and the ^{17}O nmr spectrum of $Fe(CO)_5$[1a]. Instead of two peaks corresponding to the two chemically inequivalent nuclei (axial and equatorial) which is expected for the known trigonal bipyramidal geometry, only one was observed. Other examples of five-coordinate compounds behaving in this way indicated that the equivalence could not be due to rapid ligand dissociation and recombination. It was proposed therefore, that axial $\rightleftharpoons$ equatorial ligand exchange could take place without breaking the metal ligand bond, the process being termed Berry pseudo-rotation.

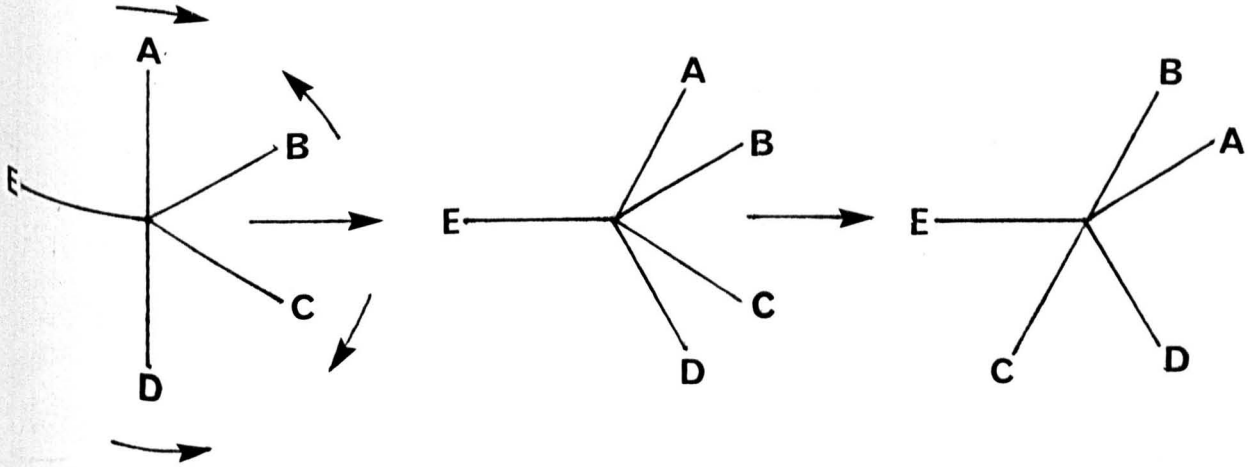

Scheme 4.1

Seven coordinate complexes also display intramolecular isomerisations and usually adopt one of three different geometries: monocapped octahedron, pentagonal bipyramid or monocapped trigonal prism. As with the five coordinate compounds, energy barriers between isomers are small. In direct contrast to these five and seven coordinate systems whose stereochemistries are relatively non-rigid, the six-coordinate octahedron is relatively rigid. However there is an increasing awareness that neutral low valent six-coordinate molecules can undergo fairly low energy intramolecular ligand rearrangements, the pathway proceeding through either a trigonal prismatic[1b-6] or bicapped tetrahedral[7] intermediate or transition state. Several qualititative observations on these processes have been reported in the literature[8-15], but only more recently have quantitative studies been reported[16-21] involving cis/trans isomerisations of $L_2M(CO)_4$ complexes (M=Cr,Mo,W; L = phosphine, phosphite) and analogous mer/fac isomerisations of some trisubstituted complexes.

It has been noted that some of the substitution reactions discussed in Chapter 3 are complicated by concomitant fac/mer isomerisation of the $L_3Cr(CO)_3$ complex so formed. This chapter is concerned with two problems:

(i) an investigation of the formation of the mer isomer directly from the phosphite substitution reaction of the type

$$(\text{polyene})M(CO)_3 + 3L \longrightarrow \text{fac/mer-}L_3M(CO)_3 + \text{polyene}$$

and (ii) a detailed study of the fac/mer isomerisation

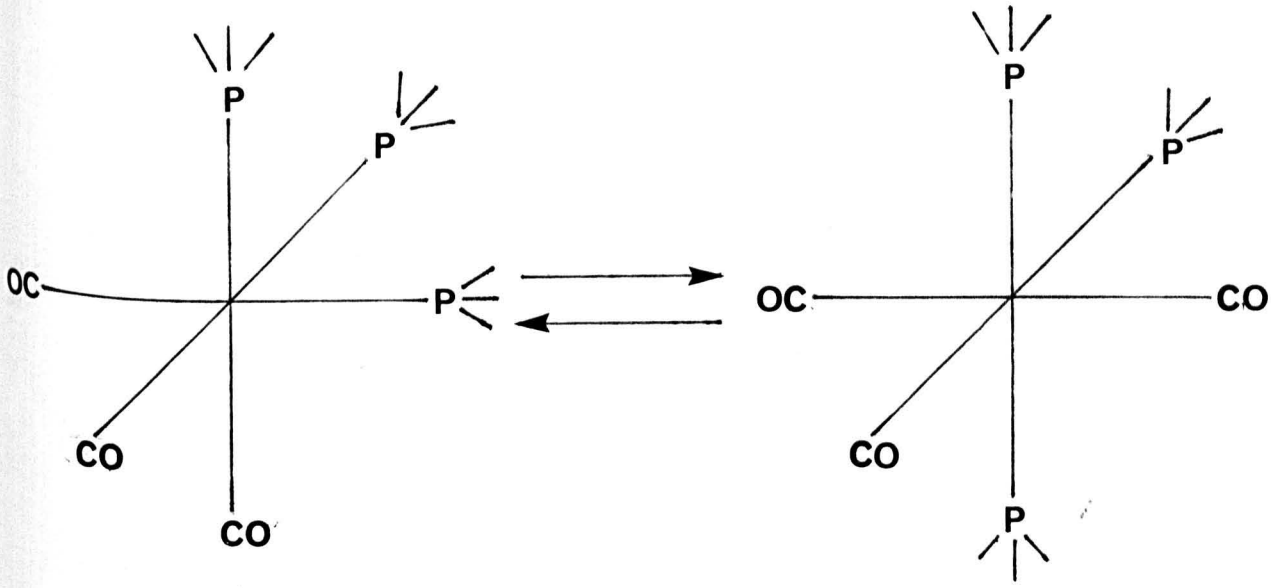

fac isomer mer isomer

M=Cr,Mo,W

Scheme 4.2

4.2 Experimental

4.2.1 Reagents and Materials

(Polyene)$Cr(CO)_3$ complexes were prepared as outlined in Chapter 2. (Cycloheptatriene)$Mo(CO)_3$ was prepared from $Mo(CO)_6$ according to the method outlined in Chapter 2 for the corresponding $Cr(CO)_3$ complex. (Cycloheptatriene)$W(CO)_3$ was prepared by reacting $(MeCN)_3W(CO)_3$[22] with excess cycloheptatriene in refluxing 100/120 petroleum ether[23]. Fac-$[P(OMe)_3]_3M(CO)_3$ complexes (M=Mo,W) were prepared by reacting (cycloheptatriene)$M(CO)_3$ with excess $P(OMe)_3$ in hexane at room temperature for about 1 hour (see Chapter 3 for preparation of fac-$[P(OMe)_3]_3Cr(CO)_3$).

Preparation of mer- $[P(OMe)_3]_3M(CO)_3$ (M=Cr,W)

The corresponding fac isomers were dissolved in 60/80 petroleum ether and heated for several hours under nitrogen. Solvent evaporation and subsequent thin layer chromatography using a 25% ethyl acetate in 60/80 petroleum ether mixture as eluent yielded mer-$[P(OMe)_3]_3Cr(CO)_3$ as the first band, whilst elution of the crude material from the tungsten reaction yielded mer-$[P(OMe)_3]_3W(CO)_3$ as the second band. Solvent evaporation and crystallisation from 40/60 petroleum ether afforded the pure mer isomers. The corresponding molybdenum complex proved difficult to crystallise. All analytical data for these and the other complexes are shown in Table 4.1.

Decalin and toluene solvents were purified as outlined in Chapter 2. Tributyl phosphine and trimethyl phosphite were purified as outlined in Chapter 3. Cyclohexane was refluxed and distilled from sodium.

4.2.2 Kinetic Measurements

Kinetic monitoring of the fac/mer isomerisation by uv/visible spectroscopy was carried out in the adapted cells used in the kinetic experiments outlined in Chapters 2 and 3. Solutions (typically 5×10^{-4} mol dm^{-3} in decalin) were degassed by passing through a stream of dry oxygen free argon, with the cells subsequently sealed under a positive pressure of argon (5 psi). Isomerisations of the chromium complex involved temperatures below 90 ^{o}C and were carried out using the experimental techniques of direct monitoring described for the substitution reactions in Chapter 3. The less labile molybdenum and tungsten complexes were monitored by the method described in Chapter 2 for the exchange reactions using the high temperature oil bath.

Table 4.1

Complex	ν_{CO}/cm^{-1} (decalin)	Microanalysis found	calc
$(chpt)Cr(CO)_3$	1982	C=52.60	52.63
	1920	H= 3.47	3.51
	1896		
$fac\text{-}[P(OMe)_3]_3Cr(CO)_3$	1962	C=28.36	28.35
	1888	H= 5.35	5.30
	1874		
$mer\text{-}[P(OMe)_3]_3Cr(CO)_3$	1975	C=27.73	28.35
	1890	H= 5.55	5.30
	1875		
$fac\text{-}[P(OMe)_3]_3Mo(CO)_3$	1974	C=26.40	26.11
	1898	H= 5.16	4.89
	1884		
$fac\text{-}[P(OMe)_3]_3W(CO)_3$	1970	C=22.43	22.53
	1893	H= 4.27	4.22
	1878		
$mer\text{-}[P(OMe)_3]_3W(CO)_3$	1986	C=22.81	22.53
	1902	H= 4.34	4.22
	1878		

Rate constants were calculated from the change in absorbance at 310 nm (Mo and W complexes) and 320 nm (Cr complex).

^{31}P nmr experiments were conducted on a Jeol Fx-100 spectrophotometer. $(Chpt)M(CO)_3$ complexes (1.0×10^{-1} mol dm^{-3}) were dissolved in cyclohexane or toluene and introduced into an nmr tube, subsequently sealed with a plastic cap. At the temperatures used, the time required for signal accumulation was not significant. Relative rates (k_1/k_2) of fac/mer isomer formation were calculated from the change in the integrated peaks of fac isomer, mer isomer and uncomplexed free $P(OMe)_3$.

Rate constants for the isomerisation reactions (fac $\rightleftharpoons$ mer) in decalin were calculated from the changes in fac/mer ratio. Free $P(OMe)_3$ (2.0 mol dm^{-3}) was added in some experiments.

4.3 Results and Discussion

4.3.1 Mer $L_3M(CO)_3$ Formation

The substitution reaction studied by ^{31}P nmr

$$(polyene)Cr(CO)_3 + 3P(OMe)_3 \longrightarrow fac/mer[P(OMe)_3]_3Cr(CO)_3 + polyene$$

Polyene = chpt, naphthalene, 2,5-dimethylthiophene

shows qualitatively that the formation of mer isomer occurs at rates much greater than the rate of fac $\longrightarrow$ mer isomerisation. This is of some interest in terms of the mechanism of the substitution reaction. Analysis of the ^{31}P nmr spectrum can be used to determine the fac/mer ratio of isomers produced directly from the reaction.

Consider the kinetic scheme below

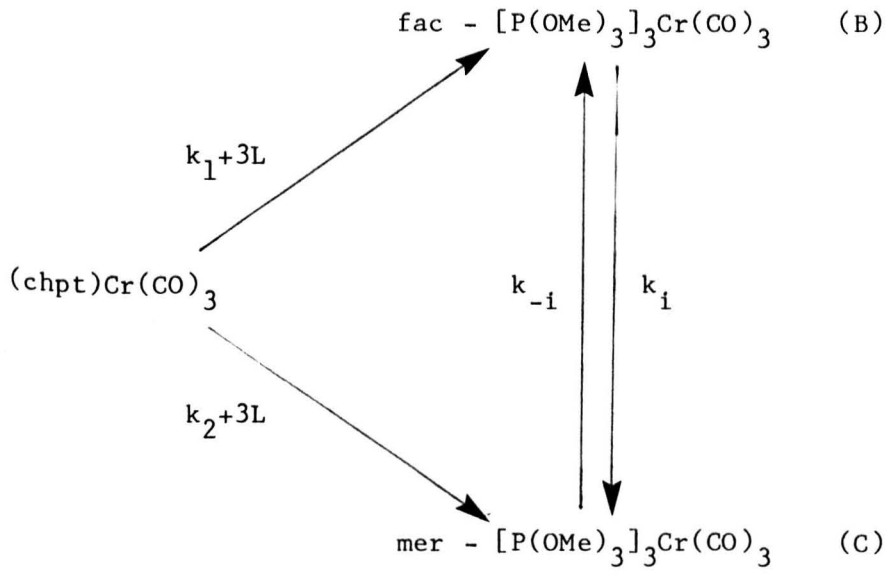

Scheme 4.3

where k_1 and k_2 are the rate constants for the formation of fac and mer isomers respectively and k_i and k_{-i} the rate constants for isomer inter-conversion. From this it can be shown that

$$\frac{[B] - [B_\infty]}{[A_o]e^{-(k_i+k_{-i})t}} = \frac{(k_1 - k_{-i})}{(k_i+k_{-i}-k_1-k_2)} \cdot \frac{[A]}{[A_o]e^{-(k_i+k_{-i})t}}$$

$$+ \frac{k_1k_i - k_2k_{-i}}{(k_i+k_{-i})(k_i+k_{-i}-k_1-k_2)}$$

The derivation of the above equation is as follows

$[A] + [B] + [C] = [A_o]$ [A][B] and [C] evaluated from integrated ^{31}P nmr peaks

$$\frac{d[A]}{dt} = -k_1[A] - k_2[A] \qquad (4.1)$$

$$\frac{d[B]}{dt} = k_1[A] - k_{-i}[C] - k_i[B]$$

$$= (k_1 - k_{-i})[A] - (k_i + k_{-i})[B] + k_{-i}[A_o] \qquad (4.2)$$

$$\frac{d[C]}{dt} = k_2[A] + k_i[B] - k_{-i}[C]$$

if $[A] = [A_o]$ at time $t = o$ then from (4.1)

$$\ln\frac{[A]}{[A_o]} = -(k_1 + k_2)t$$

$$\therefore \quad [A] = [A_o]e^{-(k_1 + k_2)t}$$

Substituting for [A] in equation (4.2)

$$\frac{d[B]}{dt} + (k_i + k_{-i})[B] = [A_o](k_1 + k_{-i})e^{-(k_1+k_2)t} + k_{-i}[A_o]$$

multiplying by the integrating factor $e^{(k_i + k_{-i})t}$

$$\left[\frac{d[B]}{dt} + (k_i + k_{-i})[B]\right] \cdot e^{(k_i+k_{-i})t} = (k_1-k_{-i})e^{(k_i+k_{-i}-k_1-k_2)t}[A_o] + k_{-i}[A_o]e^{(k_i+k_{-i})t}$$

$$\therefore \frac{d([B]e^{(k_i+k_{-i})t})}{dt} = [A_o](k_1-k_{-i})e^{(k_i+k_{-i}-k_1-k_2)t} + k_{-i}[A_o]e^{(k_i+k_{-i})t}$$

on integrating

$$[B]e^{(k_i+k_{-i})t} = \frac{[A_o](k_1 - k_{-i})e^{(k_i+k_{-i}-k_1-k_2)t}}{(k_i+k_{-i}-k_1-k_2)} + \frac{k_{-i}[A_o]e^{(k_i+k_{-i})t}}{(k_i+k_{-i})} + \text{const.}$$

if $[B] = 0$ at $t = 0$, then

$$0 = \frac{[A_o](k_1-k_{-i})}{(k_i+k_{-i}-k_1-k_2)} + \frac{k_{-i}[A_o]}{k_i+k_{-i}} + \text{const}$$

$$\therefore [B]e^{(k_i+k_{-i})t} = \frac{[A_o](k_1-k_{-i})e^{(k_i+k_{-i}-k_1-k_2)t}}{(k_i+k_{-i}-k_1-k_2)} + \frac{k_{-i}[A_o]e^{(k_i+k_{-i})t}}{(k_i+k_{-i})} - \frac{[A_o](k_1-k_{-i})}{(k_i+k_{-i}-k_1-k_2)} - \frac{k_{-i}[A_o]}{(k_i+k_{-i})}$$

dividing by $e^{-(k_i+k_{-i})t}$

$$[B] = \frac{[A_o](k_1-k_{-i})e^{-(k_1+k_2)t}}{(k_i+k_{-i}-k_1-k_2)} + \frac{[A_o]k_{-i}}{(k_i+k_{-i})} -$$

$$\frac{[A_o](k_1k_i-k_2k_{-i})e^{-(k_i+k_{-i})t}}{(k_i+k_{-i})(k_i+k_{-i}-k_1k_{-2})}$$

as $t \longrightarrow \infty$ $\quad [B] \longrightarrow \frac{[A_o]k_{-i}}{(k_i+k_{-i})}$

$$\therefore [B]-[B_\infty] = \frac{(k_1-k_{-i})[A_o]e^{-(k_1+k_2)t}}{(k_i+k_{-i}-k_1-k_2)} -$$

$$\frac{[A_o](k_1 \cdot k_{-i}-k_2k_{-i})e^{-(k_i+k_{-i})t}}{(k_i+k_{-i})(k_i+k_{-i}-k_1-k_2)}$$

dividing by $[A_o]e^{-(k_i+k_{-i})t}$ yields the equation

$$\frac{[B] - [B_\infty]}{[A_o]e^{-(k_i+k_{-i})t}} = \frac{(k_1-k_{-i}) \cdot [A]}{(k_i+k_{-i}-k_1-k_2)[A_o]e^{-(k_i+k_{-i})t}} +$$

$$\frac{k_1k_i - k_2k_{-i}}{(k_i+k_{-i})(k_i+k_{-i}-k_1-k_2)}$$

hence a plot of $\quad \frac{[B] - [B_\infty]}{[A_o]e^{-(k_i+k_{-i})t}} \quad$ against $\frac{[A]}{[A_o]e^{-(k_i+k_{-i})t}}$

gives a straight line from which the ratio k_1/k_2 may be evaluated from the slope or intercept. Such a plot is shown in Figure 4.1 for the substitution reaction of $(chpt)Cr(CO)_3$ with $P(OMe)_3$ in toluene.

Plot of $\frac{B - B_\infty}{A_o e^{-(k_i + k_{-i})t}}$ against $\frac{A}{A_o e^{-(k_i + k_{-i})t}}$ for the reaction

$$(chpt)Cr(CO)_3 + 3P(OMe)_3 \longrightarrow fac/mer\text{-}\left[P(OMe)_3\right]_3 Cr(CO)_3 + chpt$$

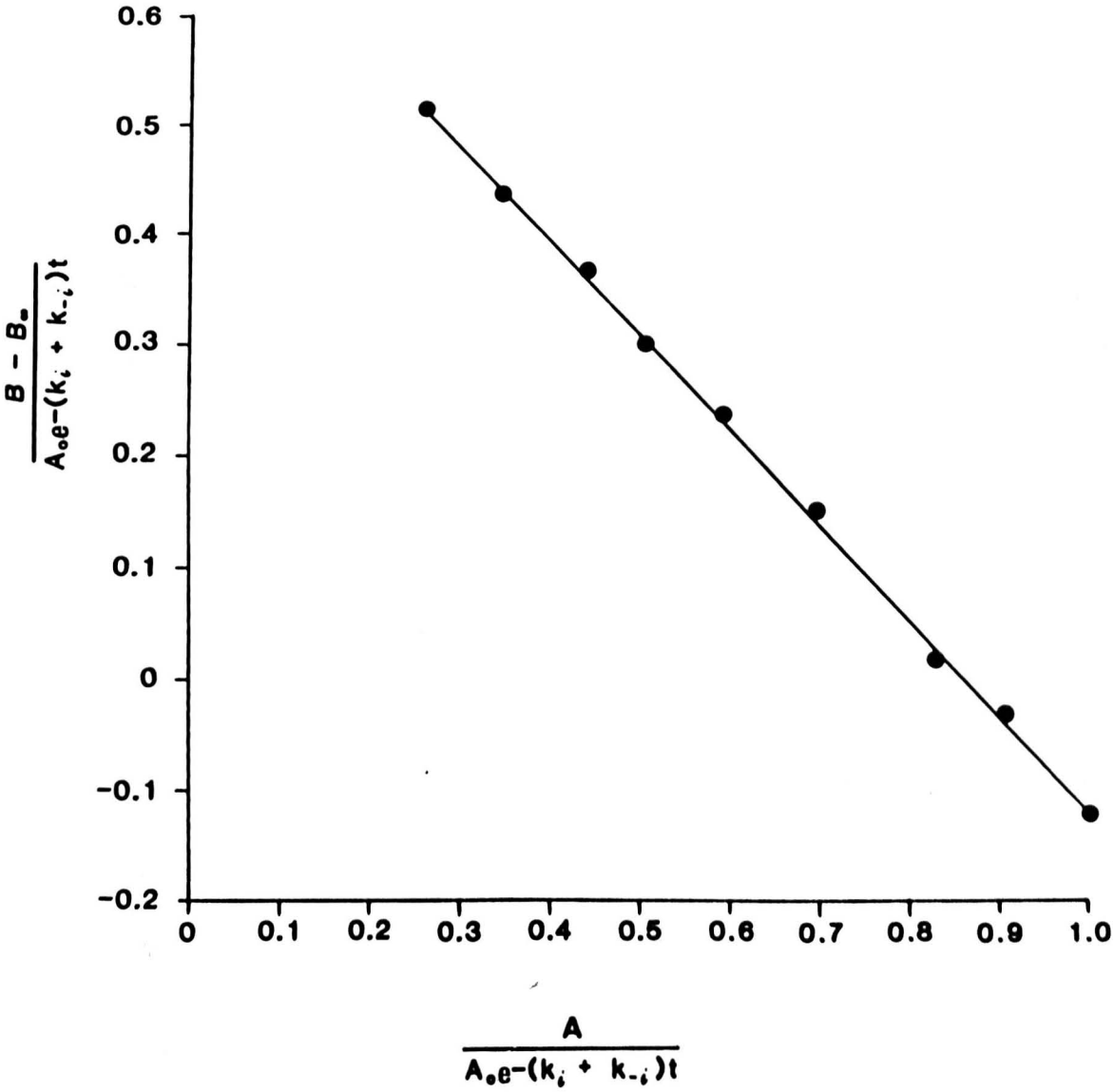

Fig. 4.1

A similar plot is obtained for this reaction in cyclohexane. Mer isomer formation varies according to solvent, metal and bound polyene. For (chpt)$Cr(CO)_3$ with $P(OMe)_3$ in cyclohexane approximately 15% is formed directly compared to 9% in toluene. Qualitative observations indicate lower levels of the mer isomer obtained from the reactions of (naphthalene)$Cr(CO)_3$ and (2,5-dimethylthiophene)$Cr(CO)_3$ with $P(OMe)_3$, $\simeq$ 5% in both cases. Changing the metal to molybdenum or tungsten also results in a reduced yield of mer isomer.

On the basis of the findings in Chapter 3 which indicate a substitution mechanism involving rate determining addition of phosphite (at low concentrations of phosphite), several possibilities exist which may account for the independent formation of both mer and fac isomers. Two of these possibilities involve isomerisation of the six-coordinate intermediates (A) and (B) of Scheme 4.4.

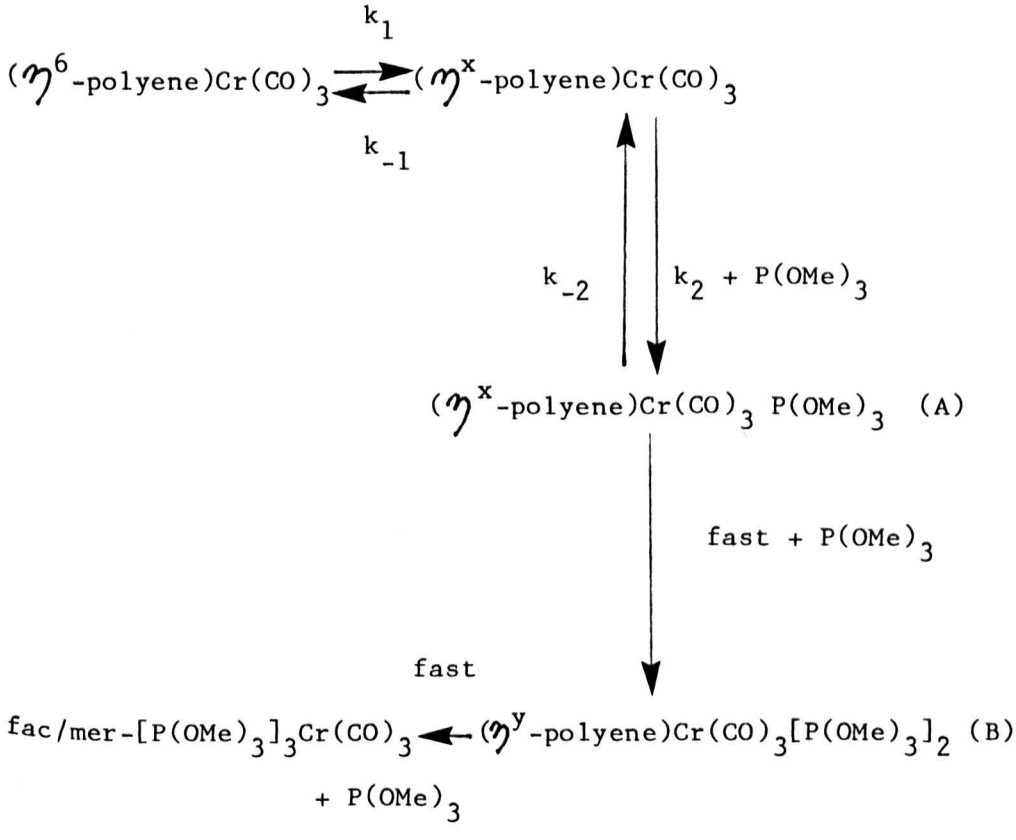

Scheme 4.4

Representing (A) as an η^4-coordinated intermediate (Scheme 4.5.1) intramolecular isomerisation involving a trigonal twist would shift $P(OMe)_3$ into a position trans to one of the coordinated double bonds (Scheme 4.5.2)

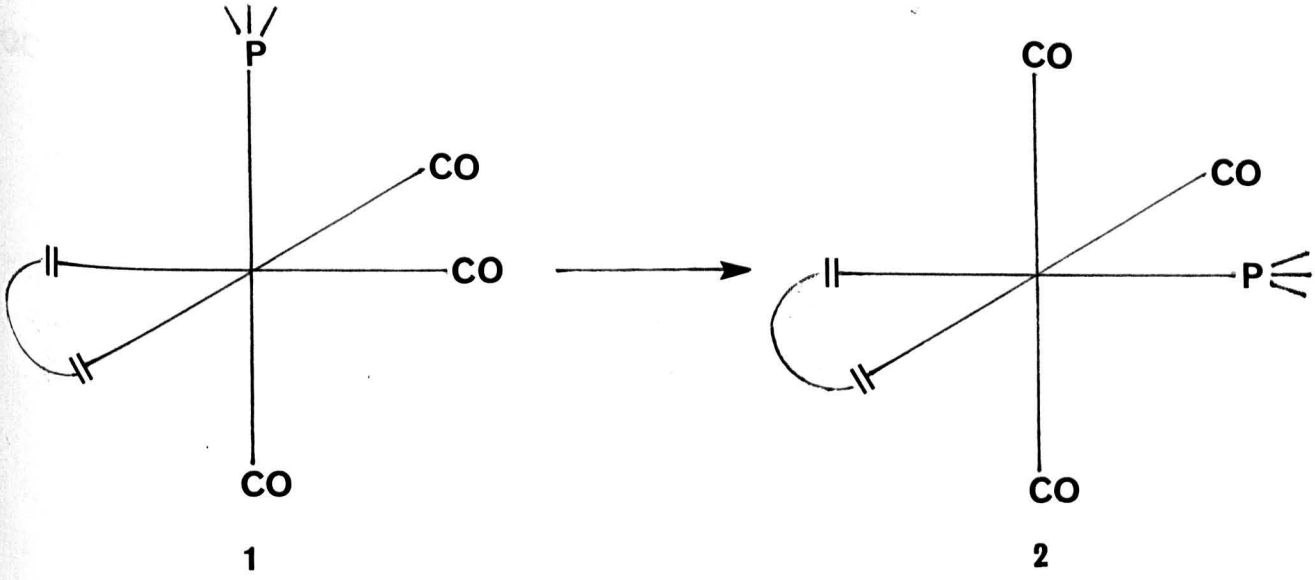

Scheme 4.5

Subsequent reaction with two molecules of $P(OMe)_3$ yields the mer isomer. Experimentally determined activation parameters for a trigonal twist in (penta-2,4-diene)$Cr(CO)_3P(OMe)_3$ shows an energy barrier of 62.8 kJ mol^{-1} [24]; associated rate constants being of the same order as the substitution reaction in this work. Assuming a similar energy barrier involved for the transformation in Scheme 4.5, it is unlikely that the above mechanism can account for mer isomer formation. Indeed, activation energies more consistent with its formation are likely to be of the order 5-10 kJ mol^{-1} and insignificant compared to the energy barrier for the initial ring opening.

A similar argument can be applied to the isomerisation of intermediate (B), the disubstituted phosphite complex. Isomerisation of the cis isomer yields the trans isomer (with respect to phosphite)

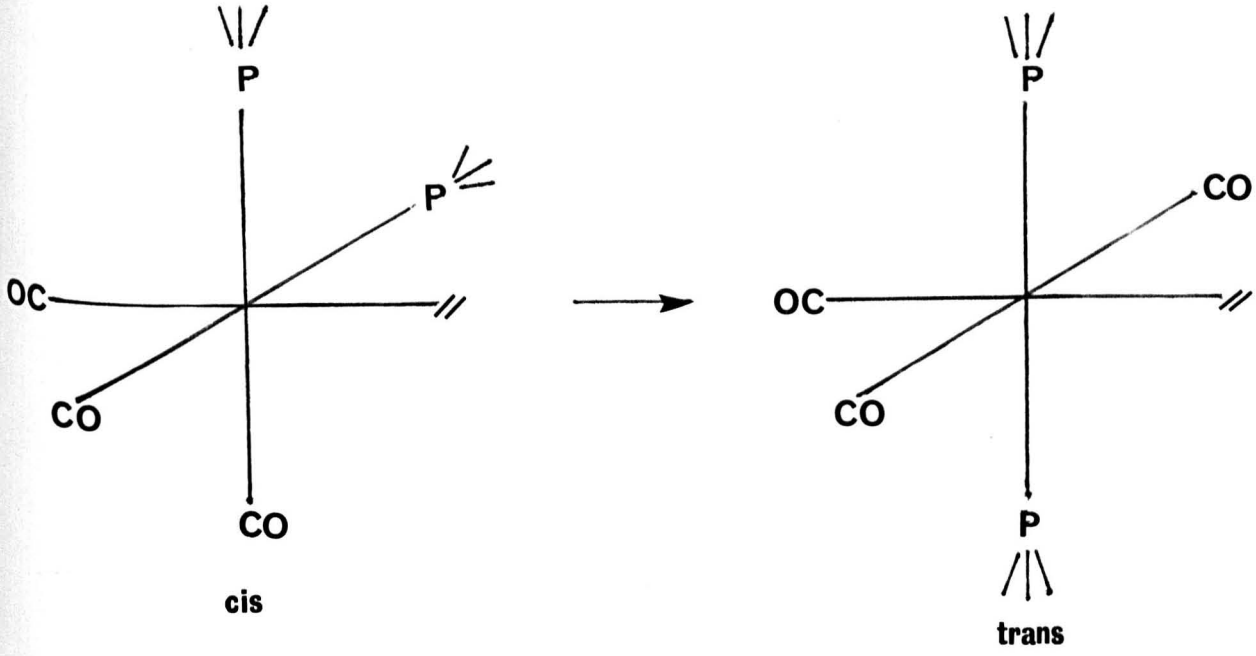

Scheme 4.6

Reaction of the cis and trans isomers with one further molecule of $P(OMe)_3$ yields the fac and mer isomers respectively. Similar energy barriers exist for the related isomerisation

$$cis\text{-}[P(OMe)_3]_2Cr(CO)_4 \rightleftharpoons trans\text{-}[P(OMe)_3]_2Cr(CO)_4$$

to the energy barrier involved in the (penta-2,4-diene)$Cr(CO)_3/P(OMe)_3$ system[19]. Hence from the above, mer isomer is unlikely to be formed from a preceeding six-coordinate isomerisation. However, other more plausible possibilities involve lower energy five-coordinate isomerisations. With reference to Scheme 4.4 such intermediates may exist prior to (Figure 4.2.1) or subsequent to (Figure 4.2.2) the formation of intermediate (B)

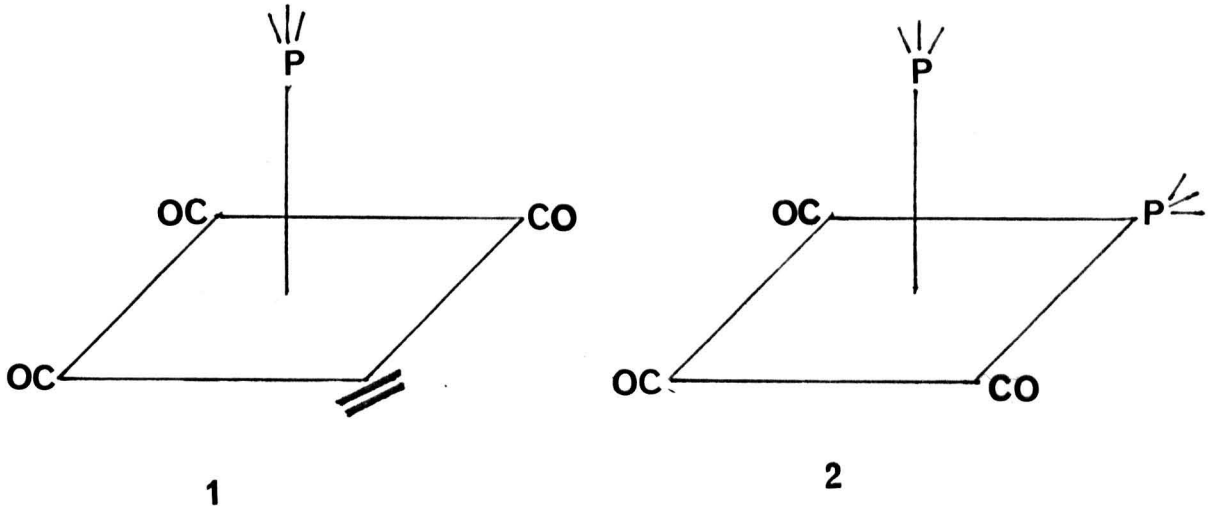

Fig. 4.2

It has been shown that five-coordinate intermediates of this type isomerise at rates of the same order as the rates of ligand association to form six-coordinate complexes[17]. The ratio fac/mer therefore reflects the ratio of ligand association to isomerisation, and in this case indicates a ratio of the order 10:1.

Of the possibilities discussed above, from a kinetic basis the five-coordinate isomerisation appears the most attractive. However, it must be noted that arguments against a six-coordinate isomerisation are based on data from assumedly similar systems. Additionally, six-coordinate isomerisations have been recently proved in complexes which had previously been interpreted to isomerise via a five-coordinate intermediate[20].

4.3.2 Fac/mer Isomerisation in $[P(OMe)_3]_3M(CO)_3$ Complexes

Rate data and activation parameters for the isomerisation

$$\text{fac-}[P(OMe)_3]_3M(CO)_3 \underset{k_{-i}}{\overset{k_i}{\rightleftharpoons}} \text{mer-}[P(OMe)_3]_3M(CO)_3$$

M= Cr,Mo,W

are given in Table 4.2 and 4.3. A uv/visible spectrum of the isomerisation of the molybdenum complex is shown in Figure 4.3. Similar spectra are obtained for the isomerisations of the Cr and W complexes. The clear isosbestic point confirms the occurrence of only the isomerisations reaction. Figure 4.4 shows the ^{31}P nmr spectrum of fac and mer $[P(OMe)_3]_3Cr(CO)_3$. Whilst the fac isomer gives rise to only one peak (as all the $P(OMe)_3$ groups are chemically equivalent), the mer isomer constitutes an AB_2 system consisting of two mutually trans $P(OMe)_3$ groups and a third $P(OMe)_3$ group cis to both of these. Rate constants for isomerisations monitored by both uv/visible spectroscopy (in decalin) and ^{31}P nmr spectroscopy (in toluene) are in good agreement considering the different concentrations and solvents used.

The isomerisation process, as represented below,

$$\text{fac-}L_3M(CO)_3 \underset{k_{-i}}{\overset{k_i}{\rightleftharpoons}} \text{mer-}L_3M(CO)_3$$

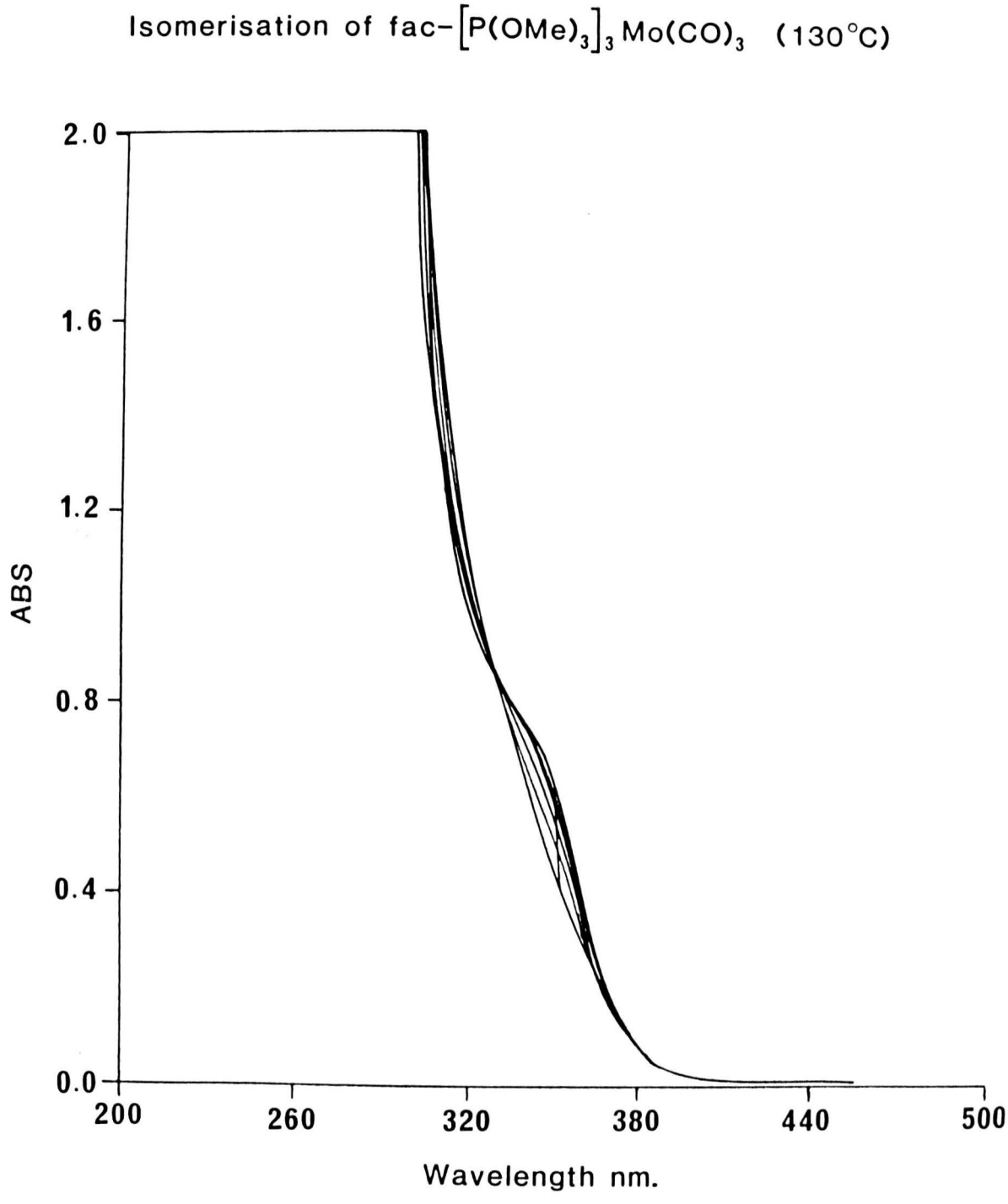
Isomerisation of fac-[P(OMe)3]3 Mo(CO)3 (130°C)
2.0
1.6
1.2
0.8
0.4
0.0
ABS
200
260
320
380
440
500
Wavelength nm.

Fig. 4.3

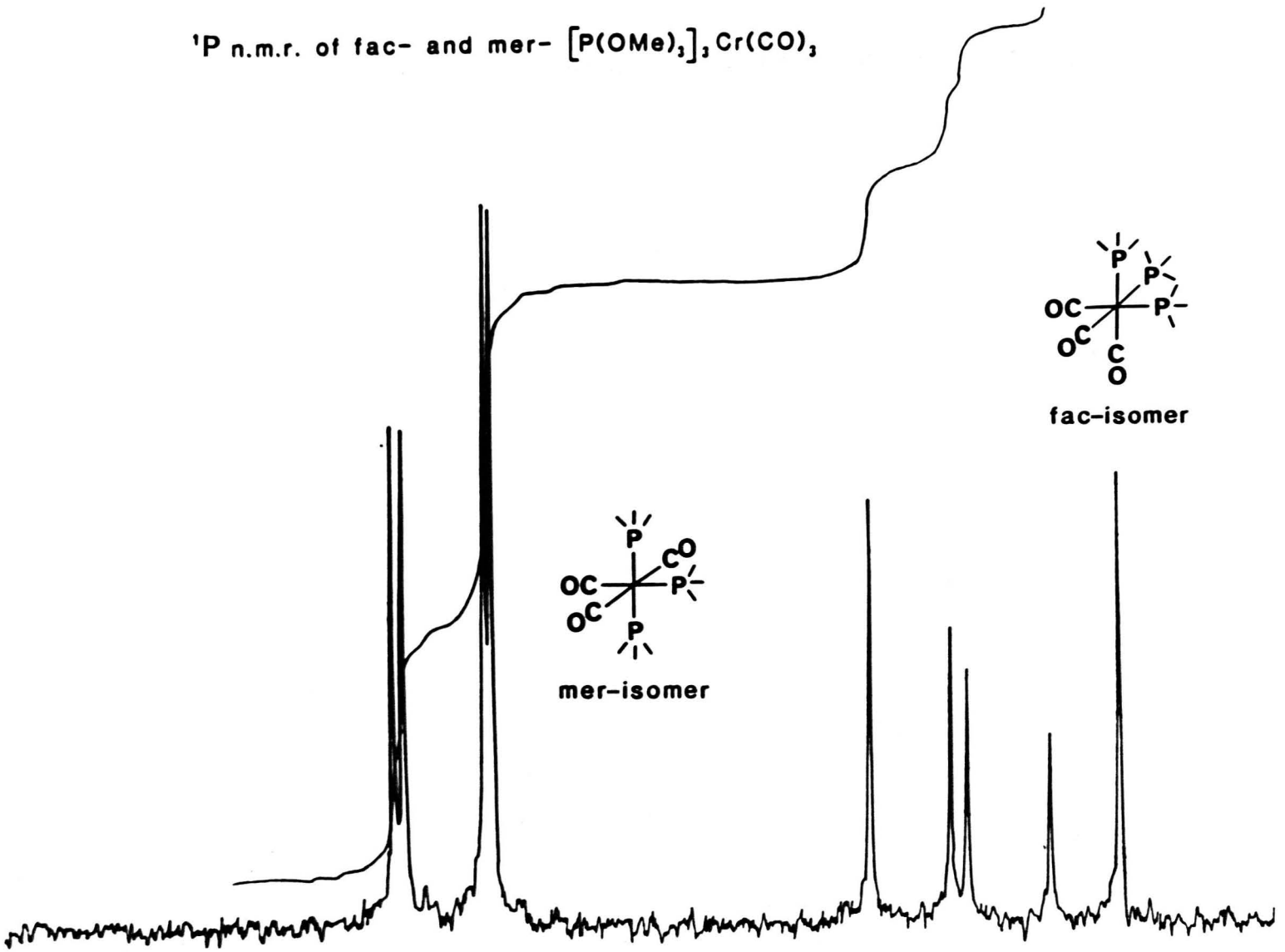

Fig. 4.4

the following equation can be derived[25]

$$-(k_i + k_{-i})t = \ln \frac{Z_e - Z_t}{Z_t + 1} + \ln \frac{Z_o + 1}{Z_e - Z_o}$$

where $Z_e = [mer]/[fac] = K_{eq}$ and is equivalent to the intensities of the fac and mer ^{31}P resonances. Therefore a plot of $\ln(Z_e - Z_t)/(Z_t + 1)$ against time yields a slope of value $-(k_i + k_{-i})$. From the equilibrium value K_{eq} (k_i/k_{-i}) individual values of k_i and k_{-i} may be determined. The plot for the isomerisation of fac-$[P(OMe)_3]_3Cr(CO)_3$ is shown in Figure 4.5. From uv/visible spectroscopy plots of $\ln(A_t - A_e)$ against time yield slopes equal to $-(k_i + k_{-i})$ individual values k_i and k_{-i} may be obtained from the equilibrium constant (which is temperature independent) determined from nmr spectroscopy.

In all cases, negligible effect on the rate of isomerisation on adding free ligand suggests that the isomerisations proceed by an intramolecular rearrangement mechanism. The octahedral complexes studied here are postulated to rearrange intramolecularly through either trigonal prismatic or bicapped-tetrahedral intermediates. Recent work however, has been able to distinguish between these mechanisms by 2-D nmr studies on $[P(OMe)_3]_3Cr(CO)_2CX$ (X=S,Se,Te) and concludes with convincing evidence the trigonal prismatic intermediate to be involved[21]. This intermediate is obtained by rotating one trigonal face of the octahedron.

Plot of $\ln\left[\frac{Z_e - Z_t}{Z_t + 1}\right]$ against time for the isomerisation of $[P(OMe)_3]_3Cr(CO)_3$ in toluene at 65 °C

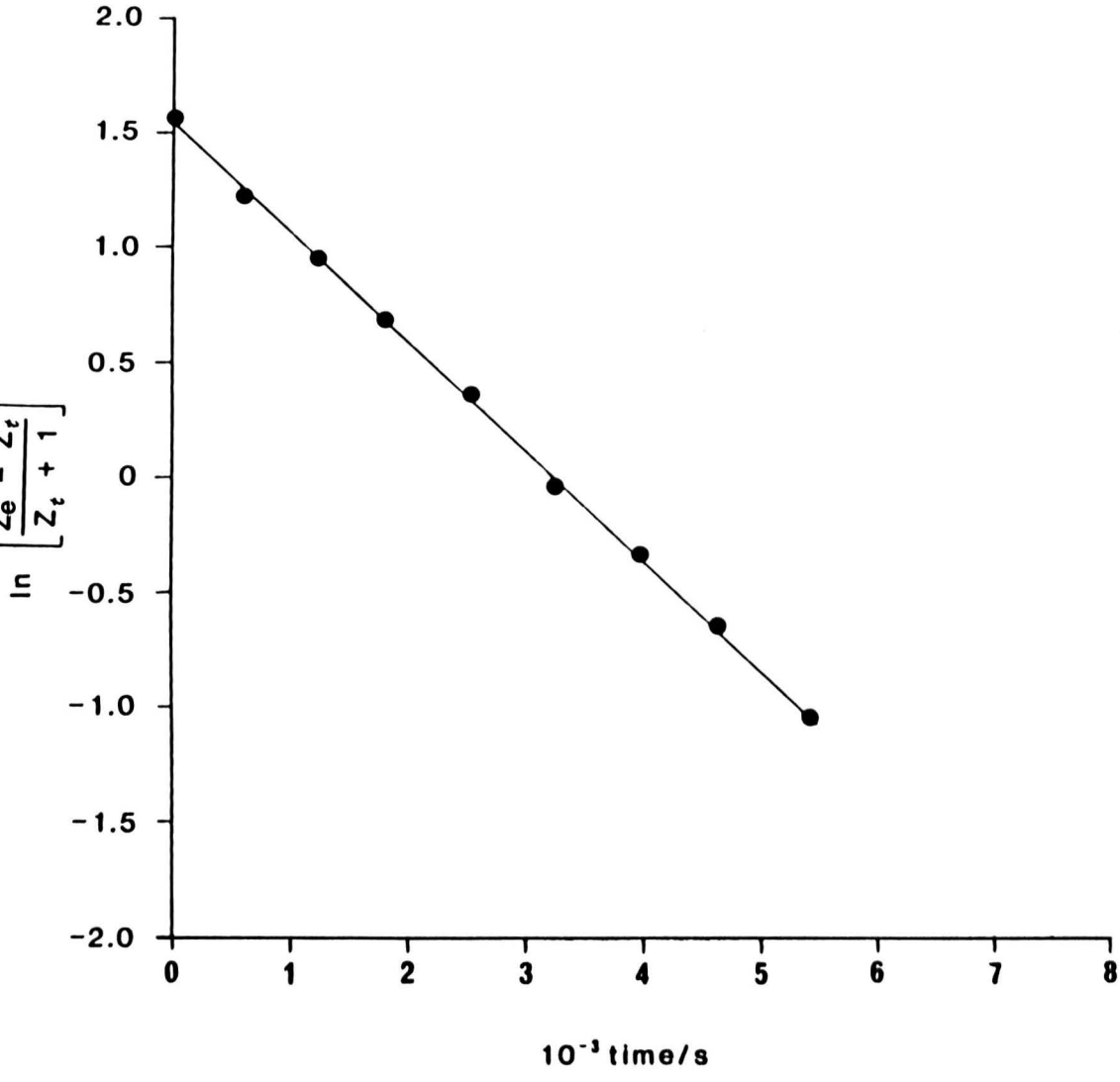

Fig. 4.5

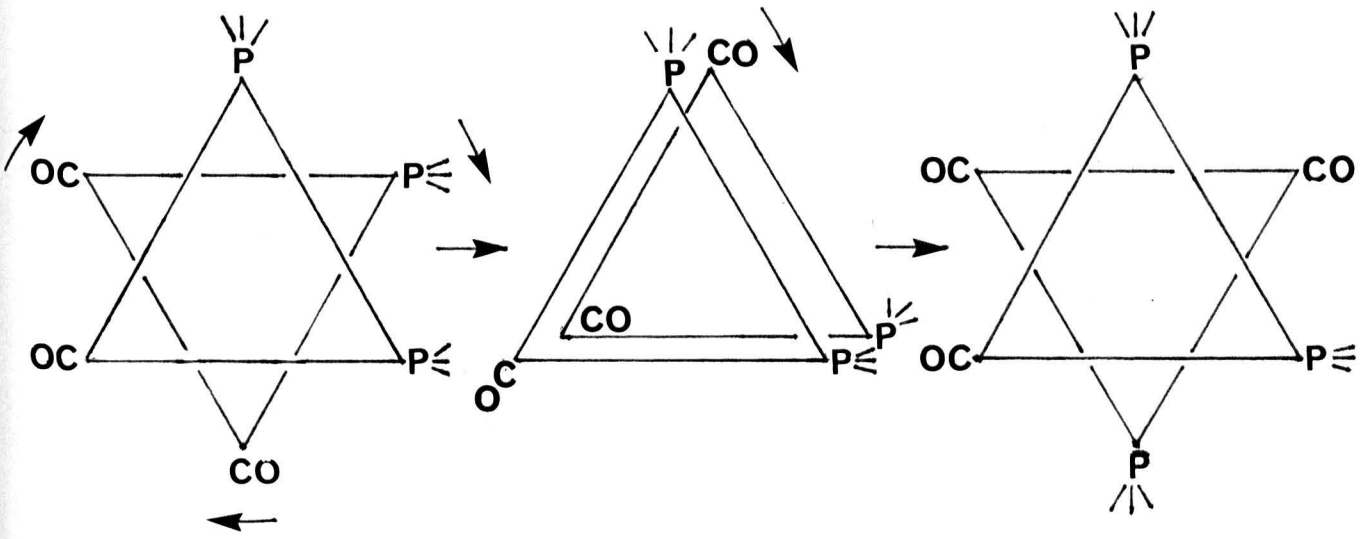

fac isomer trigonal prism mer isomer

Scheme 4.7

From the above diagram the fac ⟶ mer transformation involves eclipsed $P(OMe)_3$ groups in the trigonal prismatic intermediate, a situation which probably accounts for the increased rates of isomerisation observed in the disubstituted complexes $[P(OMe)_3]_2M(CO)_4$ (M=Cr,Mo,W), where this phosphite eclipsed intermediate may be avoided by opposite rotation. It is interesting to note at this point rates of isomerisation of $[P(OMe)_3]_xM(CO)_{6-x}$ complexes along the series x = 1 to 4, where rate increases from x = 1 to x = 2 and x = 3 to x = 4 are observed. The discontinuum between x = 2 and x = 3 separates complexes having eclipsed phosphite intermediates from those having non-eclipsed phosphite intermediates.

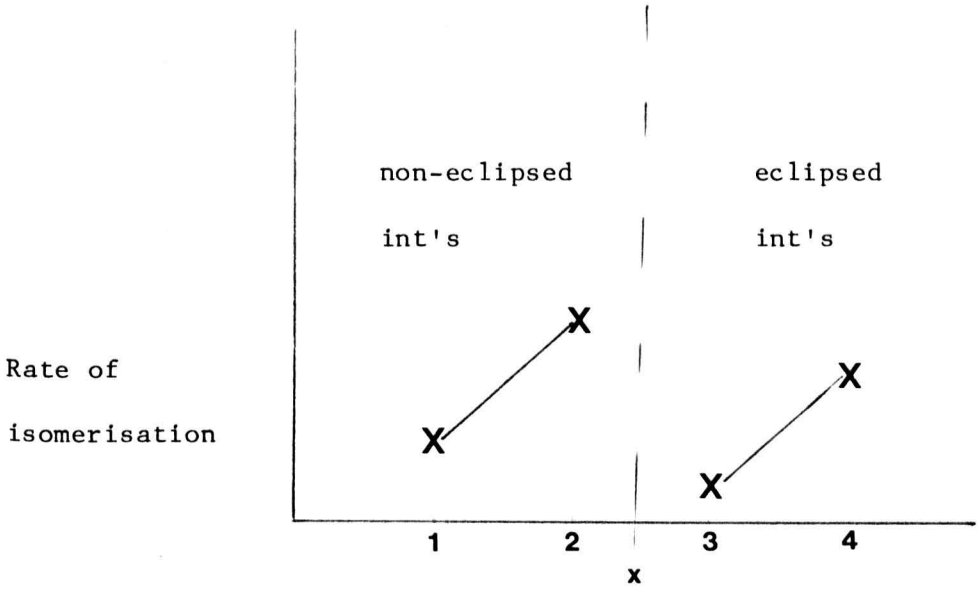

Fig. 4.6

Equilibrium position depends primarily on steric factors, the larger ligand (as measured by cone angle[26]) preferring the mer configuration as demonstrated by the higher mer/fac ratio of $[PBu_3]_3Cr(CO)_3$ compared to $[P(OMe)_3]_3Cr(CO)_3$. However, a smaller electronic effect which favours cis rather than trans CO configurations may also be involved, but overshadowed. Though both $P(OMe)_3$ and PBu_3 are both good electron donors, the latter is a considerably better one, but is a poorer electron acceptor. A fac configuration for the phosphine complex would hence seem electronically a more stable arrangement than the corresponding fac-phosphite configuration. In terms of metal, the mer/fac ratio for a given ligand is Cr >> Mo ≃ W and correlates with the increase in covalent radii between first and second/third row transition metals [Mo(1.62 A) > Cr(1.48 A)].

The rates of the fac ⟶ mer transformation of $[P(OMe)_3]_3M(CO)_3$ (M=Cr,Mo,W) follow the order Cr >> W > Mo. The higher rate of the chromium complex compared to the molybdenum complex is enthalpy controlled, whereas compared to the tungsten complex the higher rate is entropy controlled.

A similar entropy factor has been observed in ^{13}CO scrambling in the complexes cis-$(PEt_3)Cr(CO)_4(^{13}CO)$ and cis-$(PEt_3)W(CO)_4(^{13}CO)$[18] Two distinct pathways are presumed operative; for the tungsten complex, a pathway involving a highly sterically strained intermediate with little lengthening of the W-P bond, while for chromium, an intermediate involving considerable lengthening of the Cr-P bond is postulated. Hence the latter situation involves a more significant enthalpy term, but a less negative entropy term. The data presented here for $L_3M(CO)_3$ complexes show that the molybdenum complex is more similar in terms of $\Delta S^{\ddagger}$ to the chromium complex. The larger $\Delta H^{\ddagger}$ value of molybdenum compared to chromium probably reflects the greater Mo-P bond enthalpy. Indeed, it has been shown that some six-coordinate molybdenum systems for example $[P(OPh)_3]_2Mo(CO)_4$[19] tend to undergo isomerisations via an initial ligand dissociation, in contrast to the corresponding chromium and tungsten systems. Apart from the finer points of the mechanism, the results however do substantiate the increasing awareness that neutral six-coordinate molecules can undergo ligand rearrangements in their intact state.

Table 4.2

Rate Constants and Equilibrium Constants for the Isomerisations

$$\text{fac-}[P(OMe)_3]_3M(CO)_3 \underset{k_{-i}}{\overset{k_i}{\rightleftharpoons}} \text{mer-}[P(OMe)_3]_3M(CO)_3$$

i) obtained from uv/visible spectroscopy in decalin

M	temp/ ^{o}C	K_{eq}	$10^5(k_i+k_{-i})/s^{-1}$ [a]	$10^5k_i/s^{-1}$	$10^5k_{-i}/s^{-1}$
Cr	52.5	7.2	9.21(0.56)	8.08	1.13
	64.0	"	34.80(7.0)	30.60	4.20
	75.0	"	93.20(8.2)	81.80	11.40
	87.2	"	226.00(15.0)	198.00	27.00
Mo	100	3.0	3.33(0.32)	2.50	0.83
	110	"	7.02(0.60)	5.26	1.76
	120	"	18.50(1.20)	13.90	4.62
	130	"	36.80(2.60)	27.60	9.20
W	80	4.2	4.79(0.56)	3.87	0.92
	90	"	10.90(1.0)	8.80	2.10
	100	"	18.50(2.6)	14.90	3.60
	110	"	34.10(7.8)	27.50	6.60

Table 4.2 continued

ii) obtained from ^{31}P nmr spectroscopy in toluene

M	Temp/ ^{o}C	K_{eq}	$10^5 k_i / s^{-1}$	$10^5 k_{-i} / s^{-1}$
Cr	65	7.2	41.7	5.79
[+$P(OMe)_3$]	"	"	38.4	5.35
W	100	4.2	19.5	4.75
[+$P(OMe)_3$]	"	"	18.5	4.51

Notes: a) Error (2 standard deviations)

Table 4.3

Activation Parameters for the Isomerisations

$$\text{fac-}[P(OMe)_3]_3M(CO)_3 \underset{k_{-i}}{\overset{k_i}{\rightleftharpoons}} \text{mer-}[P(OMe)_3]_3M(CO)_3$$

M		$\Delta H^{\ddagger}$ /kJ mol^{-1} [a]	$\Delta S^{\ddagger}$ /J K^{-1} mol^{-1}
Cr			
fac	mer	87.2 (10.4)	-55.2 (30.4)
mer	fac	87.0 (9.2)	-72.4 (27.0)
Mo			
fac	mer	99.0 (10.0)	-70.0 (25.2)
mer	fac	99.0 (9.4)	-79.1 (25.0)
W			
fac	mer	69.1 (7.0)	-134.5 (21.4)
mer	fac	69.3 (8.4)	-146.1 (22.8)

Notes: a) Error (2 standard deviations)

REFERENCES

1a. See Inorganic Reaction Mechanisms, M.L. Tobe, Plll.

1b. J.C. Bailar Jr., J. Inorg. Nucl. Chem., 1958, 8, 165.

2. P. Ray and N.K. Dutt, J. Indian Chem. Soc., 1943, 20, 81.

3. C.S. Springer Jr. and R.E. Sievers, Inorg. Chem., 1967, 6, 852.

4. W. Majunke, D. Liebfritz, T. Mack and H. tom Dieck, Chem. Ber., 1975, 108, 3025.

5. N. Serpone and D.G. Bickley, Prog. Inorg. Chem., 1972, 17, 391.

6. L.G. Vanquickenborne and K. Pierloot, Inorg. Chem. 1981, 20, 3673.

7. R. Hoffman, J.M. Howell and A.R. Rossi, J. Amer. Chem. Soc., 1976, 98, 2484.

8. R. Mathieu and R. Poilblanc, Compt. Rend., Ser. C, 1967, 264, 1053.

9. F.B. Ogilvie, J.M. Jenkins and J.G. Verkade, J. Amer. Chem. Soc., 1970, 92, 1916.

10. J. Chatt and H.R. Watson, J. Chem. Soc., 1961, 4980.

11. R. Poilblanc and M. Bigorgne, Compt. Rend., 1960, 250, 1064.

12. R. Poilblanc and M. Bigorgne, Bull. Chim. Soc. France. 1962, 1301.

13. J.M. Jenkins, J.R. Moss and B.L. Shaw, J. Chem. Soc. (A), 1969, 2796.

14. D.J. Darensbourg, Inorg. Chem., 1979, 18, 2821.

15. M.J. Wovkulich, S.F. Feinberg and J.D. Atwood, Inorg. Chem., 1980, 19, 2608.

16. D.J. Darensbourg, Inorg. Chem., 1979, 18, 14.

17. D.J. Darensbourg, R. Kudaroski and W. Schenk, Inorg. Chem., 1982, 21, 2488.

18. D.J. Darensbourg and R.L. Gray, Inorg. Chem., 1984, 23, 2993.

19. D.T. Dixon, J.C. Kola and J.A.S. Howell, J.C.S. Dalton, 1984, 1307.

20. E.R. Dobson, H.H. Awad and S.S. Basson, Inorg. Chim. Acta., 1986, 118, L5.

21. A.A. Ismail, F. Sauroil, J. Sedman and I.S. Butler, Organometallics, 1985, 4, 1914.

22. D.P. Tate and W.R. Knipple, J.M. Augl, Inorg. Chem., 1962, 1, 422.

23. R.B. King and A. Fronzaglia, Chem. Comm., 1965, 547.

24. M Kotzian, C.G, Kreitner, M. Gunther and S. Özkar, Chem. Ber., 1983, 116, 3637.

25. J Kola, Ph.D. Thesis, University of Keele, 1983.

26. C.A. Tolman, Chem. Rev., 1977, 77, 313.